THE UNIVERSITY *of* EDINBURGH

Characterisation of the Direct Antiproliferative Effects of a Gonadotrophin-releasing Hormone Analogue

Colette Meyer

A thesis submitted in fulfilment of the requirements of the degree of Doctor of Philosophy

The University of Edinburgh

2012

Abstract

Gonadotrophin-releasing hormone (GnRH) can inhibit proliferation of multiple reproductive tissue cancer cell lines through direct interaction with GnRH receptors (GnRHR) on tumour cells. GnRH analogues may therefore have a role in treating some cancers. The signalling pathways associated with these inhibitory effects are poorly defined, and characterising them may help to understand therapeutic sensitivity. To elucidate these pathways, transcriptomic and proteomic approaches were used to compare the effects of the GnRH agonist Triptorelin in responsive GnRHR-transfected HEK293 cells (SCL60) and unresponsive (HEK293) cells both *in vitro* for up to 24h and *in vivo* for up to 7 days. Gene expression profiling demonstrated that SCL60 gene expression was temporally regulated with Triptorelin treatment, with expression of some genes increased at one time point but decreased at another. Early and mid-phase gene expression changes comprised mainly transcription factors and late changes included the hormonal signalling component *CGA*. Pathway analysis implicated mitogen-activated protein kinase and cell cycle pathways, supporting the detection of G_2/M arrest. Signalling effects within SCL60 xenografts, 4 and 7 days following Triptorelin treatment, were investigated using a phosphoproteomic antibody array. Changes included cell cycle and apoptosis regulators, as well as cell surface receptors and NFκB signalling pathway members. Reverse-phase protein arrays and western blotting also showed that pAkt was decreased and pNFκB-p65 was increased after Triptorelin treatment *in vitro*. An NFκB inhibitor enhanced the anti-proliferative effect of Triptorelin in SCL60 cells *in vitro,* suggesting that NFκB acts as a survival factor in the response to GnRHR stimulation. A range of GnRHR expression was observed in breast cancer tumours by immunohistochemistry, and on average GnRHR expression was significantly higher in the Triple Negative Phenotype (TNP) subgroup and in grade 3 tumours. A GnRHR-transfected breast cancer cell line, MCF7-h14, was developed. Despite this expressing a similar level of GnRHR to responsive SCL60 cells, MCF7-h14 cells were not inhibited by GnRHR activation, indicating that a high level of GnRHR is insufficient for the antiproliferative effects of Triptorelin.

Declaration

The work in this thesis is solely my own work unless otherwise indicated, where credit to the contributor is given. No part of the work has been submitted for any other degree.

Colette Meyer

Acknowledgements

I thank my supervisors Simon Langdon, Andy Sims, Kevin Morgan, Dana Faratian and David Harrison.

I thank all my colleagues in the Breakthrough Research Unit, Edinburgh who have assisted me with experiments. I would also like to thank Kevin Morgan and Nicola Miller of the MRC Human Reproductive Sciences Unit, Queen's Medical Research Institute, Edinburgh for their support and expertise.

The SCL60 and SCL215 cell lines and their parental HEK293 cells were provided by Kevin Morgan.

Mouse SCL60 and HEK293 xenograft experiments were performed by Morwenna Muir (University of Edinburgh Cancer Research Centre, Western General Hospital, Edinburgh) as a scientific service. Tissue from the SCL60 xenografts was used in immunohistochemical assays. Inhwa Um (Research Assistant, Breakthrough Research Unit, Edinburgh) constructed tissue microarrays from the SCL60 xenografts. Immunohistochemical staining for all markers except GnRHR was performed by myself, with the supervision of Simon Langdon, who also scored some of the slides. I prepared samples for flow cytometry analysis, which were processed on the flow cytometer by Elisabeth Freyer (Flow Cytometry Service, MRC Human Genetics Unit, Western General Hospital, Edinburgh) as a scientific service.

I designed the gene expression microarray study with the supervision of Simon Langdon and Andy Sims. I performed the cell treatments, RNA extractions, purifications and labelling. Alexey Larionov (Research Fellow, Breakthrough Research Unit, Edinburgh) provided advice on the labelling procedure. Charlene Kay (Research Assistant, Breakthrough Research Unit, Edinburgh), Annelein Zweemer (Student, Breakthrough Research Unit, Edinburgh) and Huizhong Hu (Student, Breakthrough Research Unit, Edinburgh) assisted with the procedure for biotin-labelling RNA under my direction. The microarrays were processed by the Wellcome Trust Clinical Research Facility, Western General Hospital, Edinburgh as a scientific service. I filtered and normalised the resultant data, and performed quality control checks. I performed the analyses to detect differential gene expression.

SCL60 xenografts antibody arrays were performed by Eurogentec as a scientific service. They provided data for phosphorylated protein normalised to non-phosphorylated protein, which I analysed for significant differences between treatment groups.

Peter Mullen (Research Assistant, Breakthrough Research Unit, Edinburgh) provided advice on processing the reverse-phase protein arrays. I designed the experiments, collected the protein, standardised the protein concentration across samples, performed the arrays and analysed the data. I performed all western blots in chapter 3.3.

Ilgin Cagnan, a student working under my supervision, measured GnRHR expression by quantitative immunofluorescence. The tissue microarrays used were provided by Dana Faratian, and are detailed in the publication "Quantitative analysis of changes in ER, PR and HER2 expression in primary breast cancer and paired nodal metastases, Aitken *et al*, Ann Oncol, 2009" [1]. The resulting data was analysed by myself. Andy Sims and I both analysed the mRNA level of GnRHR in published datasets of breast cancers. Andy Sims provided Figure 61.

Kevin Morgan performed the stable transfection of breast cancer cell lines, and experiments in chapter 3.6 of this thesis were done collaboratively between Kevin Morgan and myself, with the exception of Figure 78 and Figure 84, which were provided by Kevin Morgan.

Funding for this research project was provided by Breakthrough Breast Cancer.

Part of this thesis is published in the BMC cancer paper:
"GnRH receptor activation competes at a low level with growth signaling in stably transfected human breast cell lines, Morgan K, Meyer C, Miller N, Sims AH, Cagnan I, Faratian D, Harrison DJ, Millar RP, Langdon SP, 2011".
Kevin Morgan prepared the manuscript. Kevin Morgan, myself and Nicola Miller performed ligand binding assays, SRB assays and western blots. Ilgin Cagnan measured GnRHR primary breast tissue microarrays by immunofluorescence. I analysed the immunofluorescence data. Dana Faratian and provided tissue and clinical data for immunofluorescence analysis. Andy Sims, Dana Faratian, David Harrison, Robert Millar and Simon Langdon contributed intellectually, in supervision, and in manuscript preparation.

List of Contents

List of Figures

List of Tables

List of Abbreviations

15d-PGJ_2	15-Deoxy-(Delta)12,14-Prostaglandin J2
AMPS	Ammonium persulphate
ANOVA	Analysis of Variance
AQUA	Automated Quantitative Analysis
BAFF	B-cell activating factor
BRCA	Breast cancer susceptibility protein
BSA	Bovine Serum Albumin
cAMP	Cyclic adenosine monophosphate
CDK	Cyclin-dependent kinase
cpm	counts per minute
DAB	3,3'-Diaminobenzidine
DAG	Diacylglycerol kinase
DAPI	4',6-diamidino-2-phenylindole
DAVID	Database for Annotation, Visualization and Integrated Discovery
DCIS	Ductal carcinoma in situ
DGK	Diacylglycerol kinase
DMEM	Dulbecco's Modified Eagle Medium
DMSO	Dimethyl Sulphoxide
DPX	Di-N-butyl Phthalate in Xylene
DUSP	Dual Specificity Phosphatase
ECF	Enzyme-amplified Chemifluorescence
ECM	Extracellular matrix
EDTA	Ethylenediaminetetraacetic acid
EGF	Epidermal growth factor
EGFR	Epidermal growth factor receptor
Egr	Early growth response
EGTA	Ethylene glycol tetraacetic acid
ER	Oestrogen Receptor
ERBB2	Human Epidermal growth factor Receptor
ERK	Extracellular signal–regulated kinase

FADD	Fas-Associated protein with Death Domain
FCS	Foetal Calf Serum
FDR	False Discovery Rate
FSH	Follicle Stimulating Hormone
GDP	Guanosine diphosphate
GnRH	Gonadotrophin releasing hormone
GnRHR	Gonadotrophin releasing hormone receptor
GPCR	G-Protein Coupled Receptor
GTP	Guanosine triphosphate
HEK	Human Embryonic Kidney
HEPES	4-(2-hydroxyethyl)-1-piperazineethanesulfonic acid
HER2	Human Epidermal growth factor Receptor 2
IGF	Insulin-like growth factor
IGF-I-R	Insulin-like growth factor 1 receptor
IKK	IκB kinase
IP3	Inositol triphosphate
IκB	Inhibitor of kappa B
JNK	c-Jun N-terminal kinase
KEGG	Kyoto Encyclopedia of Genes and Genomes
LH	Luteinising Hormone
LSB	Laemmli Sample Buffer
MAPK	Mitogen Activated Protein Kinase
MEF	mouse embryonic fibroblasts
MEK	MAPK kinase
MMP	Matrix metalloproteinase
MTOR	Mammalian target of rapamycin
NCBI	National Center for Biotechnology Information
NFκB	Nuclear Factor Kappa B
NOD	Nucleotide-binding oligomerization domain-containing protein
p-	phosphorylated-
P/S	Penicillin & Streptomycin
PARP	Poly (ADP-ribose) polymerase

PBS	Phosphate Buffered Saline
PBS-T	PBS 0.1% Tween-20
PI3K	Phosphoinositol 3 Kinase
PKC	Protein Kinase C
PLC	Phospholipase C
PMSF	Phenylmethylsulfonyl fluoride
PR	Progesterone Receptor
PTEN	Phosphatase and tensin homolog
PVDF membrane	Polyvinylidene difluoride membrane
RPPA	Reverse phase protein array
RTK	Receptor Tyrosine Kinase
SAM	Significance Analysis of Microarrays
SDS	Sodium dodecyl sulfate
SDS-PAGE	SDS-Polyacrylamide Gel Electrophoresis
SHC	Src Homology Complex
Sos	Son of Sevenless
SRB	Sulphorhodamine B
t-	total-
TBS-T	Tris-buffered saline + 0.1% Tween-20
TCA	Trichloroacetic Acid
TDLU	Terminal Duct Locular Unit
TEMED	Tetramethylethylenediamine
TMA	Tissue Microarray
TNF	Tumour Necrosis Factor
TNP	Triple Negative Phenotype
Triptorelin	D-Trp^{6}-GnRH

Chapter 1: Introduction

1 Introduction

1.1 Breast cancer

1.1.1 The Hallmarks of Cancer

Normal cell division is carefully controlled to ensure that cells do not divide inappropriately and cause harm to the host, such as when the cell is damaged. This regulation is sometimes lost as a result of mutations (either genetic or epigenetic) accumulating in the cell and can lead to tumour formation. Tumour-promoting mutations include the loss of tumour suppressor gene function [2] or the gain of function of oncogenes [3]. Tumour suppressors inhibit growth, for instance by implementing checkpoints in the cell cycle to prevent damaged DNA being replicated [2]. Oncogenes promote growth, for example by promoting the passage through cell cycle checkpoints, or by increasing the activity of particular growth factors in the cell [3]. It is the balance of tumour suppressor and oncogene activities that is important in maintaining the regulation of cell growth and proliferation.

When regulation becomes aberrant, the surrounding cells usually recognise the rogue cell and destroy it as though it were an invading pathogen. However, since the rogue cell is derived from a normal host cell it may escape detection. In this rare event the cell may be permitted to survive in the tissue and proliferate without control. Many of the daughter cells will die, but due to the increased rate of proliferation and the competitive environment in which the cells are being produced, the number of surviving cells may increase, passing on the mutations required to survive in such an environment to their daughter cells. In this manner a tumour may be formed.

A tumour (or neoplasm) is defined as a mass of tissue resulting from abnormal growth of cells. For a tumour to be considered cancerous, additional features must be present. Hanahan and Weinberg suggested six hallmarks of cancer [4] to aid its definition; these are listed below [4].

1. Self-sufficiency in growth signals
2. Insensitivity to anti-growth signals
3. Ability to evade apoptosis
4. Limitless potential for replication
5. Sustained angiogenesis
6. Tissue invasion and metastasis

The authors have recently suggested the addition of a further two hallmarks: Deregulating cellular energetics and Avoiding immune destruction [5] and provide a detailed review of all eight hallmarks [5].

These hallmarks are a useful way to think about the processes involved in cancer. A tumour may not necessarily become cancerous. Proliferation may be successfully limited by the tissue microenvironment, and equilibrium may be reached between the level of proliferation and death, that maintains the size of the tumour. Equally, a tumour may continue to grow, but grows so slowly that it may never cause pathological damage to the host. These tumours are referred to as being benign. They are self-limiting and do not invade surrounding tissues nor metastasise (spread to other parts of the body).

1.1.2 Breast Biology

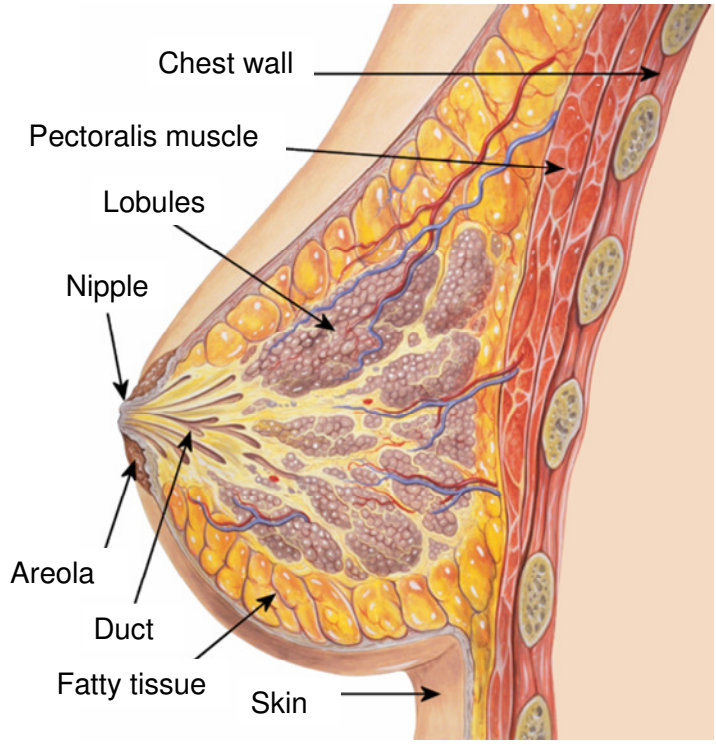

Figure 1: Breast Anatomy.
Adapted from the original image by Patrick J. Lynch, medical illustrator and C. Carl Jaffe, MD, cardiologist [6] and permission for reproduction of the figure was granted under the terms of the Creative Commons Attribution 3.0 Unported license.

A schematic of the human female breast anatomy is illustrated in Figure 1. The breasts are situated in front of the pectoralis muscle on the chest wall [7]. Each breast comprises a ductal system surrounded by stroma and fatty tissue [8]. The ducts meet at the nipple, from which milk is ejected during breastfeeding [8].

The breast is highly sensitive to hormones. It changes in composition and appearance during a woman's life from puberty, through each menstrual cycle, pregnancy and the menopause [8, 9]. The breasts can also change in shape and size with variation in the woman's body weight, since the breast is composed largely of adipose tissue [8, 9].

The adult breast is comprised of 15-25 major (segmental) ducts that branch into smaller (subsegmental) ducts [8, 9]. Lobules (terminal duct lobular units, TDLUs) bud from subsegmental ducts [8, 9] and are composed of intralobular stroma and

acini (small tubules) [8]. As a woman continues to age, particularly past the third decade, her breasts become less dense (more fatty) [8]. For a detailed review of breast anatomy see references [8] and [9].

1.1.3 Breast Cancer Background

1.1.3.1 Epidemiology

Breast cancer is a heterogeneous disease from which 12,000 women in the UK died in 2008 [10]. It almost always occurs in the female breast, with nearly 46,000 women diagnosed with breast cancer in the UK in 2007 compared to less than 300 men [10].

1.1.3.2 Risk factors

Other than gender, factors that influence the risk of developing breast cancer include age, family history, exposure to radiation or other carcinogens such as certain chemicals or alcohol, ethnic group, and lifestyle factors such as diet and exercise [11, 12]. Because breast tissue is highly sensitive to levels of circulating oestrogen, life events and choices such as the age at which a woman first gives birth, the number of children she has, early menarche, late menopause, breastfeeding, the use of the contraceptive pill and hormone replacement therapy can all affect breast cancer risk [11, 12].

1.1.3.3 Pathology

The majority of breast cancers are thought to originate in the epithelial lining of the TDLU [8] as ductal hyperproliferation. This develops into ductal carcinoma *in situ* (DCIS) as the cells acquire further genetic and epigenetic aberrations [8]. As the disease progresses it acquires the ability to invade and metastasize (invasive carcinoma) [8].

Tumours are composed, much like healthy tissues, of epithelial cells and stroma, but breast carcinomas have increased necrosis, vascularisation and invasion compared to

healthy breast tissue [8]. The cancerous epithelial tissues often appear poorly differentiated and more heterogeneous than healthy tissue [8].

1.1.3.4 Subtypes

It is now generally accepted that there are five major molecular subtypes of breast cancer. The five subtypes are: Luminal A, Luminal B, Basal-like, Human Epidermal growth factor Receptor 2 (HER2) positive/Oestrogen Receptor (ER) negative, and normal breast-like [13]. This classification has been deduced from gene expression profiling of primary breast tumours and has been reproduced across different microarray platforms using multiple datasets [14, 15]. It is also supported by previous classifications based on histological and immunological characteristics of breast cancers [14]. Each subtype has distinct characteristics and responds differently to treatment [13].

1.1.3.5 Diagnosis

Early detection of breast cancer is essential for improved prognosis [16]. Breast screening by mammography is currently in place in the UK for women 50-70 years of age [17]. Diagnosis is made following screening or through the identification of a palpable lump in the breast [17]. A breast biopsy is taken and the cells are tested for presence of oestrogen receptor, progesterone receptor and HER2 [17]. The presence or absence of each of these biomarkers can determine the subtype, and the most suitable treatment [17].

1.1.3.6 Treatment

Surgery is usually the first treatment for breast cancer after diagnosis [17]. Only the tumour may be removed if it is small enough, or it may be necessary to remove the entire breast and surrounding lymph nodes [17]. Surgery can often be an effective treatment if the cancer has not yet metastasized, but surgery is not always possible and in many cases the disease recurs even after the apparent removal of all the cancer cells [18]. This may be due to the presence of cancer stem cells [18, 19].

1.1.3.6.1 Cytotoxic therapy

All cancer cells originate from a host cell, so at least initially are very similar to healthy cells. The development of effective treatments depends on the ability to exploit subtle differences between the healthy and abnormal cells. Chemotherapy (treatment with cytotoxic drugs) and radiotherapy (treatment with radiation) exploit the higher growth rate of tumours [20]. They cause damage to all cells but have a greater impact on the cells that are rapidly dividing because cells are committed to apoptosis only after the damage is identified by checkpoints in the cell cycle. By giving this treatment in doses spread out over time, normal cells that are dividing at a slower rate have enough time to recover from this damage [20]. The side effects of this therapy result from damage to cells in the body that have a higher rate of proliferation such as bone marrow cells, which results in a compromised immune system and an increased risk of serious infection [20].

1.1.3.6.2 Molecular targeted therapy

The rationale for molecular targeted therapy is based on the premise that growth or invasion of the cancer cell is reliant on a particular pathway and therefore its inhibition would be of therapeutic benefit. It also stems from the concept of oncogene addiction i.e. the theory that cancer cells may become reliant on (addicted to) the activity of a single oncogene such that when this oncogene is inhibited the cancer cell dies [21]. A single oncogene can be targeted by designing drugs to specifically inhibit it. This is known as molecular targeted therapy [21].

These treatments often have fewer side effects because they are more selective for the tumour cells over the host cells, since only the tumour cells are so dependent on the target molecule. Some targeted therapies for breast cancer and their drug targets are summarised in Table 1.

Drug (Brand Name)	Target
Tamoxifen (Nolvadex)	Oestrogen Receptor Alpha (ERα)
Exemestane (Aromasin)	Aromatase cytochrome P450
Anastrazole (Arimidex)	Aromatase cytochrome P450
Letrozole (Femara)	Aromatase cytochrome P450
Trastuzumab (Herceptin)	Human Epidermal Growth Factor Receptor 2 (HER2)
Pertuzumab (Omnitarg)	Human Epidermal Growth Factor Receptor 2 (HER2)
Lapatinib (Tykerb)	Human Epidermal Growth Factor Receptor 1, 2 (HER1, HER2)

Table 1: Some targeted therapies for breast cancer in current clinical use

Another important concept in cancer biology is synthetic lethality [22]. Two gene products are synthetically lethal if mutation or inhibition of one of them leaves the cell viable, but inhibition of both leads to cell death [22]. As in oncogene addiction, the cell is extremely dependent on one of these genes, but only when the other is not functional. The two gene products may [22]:

- serve the same essential function (directly compensate each other's loss)
- be two subunits of an essential protein complex
- be two interconnected components in an essential pathway
- participate in parallel essential pathways

Where it is possible to identify a synthetically lethal pair of genes, cell death may be induced by combining targeted treatments for the individual genes [22]. One example of this is the BRCA mutation. If either of the *brca1* or *brca2* genes is mutated such that the BRCA protein is unable to perform its usual role in DNA repair, the cell survives but becomes dependent on PARP-mediated DNA repair [23]. This makes the cells very sensitive to inhibition of PARP activity. PARP inhibitors have been shown to cause cell cycle arrest and apoptosis in BRCA-mutated breast cancer cells [23] .

1.1.3.6.3 Limitations of current therapies

1.1.3.6.3.1 Heterogeneous response

The response to treatment is heterogeneous both between patients and within the same patient or tumour [20]. Current biomarkers do not adequately select patients for response [24]. Drug side effects can have a large impact on a patient's quality of life, often without guaranteeing an improvement in prognosis [20]. There is a need to identify patients who will respond to a drug more accurately, so that individuals who will not respond are not treated unnecessarily [20].

1.1.3.6.3.2 Resistance

Cancers are often resistant to treatment, either from the outset (intrinsic resistance) or after time and with ongoing treatment (acquired resistance) [20]. Initially, the cells may appear only to be dependent on one molecule, but when this is inhibited the second molecule may begin to compensate for the loss of the first [20]. In this case combination treatment may be more effective than a single treatment [20].

1.2 Gonadotrophin-releasing hormone in breast cancer

Gonadotrophin-releasing hormone (GnRH) agonists and antagonists have been shown to have antiproliferative effects on breast cancer cells [25-32], but further research is required to improve efficacy and prediction of response [32]. To explore potential mechanisms of GnRH analogues, it is first necessary to understand the structure of GnRH and its receptor, and its role in the normal physiological context.

1.2.1 GnRH

1.2.1.1 GnRH Structure

GnRH is a decapeptide, of which 23 forms have been identified across protochordate and vertebrate species [33]. There are often several isoforms present in one species; in mammals there are one or two isoforms per species [33]. The amino acid structures of GnRH-I and GnRH-II, the two forms present in humans, are shown in Figure 2.

GnRH-I: **pGLu-His-Trp-Ser**-Tyr-Gly-Leu-Arg-**Pro-Gly-NH_2**
GnRH-II: **pGLu-His-Trp-Ser**-His-Asp-Trp-Tyr-**Pro-Gly-NH_2**

Figure 2: Amino acid structure of GnRH-I and GnRH-II
Highly conserved residues are indicated in bold type. This figure was adapted from Millar *et al* [33] .

The conserved amino and carboxyl termini (which are post-translationally modified to form pyroGlu and Glycine amide) are important for function, and the non-conserved residues are thought to determine ligand-specificity or may be functionally redundant [33].

1.2.1.2 GnRH Receptor Structure

The GnRH receptor (GnRHR) is a seven transmembrane G-protein coupled receptor (GPCR). There are three major subfamilies of GPCRs: A, B and C. The GnRHR belongs to family A, which includes receptors related to rhodopsin and the β2-adrenergic receptor [34, 35]. The most notable feature of the human GnRHR's

primary structure is that it lacks the carboxyl terminal intracellular tail normally found on GPCRs [35] (Figure 3). Other species do have a C-terminal tail, which acts as a regulatory domain and has a role in receptor internalisation [35]. Figure 3 also shows areas of the receptor that are believed to be involved in ligand binding, receptor activation and G-protein coupling.

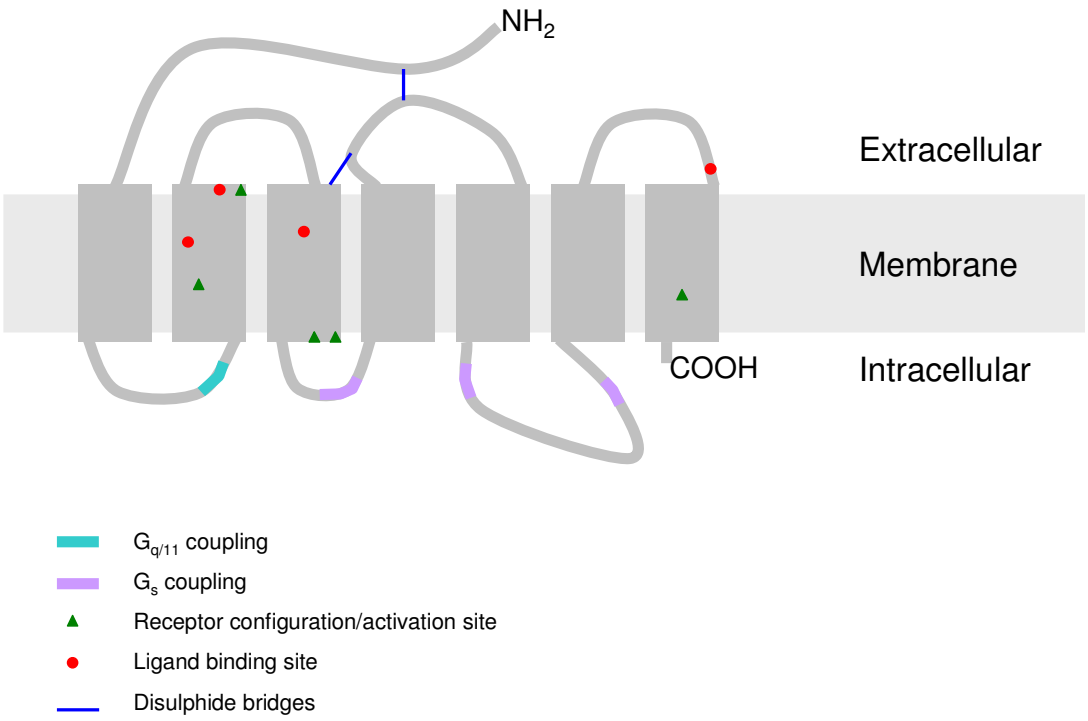

Figure 3: Human GnRH receptor structure.
Adapted from Millar et al 2004: GnRH and GNRHRs [36]. The GnRHR lacks the intracellular carboxyl terminal tail present in other GPCRs. Other notable features shown above are domains for G-protein coupling (light blue and purple), disulphide bridges (dark blue), ligand binding sites (red), and receptor activation sites (green).

Interestingly, a large percentage of human GnRH receptors are retained in the endoplasmic reticulum. This is thought to be a result of incorrect disulphide bridge formation [37]. This is not the case with rat and mouse GnRHR, of which most is efficiently directed to the plasma membrane [34]. Two disulphide bridges are required for effective routing of the human GnRHR to the plasma membrane, whereas only one of these bridges is required in rat and mouse GnRHR [37].

1.2.2 The normal physiological functions of GnRH

Most vertebrate species appear to have at least two of the structural variants of GnRH, but some have three. The different forms have diverse functions depending on the resident tissue and species [36]. They may operate in a neuroendocrine, paracrine, autocrine or neurotransmitter/neuroregulatory manner [36]. GnRH exists in two forms in humans, GnRH-I and GnRH-II [36]. GnRH-I is well-known to regulate gonadotrophin production and release in the pituitary [36], whereas the role of GnRH-II is less well defined. The GnRH-II system appears to have been adapted during evolution such that either one or both of GnRH-II and GnRH-II-R appear to be inactivated in a range of mammalian species [38].

GnRH-I is released in pulses every 30-120min from nerve endings to stimulate synthesis and secretion of Luteinising Hormone (LH) and Follicle Stimulating Hormone (FSH) from the pituitary gland, resulting in the production of sex steroid hormones in the ovary or testes [36]. It is thought that GnRH-II may also have a role in reproductive behaviour [36].

Although GnRH-II appears to be functional, it does not interact with a specific GnRH-II receptor, since the gene encoding GnRH-II-R has a premature stop codon in humans [36]. It is therefore believed that GnRH-II couples to GnRH-I-R. The different ligands are thought to induce differential receptor conformations, which stabilise differential intracellular signalling complexes to mediate distinct cellular outcomes [39]. GnRH-II-R may help to modulate the expression of GnRH-I-R, since when both were transiently transfected in fibroblast-like COS-7 cells, expression of the GnRH-I-R was reduced, and signalling through the receptor was impaired [40].

1.2.3 Current role of GnRH in Therapy

1.2.3.1 GnRH Agonists and Antagonists

Aside from the endogenous GnRH-I and GnRH-II molecules, some synthetic analogues have been designed to target the GnRHR and have been studied in relation to manipulation of the reproductive system by targeting the pituitary gland. These

can be classified as agonists, antagonists, or inverse agonists. Figure 4 shows how the structures of GnRH agonists and antagonists are modified compared to the naturally occurring GnRH sequence.

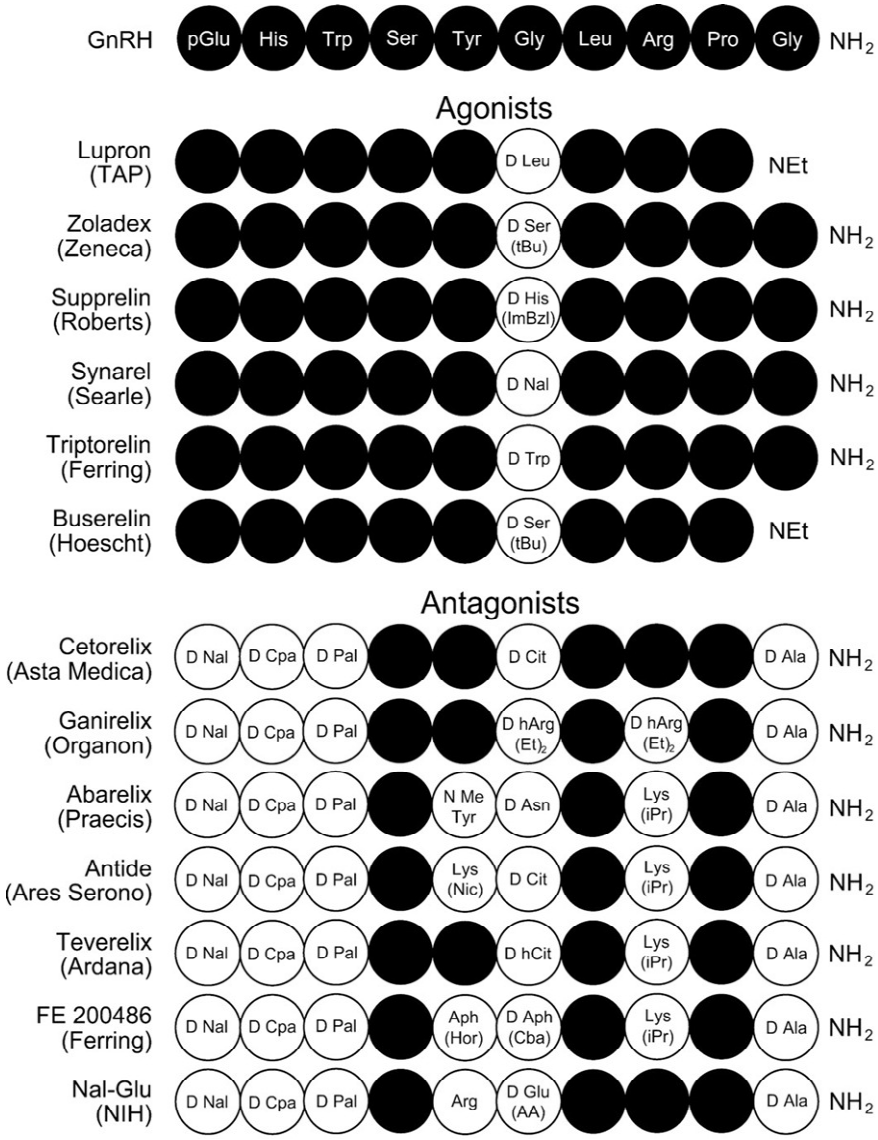

Figure 4: The amino acid structure of GnRH agonists and antagonists. This figure is adapted from [36].

In naturally occurring GnRH structural variants, the NH_2- and COOH-terminal residues (amino acids in positions 1-4 and 9-10) are highly conserved throughout different species [36]. These residues are involved in receptor binding [36]. D-amino acid substitution in position 6 enhances binding affinity at GnRH receptors by stabilising it in a folded conformation (with the receptor-binding domains spatially

near to each another), and reduces metabolism of the peptide [41]. All synthetic GnRH agonists and antagonists have this D-amino acid substitution [36]. The amino acid in position 8 appears to be important for ligand-selectivity and may determine binding affinities for different GnRH receptors [36]. Several GnRH antagonists have substitutions in this position. Antagonists also have D-amino acid substitutions at positions 1-3 and 10, and some have additional substitutions in position 5 (Figure 4).

Low pulsatile doses of GnRH agonists are used effectively to treat hypogonadism (infertility) and delayed puberty [36]. Contrarily, high doses of agonists desensitise the GnRHR to decrease the production of LH and FSH in the pituitary, thus reducing fertility [36]. This chemical castration can be beneficial for some hormone-dependent diseases such as breast cancer.

After activation, a GPCR is usually rapidly desensitised and internalised (through phosphorylation of C-terminal serine and threonine residues by GPCR-kinases and second messenger kinases) [42-44]. However, since the GnRH receptor does not have this C-terminal tail, it is somewhat resistant to this rapid desensitisation [42, 45, 46]. Desensitisation of GnRH receptor signalling therefore requires a high dose of agonist, which causes an unavoidable hyperstimulation before desensitisation [33, 36, 44]. This has clinical implications when used therapeutically: any disease symptoms that are dependent on GnRH signalling are likely to worsen substantially before they regress.

Antagonists also inhibit GnRHR-mediated signalling by competing with endogenous GnRH [33]. However, the required doses of antagonists are much higher than that required for the same effect mediated by receptor desensitisation [33]. Antagonists would be more desirable since they avoid the need for the undesirable hyper-stimulation that must occur for desensitisation [33, 36], but because a much higher dose is required, work is needed to improve this approach before it replaces agonist therapy [36].

Oestrogen is required for the growth of some breast cancers. To induce oestrogen production, GnRH must be released in pulses. GnRH agonists have been used to treat oestrogen-dependent breast cancer by continuously stimulating GnRHR activity in the pituitary [47, 48]. This causes signal inhibition and thereby prevents oestrogen production.

1.2.3.1.1 Triptorelin

Triptorelin is a GnRH agonist that differs from the physiological GnRH-I decapeptide by a single amino acid substitution at position 6 of Gly to D-Trp (Figure 5). Triptorelin is a superagonist [49], and the estimated binding affinity for Triptorelin has an IC_{50} of 0.4nM [50].

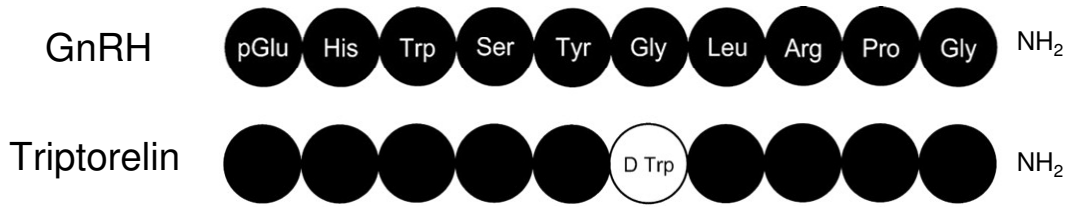

Figure 5: The amino acid structure of Triptorelin.
The synthetic GnRH agonist Triptorelin differs from naturally occurring mammalian GnRH by a single amino acid substitution at position 6 of Gly to D-Trp. This figure is adapted from [36].

Triptorelin is able to bind GnRHR and activate downstream signalling in both pituitary and extrapituitary tissues such as breast and prostate cancer cell lines [25-32, 50, 51].

Triptorelin has most extensively been used and studied for its ability to simulate hypothalamic GnRH in the pituitary. Triptorelin (D-Trp^6-GnRH) has been used to treat prostate cancer since the 1980s [52], and more recently clinical trials have explored its use in other cancers such as breast cancer [53, 54]. Triptorelin is marketed in the UK under the brand names Decapeptyl® (Ipsen) and Gonapeptyl® (Ferring Pharmaceuticals). Triptorelin is currently used to treat patients with prostate cancer, uterine myoma, endometriosis or precocious puberty [55]. These are all hormone-dependent conditions and Triptorelin works by suppressing hormone production. Triptorelin is administered by intramuscular injection every 4-12 weeks

[55]. Most side effects are as a result of the lowered level of oestrogen or testosterone [55]. Although unpleasant, the side effects are generally well-tolerated and less severe than those of other treatments such as cytotoxic therapy [20, 55].

1.2.3.2 Current limitations of GnRH analogues in therapy

The use of GnRH agonists, through the hormone-suppressive mechanism described above, can only be useful in hormone-dependent cancers, thereby failing to deal with a significant proportion of oestrogen receptor (ER)-negative breast cancers. Currently, clinical trial data does not support a role for GnRH agonists in improving breast cancer patient survival [48]. However, GnRH agonists are known to have relatively well-tolerated side-effects compared to other cancer treatments [52].

1.2.4 GnRH has antiproliferative effects in some cancer xenograft models and in some cancer cell lines

It has been demonstrated that some post-menopausal breast cancer sufferers [30], and patients with ER-negative breast cancer [56], responded positively to GnRH agonist therapy. This implied a mechanism of GnRH signalling outwith its role in the pituitary. This new role for GnRH analogues may represent a currently unexploited treatment option for hormone-independent cancers. A direct anti-proliferative action of GnRH agonists and antagonists *in vitro* has now been verified by various groups in an array of reproductive and non-reproductive cancer cells [27, 32, 39, 50, 57-67].

In 1985, Miller *et al* reported major inhibitory effects of the GnRH agonist Buserelin on the MCF7 breast cancer cell line [29]. This effect was blocked by a GnRH antagonist, indicating that the antiproliferative effects arose from interaction between the GnRH agonist and specific receptors [29]. A direct inhibitory effect of GnRH agonists on MCF7 cells was also demonstrated in that year by others such as Blankenstein *et al* [68]. However, Mullen *et al* in 1991 could only show that one out of four clonal variants of MCF7 cells responded to Buserelin [69].

Eidne *et al* confirmed the presence of specific GnRH binding sites in human breast cancers [70]. They showed that these binding sites were predominantly in ductal

breast carcinomas rather than lobular breast carcinomas, and were not observed in normal breast tissue [70]. The authors later confirmed an inhibitory effect of GnRH antagonists in several breast cancer cell lines [28].

In 1988, Sharoni *et al* demonstrated that application of two GnRH antagonists (SB29 and SB30) to MDA-MB-231 cells resulted in up to 40% reduction in [^{3}H]thymidine incorporation [71]. An older antagonist had less effect and the agonist Buserelin had no effect on [^{3}H]thymidine incorporation. Similar results were observed on cell growth: SB29 and 30 inhibited cell number, whereas Buserelin did not [71].

A direct interaction between GnRH and its receptor is supported by the expression of GnRHR in 50-64% of breast cancers [72-75], and the finding that both GnRH-I and GnRH-II are expressed in both normal and malignant breast cells [76]. It has long been speculated that GnRH may act in an autocrine or paracrine manner in breast cancer [28]. GnRH-I and GnRH-II have been reported to be overexpressed at the mRNA level in breast malignant tissue (compared to healthy tissue from the same individual) [76]. Emons, Grundker *et al* in particular have published extensively showing inhibitory effects of GnRH agonists and antagonists in ovarian, endometrial and breast cancer cell lines [60-67].

More recently, Saleh-Abady *et al* observed that Triptorelin inhibited SKBR3 and T47D cells *in vitro* [77] and Grundker *et al* showed that the GnRH-II antagonist [Ac-D2Nal^{1}, D-4Cpa^{2}, D-3Pal^{3,6}, Leu^{8}, D-Ala^{10}]GnRH-II induced apoptosis in MCF7 and MDA-MB-231 cells *in vitro* and slowed growth of xenografts derived from these cell lines *in vivo* [78]. However, the antiproliferative effect of the GnRH-II antagonist persisted after GnRHR was knocked down, making it unclear how GnRH-II is mediating its effects [78]. Schubert *et al* recently demonstrated that agonists and antagonists of GnRH-I (Triptorelin and Cetrorelix) and GnRH-II (developed in-house by the authors) reduced metastasis formation in MDA-MB-453 and MDA-MB-231 cells *in vivo* [25].

Although clinical trial data does not currently support a role for GnRH agonists or antagonists in the treatment of breast cancer [48], the details above indicate that GnRH analogues have antiproliferative effects in some breast cancer cell lines and with further research, GnRH signalling may represent a currently unexploited target for breast cancer treatment.

1.2.5 Problems to overcome for the direct antiproliferative effect of GnRH analogues to become a viable treatment option

Only a subset of breast cancers are thought to be responsive to the direct action of GnRH analogue treatment, and it is necessary to identify the factors involved in GnRH signalling in this context to improve prediction and efficacy of response to target the therapy appropriately.

There has been difficulty in reproducing the antiproliferative effects of GnRH agonists in breast cancer cell lines between research groups. For example, in a range of reproductive cancer cell lines (ovary, endometrium, breast), it was found that high doses are required to elicit only modest antiproliferative effects [42]. There is a need to establish which factors are required for the response. Through increased understanding of the signalling mechanism, the antiproliferative effect of GnRH may be enhanced, for example in combination with other therapies.

Although there are similarities between breast and other reproductive cancers, there may be crucial differences between the mechanisms of GnRHR signalling in these tissues. However, it is likely that at least some features of GnRH signalling will be common across a variety of tissues, so information from studies on a range of cell lines is considered to be relevant.

1.2.6 Factors determining the antiproliferative response to GnRH

Possible factors determining an antiproliferative response to GnRH:

1. Level of receptor
2. Ligand subtype
3. G-protein alpha subunit type
4. Extracellular signal-regulated kinase activation
5. Other signalling factors

These are discussed in more detail below.

1.2.6.1 Levels of GnRHR protein

A high level of functional GnRHR (GnRH-I-R) at the cell surface appears to be essential for the antiproliferative effects of GnRH agonists [79]. The extent of the inhibitory effects of a GnRH agonist on a given cell line appears to be proportional to the level of functional GnRHR in that cell line [79, 80]. The authors of that study found that a panel of several breast cancer cell lines had levels of GnRHR undetectable by radioligand binding assay [80]. This may explain why a GnRH agonist did not inhibit proliferation in these cells.

The level of GnRHR protein expression in breast cancer and its association with other features of breast cancer is not well defined. There is a need to define the expression of GnRHR in primary breast tumours in order to establish the target population for this application of GnRH agonists.

1.2.6.2 Ligand

1.2.6.2.1 GnRH-I vs. GnRH-II

GnRH-I and GnRH-II have been found to have inverse potency ratios with respect to how well they mediate the classical GnRH-I-R signalling in the pituitary via inositol phosphate accumulation, and the alternative direct antiproliferative effects [81].

GnRH-II has been found to be most potent at causing a direct antiproliferative effect [81].

1.2.6.2.2 Analogues

From various models built in attempts to explain the binding of ligand to the GnRH receptor, it appears that the receptors are in a state of equilibrium between the inactive and active conformations [34]. Agonists shift the balance towards the active state, whereas inverse agonists shift it the other way [34]. Inverse agonists can inhibit agonist-independent receptor activity [34]. Because inverse agonists bind to both conformations, they compete with agonist for binding to the active receptor [34].

1.2.6.2.3 Ligand-induced selective signalling

The term Ligand-induced Selective Signalling has been used to suggest how different ligands may bind the GnRHR to induce differential intracellular responses (Figure 6) [36]. It is thought that different active receptor states may exist and a particular ligand binds a particular receptor state [36]. A signalling complex is formed that then stabilises this receptor conformation. Different ligands may cause the receptor to bind to different G-proteins to induce differential downstream effects [36]. This is ligand-selective signalling, because the signalling pathway is determined by the ligand.

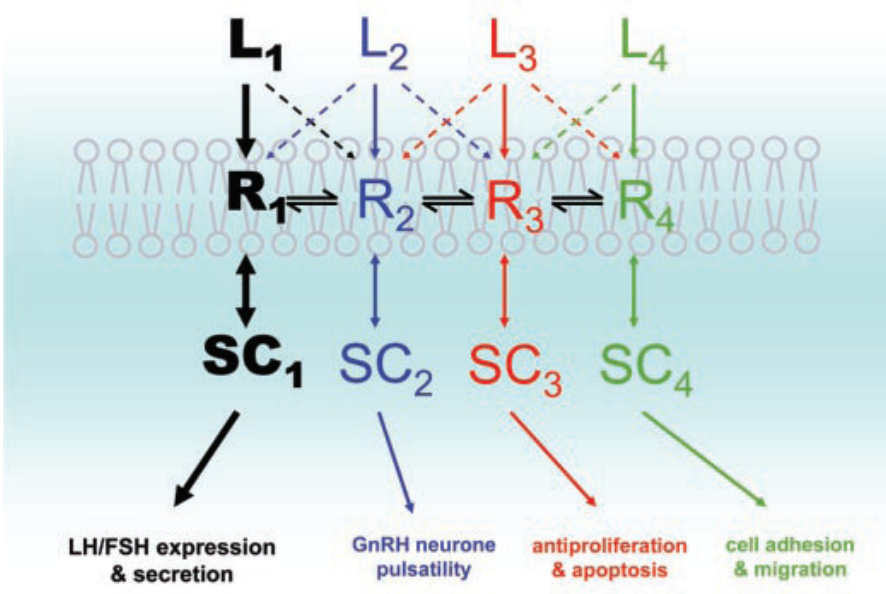

Figure 6: Ligand-induced Selective Signalling.
L = Ligand, R = Receptor state, SC = Signalling Complex. This figure is taken from [82].

1.2.6.3 Receptor G-protein coupling

G-proteins are composed of three subunits: α, β and γ. When an agonist binds the GPCR, GDP is converted to GTP on the α subunit of the G-protein (Gα). Gα dissociates from the remaining subunits (Gβγ) and activates downstream effector molecules to mediate a functional outcome. Gα has intrinsic GTPase activity, which deactivates the signal by hydrolysing Gα-GTP to Gα-GDP, which re-associates with Gβγ [34] (Figure 7).

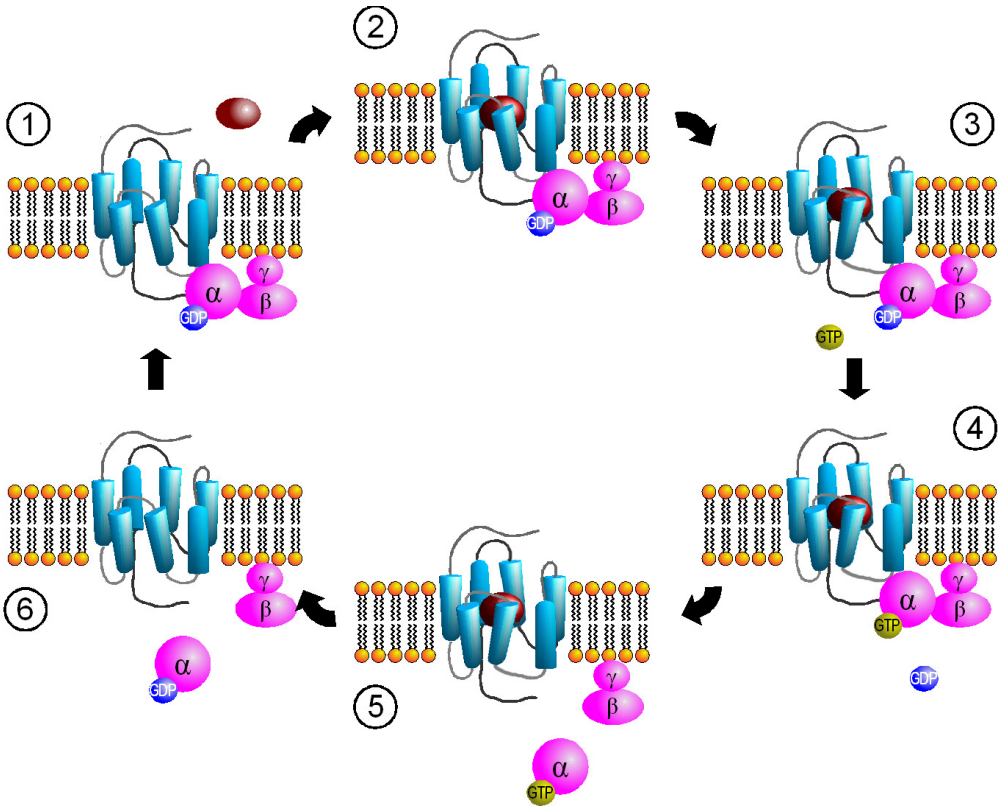

Figure 7: Activation of the Gα protein subunit after a ligand binds to the GPCR.
This figure is provided by the author Sven Jähnichen (24 April 2006) [83] and permission for reproduction of the figure was granted under the terms of the GNU Free Documentation Licence.

When a ligand binds to it, the GnRHR couples to a Gα-protein on the intracellular side of the plasma membrane to form a signalling complex. Gα subunits can be divided into four families with varying functions such as activation of PLC and adenylyl cyclase (Table 2) [34]. The Gβγ complex can also regulate downstream effectors such as PLC-β, K^+ channels, adenylyl cyclase and PI3K [84, 85].

G-protein family	Function
$G\alpha_{q/11}$	activates PLC
$G\alpha_{s}$	activates adenylyl cyclase
$G\alpha_{i/o}$	inhibits adenylyl cyclase
$G\alpha_{12/13}$	activates small GTPases

Table 2: Functions of the four families of Gα subunits.

GnRHR couples to different G-proteins depending on cell type and ligand stimulation. In some cells it can couple to multiple G-proteins [34]. For example, in GT1-7 neurons it has been shown that under a high GnRH agonist concentration the

receptor couples to $G\alpha_i$, whereas with low GnRH agonist concentration the receptor couples to $G\alpha_s$ [34].

The $G\alpha_q$ subunit is known to mediate GnRHR signalling in the pituitary [86]. The G-protein subunit to which GnRHR couples has been suggested to determine the functional outcome [81]. There is some evidence to suggest that $G\alpha_i$ mediates the antiproliferative effect of GnRH agonists [59, 66, 87]. However, more recently, White *et al* found that in mouse embryonic fibroblasts (MEF) and stably GnRHR-transfected Human Embryonic Kidney-293 (Stable Cell Line number 60, SCL60) cells, only $G\alpha_q$, and not $G\alpha_i$ nor $G\alpha_s$ coupled to the GnRHR [88]. The authors suggest that RTK transactivation may explain previous reports that have suggested receptor coupling to $G\alpha_{i/o}$ [88]. This is in light of the recent suggestion that growth factor RTKs can directly activate Gα subunits (Delcourt *et al*, 2007, as cited in [88]).

1.2.6.4 Extracellular signal-regulated kinases (ERK1/2)

A perturbation of phosphorylated ERK1/2 occurs in a number of cell lines following GnRH agonist treatment [79]. Although the nature of this change is not the same in all cell lines, it is thought to be important in mediating the antiproliferative effects of GnRH agonists [79]. Figure 8 outlines how GnRH is thought to signal through the GnRH receptor to ERK1/2.

It is not clear how this change in the level of ERK1/2 activity contributes to cell fate, but it has been noted that the timing, duration and intensity of ERK1/2 activation are all important in determining cellular outcome [89]. Although ERK1/2 activation often drives proliferation, ERK1/2 activation has been associated with cell-death in many different cell types (reviewed in [89-91]). DNA-damage-induced ERK1/2 activation causes cell cycle arrest, although the details of the mechanism are not yet clear (reviewed in [91]). EGFR-mediated activation of MAPK has been shown to cause G2 arrest [92]. Intracellular localisation of ERK1/2 may be relevant to its role in determining cellular fate (reviewed in [93]).

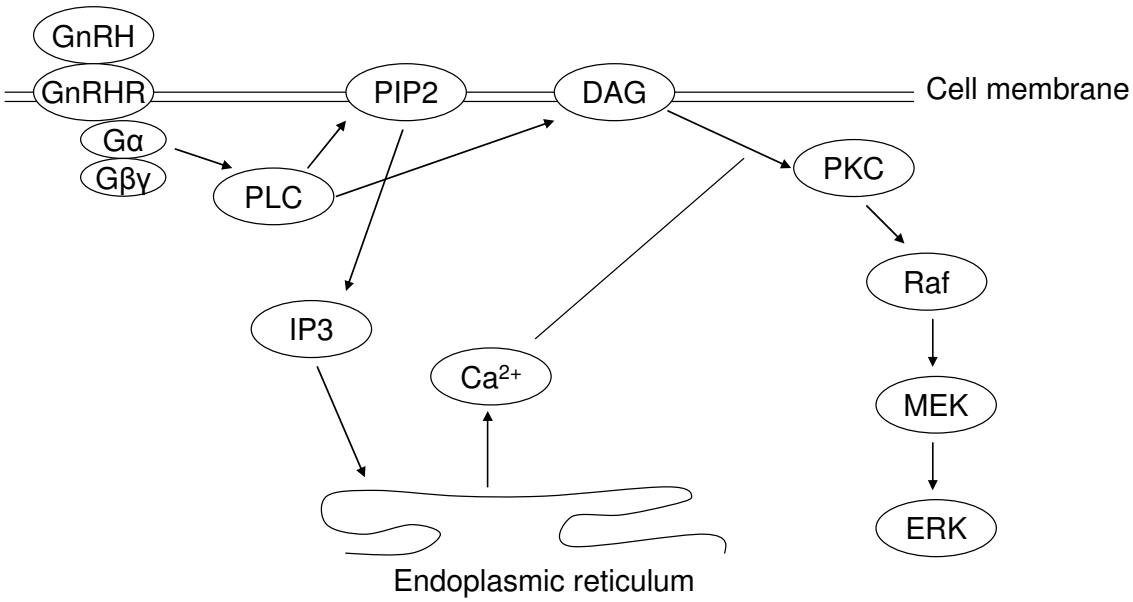

Figure 8: GnRH receptor signalling to ERK1/2

Figure 8 outlines how GnRH (or a GnRH analogue) is thought to signal through the GnRH receptor to ERK1/2. GnRHR can signal through $G\alpha_{q/11}$ to stimulate PLCβ in a Ca^{2+} independent manner. This induces further PLCβ activation via a Ca^{2+}-dependent mechanism. Activation of PLCβ cleaves PIP_2 to produce IP_3. IP_3 activates calcium channels in the endoplasmic reticulum to release Ca^{2+}. In association with DAG, Ca^{2+} activates PKC [34]. Once active, PKC phosphorylates Raf which in turn activates MEK and downstream ERK1/2 [34].

1.2.6.5 Other signalling factors implicated in GnRHR signalling

Several of the putative GnRH receptor signalling pathway members shown in Figure 8 have been investigated prior to this study. Morgan *et al* used a panel of inhibitors in two GnRH agonist-sensitive cell lines, B35-2 (rat neuronal cells expressing a high level of GnRHR) and SCL60 (HEK293 cells expressing a high level of GnRHR) to determine which of these suggested pathway members are required for the antiproliferative effect of GnRH [79]

As well as the ERK1/2 pathway, the JNK and p38 MAPK pathways have been implicated in mediating the antiproliferative effects of GnRH [34]. JNK and p38 MAPKs are activated by stress [94]. They affect a wide range of cellular processes

and, similarly to ERK1/2, their effect on cell fate is complex and they can both promote and inhibit cell survival and proliferation [94]. White *et al* sought to clarify which of these is required for the antiproliferative effects: JNK and p38 inhibitors were unable to rescue mouse embryonic fibroblast (MEF) cells from the growth-inhibitory effect of GnRH whereas ERK inhibitors successfully restored the growth of the cells to ~90% that of controls [88]. Morgan *et al* found that a p38 inhibitor had no effect in either SCL60 or B35-2 cells [79]. Interestingly, the authors were unable to show that MEK was essential in mediating the direct antiproliferative effect of a GnRH agonist: A MEK inhibitor (18μM PD98059) had no effect on B35-2 cells and only partially rescued SCL60 cells (8%), which was not statistically significant [79].

A PKC inhibitor which inhibits PKCα and possibly other isoforms (100nM Ro 32-0432) was able to completely rescue SCL60 cells from the antiproliferative effect of a GnRH agonist [79]. However, a specific PKCδ inhibitor (0.5μM Rottlerin) did not alter the effect of GnRH treatment [79], suggesting that whilst PKC is an essential factor in signalling the GnRH-mediated antiproliferative effect, the PKCδ isoform is not.

Despite the lack of effect of the MEK inhibitor, the crucial role of PKC and the profound change in pERK1/2 levels in SCL60 cells following GnRHR stimulation makes it difficult to discount the MEK-ERK pathway. Neither of the PKC inhibitors, nor the MEK inhibitor, had any effect on B35-2 cell number following treatment with the GnRH agonist Triptorelin [79]. Only the caspase inhibitor partially rescued B35-2 cells from Triptorelin treatment [79]. This occurred to the same extent as in SCL60 cells (40%) [79]. This suggests that the GnRH receptor may mediate its antiproliferative effect by distinct mechanisms in different cell lines, although caspase-mediated cell death appears to be involved in both cases in at least a proportion of cells.

Neither a FasL antagonist nor ceramide synthesis blockage affected the response of either cell line to a GnRH agonist [79]. This indicated that cell death was unlikely to be occurring through the Fas death receptor in these cell lines.

An IP_3 Ca^{2+} channel blocker had no effect in either of the cell lines, whereas a Ca^{2+} chelator had an additive effect in both cell lines [79]. It has been presumed that intracellular Ca^{2+} elevation is involved in GnRHR antiproliferative signalling, but these results do not support this.

cAMP is usually activated by $G\alpha_s$ and inhibited by $G\alpha_i$ [34]. Since $G\alpha_i$ has been thought to be responsible for the direct antiproliferative effect of GnRH agonists, exogenous cAMP was expected to reduce this effect. However, exogenous 8-Br-cAMP added to the antiproliferative effect of the GnRH agonist Triptorelin in SCL60s [79]. This was also observed in B35-2 cells (rat neuronal cells expressing high GnRHR) [79]. This may suggest that endogenous and exogenous cAMP do not influence the cell in the same way [79].

1.2.6.5.1 Crosstalk with Receptor Tyrosine Kinases

The antiproliferative effects of GnRH agonists and antagonists are thought to be at least partly mediated by antagonism of growth factors, such as epidermal growth factor (EGF) and insulin-like growth factor (IGF) [95], but the level of involvement and its precise role is unclear. They may also involve ligand-regulated transcription factors such as oestrogen receptors alpha and beta (ERα, ERβ). These may be activated by signalling molecules downstream of growth factor receptors such as PI3K and ERK1/2, and this can occur in the absence of oestrogen [96].

Growth factor receptors belong to the receptor tyrosine kinase (RTK) family. Of the 90 members of this family, 58 are receptors, which can be divided into 20 subfamilies based on their structural similarities [97]. RTKs have a single transmembrane domain, with an intracellular tyrosine kinase domain. The kinase region is composed of a particular combination of conserved elements that is distinct

to each RTK subfamily [98]. RTK ligand binding induces a conformational change that allows receptors to dimerise. Dimerisation increases the kinase activity of the receptor, and autophosphorylation of specific tyrosine residues allows proteins with Src homology 2 (SH2), and phosphotyrosine binding domains to bind [98]. These recruit Src, PLCγ, or other adaptor proteins to activate further downstream signalling. For example, the SHC-Grb2-Sos complex and Ras link RTKs to the ERK/MAPK pathway to promote proliferation [98].

There is some evidence to implicate growth factor receptor signalling in mediating the antiproliferative effect of GnRH analogues. The GnRH agonist Buserelin inhibited proliferation of MCF7 cells, but this was prevented by addition of insulin or EGF [99]. This suggests that GnRH may exert its antiproliferative effect by antagonising growth factor signalling [99]. The GnRH-I analogue Triptorelin, and the GnRH-II analogue [D-Lys^6]GnRH-II, both superagonists, have been shown to have an antiproliferative effect on the human breast cancer cell lines MCF7 and T47D [95]. The authors demonstrated that these agonists inhibited EGF-induced autophosphorylation of EGFR and inhibited MAPK and ERK1/2 activity [95]. A similar antiproliferative effect of Triptorelin has been shown in ovarian and endometrial cell lines, in which the effect was mediated by $G\alpha_i$-induced activation of phosphotyrosine phosphatase, which then inhibited the EGF-induced autophosphorylation of EGFR [66]. Reduced EGFR signalling inhibited ERK1/2 activation of c-fos and oestrogen responsive elements, thereby reducing cell proliferation [66]. However, other studies have shown that in some cell lines ERK1/2 activation is (at least initially) increased following GnRHR stimulation, and this is thought to be important in mediating the antiproliferative effect of GnRH agonists and antagonists [79]. As described above, the relationship between ERK1/2 activity and cell fate is complex, and it is possible that activation of ERK1/2 may also lead to reduced cell proliferation or cell death. The mechanism by which GnRH analogues may exert their antiproliferative effects through signalling to ERK1/2 is not yet clear. G-protein coupled receptors (GPCR) have been shown to be able to transactivate RTKs such as EGFR by inducing cleavage of EGF-like growth factor pre-cursor via matrix metalloprotease activation [98]. It is possible that GnRHR may be able to

transactivate EGFR or another growth factor receptor in this way. Together, these data suggest that there may be a role for growth factor receptor signalling in the response to GnRH analogues.

1.2.6.5.2 NFκB and the survival or suicide decision

Activation of NFκB, mediated through $G\alpha_i$, has been shown to occur in Triptorelin-treated ovarian cancer cell lines, EFO-21 and EFO-27, to inhibit apoptosis [42, 65]. GnRH has also been shown to stimulate the rapid phosphorylation of NFκB-p65 in LβT2 cells [100]. This may represent another pathway that may be involved in mediating the antiproliferative effect of a GnRH agonist. However, this has not been explored in any depth in these or other models.

The NFκB family consists of five members: RelA/p65, c-Rel, RelB, NFκB1 (p50) and NFκB2 (p52) [101]. These are transcription factors that activate a wide range of genes [101]. NFκB signalling plays a particularly important role in the inflammatory pathway, and is often constitutively active in cancers [101]. NFκB is usually held inactive in the cytoplasm by inhibitors of NFκB (IκB proteins): IκBα, IκBβ, IκBε, and IκBζ. p50 and p52, and their full length counterparts p105 and p100 also act as IκB proteins [101]. The main inactive form of NFκB is a trimer consisting of the p50 and p65 subunits and IκBα [101]. This is held inactive in the cytoplasm until phosphorylated by an IκB kinase (IKK). Often in response to an inflammatory stimulus, such as TNFα, IκBα kinase (IKKα) phosphorylates IκBα, which targets it for ubiquitination and degradation by the proteasome [101, 102]. The degradation of IκBα releases p50-p65 (which is also phosphorylated by IκBα) to translocate to the nucleus where it activates transcription [101, 102]. The p65 subunit undergoes further modifications by acetylation and methylation at the site of the NFκB-responsive promoters and the function of p65 is further enhanced by interaction with transcriptional coactivators [101]. This is known as the classical pathway of NFκB activation, and usually confers cell survival (reviewed in [102] and [103]).

An alternative pathway of NFκB activation relates to another inactive form of NFκB: a dimer of the p52 precursor p100 and RelB [101, 102]. In response to an external

stimulus, such as B-cell activating factor (BAFF), p100 is phosphorylated by IKKα and is processed to p52 to form the p52-RelB complex [101, 102].

Other pathways of NFκB activation have been reported in response to cellular stressors such as DNA damage, oxidative stress, heat shock, and cell cycle disruption [102]. These pathways may involve IKK other than IKKα; however, some IKK-independent pathways of NFκB activation have also been reported, although these are uncommon and less well-described than the classical and alternative pathways mentioned above.

1.3 Previous approaches to study GnRHR signalling

1.3.1 Mouse Embryonic Gonadotrope Tumour Cell Lines

Previous approaches to examine GnRH signalling have generally focused on the target cells of GnRH in its normal physiological role, which include the gonadotropes of the anterior pituitary gland. LβT2 cells are mouse embryo pituitary gonadotrope tumour cells that have been used to study the mechanism of GnRH in the pituitary. LβT2 cells have been shown to express both LHβ and FSHβ genes, as well as GnRHR. αT3-1 is another pituitary gonadotrope cell line that has been used to study GnRHR signalling [104-106]. This cell line is less widely used than the LβT2 cell model. The GnRHR signalling network in LβT2 pituitary cells has been well-described, and the resulting data has recently been collated into an online resource by Fink *et al* (see [107]).

To explore the effect of a GnRH agonist on gene transcription in the pituitary, Kakar *et al* performed gene expression analysis on mouse pituitary gonadotrope tumour (LβT2) cells to examine the transcriptional changes resulting from GnRH agonist treatment [108]. The authors of that study reported a list of 68 genes whose expression was altered following treatment with the GnRH agonist des-gly^{10},[D-Ala^{6}]GnRH. Although the study only considered two time-points, it showed marked differences of GnRH agonist-regulated gene profiles at 1h and 24h after treatment with the GnRH agonist des-gly^{10},[D-Ala^{6}]GnRH [108]. Genes that were changed in

expression encoded proteins including transcription factors, ion channel proteins, cytoskeletal proteins, and other signalling proteins such as those involved in proliferation and apoptosis [108]. This was the first microarray analysis of GnRH agonist-regulated gene expression and provides a useful resource for comparisons between the response to GnRH agonist treatment in pituitary-derived cells (which may be similar signalling to the normal physiological role of GnRH) and the antiproliferative response to GnRH agonist in extrapituitary tissue-derived cells.

An earlier study by Wurmbach *et al* also examined gene expression changes as a result of GnRHR activation in LβT2 cells [109]. This study used focussed microarray analysis, in which 956 cDNAs were carefully selected for measurement. The authors showed differential expression of genes including many transcription factors, as well as other proteins involved in cell signalling, cytoskeletal regulation and channel regulators [109]. This shares similarities with the Kakar *et al* study, which supports several of the gene expression changes observed at 1h after GnRHR stimulation, such as Egr1, Nr4a1 and Rgs2. However, the data presented in this study is limited, largely by the constraints of technology at the time, and the Kakar *et al* study provides a more thorough, less biased approach to the gene expression analysis.

1.3.2 SCL60 model

The direct antiproliferative effect of GnRH agonists and antagonists in extrapituitary tissues has been demonstrated in several cancer cell lines, but has not been explored in depth in these cells and there have been difficulties in reproducing the antiproliferative response in some of these cell lines between research groups. To investigate the direct antiproliferative effect of GnRH signalling, the SCL60 model has been developed.

SCL60 is a Human Embryonic Kidney-293 (HEK293) cell line that has been stably transfected with rat GnRHR cDNA. The HEK293 cell line is derived from human embryonic kidney epithelial cells, transformed by adenovirus E1a [110]. It is poorly adherent and is tumourigenic in nude mice. Radioligand binding assays have

confirmed that SCL60 cells express high levels of functional GnRHR (similar levels to LβT2 cells) at the cell surface [79]. Rat GnRHR is used because rat GnRHR is more efficiently trafficked to the plasma membrane than human GnRHR, so facilitates a higher level of GnRHR protein expression at the cell membrane. The SCL215 model is a HEK293 cell line that has been stably transfected with a modified form of human GnRHR, which is inactivated by the fusion of a catfish GnRHR cytoplasmic tail domain [111]. The fusion protein binds GnRH but does not signal effectively in terms of inositol phosphate production [111]. SCL60 cells *in vitro* and SCL60-derived xenograft tumours treated with the GnRH agonist Triptorelin showed significantly reduced growth compared to those treated with a vehicle control [79, 112] at days 7 (P=0.0002), 10 (P=0.0005) and 14 (P=0.0005) after treatment (Figure 9). Growth of HEK293- and SCL215-derived xenografts was not inhibited by Triptorelin (Figure 9, [79]).

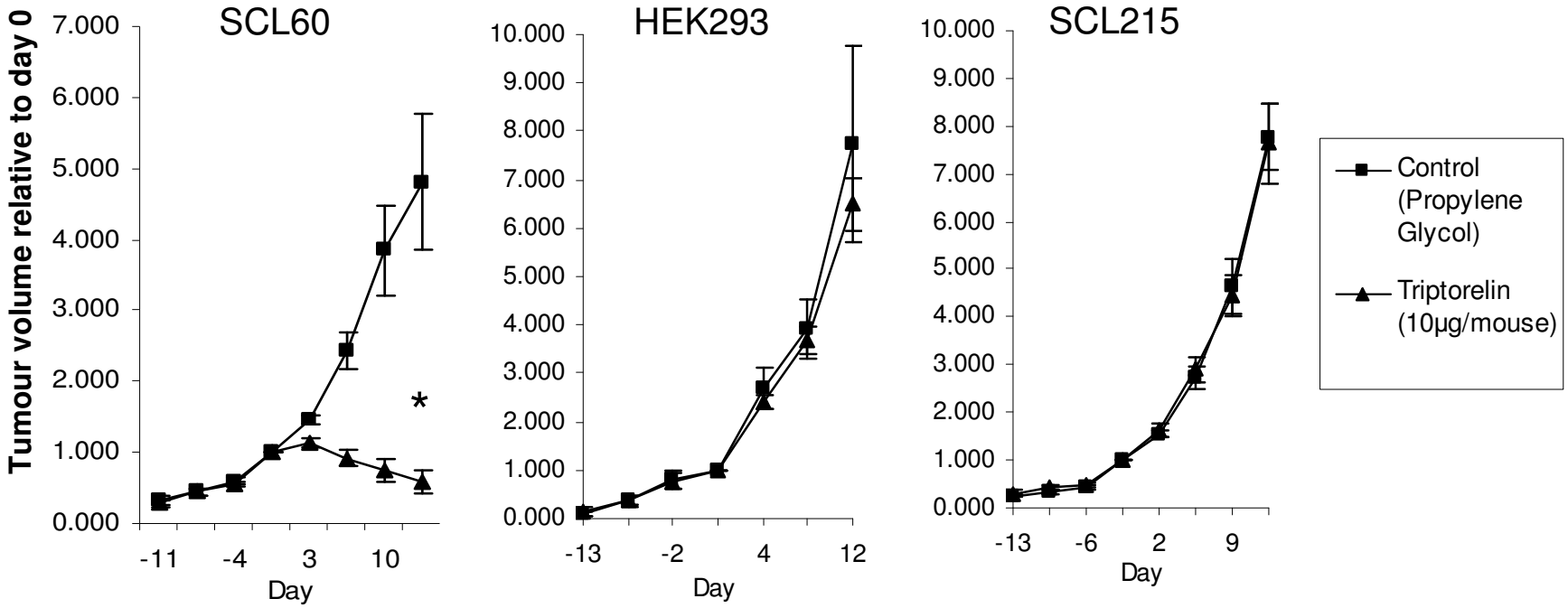

Figure 9: Growth of SCL60-, HEK293- and SCL215-derived xenografts treated with Triptorelin (10µg/mouse) for up to 14 days.
The graphs show the tumour volume relative to the tumour volume at day 0, when treatment was initiated. Error bars show +/- standard error of the mean. The data in this figure is published in Morgan *et al*, 2008 Cancer Research. * indicates a significant difference (P<0.05, 2-sample t-test) between control and Triptorelin xenografts at days 7 (P=0.0002), 10 (P=0.0005) and 14 (P=0.0005).

Miles *et al* treated SCL60 cells with the GnRH agonist Triptorelin and observed a very small but significant increase in the percentage of apoptotic cells by flow cytometry, although this could not account for the large decrease in cell number [112]. They also observed G_2/M arrest in the cell cycle [112]. A caspase inhibitor partially rescued SCL60 cells from Triptorelin treatment [79], indicating that the GnRH receptor may mediate its antiproliferative effect at least in part by apoptosis.

The cell cycle consists of four phases: Mitosis (M phase), Gap 1 (G1 phase), DNA synthesis (S phase), and Gap 2 (G2 phase). These phases vary in duration: typically G2 lasts approximately 4h, S phase 6, G1 phase approximately 10h, and mitosis lasts only 1-2h [113, 114]. There are checkpoints throughout the cell cycle that prevent the inappropriate replication of cells and these checkpoints are controlled by complexes of cylins and cyclin-dependent kinases [114, 115]. Cyclin D and CDK4 and 6 control progression from G1 to S phase; Cyclin E, A and CDK2 are responsible for the initiation of DNA synthesis in S phase; and the transition from G2 to M phase is controlled by Cyclin B and CDK1 [114, 115]. GnRHR signalling may disrupt the cell cycle for example at S phase by disrupting DNA replication, or at M phase by disrupting spindle assembly and/or alterating of the dynamics of chromosome segregation.

As mentioned previously (on page 38), White *et al* found that in SCL60 cells, only $G\alpha_q$, and not $G\alpha_i$ nor $G\alpha_s$ coupled to the GnRHR [88]. As described on page 37, Morgan *et al* demonstrated that despite an intense transient activation of pERK1/2 observed following Triptorelin treatment, a MEK inhibitor only partially rescued SCL60 cells (8%), which was not statistically significant [79]. PKC appears to be an essential factor in signalling the GnRHR-mediated antiproliferative effect, although not the PKCδ isoform [79]. Neither a FasL antagonist nor ceramide synthesis blockage affected the response of either cell line to a GnRH agonist [79]. This indicated that cell death was unlikely to be occurring through the Fas death receptor in these cell lines. An IP_3 Ca^{2+} channel blocker had no effect in either of the cell lines, whereas a Ca^{2+} chelator had an additive effect in both cell lines [79]. It has

been presumed that intracellular Ca^{2+} elevation is involved in GnRHR signalling, but these results do not support this.

GnRH has been shown to lead to activation of lipid-directed kinases such as diacylglycerol kinase (DGK)-ζ [116]. Increased DGK-ζ reduced the time scale of ERK1/2 activation [116]. DGKs phosphorylate diacylglycerol (DAG), therefore this may reflect feedback metabolism of DAG generated by Gαq-PLC activation. As discussed earlier, the length of ERK1/2 activation could be important in determining the functional outcome of this signalling [89].

GnRHR signalling may induce downstream signalling of the stress-activated protein kinases JNK and p38 [34]. These proteins have been shown to play a role in cell cycle arrest and apoptosis [94]. However, like ERK1/2, they can both promote and inhibit proliferation, and it is the duration and intensity of their activation that is crucial in determining the functional outcome [94].

In SCL60 cells, GnRHR stimulation by GnRH-I, GnRH-II, and other agonists (but not antagonists) caused an increase in cell adherence and change in morphology [117]. This was dependent on Tyr-kinases and Src but not EGFR or JNK [117]. This indicated that GnRH agonists can cause cytoskeletal reorganisation and affect cell adherence. Inappropriate cytoskeletal changes could play a role in GnRHR-mediated cell death or reduced proliferation. Progression through the cell cycle, particularly mitosis, is dependent on carefully controlled cell adhesion. If cell adhesion is altered inappropriately, via signalling to adhesion molecules, the cell cycle may be halted.

GnRHR signalling may lead to cell cycle arrest or apoptosis via changes at the transcriptional level. Inappropriate gene expression may result directly from GnRHR-mediated signalling, or as a consequence of cellular stress and the activation of p38 and JNK signalling. For example, altered transcription of one or more CDK or cyclins could lead to cell cycle arrest. Many diverse signalling factors interact with the cell cycle and apoptotic machinery within the cell and aberrant transcription of any of these could impact on cell survival and proliferation.

1.3.3 Other cell line models

Other reproductive cancer cell lines have been used to study GnRHR signalling, such as EFO-21 and EFO-27 ovarian cancer cell lines [65, 66, 118], breast cancer cell lines including MCF-7 [31, 68, 69, 99, 119] and MDA-MB-231 [78, 120], and Ishikawa and Hec-1A endometrial cancer cell lines [66, 118]. Several GnRHR-transfected cell lines have also been studied previously, such as the kidney-derived cells Cos-1 [45], the breast cancer cell line MCF-7 (transient transduction) [27, 121], and the stably transfected prostate-derived WPE-1-NB26 cells [50].

1.4 Aims of the current study

1. To identify signalling factors that may be involved in mediating the antiproliferative effect of a GnRH agonist using a cell line model both *in vitro* and *in vivo*, and at both the transcriptomic and proteomic level.
2. To identify the extent of GnRHR expression in breast tumours and cell lines.
3. To develop a model to study GnRHR signalling in breast cancer.

These aims will contribute to the long-term objective to identify drug treatments that can exploit the GnRH receptor anti-proliferative pathway as a feasible cancer treatment.

1.5 Approach

As discussed above, the mechanism by which GnRHR activation causes a direct antiproliferative effect in various cell lines is not clear. There is some evidence to indicate the involvement of MAPK activity, and possibly cross-talk with RTKs, but the details remain poorly defined. A global data-driven approach was taken to identify candidate molecules that might be involved in mediating this effect. This approach focussed on the high GnRHR-expressing cell line SCL60.

Section 3.1 is devoted to the molecular characterisation of the SCL60 cell line model. This cell line model was used to investigate the antiproliferative effect of the GnRH

agonist Triptorelin. The SCL60 cell line has previously been established as a model in which to study GnRHR-mediated antiproliferative signalling [79, 104, 112, 122], but this was the first attempt to comprehensively examine GnRHR signalling using a data-driven transcriptomic and proteomic approach, both *in vitro* and *in vivo*. In section 3.1 the SCL60 cell line is compared to HEK293 (untransfected) and SCL215 cells to confirm their response to GnRHR stimulation and to explore the mechanism by which this may occur. Sulphorhodamine Blue (SRB) assays were used to observe the effect of Triptorelin on SCL60, SCL215 and HEK293 cell number; flow cytometry was used to assess changes to the cell cycle as a result of Triptorelin treatment; and immunohistochemistry was used to observe changes in markers of apoptosis and proliferation in SCL60 xenografts following Triptorelin treatment.

To allow focus, only the GnRH agonist Triptorelin was used because it is one of the most potent agonists with demonstrated *in vivo* antiproliferation activity [79]. Effects on cell behaviour following treatment with Triptorelin were compared relative to vehicle alone (0.02% propylene glycol solution), which did not appear to have any effect, suggesting that the observations were caused directly or indirectly by GnRHR activation only.

The SCL60 and HEK293 cell lines provide a useful model to study GnRHR signalling because the SCL60 cells express high levels of GnRHR whereas the HEK293 cells do not express detectable levels of GnRHR. This model was used to identify novel GnRH agonist-driven signalling processes. GnRHR signalling was explored at the transcriptomic level (section 3.2), before focusing on the proteomic level (section 3.3).

GnRHR-induced cell cycle arrest and/or apoptosis could result from altered gene expression. For example, increased transcription and synthesis of pro-apoptotic factors or altered levels of cell cycle regulators. Events during the cell cycle require carefully regulated changes to the cytoskeleton. Dysregulated signalling to the cytoskeleton could result in cell cycle arrest. Concurrently, GnRH agonist-induced stress may activate cell survival responses. For example de novo synthesis of heat

shock proteins, which prevent cell damage by playing a role in refolding proteins [123]; inhibition of pro-apoptotic factors, and increased synthesis of the survival protein Akt, could all contribute to the cell survival response. The balance of the damaging events and the cell survival processes in response to GnRHR stimulation determine cell fate. It was therefore interesting to explore the role of de novo gene transcription and protein synthesis following GnRHR stimulation in SCL60 cells. The time course of events following GnRHR stimulation is not understood, so a time-series approach was beneficial.

To investigate signalling that is relevant to the antiproliferative effect of GnRH agonists in SCL60 cells, it was interesting to explore the gene expression changes resulting from GnRHR expression (by comparing HEK293 and SCL60 cells, section 3.2), and the gene expression changes in response to GnRH agonist treatment in SCL60 cells *in vitro* (section 3.2). These data were generated by conducting a time series gene expression study to provide an unbiased, data-driven approach to identifying candidates for further investigation. A time-series study allowed the observation of dynamic gene expression changes over the treatment period. Similar studies have been conducted by Kakar *et al* and Wurmbach *et al*, but these focused on the pituitary cell line LβT2 [108, 109]. Kakar *et al* showed that most of the genes that were increased in response to GnRH agonist treatment at 1h had returned to basal levels by 24h [108]. Because they used only two time points, it was not clear how long these genes were increased for before returning to basal levels. It was therefore considered useful to expand the time-course design of the Kakar *et al* study to include more time points, as it is clear from their data that the response to GnRH is dynamic between 0 and 24h [108]. The time series gene expression study in this thesis covered six time points from 0 to 24h after Triptorelin treatment to further understand the dynamic response to GnRHR stimulation.

Phosphoproteomic antibody arrays were used to examine protein expression in SCL60 xenografts *in vivo* in response to GnRHR stimulation and immunohistochemistry was used to validate any protein changes identified (section 3.3.1). From the results of the phosphoproteomic array, and from existing literature, a

list of candidates was populated to be explored by reverse phase protein array *in vitro*. This was used as a broad screening tool to identify candidates worthy of further investigation. These results are shown in section 3.3.2. The expression profiles of selected protein candidates were then validated by western blotting (section 0).

The level of GnRHR expression in breast cancer and its association with other features of breast cancer is not well defined. There was a need to define the expression of GnRHR in primary breast tumours to establish the target population for this application of GnRH agonists. GnRHR expression was measured in primary breast cancer by quantitative immunofluorescence and association of GnRHR expression with key markers of breast cancer subtypes such as ER or HER2 expression was explored using pre-existing information about their expression in these tumours. It was anticipated that this may help to identify a subgroup of breast cancers that might be most likely to respond to GnRH agonist therapy. These results are shown in section 3.5.

To investigate GnRHR signalling in breast cancer, a model of GnRHR signalling in breast cancer was required. A suitable model was sought by screening a panel of cell lines for GnRH agonist (Triptorelin) responsiveness, and by transfecting a breast cancer cell line to stably express a high level of GnRHR at the cell surface. It was anticipated that if a suitable model can be identified or created, the GnRHR signalling pathway could be studied at greater depth in this breast cancer cell line model in the same way as for the SCL60 cell line (section 3.6). Use of targeted inhibitors could then help identify the involvement of growth factor driven pathways and their impact on GnRHR signalling.

Chapter 2: Materials and Methods

2 Materials and Methods

2.1 Materials and sources

2.1.1 Cell Culture

Material	Source
DMEM with Phenol Red and Glutamine	Invitrogen, Paisley, UK
Trypsin-EDTA	Invitrogen, Paisley, UK
Foetal Calf Serum	Harlan Seralab, AbD Serotec, Kidlington, Oxford, UK
G418 (Geneticin)	Invitrogen, Paisley, UK
Hygromycin	Sigma Aldrich, Poole, Dorset, UK
PBS	Oxoid, Basingstoke, UK
Penicillin-Streptomycin	Invitrogen, Paisley, UK

2.1.2 SRB Assays

Material	Source
TCA	Sigma Aldrich, Poole, Dorset, UK
SRB dye	Sigma Aldrich, Poole, Dorset, UK
Alamar blue reagent	AbD Serotec, Kidlington, Oxford, UK
Acetic Acid	VWR International, Leicestershire, UK

2.1.3 Protein Detection

Material	Source
HEPES	Sigma Aldrich, Poole, Dorset, UK
2-pad FAST® slide	Whatman Ltd., USA
Acrylamide	Severn Biotech, Worcestershire, UK
Ammonium persulphate (AMPS)	Sigma Aldrich, Poole, Dorset, UK
Aprotinin	Sigma Aldrich, Poole, Dorset, UK
Blotting Pads	BioRad, Hertfordshire, UK
Bromophenol Blue	Sigma Aldrich, Poole, Dorset, UK
BSA	Sigma Aldrich, Poole, Dorset, UK
ECF substrate	GE Healthcare, Buckinghamshire, UK
EDTA	Sigma Aldrich, Poole, Dorset, UK
EGTA	Sigma Aldrich, Poole, Dorset, UK
Filter Paper	Munktell, Raleigh, NC 27617, USA
Glycerol	VWR International, Leicestershire, UK
Glycine	Sigma Aldrich, Poole, Dorset, UK
Leupeptin	Sigma Aldrich, Poole, Dorset, UK

Methanol	VWR International, Leicestershire, UK
Mini-gel apparatus	BioRad, Hertfordshire, UK
Sodium Chloride	Sigma Aldrich, Poole, Dorset, UK
NP-40 Alternative	Calbiochem, EMD Biosciences, USA
Odyssey Blocking Buffer	Li-Cor Biosciences, Lincoln, NE, USA
Phosphatase Inhibitor Cocktail 1	Sigma Aldrich, Poole, Dorset, UK
Phosphatase Inhibitor Cocktail 2	Sigma Aldrich, Poole, Dorset, UK
PMSF	Sigma Aldrich, Poole, Dorset, UK
Protease Inhibitor Cocktail Tablet	Sigma Aldrich, Poole, Dorset, UK
PVDF membrane	Millipore, Billerica, MA 01821, USA
Kaleidoscope pre-stained molecular weight marker	BioRad, Hertfordshire, UK
SDS	Sigma Aldrich, Poole, Dorset, UK
TGX® Tris-Glycine gels 4-15%	BioRad
Novex® Tris-Glycine gels 4-20%	Invitrogen, Paisley, UK
Semi-dry transfer apparatus	BioRad, Hertfordshire, UK
Sodium Orthovanadate	Sigma Aldrich, Poole, Dorset, UK
TEMED	BioRad, Hertfordshire, UK
Tris	Sigma Aldrich, Poole, Dorset, UK
Tris base	Sigma Aldrich, Poole, Dorset, UK
Triton-X	Sigma Aldrich, Poole, Dorset, UK
Typhoon Phosphoimager	Amersham Biosciences
PBS	Oxoid, Basingstoke, UK
Tween-20	Fisher Scientific, Leicestershire, UK
β-mercaptoethanol	Sigma Aldrich, Poole, Dorset, UK
IRDye® 680LT Goat Anti-Mouse	Li-Cor Biosciences, USA
IRDye® 800LT Goat Anti-Rabbit	Li-Cor Biosciences, USA
Primary Antibodies	See Table 3

2.1.4 Inositol Phosphate Assay

Material	**Source**
Special DMEM	Invitrogen, Paisley, UK
^{3}H-myoinositol	GE Healthcare, Buckinghamshire, UK
GnRH agonist with –His^{5}D-Tyr^{6}	Dr Kevin Morgan, MRC-HRSU, UK
HEPES	Sigma Aldrich, Poole, Dorset, UK
Lithium Chloride	Sigma Aldrich, Poole, Dorset, UK
Formic Acid	Sigma Aldrich, Poole, Dorset, UK
Dowex Resin	Sigma Aldrich

2.1.5 Inhibitors/Drugs

Material	Source
EGFR/ErbB2 inhibitor (#324673)	Calbiochem, EMD Biosciences, USA
Triptorelin (D-Trp^6-GnRH)	Sigma Aldrich, Poole, Dorset, UK
IGF-I-R inhibitor II (#407248)	Calbiochem, EMD Biosciences, USA
15d-PGJ_2	Biomol, Enzo Life Sciences, UK
PI3K inhibitor (#528106)	Calbiochem, EMD Biosciences, USA
Propylene Glycol	Sigma Aldrich, Poole, Dorset, UK

2.1.6 Flow Assisted Cytometry

Material	Source
Sucrose	Sigma Aldrich, Poole, Dorset, UK
Trisodium Citrate	VWR International, Leicestershire, UK
DMSO	VWR International, Leicestershire, UK
Tris Base	Sigma Aldrich, Poole, Dorset, UK
Nonidet P-40	Sigma Aldrich, Poole, Dorset, UK
Trypsin Type IX-S	Sigma Aldrich, Poole, Dorset, UK
Trypsin Inhibitor	Sigma Aldrich, Poole, Dorset, UK
RNase A	Sigma Aldrich, Poole, Dorset, UK
Propidium Iodide	Sigma Aldrich, Poole, Dorset, UK
Spermine Tetrahydrochloride	Sigma Aldrich, Poole, Dorset, UK

2.1.7 Gene expression analysis

Material	Source
Stratagene Absolutely® RNA Miniprep kit	Agilent Technologies UK Ltd., Stockport, Cheshire, UK
Illumina® TotalPrep™ RNA Amplification Kit	Ambion, Warrington, UK
HumanHT-12 Expression BeadChips	Illumina, Essex, UK
Ethanol	Fisher Scientific, Leicestershire, UK

2.1.8 Immunohistochemistry/AQUA

Material	Source
DakoCytomation envision/HRP Kit	DAKO, Ely, Cambridgeshire, U.K.
Tris Base	Sigma Aldrich, Poole, Dorset, UK
EDTA	Sigma Aldrich, Poole, Dorset, UK
Tween 20 (Polysorbate 20)	Fisher Scientific, Leicestershire, UK
Sodium Citrate	Sigma Aldrich, Poole, Dorset, UK
Citric Acid	Sigma Aldrich, Poole, Dorset, UK
Mouse Anti-cytokeratin Antibody	Invitrogen, Paisley, UK
Goat anti-mouse Alexa555 antibody	Invitrogen, Paisley, UK
Goat anti-Rabbit (#A3681)	Sigma Aldrich, Poole, Dorset, UK
Primary antibodies	See Table 3

2.1.9 Antibodies

Antibody	Supplier	Catalogue Number	Host	RPPA dilution	Western blot dilution	IHC buffer	IHC conditions	IHC dilution
Ki67	DAKO	M7240	Mouse	1:250	N/A	TE buffer pH9.0	1h RT	1 in 1000
Myc	Cell Signaling	5605	Rabbit	1:50	N/A	N/A	N/A	N/A
P21	Cell Signaling	2946	Mouse	1:150	N/A	N/A	N/A	N/A
P38MAPK	Cell Signaling	9212	Rabbit	1:100	N/A	N/A	N/A	N/A
P53	Cell Signaling	2524	Mouse	1:50	N/A	N/A	N/A	N/A
pAKT	Cell Signaling	9271	Rabbit	1:50	1:1000	N/A	N/A	N/A
pAKT	Cell Signaling	4060	Rabbit	N/A	N/A	TE buffer pH9.0	1h RT	1 in 100
PARP	Cell Signaling	9542	Rabbit	N/A	1:1000	N/A	N/A	N/A
pCAV1	Cell Signaling	3251	Rabbit	1:50	N/A	N/A	N/A	N/A
pCAV1	Eurogentec	65411	Rabbit	N/A	N/A	Sodium Citrate pH6.0	1h RT	1 in 50
pCDK2	Cell Signaling	2561	Rabbit	1:50	N/A	N/A	N/A	N/A
pCHK2	Cell Signaling	2669	Rabbit	1:50	N/A	N/A	N/A	N/A
pCyclinD1	Cell Signaling	2921	Rabbit	1:50	N/A	N/A	N/A	N/A
pER	Cell Signaling	2511	Mouse	1:100	N/A	N/A	N/A	N/A
pERK1/2	Cell Signaling	9101	Rabbit	1:100	1:1000	Sodium Citrate pH6.0	1h RT	1 in 20
pHistone H3	Cell Signaling	9701	Rabbit	1:100	N/A	N/A	N/A	N/A
PI3K p110alpha	Cell Signaling	4249	Rabbit	1:133	1:1000	N/A	N/A	N/A
pMet	Cell Signaling	3121	Rabbit	1:50	1:1000	N/A	N/A	N/A

Antibody	Supplier	Catalogue Number	Host	RPPA dilution	Western blot dilution	IHC buffer	IHC conditions	IHC dilution
pMet	Eurogentec	65559	Rabbit	N/A	N/A	Sodium Citrate pH6.0	1h RT	1 in 50
pmTOR	Cell Signaling	2971	Rabbit	1:50	N/A	N/A	N/A	N/A
pNFκB	Cell Signaling	3037	Rabbit	1:50	1:1000	N/A	N/A	N/A
pP70S6K	Cell Signaling	9206	Mouse	1:50	N/A	N/A	N/A	N/A
pPDK1	Cell Signaling	3061	Rabbit	1:50	N/A	N/A	N/A	N/A
pPTEN	Cell Signaling	9554	Rabbit	1:50	N/A	N/A	N/A	N/A
pRAF	Cell Signaling	9421	Rabbit	1:133	N/A	N/A	N/A	N/A
tAKT	Cell Signaling	2920	Mouse	1:1000	1:2000	Sodium Citrate pH6.0	1h RT	1 in 200
tCAV1	Cell Signaling	3267	Rabbit	1:50	N/A	N/A	N/A	N/A
tCAV1	Eurogentec	75433	Rabbit	N/A	N/A	Sodium Citrate pH6.0	1h RT	1 in 50
tCyclinD1	Cell Signaling	2926	Mouse	1:300	N/A	N/A	N/A	N/A
tERK1/2	Cell Signaling	9107	Mouse	1:50	1:1000	N/A	N/A	1 in 250
tHER1	Cell Signaling	2239	Mouse	1:125	N/A	N/A	N/A	N/A
tHER2	Cell Signaling	2248	Mouse	1:50	N/A	N/A	N/A	N/A
tMet	Cell Signaling	3148	Mouse	1:50	1:1000	N/A	N/A	N/A
tMet	Eurogentec	7551	Rabbit	N/A	N/A	Sodium Citrate pH6.0	1h RT	
tmTOR	Cell Signaling	2972	Rabbit	1:300	N/A	N/A	N/A	N/A
tCDK2	Cell Signaling	2546	Rabbit	1:50	N/A	N/A	N/A	N/A
tNFκB	Cell Signaling	4764	Rabbit	1:50	1:1000	N/A	N/A	N/A

Antibody	Supplier	Catalogue Number	Host	RPPA dilution	Western blot dilution	IHC buffer	IHC conditions	IHC dilution
tNFκB	Eurogentec	75331	Rabbit	N/A	N/A	TE buffer pH9.0	1h RT	1 in 200
tPDK1	Cell Signaling	3062	Rabbit	1:50	N/A	N/A	N/A	N/A
tPTEN	Cell Signaling	9556	Mouse	1:300	N/A	N/A	N/A	N/A
tRAF	Beckton Dickinson	R19120	Mouse	1:133	N/A	N/A	N/A	N/A
Vimentin	Cell Signaling	3390	Mouse	1:50	N/A	N/A	N/A	N/A
Cleaved caspase-3	Cell Signaling	9661	Rabbit	N/A	N/A	Sodium Citrate pH6.0	Overnight at 4ºC	1 in 100
GnRHR	Leica Microsystems	NCL-GnRHR	Mouse	N/A	N/A	Sodium Citrate pH6.0	Overnight at 4ºC	1 in 10

Table 3: Antibodies for RPPA, Western blotting, IHC and AQUA.
t- indicates total and p- indicates phosphorylated.

2.2 Methods

2.2.1 Cell Culture

All cell culture procedures were carried out at room temperature in a class II tissue culture hood using aseptic technique. Cells were routinely maintained in 75cm^2 or 175cm^2 tissue culture flasks in a 5% CO_2 atmosphere at 37°C. All cell lines were grown in DMEM with phenol red and glutamine, supplemented with 10% FCS and 1% Pen-Strep. This mixture is hereafter referred to as complete media. SCL60 and SCL215 cells were maintained in complete media supplemented with G418 (0.5mg/ml) and MCF-7-H14 cells were maintained in complete media supplemented with G418 (0.5mg/ml) and Hygromycin (0.05mg/ml).

Cells were passaged when 60-80% confluent, approximately twice weekly. For a 175cm^2 flask, media was aspirated from the flask and cells were washed with 5ml PBS. Following the immediate removal of PBS, 5ml Trypsin-EDTA was added and the cells incubated with this for 30s-3min at 37°C. Fresh complete media was added to the dissociated cells and the mixture centrifuged at 1000g for 4min. The pellet was resuspended in 10ml fresh complete media, 20% was returned to the flask and 60ml fresh complete media was added.

Cells were routinely stored in nitrogen at -196°C. To prepare cells for freezing, cells were detached as described above, centrifuged at 1000g for 4min and the pellet resuspended in a solution of 90% FCS and 10% DMSO. For a 175cm^2 flask, the pellet was resuspended in 7ml, and 1ml aliquots were prepared in cryovials. The cells were frozen at -70°C overnight before transferring to nitrogen. To recover cells from freezing, aliquots were thawed rapidly, and immediately washed with complete media to remove DMSO. The cells were centrifuged at 1000g for 4min and then the pellet resuspended in fresh complete media.

To assist cell adherence during experiments using SCL60, HEK293 and SCL215 cells, tissue culture dishes/wells were coated with 2-3mm depth Matrigel® solution (200µl Matrigel® in 6ml serum-free media) and incubated for 24h. Immediately

before very gently adding cells, excess Matrigel® solution was aspirated to leave the dish evenly coated.

2.2.2 Flow Cytometric DNA Analysis

Cells were seeded into 6cm diameter dishes at $0.5x10^6$cells/dish. The cells were treated with Triptorelin (100nM) or 0.02% Propylene Glycol solution (vehicle control) for up to 72h. The cells were washed with PBS then detached from the dish surface by incubation with 1ml Trypsin-EDTA for 2min. The cells were transferred to 12x75mm glass tubes and centrifuged at 450 x g for 5min. Excess moisture was removed by inverting the tubes and the cells were then resuspended in 100µl pH7.6 citrate buffer (Table 4). These tubes were stored at -20°C until analysis.

Samples were thawed to room temperature. The cells were incubated at room temperature with Solution A (450µl; Table 6) for 2min with continuous agitation, then Solution B (375µl; Table 7) was added and after mixing the cells were incubated for 10min. Finally Solution C (250µl, cold; Table 8) was added and the cells were mixed and then incubated for 10min on ice and in the dark. The samples were analysed using a BD FACSAriaII SORP Flow Cytometer (Becton Dickinson) and BD FACSDiva software (Becton Dickinson, Version 6.1.2).

Component	**Quantity**
Sucrose	85.5g
Trisodium Citrate	11.76g
Distilled Water	To make final volume of 1000ml
DMSO	50ml
Hydrochloric Acid	To adjust to pH7.6

Table 4: Citrate Buffer for Flow Cytometric DNA Analysis

Component	Quantity
Trisodium Citrate	2000mg
Tris Base	121mg
Spermine Tetrahydrochloride	1044mg
Nonidet NP40	2ml
Hydrochloric Acid	To adjust to pH7.6

Table 5: Stock solution for Flow Cytometric DNA Analysis

Component	Quantity
Stock solution (Table 5)	500ml
Trypsin Type IX-S	15mg

Table 6: Solution A for Flow Cytometric DNA Analysis

Component	Quantity
Stock solution (Table 5)	500ml
Trypsin Inhibitor	250mg
RNase A	50mg

Table 7: Solution B for Flow Cytometric DNA Analysis

Component	Quantity
Stock solution (Table 5)	500ml
Propidium iodide	208mg
Spermine Tetrahydrochloride	500mg

Table 8: Solution C for Flow Cytometric DNA Analysis

2.2.3 *In vitro* Protein Detection

2.2.3.1 Protein Extraction

Cells were seeded to generate 10cm diameter dishes at 70-80% confluence. On ice, media was aspirated from the tissue culture dish, and the cells were washed with ice cold PBS. This was aspirated and 400µl complete lysis buffer A (Table 9) was added to cells in a 10cm diameter dish, or 800µl per 16cm dish. The dish was tilted and the cells scraped into the complete lysis buffer. The cells were incubated in the complete lysis buffer on ice for 5min before being transferred to a 1.5ml microcentrifuge tube. Lysates were centrifuged at 16000 x g in a microcentrifuge for 6min at 4°C. The supernatant was transferred to a fresh 1.5ml microcentrifuge tube and the pellet discarded. Lysates were stored at -70°C for up to 12 months.

The protein extraction method differed for experiments in chapter 3.6 as these experiments were performed in another laboratory: Complete lysis buffer A was substituted for Complete lysis buffer B (Table 10, Table 11 and Table 12).

Component	Quantity
Tris (50mM, pH7.5)	1ml
EGTA (5mM, pH8.5)	1ml
Sodium chloride (150mM)	3ml
Distilled water	5ml
Triton-X (1%)	100µl
Protease Inhibitor Cocktail Tablet	1
Phosphatase Inhibitor Cocktail 1	100µl
Phosphatase Inhibitor Cocktail 2	100µl
Aprotinin	50µl

Table 9: Complete lysis buffer A

Component	Quantity
Glycerol (BDH)	5ml
1M HEPES buffer pH7.4 (Sigma)	0.25ml
0.5M EDTA pH8.0 (Sigma)	0.20ml
NP-40 Alternative (Calbiochem, #492016)	0.50ml
Sodium chloride (Sigma)	0.73g
Distilled water	44ml

Table 10: NP40-based lysis buffer.
Note that NP-40 alternative is used because NP40 is no longer available.

Component	Quantity
NP40-based lysis buffer	1ml
PMSF (17mg/ml in isopropanol) (Sigma, protease inhibitor)	30µl
0.2M Na Orthovanadate (Sigma, phosphatase inhibitor)	30µl
10mg/ml Leupeptin (Sigma, protease inhibitor)	3µl

Table 11: Complete lysis buffer B

Component	Quantity
10% SDS	40ml
β-mercaptoethanol	2.5ml
Glycerol	5ml
1M Tris pH6.8	1.25ml
Distilled Water	1.25ml
Bromophenol Blue	Pinch (to make the buffer blue)

Table 12: 2x Laemmli Sample Buffer

2.2.3.2 Protein Quantification

In glass tubes (12x75mm), 5µl of each protein sample was diluted in 45µl distilled water and a protein standard was diluted to the following concentrations: 0, 50, 75, 100, 250, 500, 750, and 1000µg/ml in 50µl distilled water. Then 1ml 1:50 Bicinchoninic Acid (BCA)/Copper sulphate solution was added to each tube and the tubes were immediately incubated in a waterbath at 60°C for 15min. Duplicate 200µl samples of each tube were transferred to a flat-bottomed 96-well plate. The plate was read at 540nm on a Biohit BP800 spectrophotometer (BioHit Ltd., UK).

2.2.3.3 Immunoblotting

Complete lysis buffer (Table 9) was added to equalise the concentration of each protein sample. A 5x solution of loading buffer (Table 13) was added to protein lysates to make up 20% of the final volume.

Lysates were electrophoretically resolved by 10% SDS–PAGE. The resolving and stacking gel was prepared as shown in Table 14 and Table 15. Buffers for SDS-PAGE are described in Table 16 and Table 17. Protein lysates were denatured at 95°C for 5min, then protein was immediately loaded onto the gel and 25µl Rainbow™ molecular weight marker was loaded alongside the protein samples. The gel was resolved at 80V for 15min then 150V for 45min. After resolving, proteins were transferred to a PVDF membrane at 30V overnight. The membrane was then blocked with 50% Li-Cor blocking buffer (diluted 1:1 with PBS) for 1h. The

membrane was incubated with the primary antibody in 50% blocking buffer overnight at 4°C. Antibodies used for western blotting are listed in Table 3.

At room temperature, the membrane was washed 3x5min in PBS 0.1% Tween-20 (PBS-T) and then incubated with the secondary antibody (Table 3) diluted in 50% blocking buffer for 45min. After addition of secondary antibody, exposure of the membrane to light was minimised. The membrane was washed again 3x5min in PBS-T and 3x5min in PBS. The membrane was allowed to air-dry before scanning on a Li-Cor Odyssey scanner (Li-Cor Biosciences, Lincoln, Nabraska, USA).

For experiments in section 3.6, the immunoblotting method differed. Alterations to the procedure above were as follows:

- 2x Laemmli sample buffer was added to each sample after lysis (Table 12)
- The acrylamide gels were substituted for Novex® Tris-Glycine pre-cast gradient mini-gels (4-20%) (Invitrogen, Paisley, UK).
- Transfer to PVDF membrane was by semi-dry transfer using semi-dry transfer buffer (Table 20).
- Membranes were blocked using TBS-T + 0.4% BSA and TBS-T was used instead of PBS-T for membrane washes (Table 19).
- Specific antibody binding was detected by enzyme-amplified chemifluorescence: ECF substrate was applied to the membrane for 30s; the membrane was dried between filter paper and then scanned on a Typhoon 9400 Variable Mode Imager (GE Healthcare, Buckinghamshire, UK).

Component	Quantity
Tris	75mg
SDS	5mg
Mercaptoethanol	25ml
Glycerol	50ml
Bromophenol Blue Solution	1.664ml
Distilled Water	23.3ml

Table 13: 5x loading buffer

Component	Quantity
Acrylamide	13.5ml
1M Tris, pH8.85	15ml
10% SDS	0.4ml
Distilled Water	11.1ml
TEMED	0.1ml
10% AMPS	0.1ml

Table 14: 10% Resolving Gel

Component	Quantity
Acrylamide	3.6ml
0.375M Tris, pH6.8	10ml
10% SDS	0.3ml
Distilled Water	16ml
TEMED	0.1ml
10% AMPS	0.1ml

Table 15: 3.6% Stacking Gel

Component	Quantity
Tris Base	9.09g
Glycine	43.26g
10% SDS	30ml
Distilled water	To make up to 3l

Table 16: Running buffer

Component	Quantity
Tris	12.12g
Glycine	57.68g
Distilled water	To make up to 4l

Table 17: Transfer buffer

Component	Quantity
Tris Base	60.5g
Sodium chloride	87.6g
Distilled water	To make up to 1l

Table 18: Tris-buffered Saline (TBS)

Component	Quantity
5M Sodium chloride	300ml
1M Tris pH7.0	100ml
NP-40 alternative	5ml
Tween 20	5ml

Table 19: 10x TBS-T

Component	Quantity
Tris base	5.8g
Glycine	2.9g
SDS	0.37g
Methanol	200ml
Distilled water	800ml

Table 20: Semi-dry transfer buffer

2.2.4 Reverse-phase Protein Array

2.2.4.1 Preparing samples and slides

Protein was isolated from SCL60, HEK293 and SCL215 cells following treatment with Triptorelin (100nM) or vehicle control (0.02% propylene glycol solution) for 0, 0.5, 1, 2, 4, 8, or 24h. Protein was isolated in this way from three independent experiments. Protein was extracted and quantified as described in sections 2.2.3.1 and 2.2.3.2. Samples were diluted to 2mg/ml in complete lysis buffer (Table 9) then 2-fold serially diluted 4 times to produce 5 dilutions of each sample. Each dilution of each sample was spotted [124] in triplicate onto both pads of a 2-pad FAST® nitrocellulose-coated glass slide (Whatman Ltd., USA) such that each sample was spotted a total of 15 times. To avoid bias, samples were carefully distributed over the pads to ensure that a balance of control and treated samples were spotted by each pin. A total of 72 samples were spotted onto each pad by 4 pins using a BioRobotics Microgrid (Isogen Life Science, The Netherlands).

2.2.4.2 Probing slides with antibody for target protein

Slides were blocked for 1h at room temperature with 50% Li-Cor Blocking Buffer (50% PBS) before being incubated with primary antibody overnight at 4°C. The slides were then washed with PBS-T (3x5min) before applying the fluorescently labelled secondary antibody (Table 3) diluted in Li-Cor blocking buffer and incubating at room temperature for 45min in the dark with gentle shaking. The slides were washed in the dark with PBS-T (3x5min), then with PBS (3x5min), and then dried in an oven at 50°C.

The slides were scanned on a Li-Cor Odyssey scanner (Li-Cor Biosciences, Lincoln, Nabraska, USA) at 680nm and 780nm. The image was analysed using MicroVigene RPPA Analysis module software (VigeneTech Inc., Carlisle, MA, USA) to detect spots and quantify the spot intensities. Spot intensity is calculated from the total pixel intensity within the spot boundary minus background of 2 surrounding pixels. The means of the triplicate dilutions are used to produce a curve for each sample. The y intercept is used as a relative measure of protein concentration between curves. This quantitative measurement is used in further analysis. Measurements for phosphoproteins were normalised to the corresponding total protein.

2.2.5 Gene Expression Analysis

2.2.5.1 Experimental Design

SCL60 or HEK293 cells were seeded 48h prior to treatment to allow adherence and proliferation to 30-40% confluence. They were treated with 100nM Triptorelin, or 0.02% propylene glycol solution. The total media volume was 3ml; the media was not changed at treatment to avoid loss of loosely attached cells. RNA was collected at multiple time points (Table 21) from 4 independent experiments on different days.

	Triptorelin	**Control**
SCL60	0.5h, 1h, 2h, 8h, 24h	0h, 1h, 8h, 24h
HEK293	1h, 24h	0h, 1h, 24h

Table 21: Gene expression study time points.
Time points at which RNA was collected from SCL60 and HEK293 cell lines treated with Triptorelin or 0.02% Propylene Glycol solution (vehicle control)

2.2.5.2 RNA extraction and preparation for microarray

RNA was isolated using the Absolutely® RNA Miniprep kit (Stratagene) according to manufacturer's instructions. Briefly, cells were lysed in a buffer containing guanidine thiocyanate, which denatured proteins and prevented ribonuclease degradation of RNA. The sample was then mixed with ethanol, and passed through an RNA-binding fibre matrix. Contaminating DNA was removed from the matrix with DNase treatment, and further washing steps remove other contaminants before eluting the RNA. RNA samples were quantified using the NanoDrop™ 2000 (Thermo Scientific, USA) according to the manufacturer's instructions [125]. Purified RNA was biotin-labelled using the Illumina® TotalPrep™ RNA Amplification Kit (Ambion) according to the manufacturer's instructions.

2.2.5.3 Illumina microarrays

Labelled RNA was hybridised to Illumina® 12-sample Whole Genome Array BeadChips (HumanHT-12 v3) [126]. These chips contain 48803 probes, representing 37805 different features. The majority of these features are well-annotated coding transcripts, although there are other less well-annotated coding transcripts and a small number of non-coding sequences [126]. Each bead holds 10,000 copies of a probe, and there is an average of 30 bead types per array. The chips were scanned, and initial quality control measurements were carried out (using BeadStudio®), at the Wellcome Trust Clinical Research Facility, Western General Hospital, Edinburgh. Samples were distributed carefully over the 5 chips to ensure that a balance of Control and Triptorelin samples were on each chip, this reduces the likelihood of confounding batch effects [127, 128]. Probe annotation is taken from the NCBI RefSeq database (Build 36.2, Release 22) [129]. After hybridisation the chips were scanned on an Illumina BeadArray Reader. [126].

2.2.5.4 Normalisation

The Wellcome Trust Clinical Research Facility performed the required collation of individual hybridisation spots to produce a 'raw' dataset comprising a quantitative

value of expression for each probe sequence, and an indication of the confidence of this value.

Probe sequences were first filtered to remove those that were unreliably detected: only the probe sequences that were detected with more than 95% certainty in at least three samples were retained. The remaining probes were quantile-normalised to scale the distributions of intensities on the arrays of the five microarray chips using the beadarray package [130]. Cluster analysis confirmed that there was no significant chip or run bias. All normalisation and data analysis steps were performed using the statistical software package, R [131, 132] and associated Bioconductor packages [130, 133, 134].

2.2.5.5 Further Analysis

To identify differentially expressed genes, the normalised data were subject to Rank Product analysis [135]. This method of differential expression identification was used because it is more robust to outliers within a group than other methods such as Significance Analysis of Microarrays (SAM) [135]. This is important because outliers can particularly distort results in experiments with few samples. Differentially expressed genes were defined with a predicted false-positive level cut-off of 5% (0.05). Hierarchical clustering was performed on log2-transformed, median-centred data using Cluster [136]. The resulting similarity matrix was viewed as a heatmap using Treeview [136]. The online pathway annotation tool, DAVID [137], was used to determine whether there was significant enrichment for any pathways among the genes differentially expressed between HEK293 and SCL60 cells, or among the genes differentially expressed between Triptorelin-treated and control SCL60 cells. Significant enrichment was defined by an unadjusted P-value <0.10 from a one-tailed Fisher exact test calculated within the DAVID system. Analysis was performed on a standard personal computer in conjunction with the Edinburgh Compute and Data Facility (Eddie) where a higher processing power was required.

The flow chart below gives an overview of the gene expression microarray method.

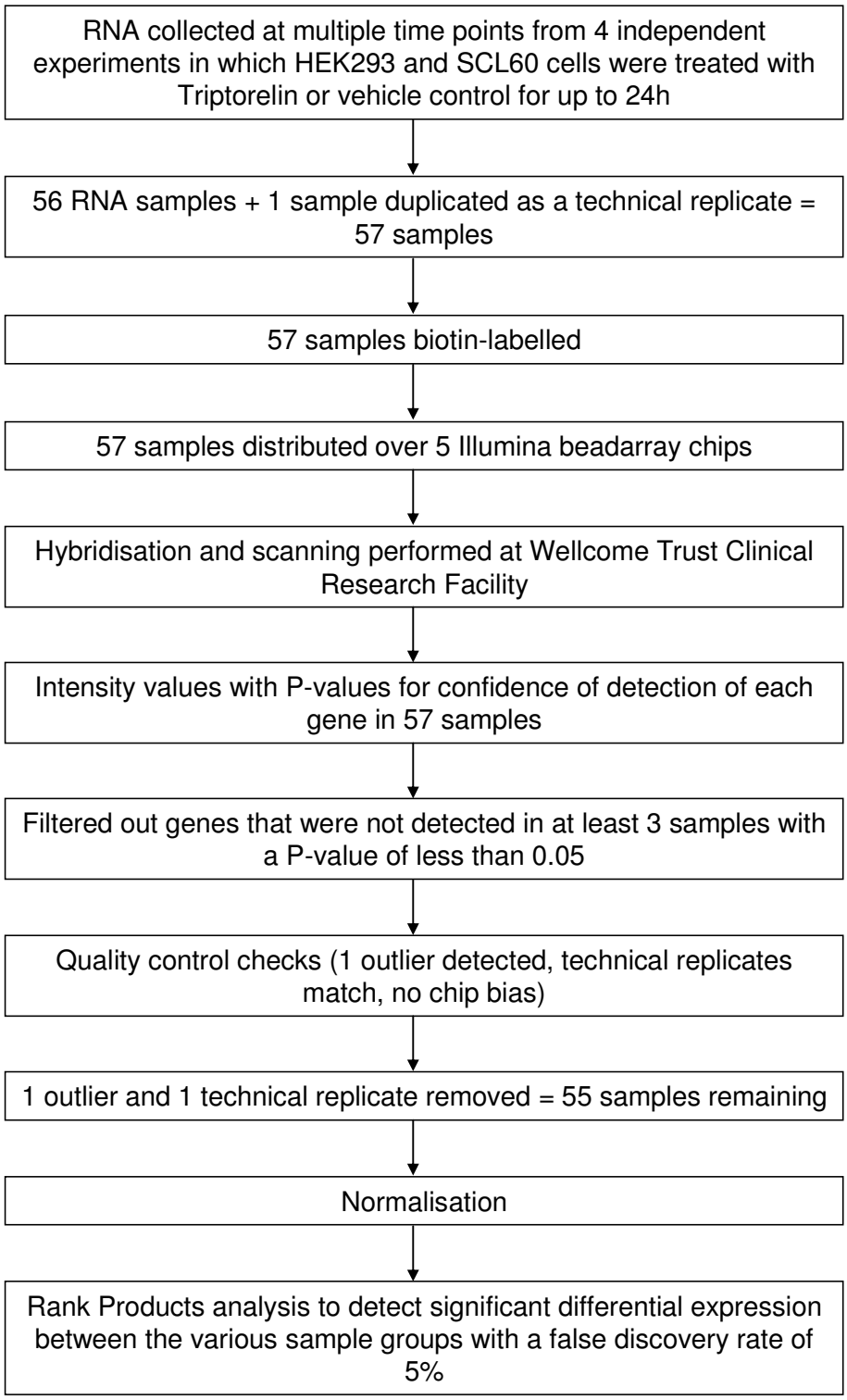

Figure 10: Flow chart for gene expression microarray study indicating steps from RNA collection to differential expression analysis

2.2.6 Radioligand Binding Assay

GnRH here refers to the GnRH agonist with –His^{5}D-Tyr^6. The ^{125}I binds to Tyr^6. Cells of each clone were seeded into 24-well plates using 1 row per clone as shown in Figure 11.

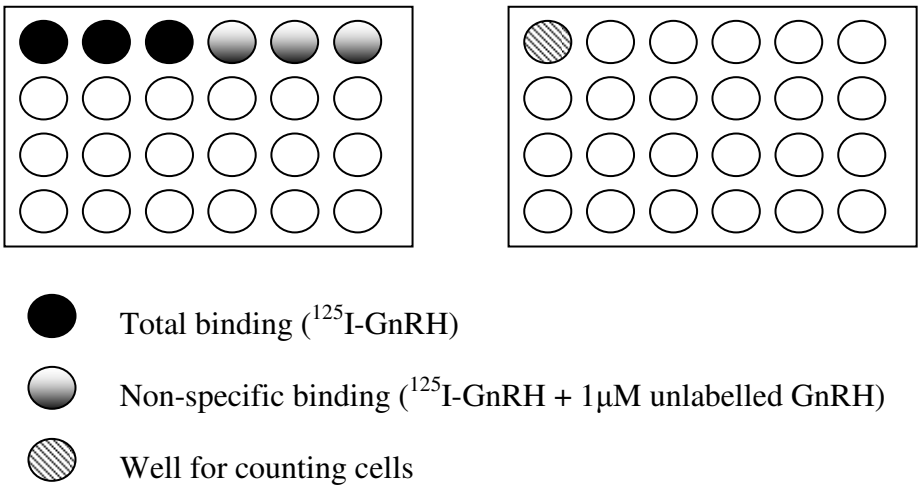

Figure 11: Radioligand binding assay plate layout.

After 24h, cells were 100% confluent. Cells in the control wells were washed with 1ml PBS to remove any non-adherent cells and debris. Cells were detached by adding 1ml trypsin per well and resuspended by repeated pipetting. The number of cells was counted using a haemocytometer.

Cells in the remaining wells were chilled to 4°C for 10min. The media was aspirated and gently replaced with either labelled (^{125}I-GnRH) or both labelled and unlabelled GnRH in 0.5ml/well DMEM + 0.1% BSA as shown above. ^{125}I-GnRH was added to 0.5ml/well DMEM + 0.1% BSA to give approximately 30,000cpm/ml media when measured using an automatic gamma counter. Unlabelled GnRH was added at 1μM. Cells were incubated at 4°C for 90min to complete binding.

On ice, media was removed and cells were gently washed 4 times with cold PBS to remove any unbound ligand. To solubilise the cells, 0.5ml 0.1mM NaOH was added per well and the cells were left on a shaking platform for 5min. The contents of each well were mixed gently by pipetting then 0.4ml was transferred to a glass tube. 0.4ml

^{125}I-GnRH, and ^{125}I-GnRH + 1μM unlabelled GnRH-I were added to 2 empty glass tubes. Radiation was measured in the tubes using an automatic gamma counter.

2.2.7 Inositol Phosphate Assay

Incubations were at 37°C, 5% CO_2 unless otherwise stated. Cells were seeded in complete media into 12-well plates at 50-70% confluence then incubated overnight to adhere. The medium was replaced with serum-free special DMEM (no inositol) and 0.5μci/ml ^{3}H-myoinositol and the cells were incubated overnight. The medium was replaced with serum-free DMEM + 10mM LiCl (inositol phosphatase inhibitor) + 10mM HEPES buffer pH7.5 and cells were incubated in this for 30min. The medium was then replaced with serum-free DMEM + 10mM LiCl (inositol phosphatase inhibitor) + 10mM HEPES buffer pH7.5 +/- GnRH agonist. After 90min the reaction was stopped by replacing the medium with 1ml/well 10mM formic acid and incubating for at least 30min at 4°C. The formic acid was removed and Dowex ion exchange chromatography was then performed as described previously [138].

2.2.8 Cell Density Assays

2.2.8.1 Sulforhodamine Blue Assay

Cells were seeded into 12-well plates at 40-50% confluence in complete media (1ml/well). After 24h the media was replaced with the relevant treatment in complete media (2ml/well). Cells were fixed on the day of treatment (Day 0) and selected time-point(s) thereafter. On ice, 25% trichloroacetic acid (TCA) solution was added gently to each well (500μl per ml media) to fix the cells. After 60min the wells were gently washed twice with water to remove any residue TCA and allowed to dry. The plates were incubated with 0.4% sulforhodamine blue (SRB) dye (750μl per well) for 30min at room temperature. The SRB solution was discarded and the wells were washed gently 4 times with 1% glacial acetic acid and allowed to dry. Tris pH10.8 (1ml) was added to each well to dissolve the dye and 50μl from each well was transferred to a 96-well plate. The absorbance was measured at 540nm using either a

Multiskan Transmit spectrophotometer (Labsystems Inc., MA, USA) or a BioHit BP800 spectrophotometer (BioHit Ltd., UK).

2.2.8.2 NFκB inhibitor assay

SCL60 cells were seeded into 12-well plates at $1x10^6$cells/ml. After 48h the cells were washed in serum-free media then treated with 3μM 15d-PGJ_2 (NFκB inhibitor) or vehicle control (dimethyl sulphoxide) in serum-free media for 30min before addition of 100nM Triptorelin or vehicle control (0.02% Propylene glycol solution) in complete media. After 4 days cell proliferation was measured by (SRB) assay as described above.

2.2.9 Proteomic (Antibody) Array

2.2.9.1 Sample preparation (SCL60 Xenografts) and the V250 array

Tumours were derived from the GnRH-R-transfected HEK293 cell line, SCL60, by subcutaneous bilateral implantation of these cells into the flank of athymic nude female mice. Nine mice with eleven tumours were treated with Triptorelin (10μg/mouse, 0.1ml). Ten mice with twelve tumours were injected with a 0.02% Propylene glycol solution, (0.1ml). Xenograft material was collected at day 4, 7 and 14.

	Control	**Triptorelin**
Day 4	671L, 671R, 643L	661L, 622R, 621R
Day 7	625L, 670L, 673R	659R, 897L, 646L

Table 22: Xenograft Samples.
This table shows the tumour codes that were assessed by antibody array. The number corresponds to the mouse, and L or R indicates the left or right tumour on this mouse.

Samples from 3 tumours following treatment with Triptorelin at day 4 and day 7, and 6 corresponding controls (Table 22), were analysed using the V250 antibody array (Eurogentec Ltd., Southampton, UK) for protein expression. This is a forward-phase protein microarray, in which immobilised antibodies capture proteins in solution (Figure 12).

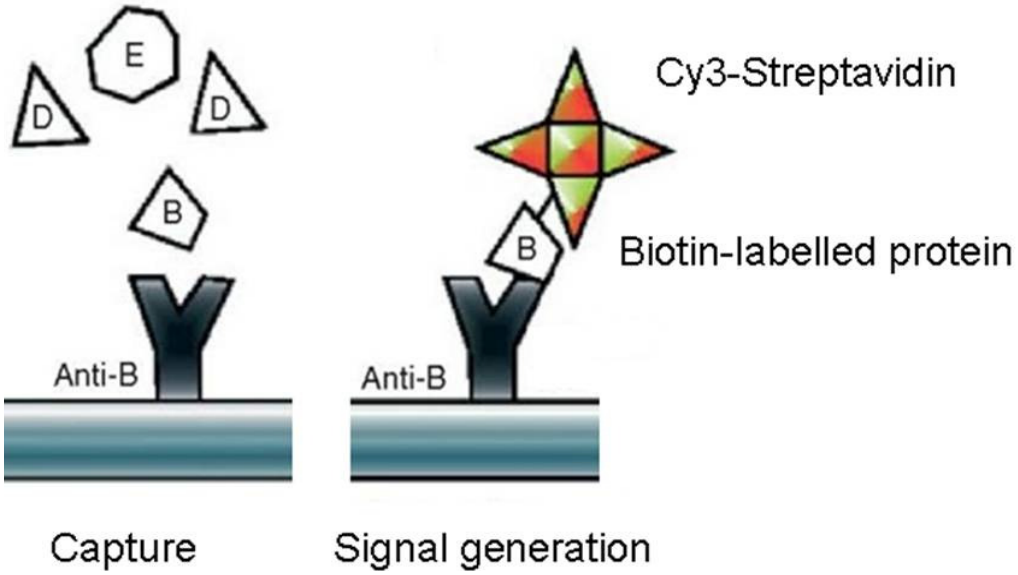

Figure 12: Forward-phase protein microarray.
Antibodies are immobilised and their biotin-labelled target protein is added in solution and allowed to hybridise. Cy3-Streptavidin is then added, which binds to the biotin and allows the antibody-protein hybridisation to be detected.
This figure is adapted from [139].

The V250 antibody array comprises 117 pairs of antibodies to detect both phosphorylated and non-phosphorylated forms of a range of proteins that are typically dysregulated in cancer-related signalling, such as proliferation and cell death signalling pathways. A full list of the antibodies used is shown in Appendix A Table 1. These antibodies, and several positive and negative controls, were covalently immobilised on a 3D-polymer coated glass slide. Six replicates of each antibody are printed onto each slide.

Protein was extracted from the xenograft tissue using bespoke Eurogentec lysis buffers. The protein concentration was measured using a BCA Protein Assay Kit before the protein was biotin-labelled. The microarrays were blocked before addition of protein to allow conjugation to the immobilised antibodies, after which any unbound protein was washed off. The microarray was then incubated in the dark with a solution of the fluorescent dye, Cy3, conjugated to Streptavidin (which binds with high affinity to biotin), before several wash steps with bespoke wash buffers followed by distilled water. This fluorescently labelled the bound protein, allowing it to be detected. The microarray slide was dried with compressed nitrogen and then

scanned using an Axon GenePix array scanner (Axon Instruments, Molecular Devices Corporation, Silicon Valley, CA, USA)

2.2.9.2 Data Analysis

The data were normalised in-house by Eurogentec and are expressed as a ratio of the intensity detected from specific binding of antibody to a phosphorylated protein, to that of its non-phosphorylated counterpart. For statistical analysis the open-source statistical language, R, was used, with associated packages [131]. The data for day 4 and day 7 were analysed as individual datasets with respect to their corresponding controls. Control and treated groups were tested for significant differences using the Mann-Whitney-U test. A correction for multiple testing was applied. However, since this returned no statistically significant differences, the uncorrected P-values were used, in combination with fold changes, to identify the protein changes most likely to be relevant to the antiproliferative effect of Triptorelin.

2.2.10 Immunohistochemistry

2.2.10.1 Tissue Microarray construction/Preparation of Slides

2.2.10.1.1 SCL60 xenograft tissue microarray

Tumours from SCL60 xenografts (prepared as described in [79]) were added to a tissue microarray as described in [140]. The tissue microarray was constructed containing 0.6mm cores from 9 control tumours (6 from day 4 and 3 from day 7) and 10 Triptorelin-treated tumours (7 from day 4 and 3 from day 7), each in triplicate. Note that 3 control day 4 and 4 Triptorelin-treated day 7 samples were derived from a second xenograft experiment but the experimental protocol was identical. Paraffin embedded sections were prepared from the TMAs (3μm thick) using a microtome and then mounted onto slides.

2.2.10.1.2 SCL60 cell line sections

Cells were grown to 70-80% confluence then detached using Trypsin-EDTA, washed and a cell pellet collected. This was fixed in formalin before being embedded into paraffin wax. Paraffin embedded sections were prepared from the TMAs (3µm thick) using a microtome and then mounted onto slides.

2.2.10.1.3 Staining slides

All washes were 2x5min with PBS-T unless otherwise indicated. All steps were performed at room temperature unless otherwise stated. Paraffin embedded sections were dewaxed by washing in xylene and then rehydrated through graded ethanol solutions (100% twice, then 80%, 50%; 2min each). The antigen retrieval buffer used was either a sodium citrate-based buffer, or a Tris-EDTA buffer, depending on antibody specification (Table 3).

Antigen retrieval buffers were prepared as detailed in Table 23 and Table 24. The antigen retrieval buffer (900ml) was heated in a microwave pressure cooker for 10min before adding the slides and heating for a further 5min. When the solution was cool the slides were washed, incubated for 10min with 3% hydrogen peroxide solution to block any endogenous peroxidase activity and then washed again. The slides were loaded onto a Sequenza® slide rack and washed again before incubating with Dako Total Protein Block for 10min.

Component	Quantity
0.1M Sodium Citrate	82ml
0.1M Citric Acid	18ml
Distilled Water	900ml

Table 23: Sodium Citrate Buffer

Component	Quantity
Tris Base	1.21g
EDTA	0.37g
Tween 20 (Polysorbate 20)	0.5ml
Distilled Water	1000ml

Table 24: Tris-EDTA Buffer

Primary antibodies (prepared in Dako Antibody Diluent) were applied (120µl) and the slides were incubated for 1h at room temperature or as otherwise advised by individual antibody specifications (Table 3). Slides were washed, then incubated with Dako Envision Labelled Polymer for 30min, then washed again. To visualise the bound antibody, DAB substrate was diluted 1:50 in DAB buffer and was applied to the slides for 10min.

The slides were washed with water, counterstained in haematoxylin, and washed again in water to remove excess stain. The sections were dehydrated through graded ethanol solutions (50%, 80%, 100% twice; 2min each), and then washed in xylene. Slides were mounted with coverslips using di-N-butylphthalate in Xylene (DPX) mountant.

2.2.10.1.4 Scoring and analysis

Slides were observed at 200x magnification on a light microscope. Negative controls (no primary antibody added) were included for each antibody and these were assessed for non-specific antibody staining.

For cleaved Caspase-3, the percentage of positively stained cells was visually estimated for each core. The mean percentage of up to three cores (some cores were removed due to poor quality) was calculated for each xenograft. Three ‘control day 4’ and three ‘control day 7’ xenografts were each compared with three ‘Triptorelin day 4’ and three ‘Triptorelin day 7’ xenografts.

For pHistone H3, an estimate of the percentage of positively stained cells in each core was obtained by counting all the positively and negatively stained cells in multiple fields per core, to reach a total cell count per core of at least 1500 cells. Three ‘control day 4’ and three ‘control day 7’ xenografts were each compared with three ‘Triptorelin day 4’ and three ‘Triptorelin day 7’ xenografts.

For all other markers, an immunoscore out of 300 was calculated for each TMA core. This was calculated by visually estimating (or counting at least 1500 cells from representative fields) the percentage of cells stained at each intensity level from 0 to 3, where 0 is negative and 3 is strongly stained. The percentage of cells at each intensity level was multiplied by 0, 1, 2 or 3 (corresponding to the intensity level). The sum of these percentages gave a total score out of 300. Mean immunoscores were calculated for control and Triptorelin-treated tumour groups at day 4 and 7. A difference in mean immunoscores with a P-value of less than 0.05 from a 2-sample t-test was considered to be significant.

2.2.11 GnRHR expression assay by immunofluorescence

2.2.11.1 TMA construction and preparation of Slides

2.2.11.1.1 Clinical breast cancer tissue microarray

Three tissue microarrays (TMAs) were constructed with triplicate samples from each of 347 primary breast carcinomas [141] as previously described [140]. The primary tissue was collected after surgical breast resection between 1999 and 2002 at the Breast Unit, Western General Hospital, Edinburgh [141]. Paraffin embedded sections were prepared from the TMAs (3μm thick) using a microtome and then mounted onto slides. Primary breast cancer TMA sections were used for antibody validation. This TMA is referred to as Ab-Val and is distinct from the TMAs described above.

2.2.11.2 Staining for GnRHR expression

2.2.11.2.1 Immunohistochemistry

Sections were stained for GnRHR expression by immunohistochemistry to determine the optimal antibody concentration, antigen retrieval buffer and incubation times to use for immunofluorescence. Immunohistochemical staining was performed as described above using pituitary whole tissue sections (positive control for GnRHR expression) and primary breast cancer TMA (Ab-Val) sections. Positive GnRHR staining was observed with the GnRHR (A9E4) Leica Microsystems antibody, and

the optimal conditions for this antibody are described in Table 3. This staining was performed by Ilgin Cagnan, a student working under my supervision.

2.2.11.2.2 AQUA®

Sections were dewaxed and rehydrated through graded alcohols as described above. Antigen retrieval was performed as described above with pH6.0 0.01M sodium citrate buffer. Slides were washed and incubated with 3% hydrogen peroxide.

Ab-Val TMA sections and pituitary whole tissue sections were used to determine optimal antibody concentration for immunofluorescence assays. The immunofluorescence assays were performed using sections from the primary breast cancer TMAs described above [141]. Slides incubated with antibody diluent and no primary antibody were included as negative controls, and formalin-fixed paraffin-embedded pituitary was used as a positive control for GnRHR expression.

Sections were prepared as for immunohistochemistry, as described in section 2.2.10.1.3, until the primary antibody incubation step. Further steps were performed using the Aquantiplex™ Epithelial Masking Kit (HistoRx). Slides were incubated with the mouse anti-GnRHR (A9E4) antibody diluted 1:4 in antibody diluent, followed by mouse anti-cytokeratin antibody (diluted 1:50, 4°C overnight). The slides were then incubated with goat anti-mouse Alexa555 antibody (1:100; Invitrogen; epithelial mask visualisation). Target visualisation was performed according to the manufacturer's instructions. Slides were counterstained and a coverslip mounted. Images (200x magnification) of the stained tissue cores were captured using an Olympus AX51 fluorescent microscope (as part of the HistoRx-PM-2000™ imaging system) in conjuction with AQUAsition™ software. DAPI, Cy3 and Cy5 filters were applied to obtain an image for each of the nucleus, cytokeratin mask, and the target protein (GnRHR). These images were analysed using AQUAnalysis™ software as previously described [142]. Analysis included the removal of image areas that either had imaging errors, corresponded to normal mammary ducts or ductal carcinoma *in situ* or constituted less than 5% epithelium.

Each core image was given a score in AQUA® units (Au) corresponding to the level of GnRHR expression. Full details of the antibodies used are described in Table 3. This AQUA staining and scoring was performed by Ilgin Cagnan.

2.2.11.2.3 Analysis

The relationship between discrete variables (Grade or Phenotype) and GnRHR expression was determined by comparing the mean GnRHR expression level for each category (Grade 0/1/2/3 or phenotype HER2/Luminal/TNP) by one-way ANOVA. 298 of the 347 samples were assigned to a molecular phenotype by hormone receptor status using the annotations given by Aitken *et al* [1]. Grade information was available for 344 of the 347 samples.

The relationship between continuous variables (ER, PR, HER2, CK5/6, EGFR expression) and GnRHR expression was determined by non-linear regression. Expression values of ER, PR, HER2, CK5/6 and EGFR were available for 335, 336, 339, 339 and 337 of the 347 samples respectively.

Minitab® software version 16.1.1.0 was used for these analyses.

Chapter 3: Results

3 Results

3.1 SCL60 response to the GnRH agonist Triptorelin in vitro and in vivo

The SCL60 cell line has been established as a model in which to study GnRHR-mediated antiproliferative signalling [79, 104, 112, 122]. The SCL60 model is a Human Embryonic Kidney-293 (HEK293) cell line that has been stably transfected with rat GnRHR. Radioligand binding assays have confirmed that these cells express high levels of functional GnRHR at the cell surface [79]. The SCL215 model is a HEK293 cell line that has been stably transfected with a modified form of GnRHR, which is inactivated by the presence of a C-terminal tail (personal communication – Dr Kevin Morgan).

In this chapter, the SCL60 cell line is compared to HEK293 (untransfected) and SCL215 cells. Stimulation of GnRHR in SCL60 cells causes increased inositol phosphate production, and a reduction in SRB activity[79]. This is not observed in HEK293 or SCL215 cells. These cell lines provide a useful model in which to study GnRHR-mediated antiproliferative signalling.

3.1.1 SRB Activity in Response to Triptorelin

The experiments in this thesis focus on the GnRH agonist, Triptorelin. This agonist has been shown to strongly reduce SRB activity of SCL60 cells *in vitro* and the growth of SCL60-derived xenografts *in vivo* [79]. It is readily available and has been the GnRH agonist of choice in similar studies of GnRH in this context [79, 143].

It is shown below that Triptorelin inhibited SCL60 but not SCL215 or HEK293 cells *in vitro*. This inhibition appeared to occur by a combination of induction of apoptosis and inhibition of proliferation *in vivo*, and involves cell cycle arrest in at least a proportion of cells *in vitro*.

3.1.1.1 Triptorelin inhibits SCL60 cells *in vitro*

The GnRH agonist, Triptorelin, has been shown to inhibit the proliferation of SCL60 cells *in vitro* [79]. To confirm this response, SCL60 cells were treated with 100nM Triptorelin or an appropriate dilution of the vehicle (0.02% Propylene Glycol solution) as a control. Cell density was measured by sulphorhodamine blue (SRB) assay after 4 days. Triptorelin caused an average 42% reduction in SRB activity of SCL60 cells (P=0.006, paired t-test; Figure 13). HEK293 and SCL215 cells were unresponsive to Triptorelin (Figure 13). Figure 13 shows a representative example of the response of SCL60, HEK293 and SCL215 cells to 100nM Triptorelin.

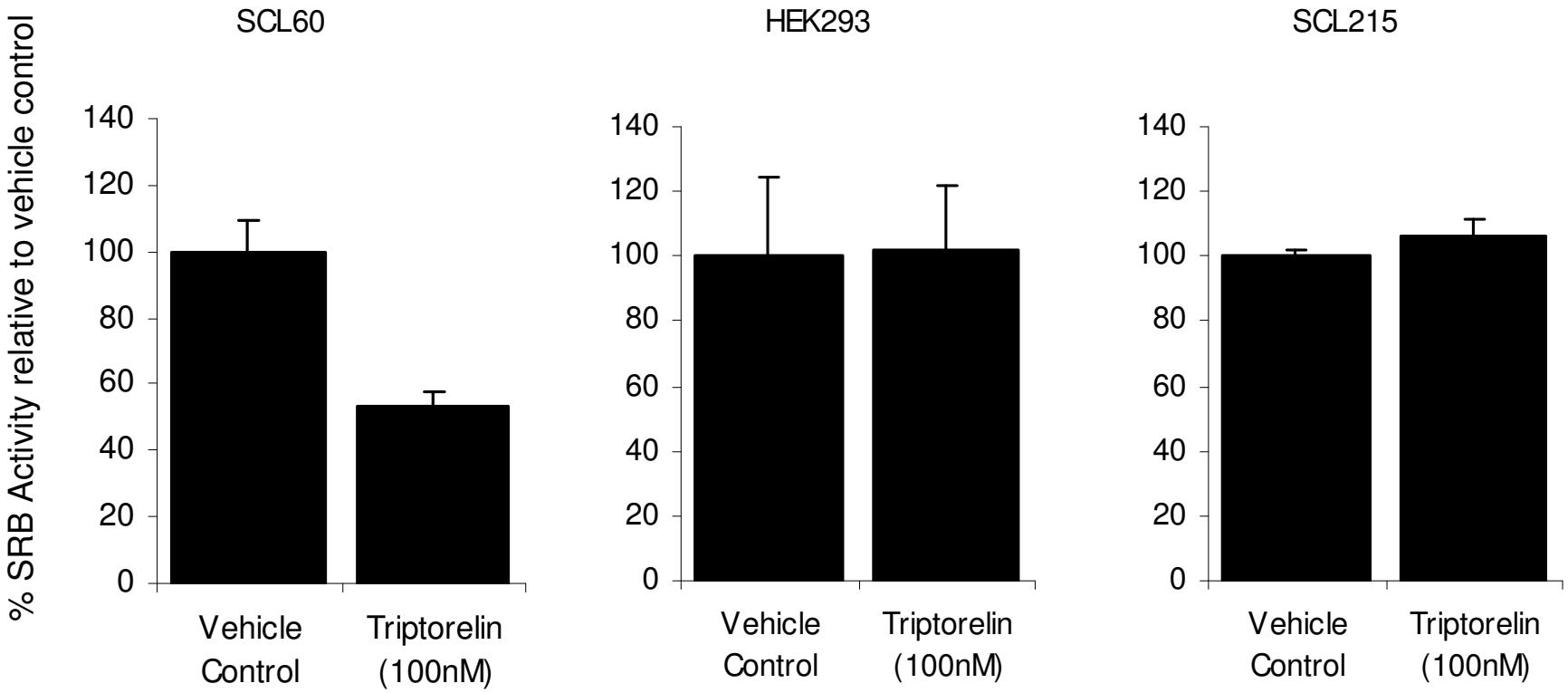

Figure 13: SRB Activity of SCL60, HEK293 and SCL215 cells 4 days after treatment with Triptorelin (100nM) or vehicle control.
Bars show the mean of 3 replicates. Error bars show standard deviation. The effect of Triptorelin on SCL60 cells is representative of 7 independent experiments (mean inhibition = 42%; P=0.006, paired T-test).

3.1.2 Exploring the mechanism by which Triptorelin reduces cell number in SCL60 cells *in vitro*

To further understand how Triptorelin reduces cell number *in vitro* and tumour volume *in vivo*, it was necessary to identify whether this occurs by an inhibition of proliferation signalling pathways, induction of cell death signalling, or a combination of both processes. This is important to help identify which signalling factors are involved in the response to Triptorelin. To do this, the impact of Triptorelin on cell cycle progression *in vitro* and on the expression of protein biomarkers of apoptosis and proliferation both *in vitro* and *in vivo* was assessed.

3.1.2.1 Triptorelin causes increased expression of apoptotic markers in SCL60 cells *in vitro*

PARP is an important protein in the cellular response to DNA damage. It is cleaved and inactivated during caspase-mediated apoptosis. Cleaved PARP (c-PARP), therefore, is often used as a marker for caspase-mediated apoptosis [144].

c-PARP expression was evaluated in SCL60 cells in response to Triptorelin using semi-quantitative western blotting. A small increase in c-PARP expression was detected in SCL60 cells by western blot 24-48h after treatment with Triptorelin, although this was much less pronounced than at 72-96h after treatment (Figure 14, Figure 15). By 72h the level of c-PARP expression in Triptorelin-treated cells was more than four times the expression in vehicle-control treated cells (Figure 15). This increase in c-PARP continued to be observed at 96h (Figure 14, Figure 15). These results support the previously published data, which identified increased c-PARP in SCL60 cells 72-96h after Triptorelin treatment [79].

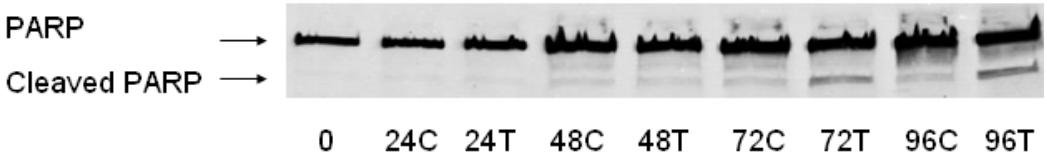

Figure 14: Western blot showing cleaved PARP expression in SCL60 cells after 24, 48, 72 and 96h after treatment with Triptorelin (T) or vehicle control (C). This is representative of two independent experiments.

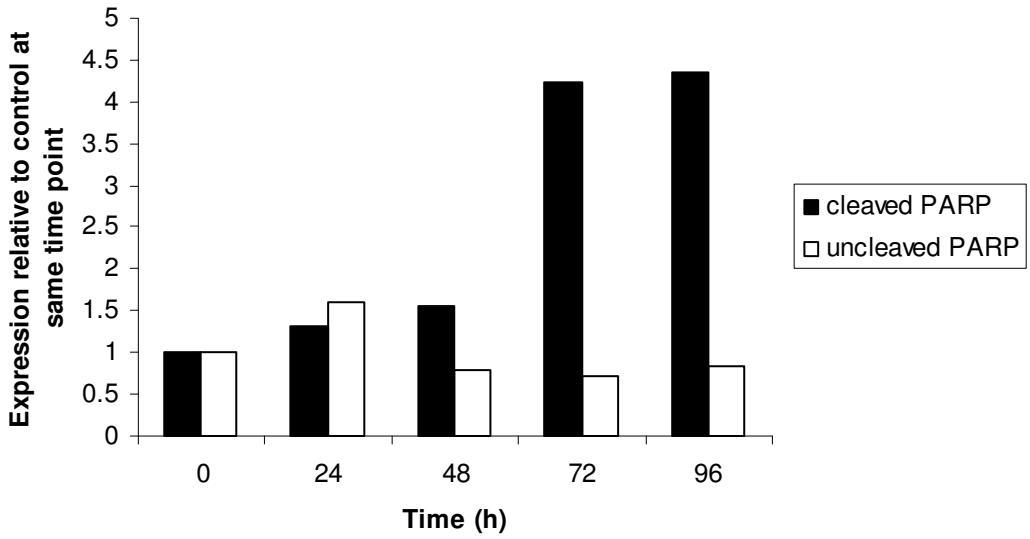

Figure 15: Quantification of the western blot for PARP and cleaved PARP.
Values for the Triptorelin-treated samples are shown relative to the corresponding vehicle control-treated samples at each time point to show the change in cleaved PARP (black bars) that occurs as a result of Triptorelin treatment. Uncleaved PARP expression is also shown (white bars). This is representative of two independent experiments.

3.1.2.2 Triptorelin causes cell cycle arrest in SCL60 cells *in vitro*

Flow cytometric cell cycle analysis showed that after 24-48h of treatment with 100nM Triptorelin, the percentage of SCL60 cells increased in the G_2/M and S phases (Figure 16). The proportion of cells in each phase of the cell cycle in the Triptorelin-treated population normalised to the vehicle control-treated population in each cell line is shown in Figure 16. The unnormalised data is shown in Figure 17. It is important to note that these data show results from a single experiment, and therefore require further work before firm conclusions may be drawn. The baseline cell cycle distributions of HEK293 and SCL60 cells were comparable (Figure 18). In the HEK293 cell population, 70% were in G_0/G_1 phases, 21% were in S phase and 9% were in G_2/M phases. In the SCL60 cell population, 67% were in G_0/G_1 phases, 24% were in S phase and 9% were in G_2/M phases. The cell cycle distributions are similar, although there is a slightly higher proportion of SCL60 cells in S phase than HEK293 cells. In HEK293 and SCL215 cells no difference in the proportion of cells in each phase of the cell cycle between control and Triptorelin-treated cells could be detected (Figure 16).

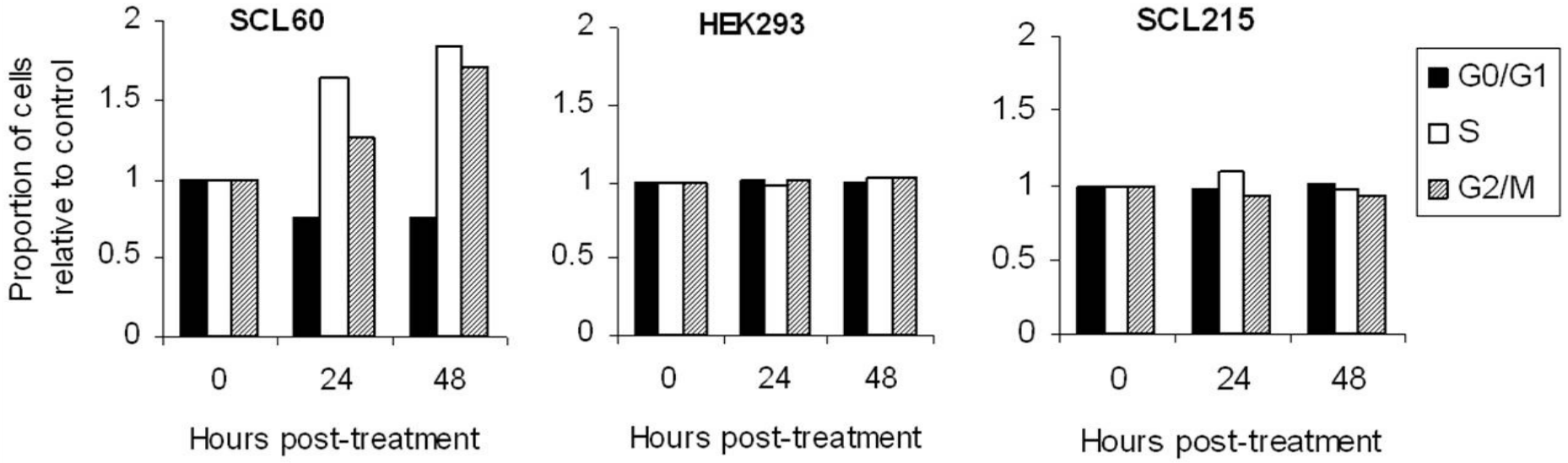

Figure 16: Flow cytometric cell cycle analysis of SCL60, HEK293 and SCL215 cells following treatment with Triptorelin (100nM) for up to 48h. Bars show the proportion of cells (relative to vehicle control at the same time point) in G_0/G_1 (black), S (white) or G_2/M (grey) phases of the cell cycle. These data are from a single experiment.

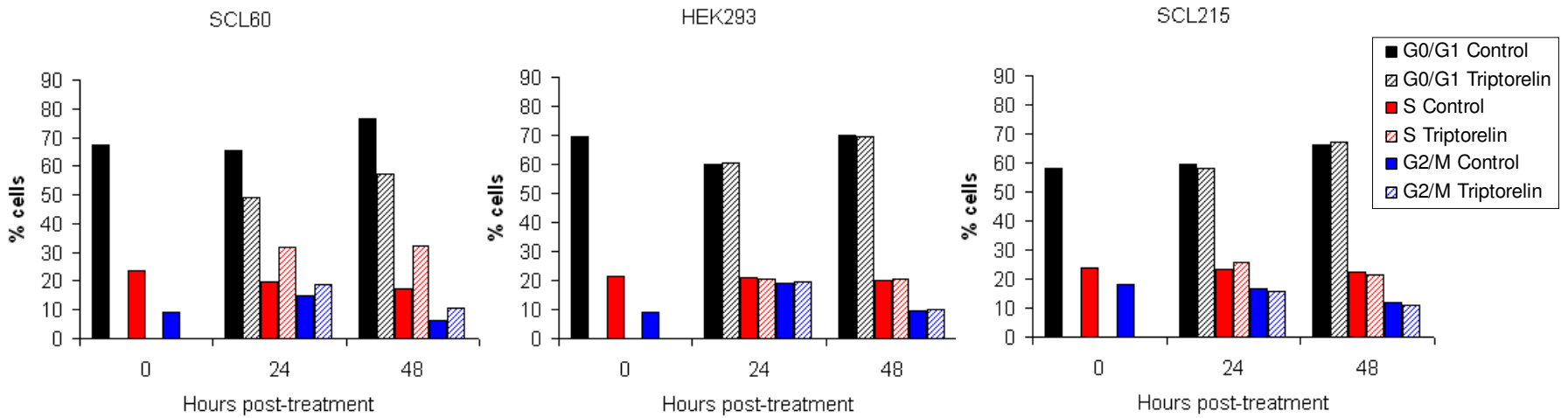

Figure 17: Flow cytometric cell cycle analysis of SCL60, HEK293 and SCL215 cells following treatment with Triptorelin (100nM) for up to 48h. Bars show the proportion of cells (relative to vehicle control at the same time point) in G_0/G_1 (black), S (red) or G_2/M (blue) phases of the cell cycle in SCL60, HEK293 and SCL215 cells treated with 0.02% propylene glycol (solid bars) or 100nM Triptorelin (shaded bars). These data are from a single experiment.

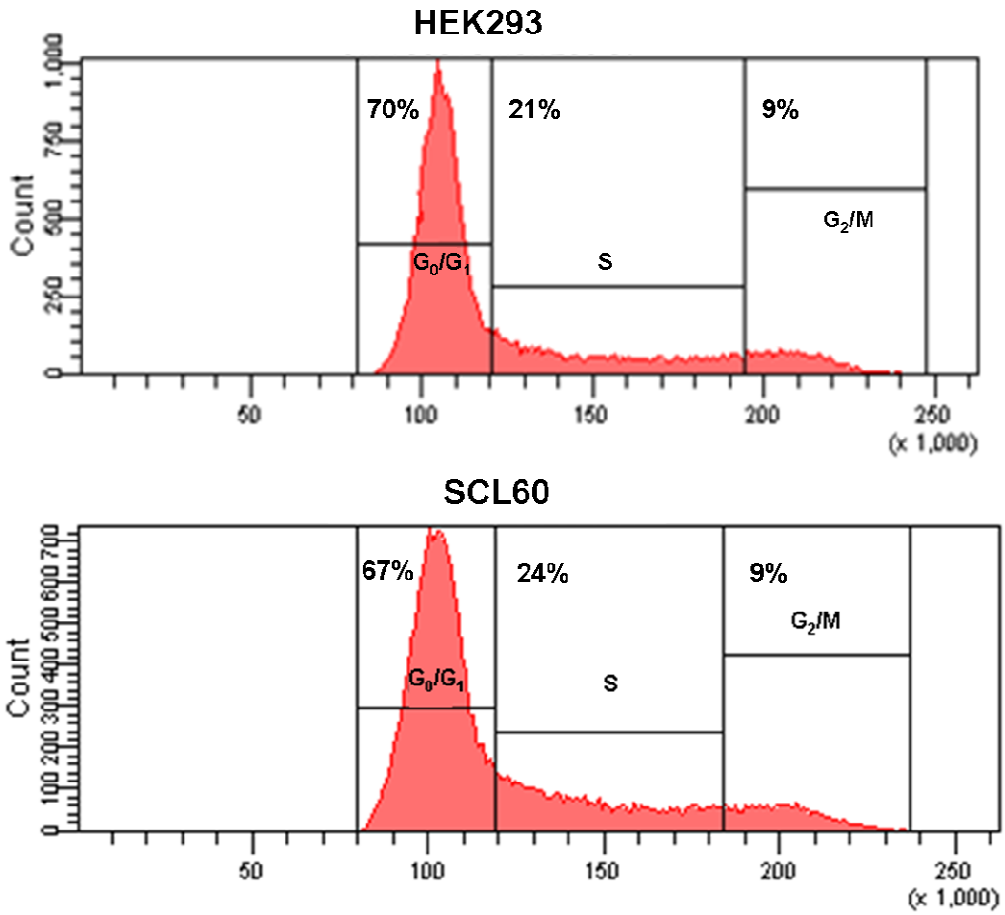

Figure 18: The cell cycle distributions of HEK293 and SCL60 cells
In the HEK293 cell population, 70% were in G_0/G_1 phases, 21% were in S phase and 9% were in G_2/M phases. In the SCL60 cell population, 67% were in G_0/G_1 phases, 24% were in S phase and 9% were in G_2/M phases. The cell cycle distributions are similar, although there is a slightly higher proportion of SCL60 cells in S phase than HEK293 cells. These data are from a single experiment.

3.1.3 Exploring the mechanism by which Triptorelin reduces the volume of SCL60 xenografts *in vivo*

Using tissue from the SCL60 xenografts treated with Triptorelin or vehicle control described in Section 1.3.2 (Figure 9), the level of phospho-Histone H3 and cleaved Caspase-3 was measured by immunohistochemistry. Phosphorylated Histone H3 is used as a marker of proliferation because phosphorylation at Ser10, Ser28 and Thr11 residues of Histone H3 is specifically correlated with mitosis [145-147]. The level of staining for phospho-Histone H3 indicates the number of cells undergoing mitosis at one point in time. If the proliferation rate of the cell population is greater, one would expect more cells to be undergoing mitosis at any one time. Caspase-3 cleavage is an essential event in initiating the death cascade in caspase-dependent apoptosis [148]. It is therefore used as a marker of the early stages of apoptosis.

3.1.3.1 Triptorelin caused a reduction in the expression of the proliferation marker pHistone H3 in SCL60 xenografts

pHistone H3 expression was significantly lower in Triptorelin-treated xenografts compared to vehicle control-treated xenografts (P=0.006, 2-sample t-test; Figure 19).

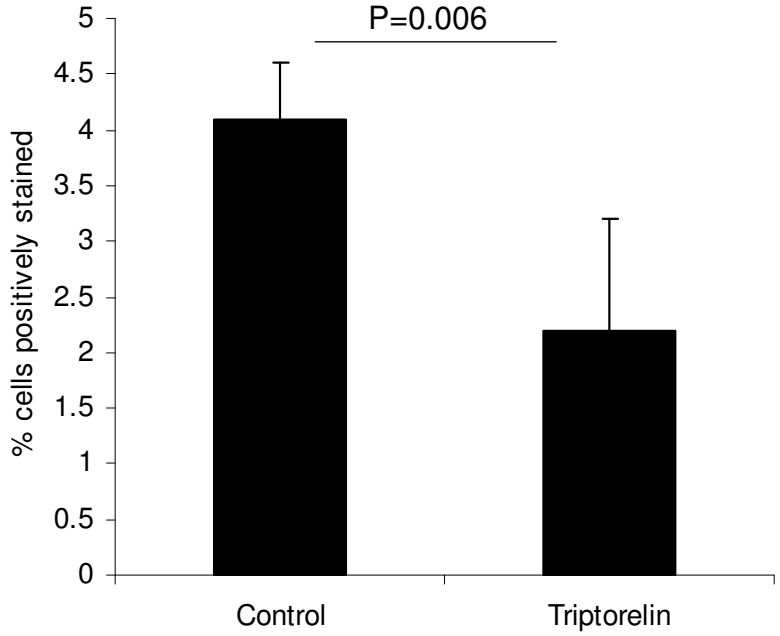

Figure 19: pHistone H3 expression in SCL60 xenografts as measured by immunohistochemistry. Bars show the percentage of cells positively stained in (triplicate cores of) 5 vehicle control-treated tumours and 6 Triptorelin-treated tumours. Tumours were treated for either 4 or 7 days. pHistone H3 expression was significantly lower in Triptorelin-treated tumours compared to vehicle control-treated tumours (P=0.006; 2-sample t-test).

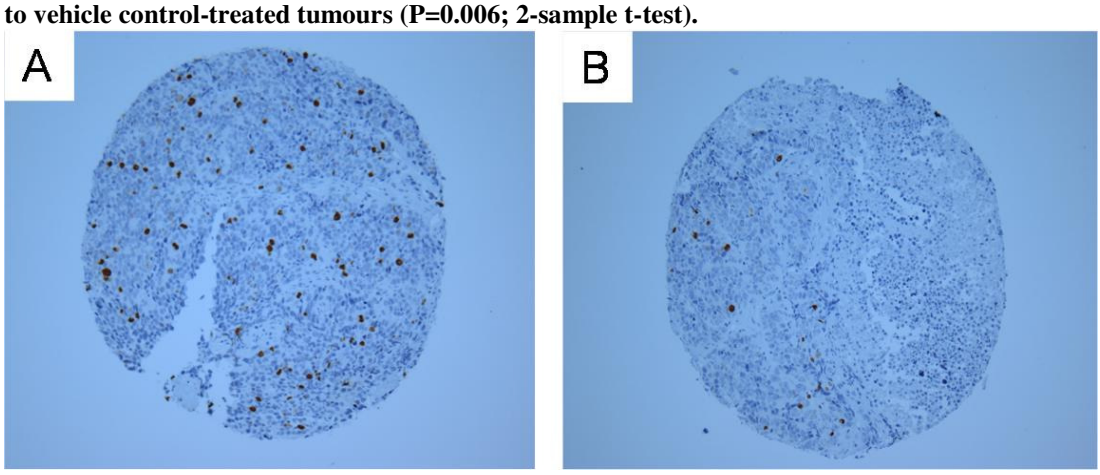

Figure 20: pHistone H3 immunostaining in TMA cores of SCL60 xenografts treated with (A) vehicle control or (B) Triptorelin for 4 days.
Brown staining corresponds to pHistone H3 expression and blue staining corresponds to haematoxylin.

3.1.3.2 Triptorelin caused an increase in the expression of the apoptotic marker cleaved caspase-3 in SCL60 xenografts

Immunohistochemical staining showed a significant 3-fold increase in cleaved caspase-3 expression in Triptorelin-treated SCL60 xenografts compared to those treated with a vehicle control (P=0.0095, 2-sample t-test; Figure 21).

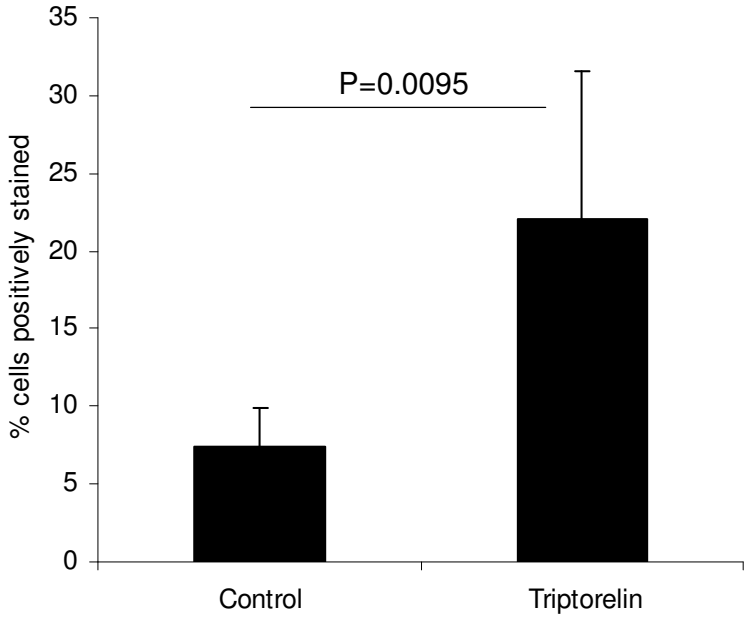

Figure 21: Cleaved caspase-3 expression in SCL60 xenografts as measured by immunohistochemistry.
Bars show the percentage of cells positively stained in 5 vehicle control-treated tumours and 6 Triptorelin-treated tumours. Tumours were treated for either 4 or 7 days. A statistically significant increase in cleaved caspase-3 expression was observed in Triptorelin-treated tumours compared to vehicle control-treated tumours (P=0.0095; 2-sample t-test).

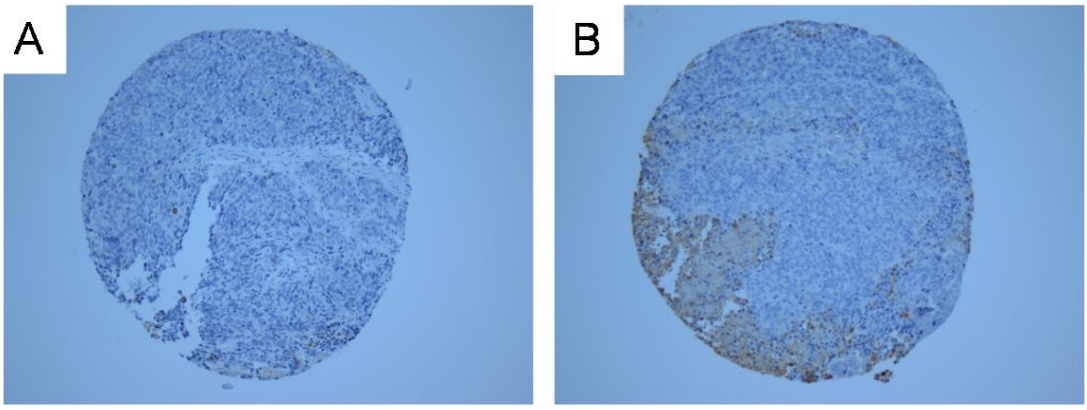

Figure 22: Cleaved caspase-3 immunostaining in TMA cores of SCL60 xenografts treated with (A) vehicle control or (B) Triptorelin for 4 days.
Brown staining corresponds to cleaved caspase-3 expression and blue staining corresponds to haematoxylin.

3.1.4 Discussion

It has been shown above that Triptorelin reduced SCL60 but not SCL215 or HEK293 cell numbers both *in vitro* [79] (Figure 13) and this has previously been shown *in vivo* [79] (Figure 9). These data support the previous finding that Triptorelin has a marked effect on SCL60 cell number, and that expression of functional GnRHR is required for a response [79]. This ability of Triptorelin to inhibit the SRB activity of SCL60 cells makes SCL60 cells a useful model with which to study the antiproliferative effect of GnRHR stimulation.

The SRB activity of HEK293 and SCL215 cells was uninhibited by Triptorelin and this is consistent with the lack of functional GnRHR. The addition of functional GnRHR appeared to be sufficient to allow Triptorelin to reduce SRB activity. This indicated that the cells have the necessary machinery to mediate an antiproliferative response to a GnRH agonist, even though they do not normally express the receptor. This may be relevant to other cell systems that do not normally express GnRHR.

To further understand how Triptorelin reduced cell number *in vitro* and tumour volume *in vivo*, the impact of Triptorelin on cell cycle progression (*in vitro*) and on the expression of protein biomarkers of apoptosis and proliferation (both *in vitro* and *in vivo*) was assessed.

Triptorelin caused an increase in PARP cleavage in SCL60 cells at 72 and 96h after treatment with Triptorelin (Figure 14, Figure 15). This was consistent with the previously published data by Morgan et al [79], which described a very small increase in cleaved caspase-9 (upstream of c-PARP) and pFADD (death receptor signalling, marker of extrinsic apoptosis) expression by 24h, but did not observe any increase in c-PARP expression until 72h [79]. A caspase inhibitor (20μM Q-VD-OPh) has been shown to partially rescue (40%, $P<0.002$) SCL60 cells from the effect of Triptorelin [79]. Together, these data indicate that at least a proportion of the cells undergo apoptosis in response to Triptorelin.

Flow cytometric cell cycle analysis showed that after 24-48h of treatment with Triptorelin, the percentage of SCL60 (but not HEK293 or SCL215) cells increased in the G_2/M and S phases (Figure 16). This is in agreement with previously published results, which showed that GnRHR stimulation caused G_2/M arrest in HEK293 cells stably expressing either human or rat GnRHR [112]. Together, these data indicate that the antiproliferative effect of Triptorelin may be mediated at least in part by cell cycle arrest. Cell cycle arrest has been observed following GnRHR stimulation in other cell lines including pituitary LβT2 cells [112], breast cancer MCF7-derived cells [69], and ovarian cancer cells EFO-21 and EFO-27 [149], although in these cases there was an increase in the proportion of cells in G_0/G_1 phase rather than the G_2/M phase.

Immunohistochemical staining showed a significant increase in cleaved caspase-3 expression, and a decrease in pHistone H3 expression in Triptorelin-treated xenografts compared to those treated with a vehicle control (Figure 19, Figure 21). This suggested that the antiproliferative effect of Triptorelin *in vivo* is mediated by a combination of increased apoptotic signalling and a decrease in proliferative signalling.

In summary, Triptorelin inhibited SCL60 but not HEK293 or SCL215 cells both *in vitro* and *in vivo*. This occurred by a combination of induction of apoptosis and inhibition of proliferation, and involved cell cycle arrest in at least a proportion of cells *in vitro*.

3.2 Transcriptional signalling in HEK293 and SCL60 cells following GnRHR stimulation

To investigate GnRHR-regulated signalling at the transcriptomic level, a global, data-driven approach was taken to identify genes that may be of interest in understanding the GnRHR-mediated antiproliferative effect. Gene expression analysis was conducted using RNA extracted from SCL60 and HEK293 cells following treatment with Triptorelin for up to 24h.

Gene expression analysis allows a genome-wide snapshot of transcriptional activity. The genes that are most differentially expressed with treatment might feasibly contain some of those most relevant to mediating the direct antiproliferative effect of Triptorelin. The aim of this experiment was to identify gene expression changes after Triptorelin treatment and to use these data to generate hypotheses about genes that may be involved in mediating the antiproliferative effect of Triptorelin.

More specifically, the aims were to examine whether genes are differentially expressed between (untreated) HEK293 and SCL60 cells, and whether the expression of any genes is influenced by Triptorelin treatment in each of these cell lines. If differential gene expression between any of these pairs of sample groups could be identified, the aim was then to determine how many genes were differentially expressed, by how much, and how their expression varied over 24h after treatment with Triptorelin. To explore these differentially expressed genes further, the most represented functions and pathways were defined. Differential gene expression was determined using Rank Product analysis with a maximum false discovery rate (FDR) of 0.05, as described in Materials and Methods.

3.2.1 Data pre-processing

Fifty-seven samples, including the 56 samples detailed in Materials and Methods (section 2.2.5.1; 4 replicates of HEK293 and SCL60 cells treated with vehicle control or Triptorelin for several time points up to 24h) and one sample duplicated as a

technical replicate, were distributed randomly over 5 Illumina HT-12 Beadchips. Other samples outwith this study filled the remaining 3 arrays on the chips. Values of the average fluorescence intensity resulting from the hybridisation of probes and their targets were recorded in BeadStudio (bespoke software) for 48803 probes on each array. In an initial similarity matrix, the technical replicates clustered together, and one outlier was identified. The outlier (from the group 'SCL60 vehicle control 1h'), and the technical replicate was removed before further analysis, leaving 55 arrays remaining. A detection P-value was calculated in GenomeStudio (bespoke software), which gives a measure of confidence that a given target transcript is reliably expressed above the background intensity of negative control probes. Probes that were detected with a P-value of less than 0.05 in at least 3 samples (arrays) were considered to be reliably detected; all other probes were excluded from the dataset. These included probes with poor hybridisation or transcripts that are not represented in HEK293 or SCL60 cells. After this filtering process, 25820 probes were retained for further analyses.

The dataset was quantile-normalised to scale the distributions across the 55 beadarrays (Figure 23). Multidimensional scaling demonstrated that there was no significant chip or run bias, samples were randomly assigned to beadchips but clustered by replicate rather than by chip (Figure 24).

A B

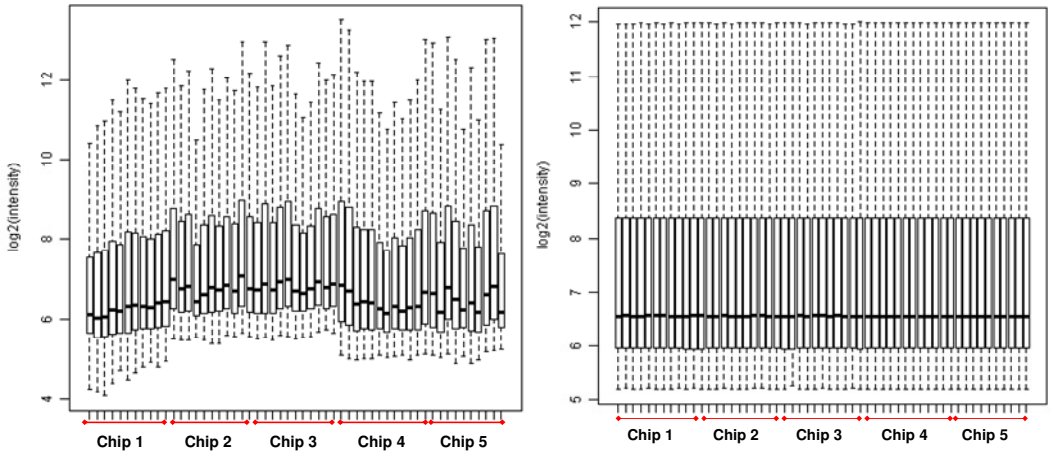

Figure 23: Boxplot showing the filtered gene expression data
(A) before and (B) after quantile normalisation. Samples are ordered from left to right by chip.

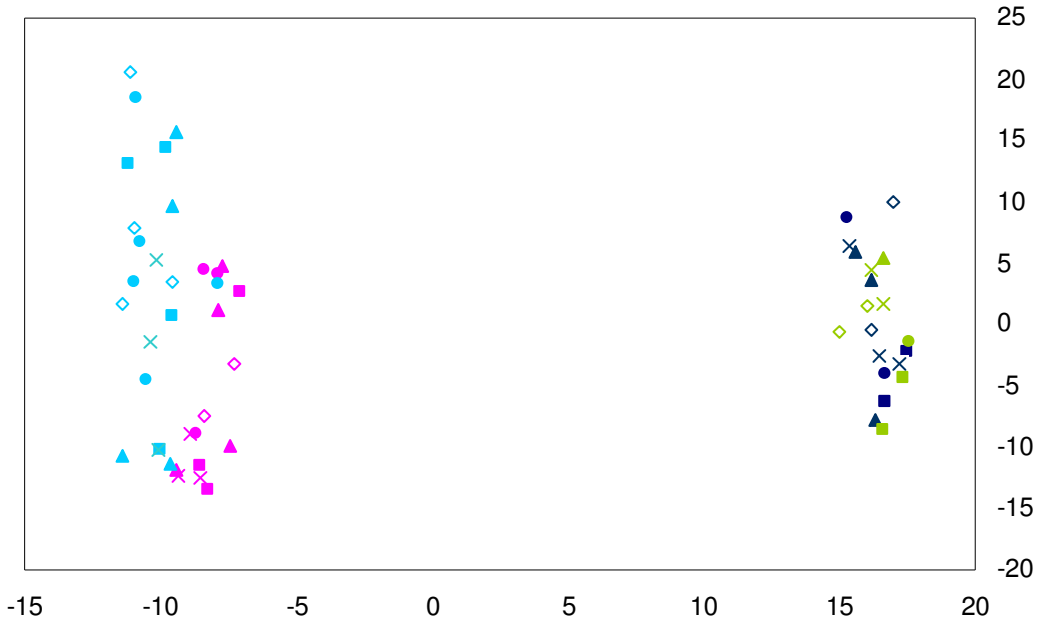

Figure 24: Multidimensional Scaling Plot.
The proximity of two points to one another on the graph represents how similar their expression profiles are. Samples cluster by cell type rather than by Beadchip or processing batch. Dark blue = HEK293 control; green = HEK293 Triptorelin; pink = SCL60 control; Light blue = SCL60 Triptorelin. Square = chip 1; circle = chip 2; cross = chip 3, triangle = chip 4; diamond = chip 5.

3.2.2 Comparison of gene expression between vehicle control- and Triptorelin-treated HEK293 cells

To identify whether any genes were differentially expressed in the untransfected HEK293 cells (which do not express GnRHR) as a result of Triptorelin treatment, four Triptorelin-treated samples were compared to four vehicle control-treated samples of the same time-point. Gene expression microarray analysis identified only four probes (representing four genes) that were increased in the Triptorelin-treated cells at 1h after treatment (PAK2, GRIPAP1, LOC100008589, and TNPO1), one that was increased at 24h (LOC100008589) and one that was decreased at 24h (CSNK1G2).

3.2.3 Comparison of gene expression between untreated HEK293 and SCL60 cells

To identify whether any genes are differentially expressed as a result of GnRHR expression, the gene expression profile of (untreated) HEK293 cells was compared to that of (untreated) SCL60 cells. Four samples of each cell line were analysed by Illumina Beadarrays. Almost 20% (4745) of the probes that were detectably expressed were differentially expressed (using a 5% false positive threshold) between the untreated HEK293 and untreated SCL60 cells (Table 25, Appendix A Figure 1).

	Number of probes	**Min fold change**	**Max fold change**
Higher expression in SCL60 cells compared to HEK293 cells	2583	+1.2	+19
Lower expression in SCL60 cells compared to HEK293 cells	2162	-1.2	-210

Table 25: Differentially expressed genes between (untreated) HEK293 and (untreated) SCL60 cells using a 5% false positive threshold.

Fold changes of genes increased in SCL60 cells ranged from +1.2 (BARX2) to +19 (SOX11), whereas genes decreased in expression with a much larger range of fold changes, from -1.2 (HS.574667) to -210 (HSPA1A) (Table 25).

The 25 probes most significantly increased and decreased in SCL60 cells compared to HEK293 cells are shown in Table 26 and Table 27 respectively. More details of these differentially expressed genes are shown Appendix A Table 2 and Appendix A Table 3.

Probes				
SOX11	KRT19	RYR3	MAL2	FLJ12684
BEX1	VANGL2	UCHL1	PRSS3	RAB17
TCEAL3 (ILMN_1734190)	HLA-DRB5	HLA-B	SFRP1	EEF1A2
TCEAL3 (ILMN_1749478)	HOPX	CYP4X1	LOC389641	CD44
TACSTD1	RUNX3	MT1F	TNFRSF10A	PTGER4

Table 26: The 25 probes most significantly increased in SCL60 cells compared to HEK293 cells. The 2583 significantly increased probes in SCL60 cells compared to HEK293 cells were ranked in order of significance (P-value). The 25 probes most significantly increased are shown above.

Probes				
HSPA1A	CMBL	NEFH	CA2 (ILMN_1662795)	CA2 (ILMN_2199439)
TMEM47	ZSCAN18	NEFM	PCDH17	NEFL
ZNF83	ZNF816A	ZNF135	ZNF702	FABP5
IFITM3	ZNF160	HS.572538	ZNF649	HOXB5
LOC400713	PCDH10	SH3PXD2A	ZNF682	HS.200774

Table 27: The 25 probes most significantly decreased in SCL60 cells compared to HEK293 cells The 2162 significantly decreased probes in SCL60 cells compared to HEK293 cells were ranked in order of significance (P-value). The 25 probes most significantly decreased are shown above.

Genes that had higher expression in SCL60 cells than in HEK293 cells included genes involved in adhesion (CD44, TACSTD1), immune response processes (HLA-B, HLA-DRB5), and transcriptional regulation (SOX11, TCEAL3, RUNX3); whilst genes that had significantly lower expression in SCL60 cells compared to HEK293 cells encode many transcription regulators (including seven zinc finger proteins) and several proteins involved in adhesion (PCDH17, PCDH10, SH3PXD2A).

3.2.3.1 Pathways represented by genes differentially expressed between HEK293 and SCL60 cells

The online pathway annotation tool, DAVID [137], was used to determine whether there was enrichment for any pathways among the genes differentially expressed

between HEK293 and SCL60 cells. This analysis used all of the 2583 significantly increased and 2162 significantly decreased genes. Enrichment with an unadjusted P-value of less than 0.10 from a one-tailed Fisher exact test was deemed of interest (see section 2.2.5.5 on page 75).

This analysis identified 30 pathways in which genes were more highly expressed in SCL60 cells compared to HEK293 cells, and 26 pathways in which genes were more lowly expressed in SCL60 cells. Most of these pathways are rather broad terms that relate to disease-specific mechanisms (for example, “Cancer-related signalling”), many of which have overlapping signalling pathways. More specific signalling pathways that were identified and the pathway members that were differentially expressed are shown in Table 28. These include Cell adhesion molecules, Cell cycle, Wnt signalling, ErbB signalling, RNA degradation, Regulation of actin cytoskeleton, and MAPK pathway signalling.

(A) Increased Pathways	Genes	P-Value	FDR
hsa04514:Cell adhesion molecules	CLDN7, HLA-DRB1, HLA-DRB3, CDH1, NEO1, HLA-DMB, CDH3, SDC4, HLA-DMA, HLA-DRB4, HLA-DRB5, CNTNAP2, HLA-DPB1, HLA-DOA, HLA-DOB, ICAM3, HLA-A, HLA-C, HLA-B, HLA-F, NCAM1, SDC1, CLDN1, CNTN1, VCAN, HLA-DPA1, JAM2	0.024	26
hsa04110:Cell cycle	CDC14B, ANAPC13, CREBBP, ANAPC4, YWHAB, SKP2, RB1, CDK7, MCM2, ORC1L, SMC3, CDC25B, CDKN1A, CDKN2A, CDKN2B, CCND2, CDKN2C, GSK3B, ABL1, GADD45A, STAG2, STAG1	0.070	59
hsa04310:Wnt signaling pathway	WNT5A, PPP2R5C, DAAM1, DAAM2, CSNK2A2, CHD8, CSNK2A1, RAC3, NFAT5, FRAT1, PPP3CB, FRAT2, CAMK2B, PLCB1, VANGL2, CREBBP, FZD2, CSNK2A1P, FZD4, PRKCB, CTNNBIP1, SFRP1, SFRP2, CCND2, GSK3B, RUVBL1	0.093	70
hsa04012:ErbB signaling pathway	MAP2K2, ERBB3, PRKCB, AKT1, LOC407835, PAK7, CBLB, CDKN1A, PLCG1, PAK2, GSK3B, NCK1, PLCG2, CAMK2B, MTOR, ABL1, PIK3R2	0.095	71
(B) Decreased Pathways	**Genes**	**P-Value**	**FDR**
hsa03018:RNA degradation	PATL1, EXOSC4, LSM7, PNPT1, EXOSC5, CNOT3, LOC647302, RQCD1, LSM3, LSM1, XRN1	0.057	52
hsa04012:ErbB signaling pathway	PIK3CB, LOC100271831, MAP2K4, RAF1, RPS6KB1, BAD, MAPK1, EIF4EBP1, CRKL, PAK2, PAK4, MAPK3, ARAF, MYC	0.075	61
hsa04810:Regulation of actin cytoskeleton	FGFR3, LOC100271831, ITGAE, LOC729841, GNA12, IQGAP2, LOC653888, CDC42, PFN2, PAK2, TIAM2, ARPC3, PAK4, CDC42P2, LOC729494, PDGFC, PDGFD, ACTN4, LIMK2, PIK3CB, RAF1, MYH9, MAPK1, ARPC1B, CRKL, CHRM3, ITGA8, ARAF, MAPK3, CYFIP1, SLC9A1	0.084	66
hsa04010:MAPK signaling pathway	MEF2C, FGFR3, LOC100271831, MAPKAPK5, GNA12, HSPA1A, HSPA1B, HSPA1L, CDC42, TNFRSF1A, FOS, MAP3K6, PAK2, CDC42P2, HSPA6, HSPA7, PPP3CC, MYC, TAOK2, TAOK1, MAP2K4, TGFBR2, ATF4C, RAF1, MECOM, FLNC, STK3, MAPK1, DUSP4, ATF4, CRKL, RPS6KA4, MAPK3, CACNA1H, RAP1B, IKBKB	0.089	68

Table 28: Genes (A) increased or (B) decreased in expression in SCLl60 cells compared to HEK293 cells are enriched for various signalling pathways. P-value is calculated within the DAVID system using a one-tail Fisher Exact test.

3.2.4 Comparison of gene expression between vehicle control- and Triptorelin-treated SCL60 cells

To identify which genes were differentially expressed in SCL60 cells as a result of Triptorelin treatment, Triptorelin-treated SCL60 cells were compared to vehicle control-treated or untreated SCL60 cells. Four replicates were generated at each of the time points (0, 0.5, 1, 2, 8 and 24h). All vehicle control and untreated (0h) samples were pooled and compared to all Triptorelin-treated samples.

An overall comparison of all the Triptorelin-treated samples with all the untreated SCL60 samples revealed that 2088 probes were significantly differentially expressed with Triptorelin treatment (1140 increased, 948 decreased, Table 29).

	Number of probes	**Minimum fold change**	**Maximum fold change**
Increased in expression with Triptorelin treatment	1140	+0.92	+16
Decreased in expression with Triptorelin treatment	948	-0.80	-2.1

Table 29: Genes that were significantly increased or decreased with Triptorelin treatment in SCL60 cells using a 5% false positive threshold.
Fold change is shown to 2 significant figures.

The range of expression (according to the signal intensity values from probe-target hybridisation) of the differentially expressed probes in untreated SCL60 cells was 37 to 22190 fluorescence units and the range in Triptorelin-treated SCL60 cells was 41 to 23402 fluorescence units. The minimum fold change of significantly differentially expressed genes was similar for increased (+0.92, CSNK1G2) and decreased (-0.80, EIF5A) genes. However, the maximum fold change of genes increased with Triptorelin treatment was much greater (+16, FOSB) than that of genes decreased (-2.1, IGFBP5) (Table 29).

An overview of the gene expression changes is shown in Figure 25. This heatmap shows the expression of the 2088 significantly differentially expressed in SCL60 cells treated with Triptorelin relative to untreated (0h) SCL60 controls. There are four replicate samples for each time point (0, 0.5, 1, 2, 8, 24h), shown from left to

right. This figure shows that most of the gene changes occur between 2 and 8h after Triptorelin treatment. Some of these gene expression changes are prolonged up to 24h, whereas others are shorter-lived. Further analysis of the time-dependent changes will be detailed later.

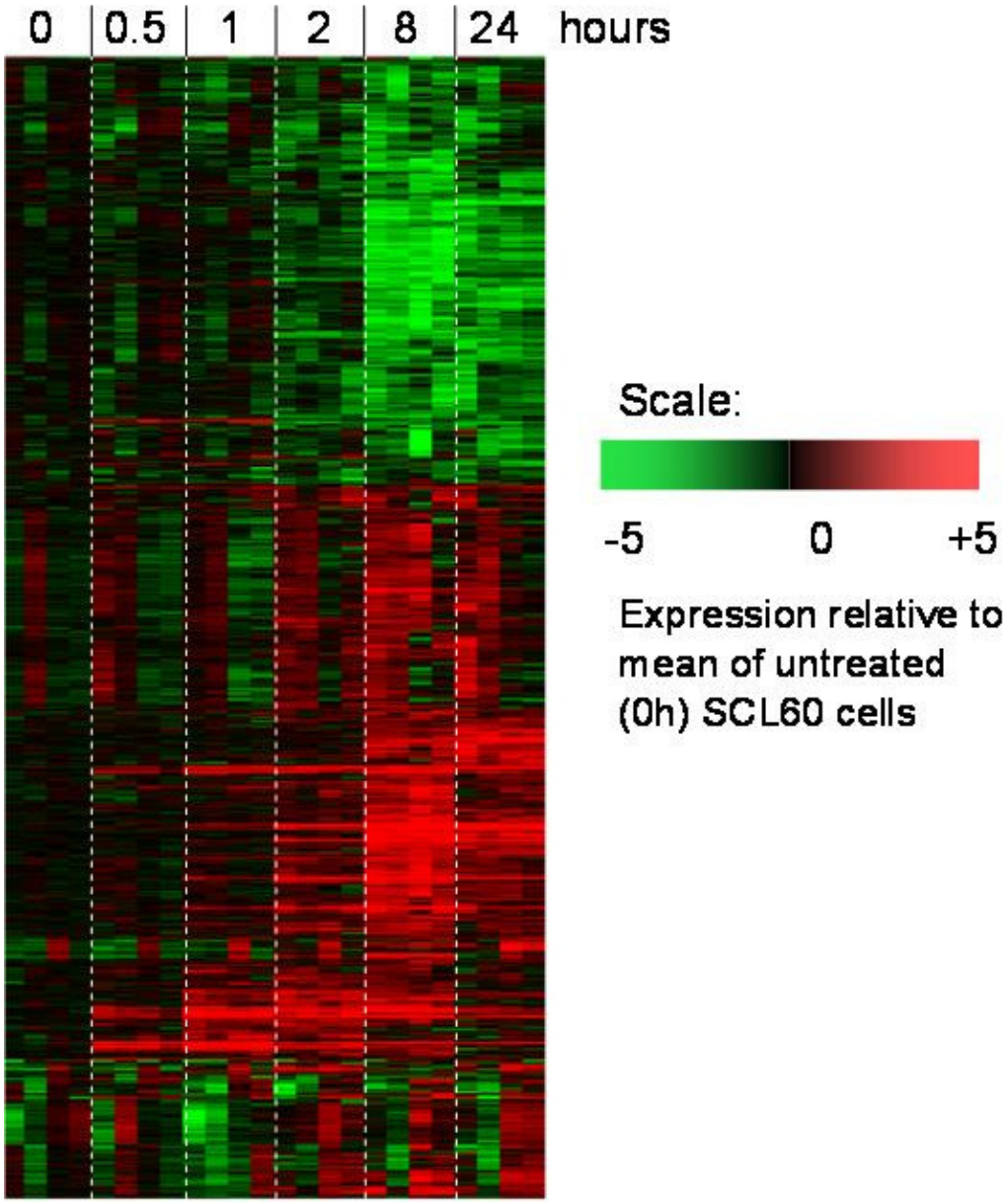

Figure 25: Heatmap showing differentially expressed probes between control and Triptorelin-treated SCL60 cells.
Samples are ordered from left to right with increasing treatment time from 0 to 24h. Four independent experiments (columns from left to right) are shown for each treatment group. Red = increased expression, green = decreased, black = unchanged expression relative to the mean of untreated (0h) controls. The range of relative expression is approximately -5 to +5, where +5 is strongly increased compared to controls and -5 is strongly decreased compared to controls. The heatmap represents the similarity between genes' temporal profiles. It is clustered to show genes that have similar temporal profiles together.

3.2.4.1 The most significantly differentially expressed genes in response to Triptorelin treatment in SCL60 cells

To explore these differentially expressed genes in more detail, the 25 probes most significantly and consistently increased and decreased in expression with Triptorelin treatment in SCL60 cells are shown in Table 30 and Table 31 respectively. The expression changes are ordered in ascending probability of each being a false positive, which for all probes in the table is less than 0.05.

The 25 most significantly increased probes (Table 30) comprise many transcription factors (FOS, FOSB, EGR1, ATF3, AXUD1, JUNB, LBH, ZFP36), as well as genes encoding IGF binding proteins (CYR61, CTGF), nuclear receptors (NR4A1, NR4A2) and ERK1/2 phosphatases (DUSP1, DUSP5). The genes represented by the 25 most significantly decreased probes (Table 31) following Triptorelin treatment are more diverse in their functions than those that are increased. They comprise a few transcription factors (HOXA13, FOXD2, ZNF503), several genes whose products may be involved in cell adhesion (AMOT, which promotes adhesion and migration [150, 151]; FLRT3, which has been shown to inhibit cadherin-mediated adhesion and increase motility [152, 153]; and LAMA5, which has been shown to promote adhesion in hepatocellular carcinoma [154]), and various other genes including IGFBP5 (IGF binding protein), MUM1 (DNA repair), FZD4 (Wnt protein receptor) and SRGAP3 (Rho GTPase activating protein).

Gene	Illumina Probe ID	Fold Change	Description
FOS	ILMN_1669523	+12	Signal transduction, Cell proliferation and differentiation
PTGS2	ILMN_2054297	+7.7	Prostanoid signalling
NR4A2	ILMN_1782305	+7.3	Nuclear receptor
CYR61	ILMN_2188264	+8.2	Secreted apoptosis/adhesion modulator
FOSB	ILMN_1751607	+16	Signal transduction, Cell proliferation and differentiation
EGR1	ILMN_1762899	+7.5	Transcription factor
CGA	ILMN_1734176	+8.2	Follicle Stimulating Hormone subunit alpha
ATF3	ILMN_2374865	+4.2	Transcription factor
CTGF	ILMN_1699829	+5.2	IGF binding protein. Cell proliferation and adhesion
DUSP1	ILMN_1781285	+4.4	ERK2 inhibitor
CCL2	ILMN_1720048	+3.9	Cytokine
NR4A2	ILMN_2339955	+4.2	Nuclear receptor
LOC387763	ILMN_1677402	+4.2	Unknown
DUSP5	ILMN_1656501	+3.9	ERK1 inhibitor
CTGF	ILMN_2115125	+4.7	IGF binding protein. Cell proliferation and adhesion
AXUD1	ILMN_1703123	+3.2	Transcription, apoptosis
TAC1	ILMN_2384409	+5.1	Neurotransmitter
JUNB	ILMN_2086077	+3.0	Transcription factor
LBH	ILMN_2315979	+4.6	Trascription factor
IL8	ILMN_2184373	+3.6	Chemokine
NR4A1	ILMN_2408566	+3.4	Nuclear receptor
ARC	ILMN_1711120	+3.0	Cytoskeleton-associated protein
PTGS2	ILMN_1677511	+3.0	Prostanoid signalling
ZFP36	ILMN_1720829	+2.4	Transcripton factor
RGS2	ILMN_2197365	+2.5	Regulator of G-protein signalling

Table 30: The 25 probes with the most significant increases in expression in SCL60 Triptorelin-treated cells compared to SCL60 control cells.
The gene changes are ordered in ascending probability of each being a false positive, which for all genes in the table is less than 0.05 (not shown). Gene descriptions were taken from the GeneCards online database [151].

Gene	Illumina Probe ID	Fold Change	Description
DDIT4	ILMN_1661599	-1.7	Inhibits cell growth (downstream of AKT)
IGFBP5	ILMN_1750324	-2.1	IGF binding protein. May inhibit or promote cell growth
IGFBP5	ILMN_2132982	-1.9	IGF binding protein. May inhibit or promote cell growth
HOXA13	ILMN_1731349	-1.6	Transcription factor. Anterior-posterior development
LRRC20	ILMN_1690523	-1.7	Unknown
CBX2	ILMN_1770678	-1.6	Transcriptional repressor
PUNC	ILMN_1744635	-1.6	Immunoglobulin
AMOT	ILMN_1792409	-1.6	Tight junction maintenance
MUM1	ILMN_1764764	-1.5	DNA repair
C5ORF13	ILMN_1680738	-1.5	Unknown
FOXD2	ILMN_1789400	-1.5	Transcription factor
SESN1	ILMN_1800626	-1.5	P53-mediated inhibition of cell growth via AMPK and MTOR.
FLRT3	ILMN_1805665	-1.5	Transmembrane protein. Possibly cell adhesion or receptor signalling
DHRS3	ILMN_1752478	-1.5	Short-chain dehydrogenase/reductase
IFIT1	ILMN_1707695	-1.5	IFN-induced protein
FZD4	ILMN_1743367	-1.5	Receptor for Wnt proteins
HS.208066	ILMN_1877593	-1.5	Unknown
SRGAP3	ILMN_2400644	-1.5	Rho GTPase activating protein
ZNF503	ILMN_1787265	-1.4	Transcription factor
SMAD6	ILMN_1767068	-1.4	Negatively regulates BMP and TGF-beta signalling
GUCY1A3	ILMN_1808590	-1.5	Catalyses GTP to cGMP
RGMA	ILMN_1717636	-1.5	Axon guidance. Possible tumour suppressor
NME3	ILMN_1669456	-1.5	Synthesis of nucleotide triphosphates. Possibly induction of apoptosis
SAMD11	ILMN_1709067	-1.4	Unknown
LAMA5	ILMN_1773567	-1.4	Laminin subunit α5. ECM component, binds collagen and integrin α2β1. Cell adhesion and migration.

Table 31: The 25 probes with the most significant decreases in expression in SCL60 Triptorelin-treated cells compared to SCL60 control cells.
The gene changes are ordered in ascending probability of each being a false positive, which for all genes in the table is less than 0.05 (not shown). Gene descriptions were taken from the GeneCards online database [151].

3.2.4.2 Temporal profiles of genes differentially expressed with Triptorelin treatment in SCL60 cells

The gene lists in Table 30 and Table 31 were produced using data from all the Triptorelin-treated cells (all the time-points together). However, by pooling these samples some information is lost because the gene expression changes do not occur uniformly across the 24h treatment period (Figure 25).

Figure 26 shows the numbers of probes that were differentially expressed at each time point and it is clear from this that most of the expression changes occur around the 8h time-point. The number of differentially expressed probes between SCL60 control and treated cells increases up to 8h post-treatment then begins to fall (Figure 26). The proportion of these that are decreased is initially very low, increasing to account for approximately half of the differentially expressed probes by 8h.

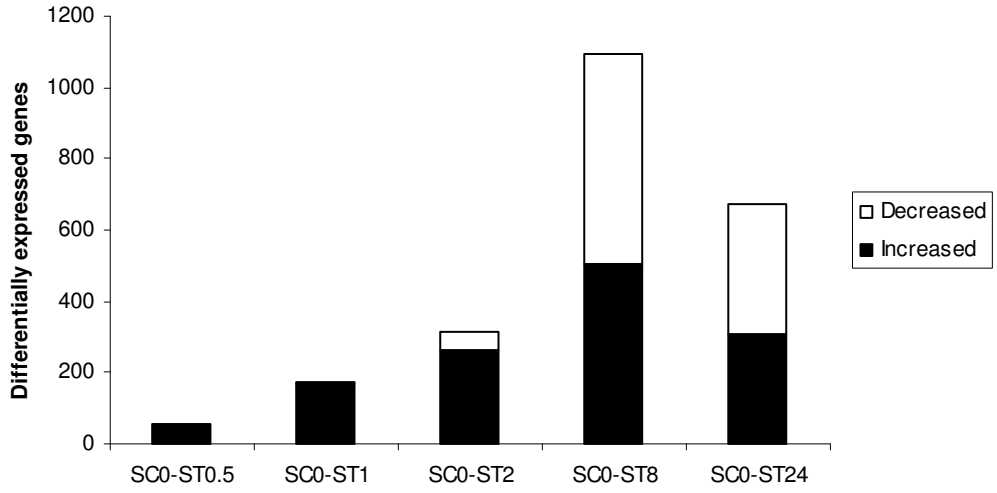

Figure 26: The number of differentially expressed probes changed between untreated (0h) SCL60 cells and Triptorelin-treated SCL60 cells at five time points using a 5% false positive threshold.
SC0 = SCL60 untreated (0h) control, STx = SCL60 treated with Triptorelin for x hours.

The temporal profiles of the top 25 increased and decreased probes are shown in Figure 27 and Figure 28. The 25 probes that were increased in expression with Triptorelin treatment clustered into three distinct groups by their temporal profile: early, mid and late changes (Figure 27). Figure 28 shows that the 25 most significantly decreased probes decreased most strongly at 8 and 24h.

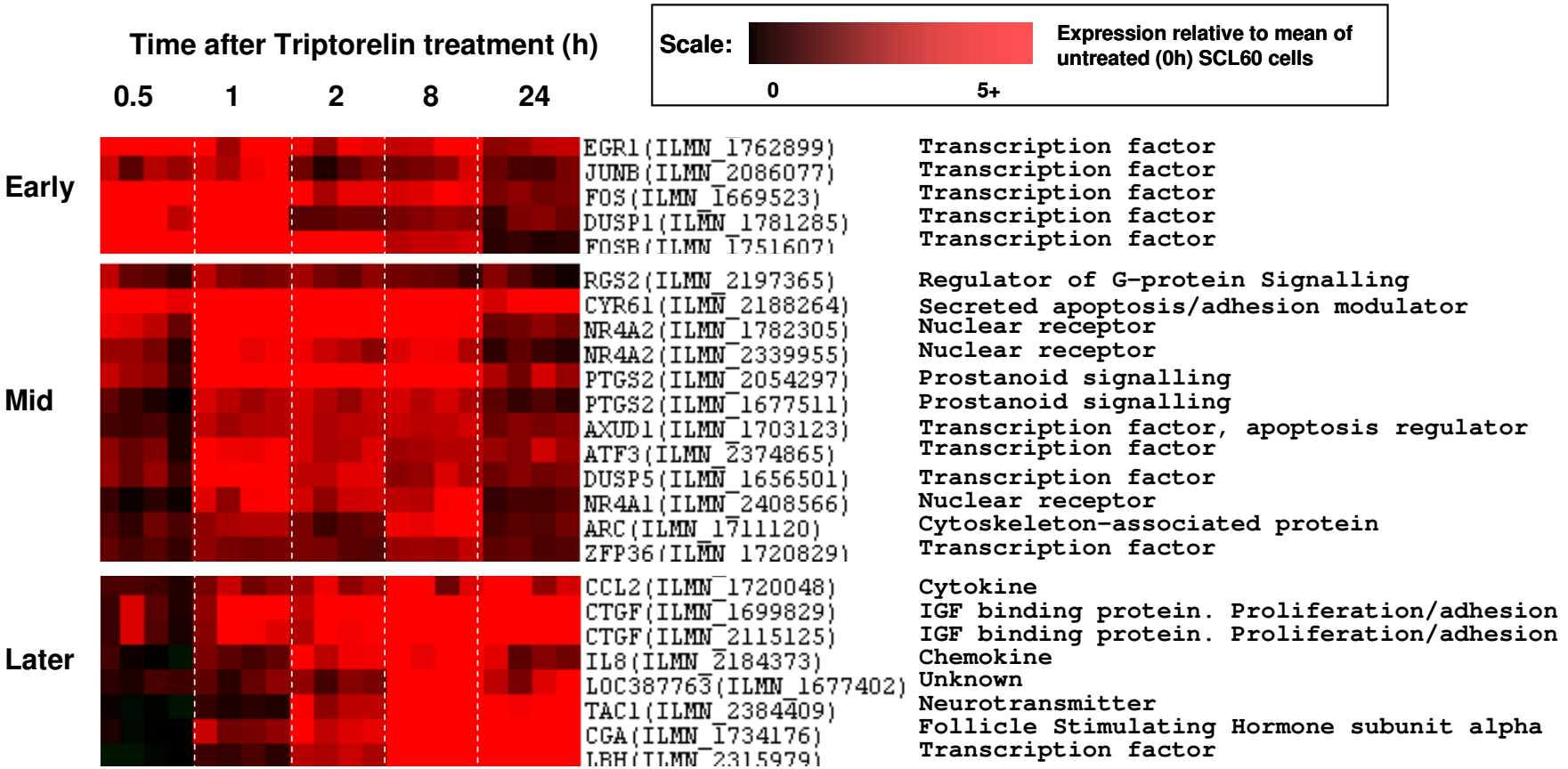

Figure 27: Heatmap to show the 25 probes most significantly increased in Triptorelin-treated SCL60 cells compared to control SCL60 cells.
Samples are ordered from left to right with increasing treatment time from 0 to 24h. Four independent experiments (columns from left to right) are shown for each treatment group. Red = increased expression, black = unchanged expression relative to the mean of untreated (0h) controls. The range of relative expression is approximately 0 to 5+. The heatmap represents the similarity between genes' temporal profiles. It is clustered to show genes that have similar temporal profiles together. These probes clustered into three distinct groups by their temporal profile: early, mid and late changes.

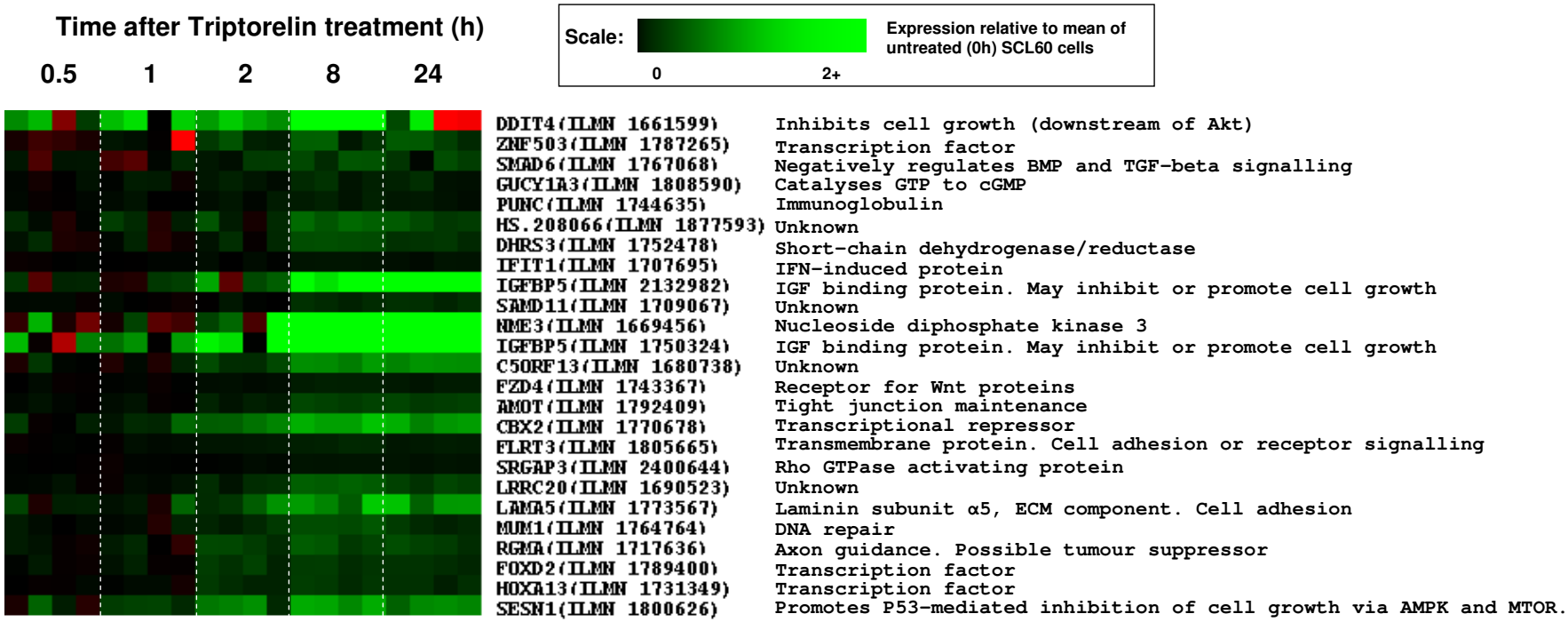

Figure 28: Heatmap to show the 25 probes most significantly decreased in Triptorelin-treated SCL60 cells compared to control SCL60 cells. Samples are ordered from left to right with increasing treatment time from 0 to 24h. Four independent experiments (columns from left to right) are shown for each treatment group. Red = increased expression, black = unchanged expression relative to the mean of untreated (0h) controls. The range of relative expression is approximately 0 to 5+. The heatmap represents the similarity between genes' temporal profiles. It is clustered to show genes that have similar temporal profiles together. These probes decreased most strongly at 8 and 24h.

3.2.4.3 Functional annotation of genes differentially expressed with Triptorelin treatment in SCL60 cells

The 25 most significantly increased and decreased probes might feasibly contain some of the most important genes in the transcriptional response to GnRHR signalling, therefore warranting the detailed annotation given above (Table 30, Table 31, Figure 27 and Figure 28). However, 2088 probes (representing 1048 genes) were significantly differentially expressed between Triptorelin-treated and control SCL60 cells and it is important to explore common functions among these genes as many of these are also likely to be important in helping to understand GnRHR signalling.

The online pathway annotation tool, DAVID [137], was used to determine whether there was significant enrichment for any pathways among the genes differentially expressed between SCL60 control and treated cells. Using an unadjusted P-value of less than 0.05 from a one-tailed Fisher exact test as significant, 5 increased pathways (Table 32A) and 5 decreased pathways (Table 32B) were identified.

Genes significantly increased with Triptorelin treatment in SCL60 cells were enriched for Cell cycle, p53 signalling, Nucleotide Oligomerisation Domain (NOD)-like receptor signalling, MAPK signalling, and Retinoic acid-Inducible Gene-I (RIG-I)-like receptor signalling pathways (Table 32A). Genes significantly decreased with Triptorelin treatment in SCL60 cells were enriched for Cell cycle, Notch signalling, ErbB signalling, Wnt signalling and Extracellular Matrix (ECM)-interaction pathways (Table 32B).

	Genes	P-Value	FDR
(A) Increased Pathways			
hsa04110:Cell cycle	CDK1, ANAPC10P1, CDC14A, CDC14B, CCNH, ANAPC10, YWHAE, CCNE2, LOC440917, CCNB1, CDKN1A, YWHAG, MAD2L1, ORC6L, MDM2, CCNA1, GADD45B, MYC, GADD45A, BUB3	0.001	0.75
hsa04115:p53 signaling pathway	CCNE2, CCNB1, CDK1, CDKN1A, CASP9, RRM2, MDM2, PMAIP1, GADD45B, SESN2, THBS1, GADD45A	0.001	1.7
hsa04621:NOD-like receptor signaling pathway	MAP3K7, HSP90B1, **CCL2, IL8**, CXCL2, CCL8, NFKBIA, TRAF6, BIRC2, CHUK, CCL7	0.002	2.8
hsa04010:MAPK signaling pathway	MAPKAPK5, NFKB2, SRF, MAP3K7, **FOS**, DUSP14, JUND, MAP3K8, TRAF6, MYC, CHUK, RELB, ATF4C, **NR4A1**, FLNC, DDIT3, DUSP5, ATF4, DUSP3, DUSP1, RRAS2, LOC100133211, JUN, RAP1B, GADD45B, DUSP8, GADD45A	0.02	18
hsa04622:RIG-I-like receptor signaling pathway	MAP3K7, DDX3X, ISG15, **IL8**, IL12A, NFKBIA, TRAF6, CHUK, AZI2, TANK	0.02	20
(B) Decreased Pathways			
hsa04110:Cell cycle	E2F2, LOC100133012, CDC14B, CREBBP, PRKDC, MCM2, CHEK2, YWHAE, MCM4, MCM5, LOC440917, RAD21, CDKN2A, EP300, MCM7, CDKN1B, CDKN2B, LOC646096, LOC731751, ABL1	5E-04	0.66
hsa04330:Notch signaling pathway	NOTCH3, CTBP1, NOTCH1, EP300, APH1A, CREBBP, JAG2, NCOR2	0.005	6.1
hsa04012:ErbB signaling pathway	LOC407835, CBLB, NRG4, CDKN1B, PAK2, PLCG1, ERBB3, MAP2K2, CAMK2G, PLCG2, ABL1	0.02	19
hsa04310:Wnt signaling pathway	WNT5A, FZD8, CTBP1, PPP2R5D, CAMK2G, CREBBP, VANGL2, FZD2, **FZD4**, CTNNBIP1, EP300, PRICKLE1, FRAT2, TBL1X	0.02	23
hsa04512:ECM-receptor interaction	SDC1, COL4A1, **LAMA5**, COL6A1, ITGB5, COL2A1, AGRN, COL4A6, HMMR	0.04	38

Table 32: Genes significantly (A) increased and (B) decreased with Triptorelin treatment in SCL60 cells were enriched for various signalling pathways. P-value was calculated within the DAVID system using a one-tail Fisher Exact test and is shown to 1 significant figure. False Discovery Rate (FDR) was also calculated within the DAVID system and is shown to 2 significant figures. Genes in bold type occur in the 25 most increased or decreased probes (Figure 27, Figure 28, Table 26, and Table 27).

To further explore the dynamic nature of the GnRHR-mediated signalling response, the most significantly differentially expressed genes were identified at each time point (0.5, 1, 2, 8 and 24h) compared to the previous time point following Triptorelin treatment in SCL60 cells (Table 33). Initial gene expression increases include transcription factors such as EGR1 and FOS, as well as the ERK1/2 inhibitors DUSP1 and DUSP5, and the IGF binding protein CYR61. Between 1 and 2h after treatment, expression of transcription factors EGR2, FOS and JUN, as well as DUSP1 is decreased. Between 2 and 8h there is a significant increase in expression of MMP10, which encodes a matrix metalloproteinase. The transcription factor DDIT3 is decreased at 8h but increased by 24h. At 24h the cytoskeletal protein encoding gene, ENAH, is increased whereas another cytoskeletal-associated protein encoding gene, ARC, is decreased (Table 33).

The gene lists of differential gene expression for each time point are much more limited than the lists for pooled data. They are less likely, therefore, to contain sufficient members of a particular pathway for the gene list to be considered enriched for that pathway. Nevertheless, several pathways were identified in these genes lists including the MAPK signalling pathway and cell cycle signalling. A full list of these pathways is shown in Appendix A Table 4.

	Gene	Illumina ID	Fold change	Description
SC0 to ST0.5				
Increased	FOS	ILMN_1669523	+55	Signal transduction, Cell proliferation and differentiation
	FOSB	ILMN_1751607	+46	Signal transduction, Cell proliferation and differentiation
	EGR1	ILMN_1762899	+14	Transcription factor
	CYR61	ILMN_2188264	+11	IGF binding protein. Cell proliferation and adhesion
	DUSP1	ILMN_1781285	+8.3	ERK2 inhibitor
ST0.5 to ST1				
Increased	NR4A1	ILMN_2408566	+4.8	Nuclear receptor
	PTGS2	ILMN_2054297	+4.3	Prostanoid signalling
	DUSP5	ILMN_1656501	+3.9	ERK1 inhibitor
	EGR3	ILMN_1722781	+4.0	Transcription factor
	NR4A2	ILMN_2339955	+3.8	Nuclear receptor
Decreased	FAM115A	ILMN_2297069	-1.9	Unknown
	LOC642333	ILMN_1696027	-1.7	Unknown
ST1 to ST2				
Increased	TAC1	ILMN_2384409	+3.5	Neurotransmitter
	IL8	ILMN_2184373	+3.2	Chemokine
	TAC1	ILMN_2342541	+3.0	Neurotransmitter
	TNFRSF12A	ILMN_1689004	+2.7	Tweak receptor. FGF inducible
	IL8	ILMN_1666733	+2.8	Chemokine
Decreased	EGR2	ILMN_1743199	-5.5	Transcription factor
	FOS	ILMN_1669523	-5.3	Signal transduction, Cell proliferation and differentiation
	DUSP1	ILMN_1781285	-4.6	ERK2 inhibitor
	C10ORF10	ILMN_1767556	-3.4	Activates transcription factor Elk1
	JUN	ILMN_1806023	-3.3	Transcription factor

Table 33: The top five increased and decreased Illumina probes between each time point using a 5% false positive threshold.
SC0 = SCL60 untreated (0h) control, STx = SCL60 treated with Triptorelin for x hours. The gene changes are ordered in ascending probability of each being a false positive, which for all genes in the table is less than 0.05 (not shown). Gene descriptions were taken from the GeneCards online database [151].

ST2 to ST8	Gene	Illumina ID	Fold change	Description
Increased	MMP10	ILMN_1741847	+14	Extracellular matrix degradation
	TAC1	ILMN_2384409	+11	Neurotransmitter
	TAC1	ILMN_2342541	+9.8	Neurotransmitter
	LOC387763	ILMN_1677402	+8.7	Unknown
	TAC1	ILMN_1790270	+8.6	Neurotransmitter
Decreased	FOSB	ILMN_1751607	-12	Signal transduction, Cell proliferation and differentiation
	DDIT3	ILMN_1676984	-5.6	Transcription factor. Stress-induced apoptosis
	HERPUD1	ILMN_2374159	-4.1	Endoplasmic reticulum. Ubiquitin-like
	HERPUD1	ILMN_2374164	-4.0	Endoplasmic reticulum. Ubiquitin-like
	IGFBP5	ILMN_2132982	-3.2	IGF binding protein. May inhibit or promote cell growth
ST8 to ST24				
Increased	DDIT4	ILMN_1661599	+4.6	Inhibits cell growth (downstream of AKT)
	H1F0	ILMN_1757467	+3.5	Histone
	STC2	ILMN_1691884	+3.1	Calcium and phosphate transport/homeostasis
	DDIT3	ILMN_1676984	+3.4	Transcription factor. Stress-induced apoptosis
	ENAH	ILMN_1716552	+2.7	Actin-associated. Cytoskeletal remodelling, migration
Decreased	TAC1	ILMN_2342541	-5.2	Neurotransmitter
	ARC	ILMN_1711120	-4.6	Cytoskeleton-associated protein
	NR4A2	ILMN_1782305	-4.4	Nuclear receptor
	TAC1	ILMN_2384409	-4.9	Neurotransmitter
	LOC387763	ILMN_1677402	-4.5	Unknown

Table 33 (continued): The top five increased and decreased Illumina probes between each time point using a 5% false positive threshold.
SC0 = SCL60 untreated (0h) control, STx = SCL60 treated with Triptorelin for x hours. The gene changes are ordered in ascending probability of each being a false positive, which for all genes in the table is less than 0.05 (not shown). Gene descriptions were taken from the GeneCards online database [151].

3.2.5 Comparison of genes differentially expressed as a result of Triptorelin treatment with genes differentially expressed in a similar study

To establish whether Triptorelin-mediated gene expression changes seen in HEK293 and SCL60 cells were more widely applicable, they were compared to a previous study by Kakar *et al* [108] that looked at gene expression in mouse pituitary gonadotrope tumour (LβT2) cells following treatment with the GnRH agonist des-gly^{10},[D-Ala^{6}]GnRH. Although that study only considered two time-points, it showed marked differences of GnRH agonist-regulated gene profiles at 1h and 24h after treatment with the GnRH agonist des-gly^{10},[D-Ala^{6}]GnRH [108]. Genes that were changed in expression encoded proteins including transcription factors, ion channel proteins, cytoskeletal proteins, and other signalling proteins such as those involved in proliferation and apoptosis [108]. Using the online gene ID conversion tool, DAVID [137], human homologues could be identified for 59 of the 67 mouse genes reported as differentially expressed (with a fold change of 4 or greater). The 8 mouse genes that could not be mapped were U85993, AI835098, AA682038, AI846236, AI428936, AW122517, 5031401C21Rik and Skir. The 59 official human gene symbols were converted to Illumina IDs to produce a list of 222 Illumina IDs (the number of Illumina IDs was greater than the number of official gene symbols because multiple probes exist for each gene).

A subset of the GnRH-regulated genes defined by Kakar *et al* in LβT2 cells were also significantly differentially expressed between control and Triptorelin-treated SCL60 cells (21 out of 59) and between HEK293 and SCL60 cells (17 out of 59), including the early response genes EGR1, FOSB, JUNB and IER2 (Table 34). The remainder of the Kakar *et al* genes (including for example cAMP-responsive element modulator, CREM, and Period circadian protein homolog 1, PER1) did not appear to change either between HEK293 and SCL60 cells, or between control and Triptorelin-treated SCL60 cells. However, the extent of differential gene expression in the subset of commonly changed genes was enough to cluster the SCL60 control and Triptorelin-treated sample groups apart (Appendix A Figure 2).

	Fold Change				Fold Change		
A	**SCL60**	**Kakar 1h**	**Kakar 24h**	**B**	**SCL60 +HEK293**	**Kakar 1h**	**Kakar 24h**
ATF3(ILMN_1791346)	+1.4	+40	+2.5	**ATF3(ILMN_2374865)**	+1.3	+40	+2.5
ATF3(ILMN_2374865)	+4.2	+40	+2.5	**BTG2(ILMN_1770085)**	+1.4	+6.2	+2.5
BTG2(ILMN_1770085)	+2.4	+6.2	+2.5	**CD68(ILMN_1714861)**	-1.3		+4.5
CD68(ILMN_1714861)	+1.2		+4.5	**CDKN1A(ILMN_1784602)**	+1.6		+6.6
CDKN1A(ILMN_1784602)	+1.5		+6.6	CHERP(ILMN_1798083)	-1.3	-15	
EGR1(ILMN_1762899)	+7.5	+160		**EGR1(ILMN_1762899)**	+0.7	+160	
EGR2(ILMN_1743199)	+3.1	+4.9		FER(ILMN_1789618)	-1.4	-6.0	
FOSB(ILMN_1751607)	+16.0	+25	+2.6	**FOSB(ILMN_1751607)**	+1.2	+25	+2.6
FOSL1(ILMN_1771841)	+1.4	+8.6	+2.5	FXYD5(ILMN_1704286)	+1.8		+6.0
GADD45B(ILMN_1718977)	+2.1	+6.1		FXYD5(ILMN_2309848)	+1.8		+6.0
GLA(ILMN_1766637)	+1.5		-4.8	GCNT2(ILMN_1680390)	-1.3	-4.0	
IER2(ILMN_1700584)	+2.0	+12		**GLA(ILMN_1766637)**	+1.5		-4.8
JUN(ILMN_1806023)	+1.9	+9.7		HADH(ILMN_1719906)	+1.3	-4.1	
JUNB(ILMN_2086077)	+3.0	+28		KIFC1(ILMN_2222008)	+1.3	-4.2	
KLF4(ILMN_2137789)	+1.8	+6.0		MAZ(ILMN_2409793)	-1.4		-4.5
KLF6(ILMN_1735014)	+1.4	+7.9	+2.2	PRSS23(ILMN_1797776)	+1.5		+4.7
KLF6(ILMN_1737406)	+1.4	+7.9	+2.2	TARBP2(ILMN_1729767)	-1.4	-4.6	
MNAT1(ILMN_2083243)	+1.1	+4.2		TARBP2(ILMN_2310253)	-1.4	-4.6	
NFKBIZ(ILMN_1719695)	+1.8	+7.9	+1.7	ZFP36(ILMN_1720829)	+1.3	+8.9	
NR4A1(ILMN_1661178)	+1.2	+100	+12.6				
NR4A1(ILMN_2408566)	+3.4	+100	+12.6				
NR4A1(ILMN_2410145)	+2.9	+100	+12.6				
PPP1R15A(ILMN_1659936)	+2.4	+17					
RGS2(ILMN_2197365)	+2.5	+6.0	+2.9				
ZFP36(ILMN_1720829)	+2.4	+8.9					

Table 34: Genes commonly significantly differentially expressed in both the SCL60 dataset and the Kakar *et al* dataset.
(A) Kakar *et al* dataset and between SCL60 all control and Triptorelin-treated (0.5-24h) groups
(B) Kakar *et al* dataset and between HEK293 and SCL60 cells
Fold change is shown to 2 significant figures. Genes in bold type were differentially expressed in both A and B comparisons.

3.2.6 Discussion

Triptorelin treatment had a minimal effect on gene expression in HEK293 cells (only four probes differentially expressed). This supports the hypothesis that HEK293 cells do not respond to Triptorelin, due to their lack of GnRHR expression. It provides reassurance for the model in that observed differential gene expression in other comparisons is likely to reflect a true biological response. Given the scale of differential gene expression in other comparisons such as between HEK293 and SCL60 cells, it is likely that the gene expression changes seen in HEK293 cells with Triptorelin treatment are false positives. This indicated that the parameters chosen for identifying differential gene expression are appropriate, since they maintain a minimal level of false positive detection, whilst being broad enough to minimise the chance of falsely excluding positive gene changes.

There were 4745 probes differentially expressed (using a 5% false positive threshold) between the untreated HEK293 and untreated SCL60 cells (Table 25, Appendix A Figure 1). This large number of differentially expressed genes indicates that there are substantial differences at the transcriptomic level between the two cell lines. There is a relatively small difference between SCL60 control cells and those treated with Triptorelin, but there is a very substantial difference between the gene expression profiles of HEK293 cells and SCL60 cells. These changes in SCL60 cells compared to HEK293 cells may have occurred due to the presence of GnRHR (and/or the G418 resistance gene used in the transfection), due to damage caused by its incorporation into the DNA or due to genetic drift as a result of random events in culture, or as a result of selection pressure in culture and repeated passage. Although these alternative explanations for the differences between the two cell lines are important to consider, these gene expression differences may have been caused by the addition of a functional GnRHR. These differentially expressed genes may therefore represent important factors in mediating the antiproliferative response to Triptorelin in SCL60 cells.

The presence of adhesion-related genes in both the genes increased and decreased in SCL60 cells compared to HEK293 cells indicates that adhesion-related signalling may be relevant to the antiproliferative effect of Triptorelin in SCL60 cells. A role for cell adhesion signalling has been previously suggested by Davidson *et al* [117]. In SCL60 cells, GnRHR stimulation by GnRH-I, GnRH-II, and other GnRH agonists (but not antagonists) caused an increase in cell adherence and a change in morphology [117]. This was dependent on Tyrosine kinases and Src but not EGFR or JNK [117]. This shows that GnRH can cause cytoskeletal reorganisation and affect cell adherence. Inappropriate cytoskeletal changes, for example during mitosis, could play a role in GnRHR-mediated cell death or reduced proliferation.

The large number of transcriptional regulators that were differentially expressed indicates that GnRHR has a large influence on transcription, and that transcription may be relevant in the GnRHR-mediated antiproliferative effect in SCL60 cells. In similar gene expression studies in LβT2 cells, Kakar *et al* [108] and Wurmbach *et al* [109] found that a large proportion of the genes differentially expressed following GnRHR stimulation were transcription factors.

Also significantly increased in expression in SCL60 cells compared to HEK293 cells was the RYR3 gene, whose product forms a calcium release channel [155]. The increased expression of this gene may be particularly relevant to the GnRHR-mediated antiproliferative effect in SCL60 cells, since calcium ion release may be important in activating PKC, upon which the GnRHR-mediated antiproliferative effect is dependent [79]. However, Morgan *et al* could not demonstrate a dependence on calcium ions of the antiproliferative effect of the GnRH agonist Triptorelin with the use of a Ca^{2+} channel blocker or a Ca^{2+} chelator [79].

Approximately 8% of detected genes (represented by 2088 probes) were differentially expressed between control and Triptorelin-treated SCL60 cells. This indicates that Triptorelin has a large impact on gene transcription in SCL60 cells. However, changes in expression were not uniform and most changes occurred between 2 and 8h after treatment (Figure 25, Figure 26). Genes with the most

increased expression after Triptorelin treatment clustered into three groups: early, mid and late changes (Figure 27), whilst repressed genes tended to decrease later in the 24h treatment period (Figure 28). It is possible that these genes may be decreased in a secondary response to some of the gene activations seen as an immediate response to GnRHR stimulation.

The altered expression of IGF binding proteins (Table 30, Table 31) could be an indication of the involvement of RTK signalling pathways in the GnRHR-mediated response, or it may be involved in mediating changes in cellular adhesion through interaction with integrin [156, 157]. Interestingly, GnRHR stimulation caused an 8.2 fold increase in expression of CGA (Table 30), which encodes the FSHα subunit [151]. This may indicate that there is some similarity between GnRHR signalling in SCL60 cells and GnRHR signalling in pituitary gonadotropes, which normally induces FSH and LH production.

Immediately following GnRHR stimulation in SCL60 cells *in vitro*, there is an intense and rapid increase in ERK1/2 phosphorylation [79]. The increased expression of early response genes such as FOS and EGR1 supports this, since it has previously been shown that when ERK1/2 is phosphorylated it translocates to the nucleus and activates various transcription factors such as these [8, 9]. FOS gene family members encode proteins that dimerise with proteins of the JUN family to form the transcription factor complex AP-1 [158]. The increased expression of both FOS and JUN family members (Table 33) make this a possible mechanism of transcriptional activation in SCL60 cells.

Given the intense ERK1/2 response, it was interesting to observe the increase in gene expression of dual specificity phosphatases, DUSP1 and DUSP5 (Table 33), whose protein products inhibit ERK2 and ERK1 respectively by dephosphorylation [151]. It is possible that these may be involved in mediating a negative feedback response to the initial MAPK activity. DUSP1 and DUSP5 activation following GnRHR stimulation is supported by the findings of Armstrong *et al*, who observed a marked increase in DUSP1, DUSP2 and DUSP5 mRNA expression following GnRH

treatment in cervical cancer-derived HeLa cells [159]. The increase in expression peaked at 1h after treatment before gradually reducing to basal levels. The authors also observed a slower increase in DUSP4, peaking at 4h after treatment.

GnRH has been shown to activate EGR1 via ERK1/2 in HeLa cells [160]. In HeLa cells, GnRH causes increased mRNA expression of DUSP1 and DUSP4 [160]. Armstrong *et al* showed that the increase in DUSP1 appeared to be reliant on endogenous ERK1/2, whereas that of DUSP4 was not [160]. In that study by Armstrong *et al*, when DUSP1, -2, and -4 were knocked out individually or together there was no change in Egr1 luciferase or pERK1/2 activity [160], arguing against a role for these DUSPs in mediating the ERK1/2 response to GnRH. However, the authors also screened 16 DUSPs for involvement in regulating the ERK1/2 response to GnRH and found that five of these influenced the amplitude of pERK1/2 or the localisation of ERK2 following GnRHR stimulation [160]. This suggests that there may be a role for DUSPs in response to GnRHR stimulation, but it may involve multiple DUSPs and it may be complicated by multiple interacting signalling pathways.

RGS2 expression was increased in SCL60 cells with Triptorelin treatment. This gene product is known to regulate G protein signalling [161, 162]. An increase in RGS2 expression in response to GnRHR stimulation was also identified by Wurmbach *et al* and Kakar *et al* in LβT2 cells [108, 109]. Interestingly, PKC is known to phosphorylate and inhibit RGS2 [163]. In SCL60 cells, the antiproliferative effect of the GnRH agonist Triptorelin is known to be dependent on PKC [79]. RGS2 transcript levels may increase as a result of protein inhibition by PKC.

The gene SRGAP3 encodes a Rho GTPase activating protein, which may inhibit the activity of G-proteins associated with GnRHR. This gene was decreased in expression with Triptorelin treatment. If this decrease in gene expression corresponded to a decrease in functional protein activity, it would act to prevent the inhibition of GnRHR, arguing against a role for this protein product in down-regulating GnRHR to mediate the antiproliferative effect of a GnRH agonist.

Genes significantly increased with Triptorelin treatment in SCL60 cells were enriched for Cell cycle, p53 signalling, NOD-like Receptor signalling, MAPK signalling and RIG-I-like receptor signalling pathways (Table 32A). Genes significantly decreased with Triptorelin treatment in SCL60 cells were enriched for Cell cycle, Notch signalling, ErbB signalling, Wnt signalling and ECM-interaction pathways (Table 32B).

The identification of the Wnt signalling pathway was interesting, as a recent study (of LβT2 cells) showed that GnRH-mediated LHB (Luteinising Hormone β subunit) transcription requires the activity of β-Catenin, a key member of the Wnt signalling pathway [164]. Nuclear accumulation of β-Catenin and up-regulation of Wnt-target genes has been shown to occur in response to GnRH agonist treatment in SCL60 and LβT2 cells [165].

No previous study has implicated RIG-I like receptor signalling, NOD-like receptor signalling or Notch signalling in mediating the antiproliferative effects of GnRH agonist. RIG-I-like and NOD-like receptors are pattern recognition receptors, usually involved in the detection of viral RNA [166, 167], therefore their relevance here is uncertain. Notch signalling is usually activated through direct cell-cell contact, and is involved in cell fate and developmental processes [168]. Notch signalling is dysregulated in several cancers, and may act to inhibit or promote cell proliferation (reviewed in [169]).

Involvement of cell cycle genes is supported by the observation of G_2/M arrest following Triptorelin treatment in SCL60 cells (Figure 16) [50, 79]. Cell cycle pathway members that are increased in expression in SCL60 cells following treatment with Triptorelin include several that encode proteins required for mitosis (CDC14A, CDC14B, ANAPC10, ANAPC10P1, and ORC6L). However, MAD2L1 is increased, which encodes a protein that forms part of the spindle assembly checkpoint and prevents anaphase until chromosomes are properly aligned [151]. BUB3 is also increased, whose product also forms part of the mitotic checkpoint to

prevent inappropriate transition to anaphase [170], and has a role in the attachment of kinetochores to microtubules [170] and dynein [171]. Also of interest is the increased expression of GADD45A and GADD45B. These genes have both been shown to activate the p38/JNK pathway to cause G_2/M arrest [172, 173], and GADD45B has been shown to play a role in mediating Fas-induced apoptosis by enhancing the interaction between p38 and Rb [173]. The temporal gene expression profiles of these selected significantly differentially expressed probes of interest from the cell cycle pathway are shown in Figure 29.

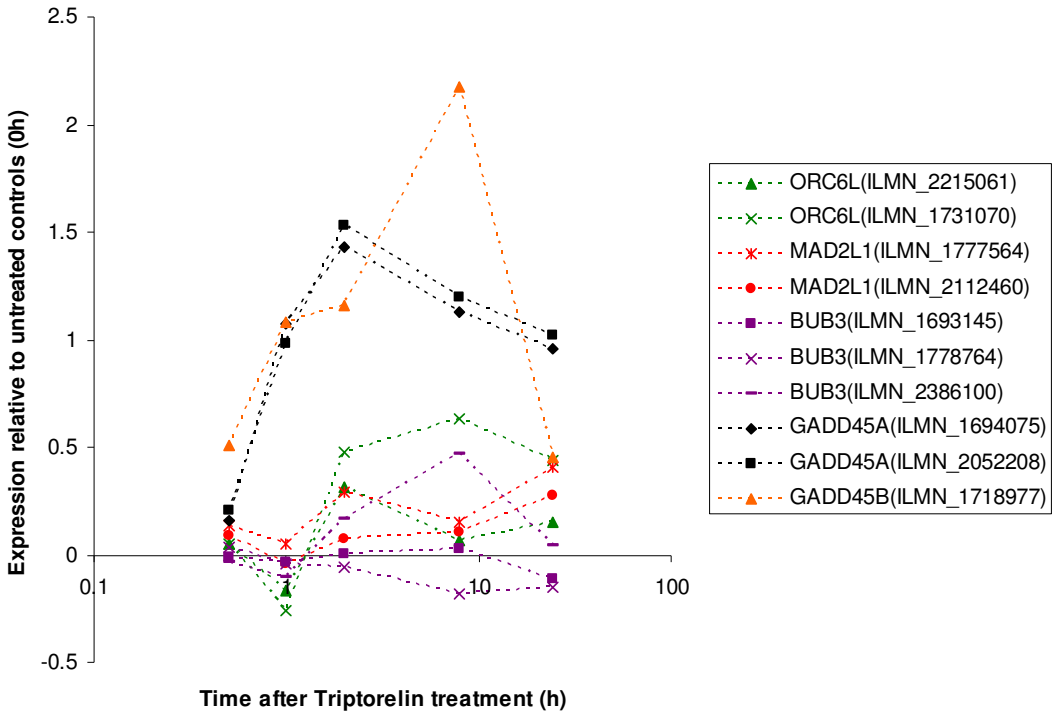

Figure 29: Time-course gene expression profile of selected cell cycle pathway members. The graph shows gene expression relative to the mean expression of each gene in of untreated controls along the y axis. Time is shown along the x axis on a log scale.

CCNB1 and CCNE2 are increased, and both are required for cell cycle progression for G_1 to S and G_2 to M transition respectively; also CDK1 is increased, which is required for cell cycle progression through G_1/S and G_2/M [151]. CDKN1A encodes an inhibitor of cyclin-CDK2 and CDK4 complexes, therefore inhibiting G_1 progression [151]. Of the cell cycle genes that are decreased, several are inhibitors of cell cycle progression such as CHEK2 and CDC14B, which are known to prevent entry into mitosis and CDKN1B and CDKN2A, which can cause cell cycle arrest in

G_1 or S phase [151]. This indicates that Triptorelin caused a decrease in cell cycle-inhibiting genes and contrasts with the cell cycle arrest observed previously. However there is also a decrease in E2F2, which normally drives transcription of genes such as cyclin E, and thus progression through G_1 to S phase [115, 151]. Some of the gene expression changes appear to promote the cell cycle, whilst others inhibit it. It is unclear which of these gene changes are the most important in mediating the antiproliferative response to Triptorelin, although the differential gene expression with Triptorelin treatment indicates that cell cycle signalling may be involved.

In a study to look at the response to UVC radiation-induced DNA damage, human skin fibroblast cells underwent cell cycle arrest (low dose) or apoptosis (high dose) [174] and transcriptional events were markedly different in the two groups of cells. Those cells that received a low dose of radiation and underwent cell cycle arrest showed a transient transcriptional response followed by recovery to basal levels by 24h [174]. Cell cycle-associated genes that exhibited altered (increased) expression levels included CCNE1, TOB1, ZNF263, CDKN1A, SNK and BTG2 [174]. CDKN1A (+1.5 fold) and BTG2 (+2.4 fold) were also significantly increased in SCL60 cells with Triptorelin treatment. The cells that received the high dose of radiation and underwent apoptosis exhibited transcriptional changes that persisted at 24h (the authors did not study transcription after 24h). Gene expression increases in these cells included GADD45A (growth arrest and DNA damage inducible α) and ATF3 (transcriptional activator), which were also both increased in SCL60 cells following Triptorelin treatment.

In SCL60 cells, many of the transcriptional changes induced by Triptorelin are transient, and the gene expression returns to basal levels by 24h. However, consistent with the fibroblasts described above, there are other genes whose expression is altered in a more prolonged manner, whereby the expression levels continue to be increased or decreased at 24h.

Interestingly, BTG2, ATF3 and CDKN1A were also increased in expression in the Kakar *et al* dataset in response to GnRHR stimulation [108]. BTG2 negatively

controls G_1 to S phase transition by inhibiting the Cyclin D1 promoter [175, 176]. CDKN1A can cause cell cycle arrest in G_1 or S phase; it binds and blocks the activity of MDM2, and blocks transcriptional activation by MYC, E2F1. GADD45A transcript levels are increased after growth arrest, this protein can activate the p38/JNK pathway. ATF3 is a transcriptional activator. These gene changes indicate one way in which Triptorelin could potentially cause cell cycle arrest.

To further explore how aberrant gene expression following GnRHR stimulation may explain the cell cycle arrest and apopotosis described in section 3.1, genes belonging to selected functional categories were identified from the genes that were significantly differentially expressed with Triptorelin treatment in SCL60 cells. Transcription factors, regulators of apoptosis, G1/S phase progression, G2/M phase progression and cytoskeletal/adhesion signalling were selected. The most strongly and consistently increased and decreased genes belonging to these functional categories are shown in Figure 30.

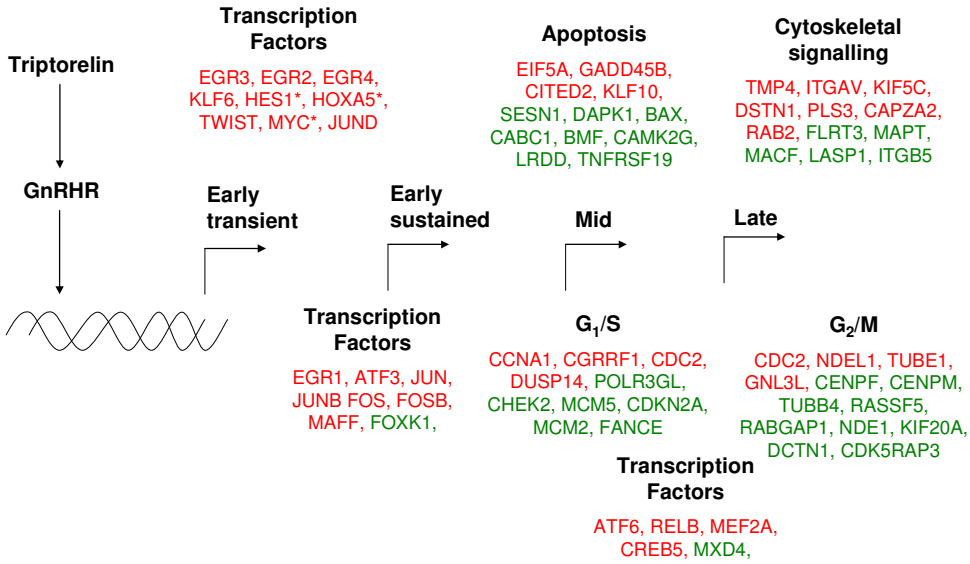

Figure 30: The order of differential expression of genes in selected functional categories following Triptorelin treatment in SCL60 cells
Transcription factors were altered in expression at both early and later phases following Triptorelin treatment. Genes involved in apoptosis and G_1/S signalling were altered in expression around 1-8h after treatment, whereas expression of cytoskeletal and G_2/M related genes was changed around 8-24h. Red indicates increased expression with Triptorelin treatment, green indicates decreased expression. * indicates that the gene initially (0.5-1h after treatment) increased in expression, followed by profoundly decreasing in expression below 0h control levels.

Genes encoding transcription factors tended to be altered in expression level very early (0.5-1h) after treatment with Triptorelin. Many of these transcription factors were increased in expression, although some decreased. Some (such as EGR2, EGR3, EGR4 and KLF6) were transiently increased or decreased, and some were initially increased in one direction followed by a profound decrease below 0h levels (such as HES1, HOXA5 and MYC). The expression level of other transcription factor genes remained elevated (such as EGR1, ATF3 and FOS) or reduced (such as FOXK1) for up to 24h after treatment. Genes involved in apoptosis (such as EIF5A, GADD45B and CABC1) and G_1/S phase signalling (such as CCNA1, CGRRF1, POLR3GL, CHEK2 and MCM5) tended to change in expression level 1-8h after treatment, but were more variable in their temporal profiles. Genes encoding proteins normally involved in cytoskeletal signalling and adhesion processes (such as TMP4, ITFAV, MAPT and ITGB5) were differentially expressed later in the 24h time course, as were genes involved in G_2/M phase progression (such as CDC2, NDEL1, CENPF and NDE1).

The differentially expressed genes shown in Figure 30 that are involved with G_2/M progression may help to explain how Triptorelin may dysregulate gene expression to cause G_2/M arrest in SCL60 cells. CENPF, CENPM, TUBB4, RASSF5, RABGAP1, NDE1, KIF20A, and DCTN1 are either components of the kinetochore (to which spindle fibres attach during mitosis), or regulate the dynamics of spindle assembly [151]. These genes are decreased in expression with Triptorelin treatment, and due to their involvement in mitosis, insufficient levels of these could potentially result in cell cycle arrest at G_2/M. CDC2, which is increased, could also be involved, as it inhibits the assembly of chromosomes at the spindle midzone [177].

Over half of the genes represented on the Illumina HT-12 beadarray are represented by more than one probe, and seeing multiple probes representing the same gene in the lists of most differentially expressed probes can increase confidence that these are reproducible changes. There was good agreement between the SCL60 and LβT2 response to GnRHR stimulation despite the use of different cell lines and GnRH agonists [108]. A subset of the GnRH-regulated genes defined by Kakar *et al* in

another system (LβT2 cells) [108] was significantly differentially expressed between control and Triptorelin-treated SCL60 cells and between HEK293 and SCL60 cells, including the early response genes EGR1, FOSB, JUNB and IER2 (Table 34, Appendix A Figure 2). This suggests that, at least at the transcriptional level, the mechanism by which the GnRHR mediates the antiproliferative effect of a GnRH agonist in SCL60 cells may share similarity to its mechanism of action in LβT2 cells.

A high throughput data-driven approach was taken, and it was anticipated that this might be useful in finding some of the most important factors in the GnRHR-mediated antiproliferative signalling response. Gene expression analysis has the advantage of looking at the entire transcriptome [126] and as such provides the basis for an unbiased data-driven approach to identifying important signalling factors. The gene expression data was useful in supporting the role of cell cycle signalling and MAPK pathway members in the GnRHR-mediated antiproliferative response [50, 79, 118, 178-181]. It demonstrates that there is a complex dynamic transcriptional response to GnRHR stimulation and indicates that gene transcription is likely to be important in this response. However, because of the complexity in this gene expression data, it is difficult to determine which gene changes are most important. There is an assumption that the strongest and most consistent changes with GnRHR transfection or with GnRHR stimulation in SCL60 cells are the most important. Whilst these changes are most likely to be valid, their biological significance in the response is not clear.

No previous study has explored the transcriptional effects of GnRHR activation in such depth. This study created a comprehensive dataset describing the gene expression changes resulting from GnRHR expression and from GnRHR stimulation in a model system: HEK293 cells either expressing or not expressing GnRHR protein. These data provide a database in which individual gene expression profiles can be examined to test hypotheses relating to the mechanism by which Triptorelin exerts its antiproliferative effect. The HEK293/SCL60 system is unlikely to reflect precisely the situation in breast cancer cells within patients, since the conditions *in vivo* are much more complex than *in vitro* culture, and this is not a breast cancer cell

line. However, SCL60 is a useful model in which to study GnRHR signalling, facets of which are likely to be applicable to more complex *in vivo* situations. It has been shown above that the transcriptional response of SCL60 cells to GnRHR activation shares similarity with the response to GnRHR activation in LβT2 cells, and may therefore be relevant to GnRHR signalling in other cell types.

The relevance of gene expression changes to the changes at the protein level may be limited since increased gene transcription does not necessarily correlate with increased expression or activity of the protein product. Protein activity may be influenced post-translation and by other proteins. It is difficult to identify which genes (and protein products) may be increased in expression to drive the antiproliferative response, and which genes may be increased in expression as part of a competing signalling network acting against the antiproliferative response as a survival response following the stimulation of the GnRHR. The functional output of any signalling network depends on a fine balance of positive and negative signals. This balance is hard to identify from such a large body of gene expression data. Computational modelling may help to show which of the gene changes are related to each other, and the likely order of activation. The genes and pathways identified above would be a useful basis on which to build and iterate a computational model.

3.3 Phosphoproteomic profiling

3.3.1 In vivo phosphoproteomic expression profiling

GnRH agonist-regulated changes were next examined at the proteomic level. A proteomic antibody array was used to explore changes in phosphoproteins in SCL60 xenografts *in vivo* following treatment with the GnRH agonist Triptorelin (section 3.3.1.1). Immunohistochemistry (section 3.3.1.2), RPPA (section 3.3.2) and western blots (section 0) were used to validate and further characterise some of the changes identified.

3.3.1.1 Phosphoproteomic array

To explore GnRHR signalling *in vivo*, a proteomic antibody array was conducted by Eurogentec, as an outsourced service, using SCL60 xenografts that had been treated with Triptorelin or vehicle control for 4 or 7 days. Tumours responsive to Triptorelin treatment were compared with vehicle control-treated tumours. The aim of this experiment was to generate hypotheses about which phosphoproteins might be involved in mediating the antiproliferative effect of Triptorelin by first identifying which proteins are differentially activated. The antibody array comprises 117 pairs of antibodies that detect both phosphorylated and non-phosphorylated forms of a range of proteins that are typically dysregulated in cancer-related signalling, such as proliferation and cell death signalling pathways. Antibodies for different phosphorylation sites on the same protein were also included. A full list of the antibodies used is shown in Appendix A Table 1. These antibodies were fixed to a glass slide and biotin-labelled protein from the xenografts was added in solution. Fluorescent Cy3-Streptavidin was used to detect the antibody-bound protein and the slides were scanned to measure the intensity of the fluorescent signal. Images of the slides are shown in Figure 31.

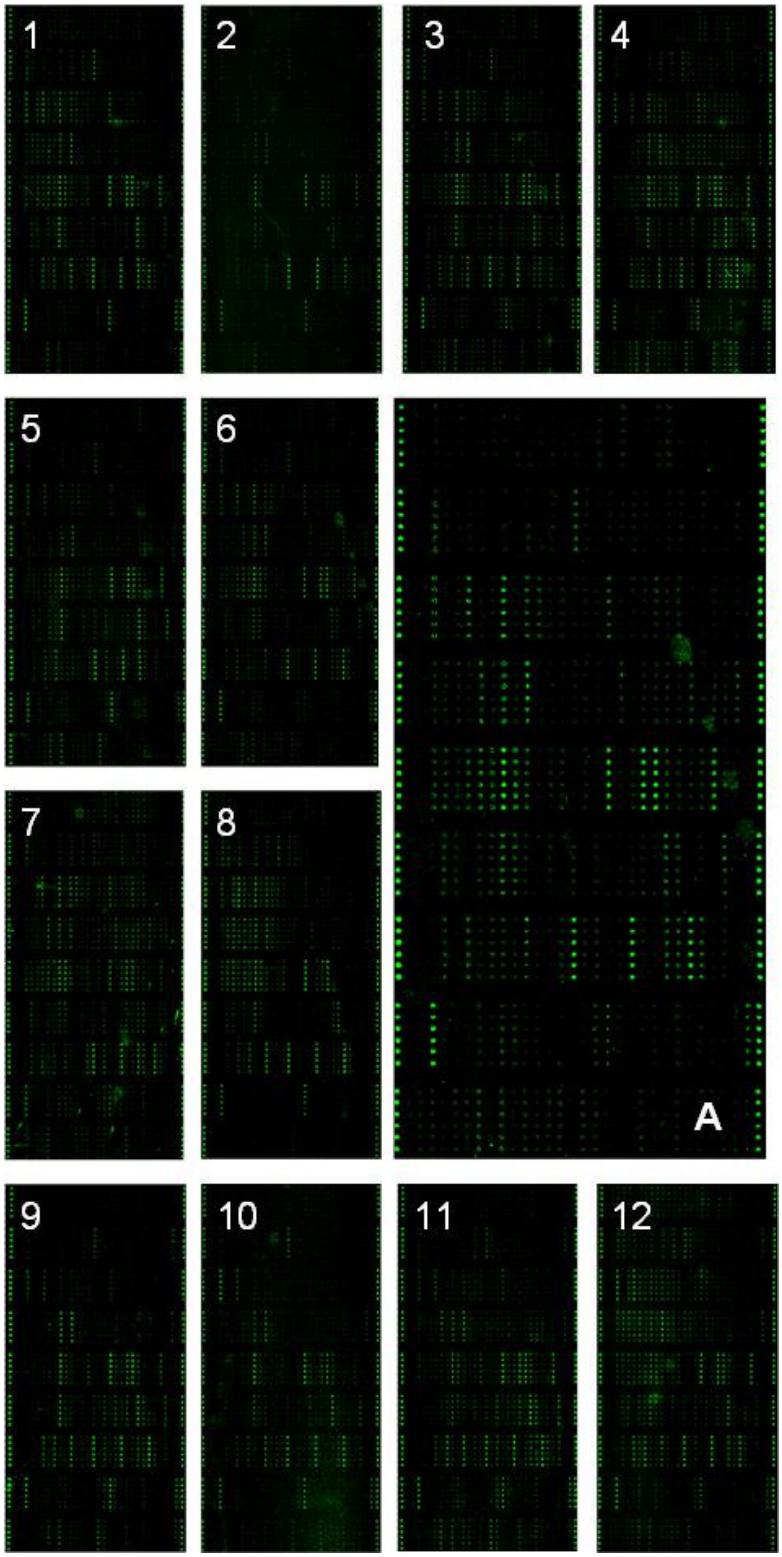

Figure 31: Twelve antibody array slides after hybridisation of antibodies with protein and fluorescent labelling.
Slides 1-3 are vehicle control day 4, 4-6 are vehicle control day 7, 7-9 are Triptorelin day 4, and 10-12 are Triptorelin day 7. A shows an enlarged image of slide 6. Six replicates of each antibody are fixed to the slide in a vertical line. Positive controls are along the outer left and right edges.

The strongest and most consistent phosphoprotein changes were identified for each time point using P-values from a Mann-Whitney-U test comparing Triptorelin- and vehicle control-treated xenografts at day 4 and day 7 after treatment. These phosphoproteins are shown in Figure 32. After 4 days of treatment, a decrease was noted in the ratio of phosphorylated to non-phosphorylated Met (growth factor receptor) and Caveolin-1 (membrane-associated protein) in Triptorelin-treated xenografts compared to control xenografts (Figure 32). In contrast, phosphorylation of Myc (transcription activator) was increased (Figure 32). Myc phosphorylation and 4E-BP1 (translation repressor) phosphorylation levels were increased with Triptorelin treatment at both 4 and 7 days compared to vehicle control-treated xenografts (Figure 32). Most phosphoproteins that were differentially modulated following treatment in the SCL60 xenografts were quite different between days 4 and 7. Other phosphoproteins that were increased with treatment at day 4 included the NFκB pathway members NFκB-p65 and IκBε. Phosphoproteins that were decreased at day 7 included Akt and Chk2 (Figure 32).

Several cell cycle-related proteins were also differentially phosphorylated: p27 (increased at day 4), CDC25C (increased at day 7), and Chk2 (decreased at day 7). Changes in the phosphorylation levels of the apoptosis regulators BCL-2 (decreased at day 7) and BAD (increased at day 4) were also observed.

A: Day 4

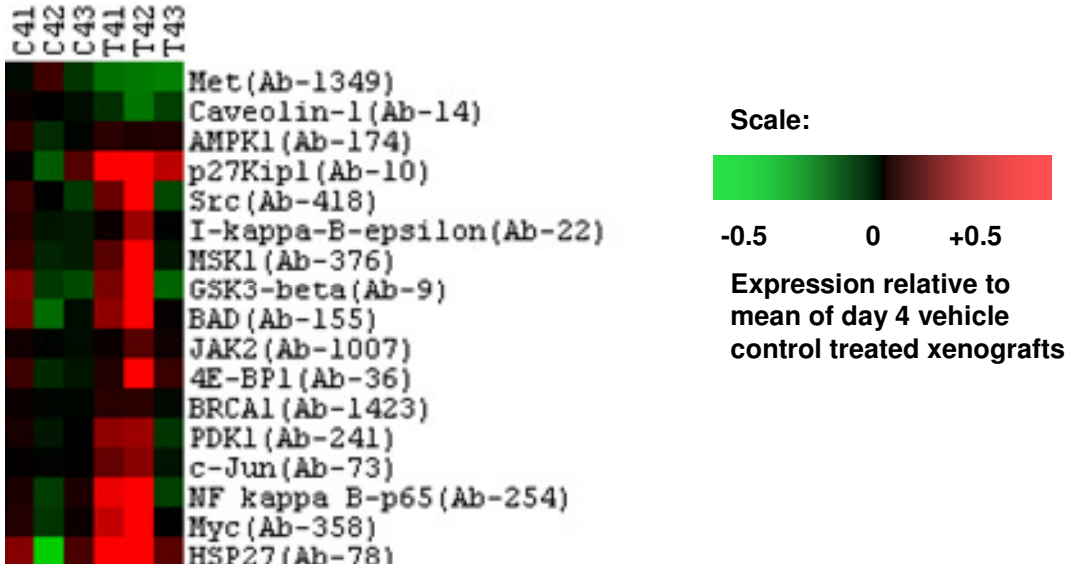

B: Day 7

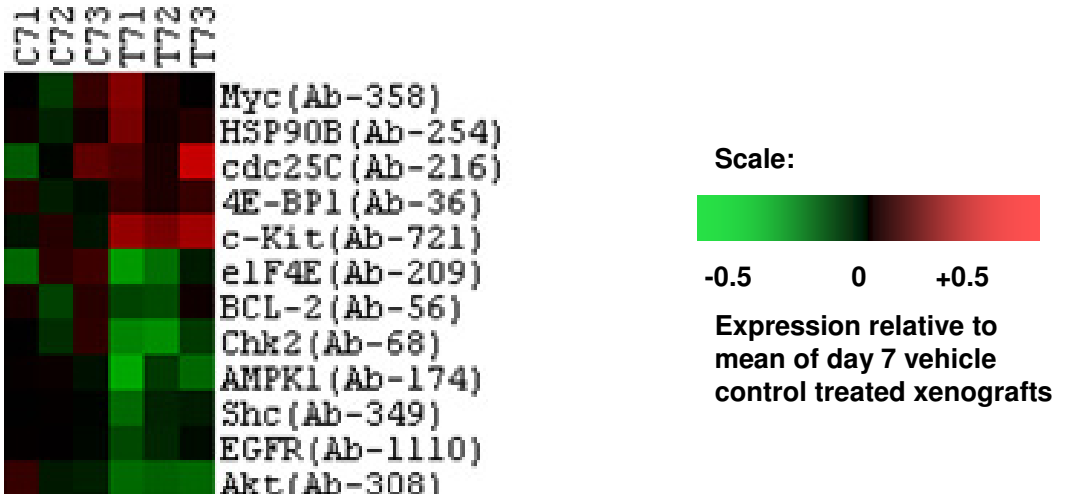

Figure 32: Proteins whose phosphorylation status was most strongly and consistently changed with Triptorelin treatment after (A) 4 days and (B) 7 days in SCL60 xenografts. Expression value is given as a ratio of phosphorylated to non-phosphorylated protein expression, and is then shown relative to the mean of the 3 control tumours. Three control (C) tumours and three Triptorelin-treated (T) tumours are shown for each day (4 and 7). Red = increased, green = decreased.

Using the online Kyoto Encyclopedia of Genes and Genomes (KEGG) pathway database [182-184], models were generated to suggest how these proteins might interact to mediate the antiproliferative effect of Triptorelin (Figure 33, Figure 34).

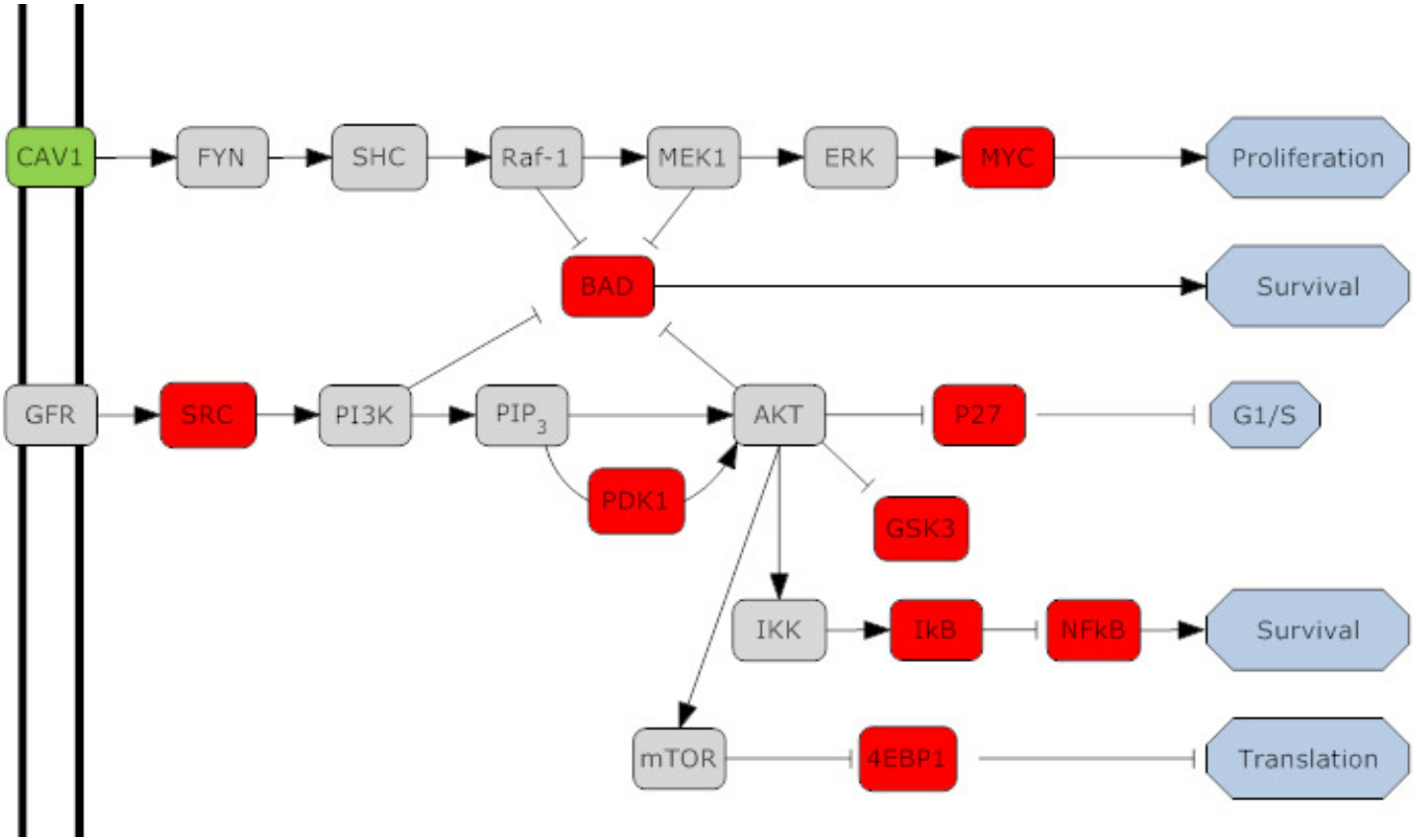

Figure 33: Model of phosphoprotein changes at day 4.
Model to show proteins whose phosphorylation status was most strongly and significantly increased (red) or decreased (green) with Triptorelin treatment in SCL60 xenografts 4 days after treatment. Proteins in grey did not appear to change with Triptorelin treatment.

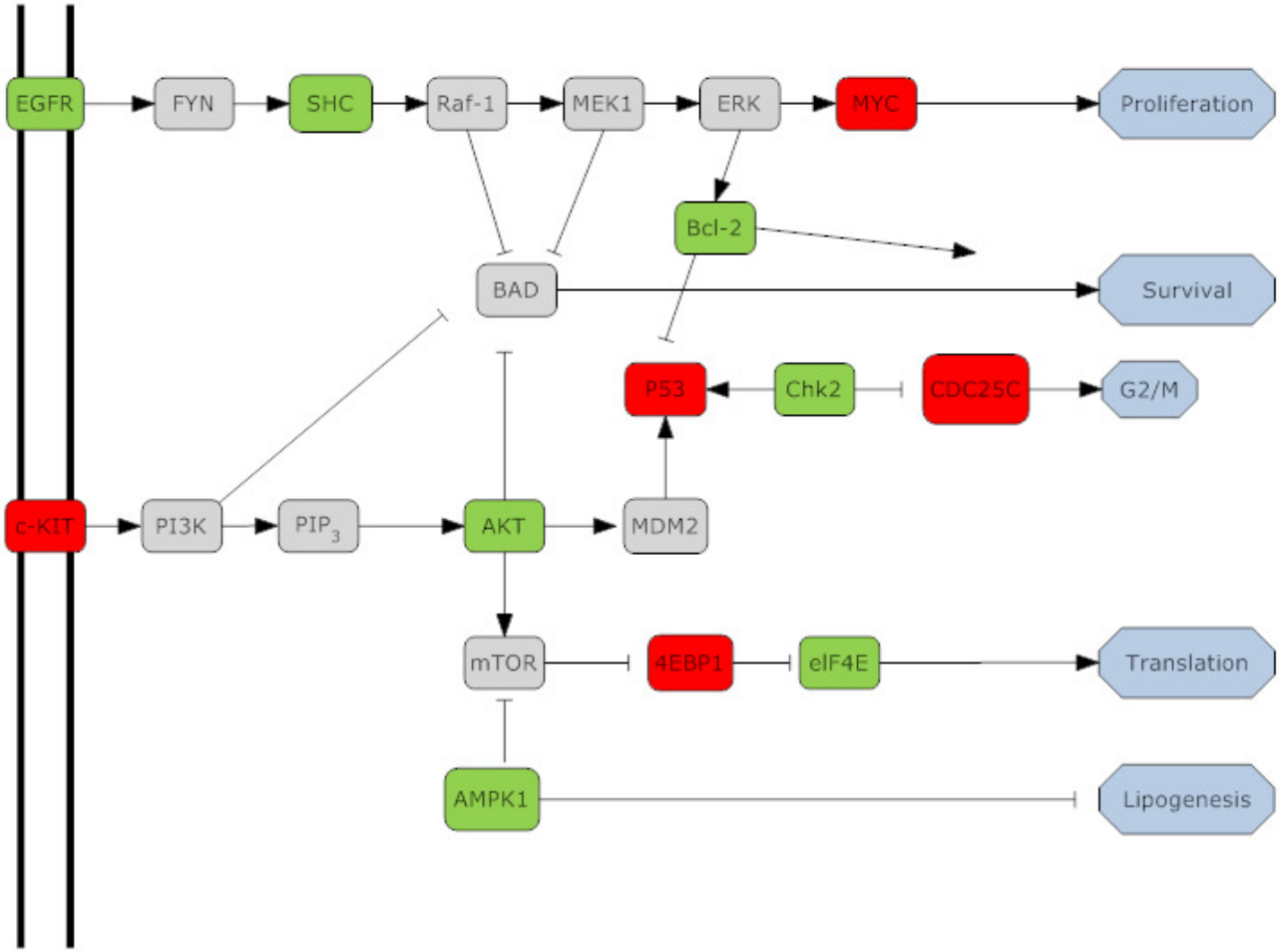

Figure 34: Model of phosphoprotein changes at day 7.
Model to show proteins whose phosphorylation status was most strongly and significantly increased (red) or decreased (green) with Triptorelin treatment in SCL60 xenografts 7 days after treatment. Proteins in grey did not appear to change with Triptorelin treatment.

3.3.1.2 Validation of proteomic responses to GnRHR stimulation

Immunohistochemistry was used to investigate in more detail the candidates identified from the *in vivo* proteomic array. The level of pNFκB (normalised to tNFκB) was significantly higher in Triptorelin-treated xenografts compared to vehicle control-treated xenografts compared to (P=0.009, 2-sample t-test; Figure 35). This difference was observed at both day 4 and day 7 (Figure 36).

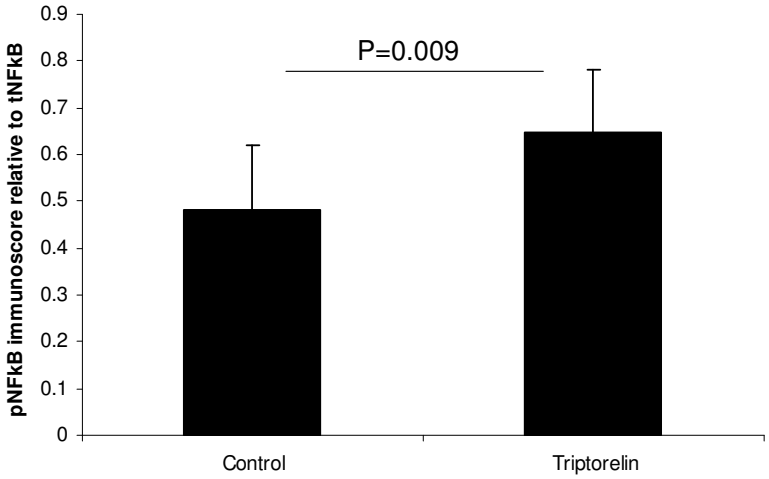

Figure 35: Immunostaining for pNFκB.
Immunostaining for pNFκB (normalised to tNFκB) was significantly lower in vehicle control-treated xenografts compared to Triptorelin-treated xenografts (P=0.009; 2-sample t-test). The bars show average immunoscores for 8 Control tumours and 9 Triptorelin-treated tumours. Error bars show standard deviation.

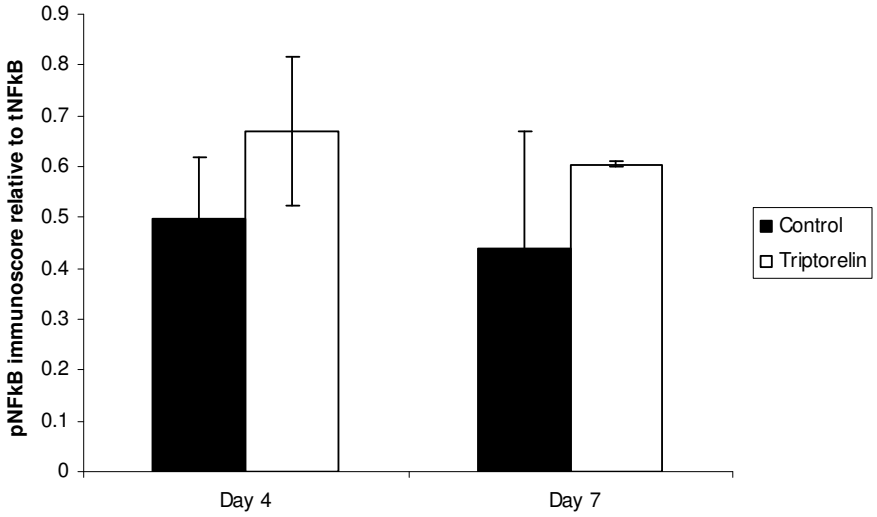

Figure 36: Immunostaining for pNFκB (day 4 and day 7).
Immunostaining for pNFκB (normalised to tNFκB) was lower in vehicle control-treated xenografts compared to Triptorelin-treated xenografts. The bars show average immunoscores for 6 vehicle control- and 7 Triptorelin-treated tumours at day 4 and 2 vehicle control- and 2 Triptorelin-treated tumours at day 7. Error bars show standard deviation.

No significant difference could be detected in the levels of pCav1, tCav1, pMet, tMet, pERK1/2, or tERK1/2 (p – phosphorylated, t – total) between Control and Triptorelin-treated xenografts when day 4 and 7 were pooled (Figure 37). Neither could a difference be detected between Control and Triptorelin-treated xenografts when day 4 and day 7 samples were analysed separately.

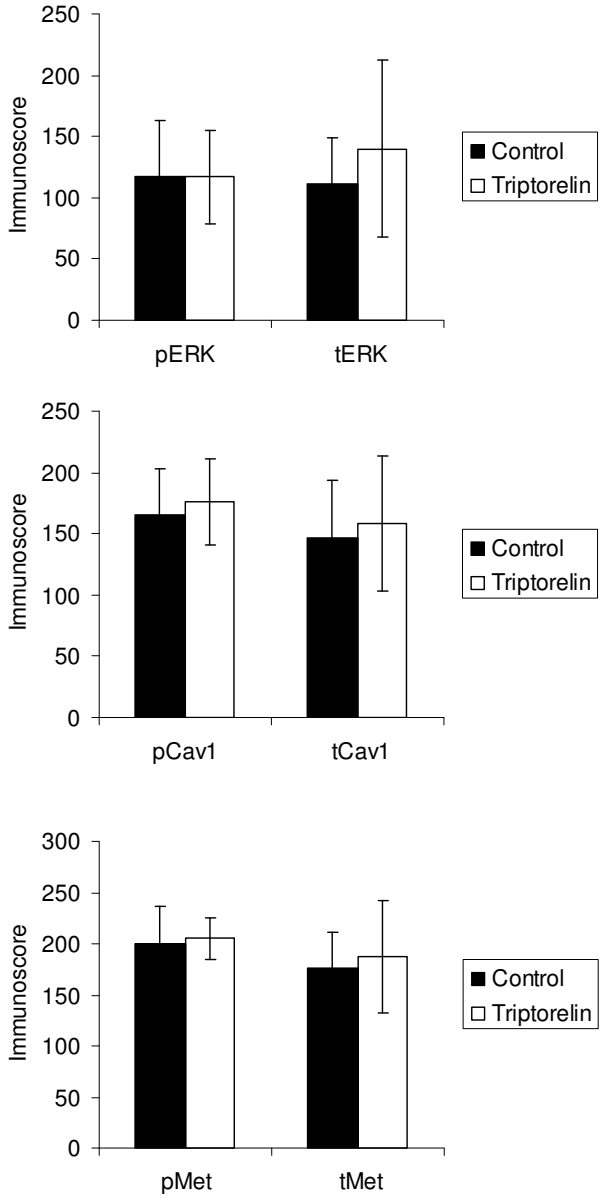

Figure 37: Immunostaining for pCav1, tCav1, pMet, tMet, pERK1/2, or tERK1/2 in SCL60 xenografts.
No significant difference could be detected in the levels of pCav1, tCav1, pMet, tMet, pERK1/2, or tERK1/2 between Control and Triptorelin-treated xenografts. The bars show average immunoscores for 6 vehicle control- and 7 Triptorelin-treated tumours at day 4 and 2 vehicle control- and 2 Triptorelin-treated tumours at day 7. Error bars show standard deviation.

3.3.2 RPPA

Reverse-phase protein array (RPPA) was used as a broad screening tool to validate some of the candidates identified from the *in vivo* antibody array and existing literature, and to identify proteins of further interest. SCL60 cells were compared with their untransfected counterparts, HEK293 cells, and with another control cell line, SCL215, which has been transfected with an extended (non-functional) form of GnRHR. Protein expression following Triptorelin treatment was also investigated in each cell line.

3.3.2.1 pNFκB, PI3K, pChk2 and pCyclinD1 differed in their baseline expression between SCL60, HEK293 and SCL215 cells

The expression of several proteins was compared between HEK293, SCL215 and SCL60 cells. These results are shown in Figure 38. The cell cycle proteins pCHK2 and pCyclinD1 were significantly different between at least two cell lines (Figure 38). pCHK2 (not normalised to total) expression was significantly (39%) lower in SCL60 cells compared to HEK293 cells (Figure 38; P=0.027, 2-sample t-test) but not compared to SCL215 cells. The baseline expression of pCyclinD1 (normalised to total CyclinD1) was significantly (3-fold) higher in SCL215 cells than HEK293 cells (Figure 38; P=0.004, 2-sample t-test). PI3K-p110α was significantly (13%) reduced in expression in SCL60 cells compared to HEK293 cells (P=0.027, 2-sample t-test). pNFκB (normalised to tNFκB) was significantly (1.8 fold) higher in SCL60 cells compared to SCL215 cells (P=0.035, 2-sample).

No expression differences were observed between the three cell lines in the proliferation markers pHistone H3 and Ki67, or the tumour suppressor total p53 (Figure 38). No difference in expression of tP21, pCAV1, pmTOR, pPTEN, pAkt, p-cRAF, pMet, pER, tHER2, tEGFR or pERK1/2, could be detected between any of the three cell lines (Figure 38).

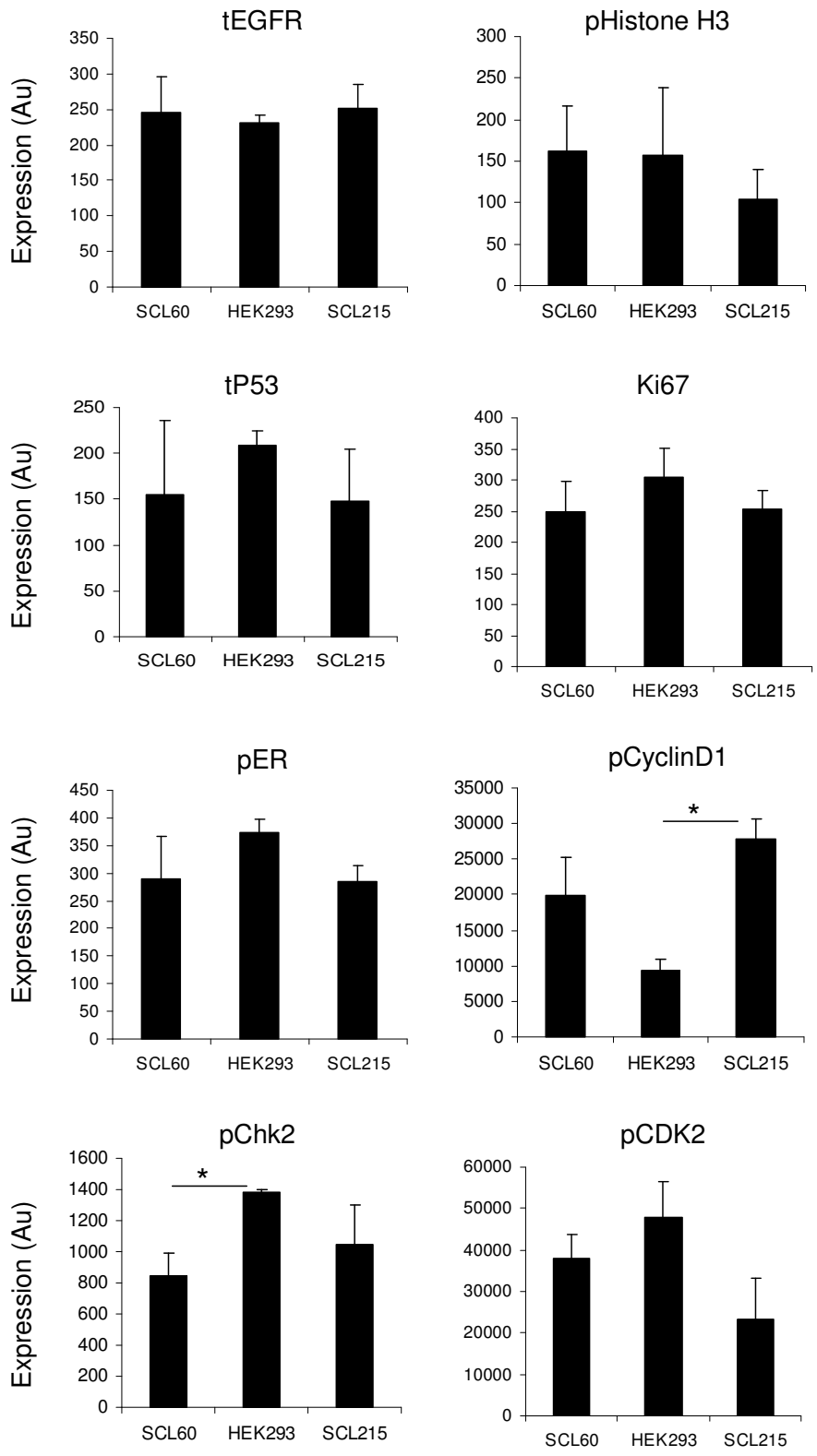

Figure 38: Baseline protein expression (measured by RPPA) in untreated SCL60, HEK293, and SCL215 cells.
*** indicates a statistically significant difference in expression (P<0.05, 2-sample t-test). Bars show mean of three independent experiments. Error bars show standard deviation. Figure continues on the next page.**

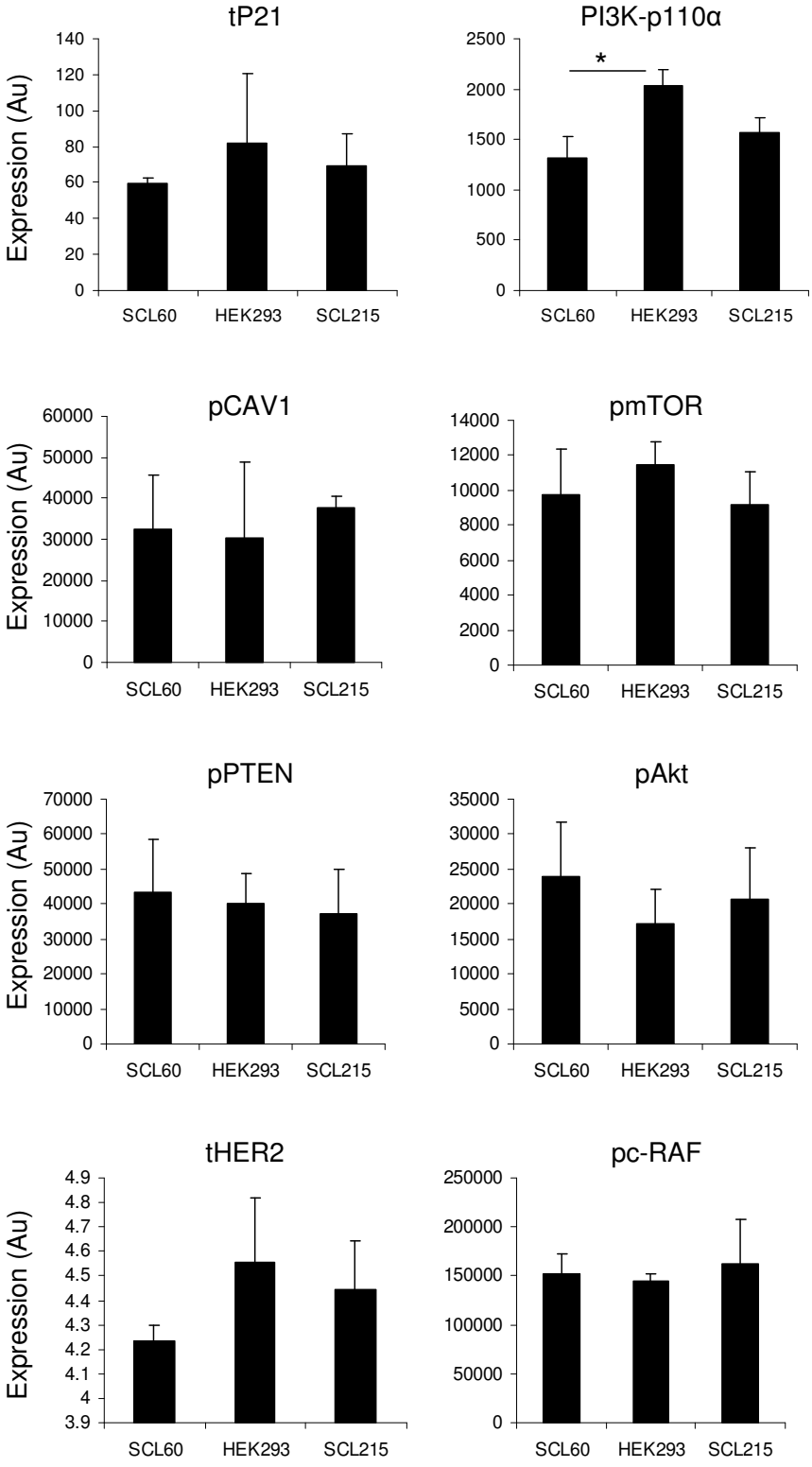

Figure 38 (continued): Baseline protein expression (measured by RPPA) in untreated SCL60, HEK293, and SCL215 cells.
*** indicates a statistically significant difference in expression ($P<0.05$, 2-sample t-test). Bars show mean of three independent experiments. Error bars show standard deviation. Figure continues on the next page.**

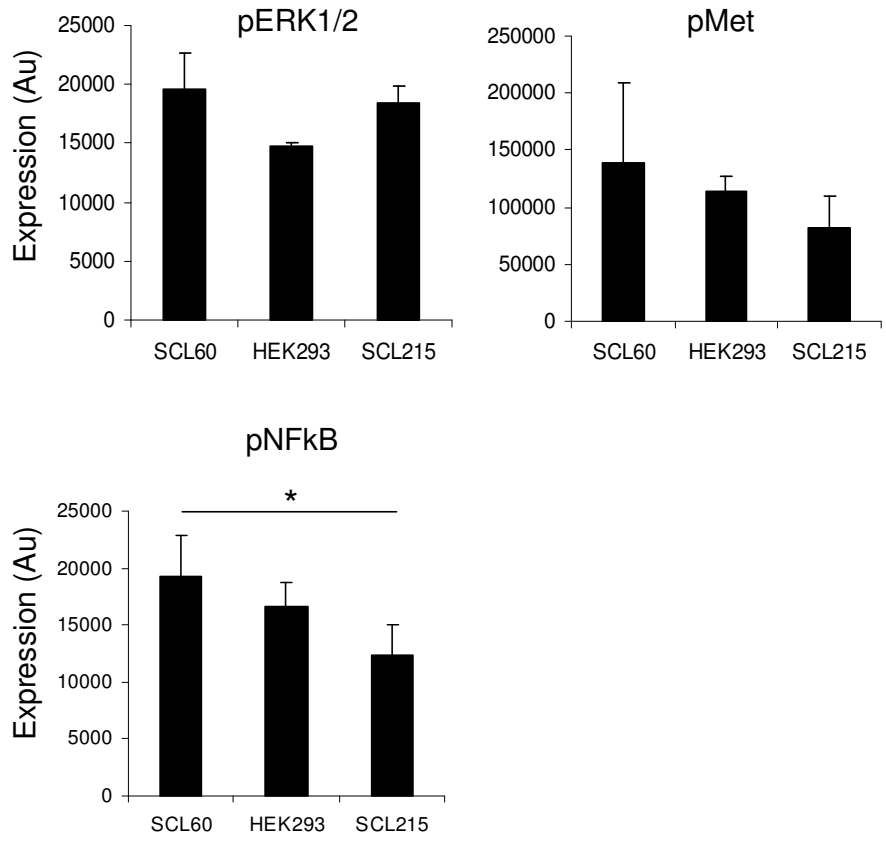

Figure 38 (continued): Baseline protein expression (measured by RPPA) in untreated SCL60, HEK293, and SCL215 cells.
*** indicates a statistically significant difference in expression (P<0.05, 2-sample t-test). Bars show mean of three independent experiments. Error bars show standard deviation.**

3.3.2.2 pERK1/2 was increased in SCL60 and SCL215 cells following Triptorelin treatment

Levels of selected phosphoproteins in HEK293 and SCL215 cells were largely unresponsive to Triptorelin treatment (Figure 39). The exception to this was a transient increase (approx 1.5 fold) in the level of pERK1/2 at 1h following treatment with Triptorelin in both SCL60 and SCL215 cells which returned to basal levels by 24h (Figure 39). Figure 39 shows protein expression levels in SCL60, HEK293 and SCL215 cells at 0, 1, and 24h after treatment with Triptorelin. The data in this figure shows protein expression in Triptorelin treated cells relative to the expression of that protein in corresponding vehicle control treated cells at the same time point. Figure 40 shows these data in more detail by showing separate values for control and Triptorelin-treated cells.

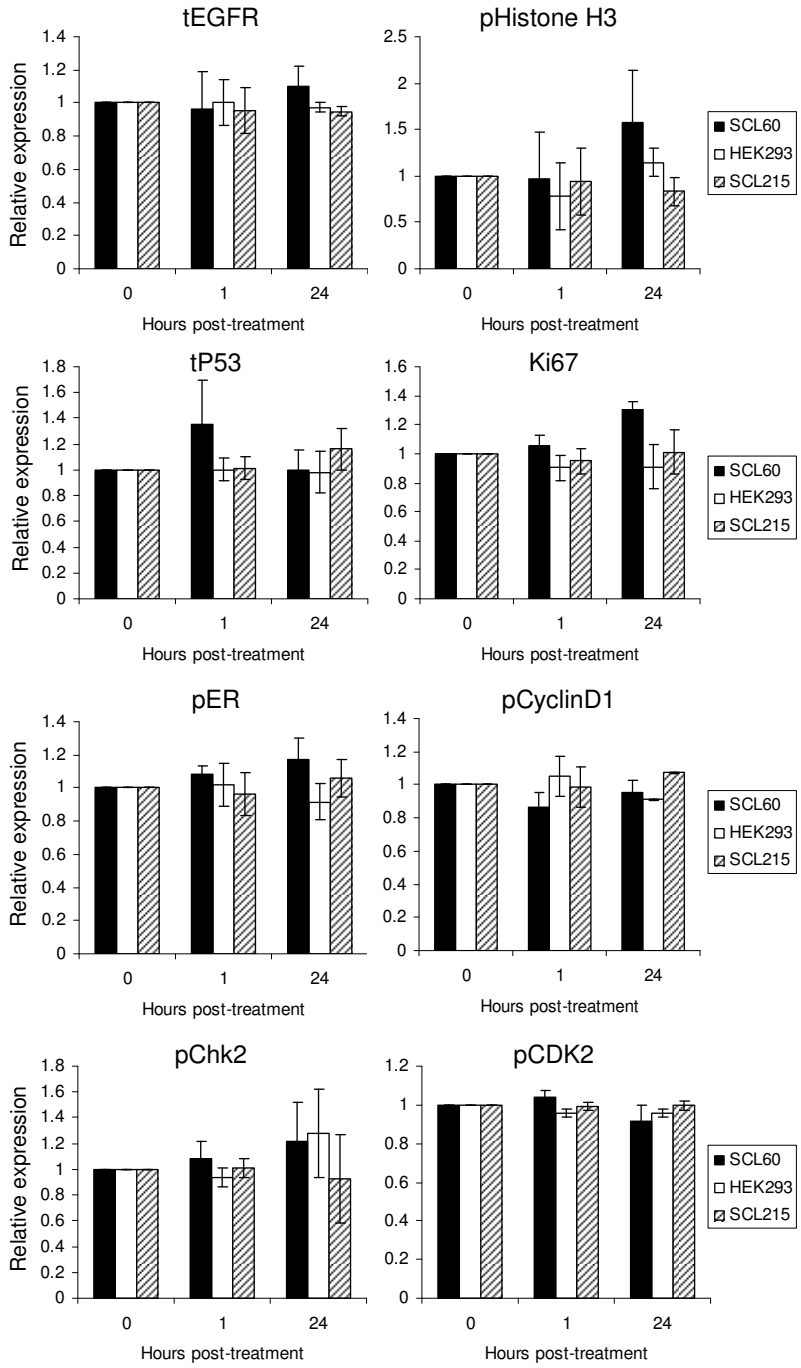

Figure 39: Protein expression (measured by RPPA) in SCL60, HEK293, and SCL215 cells following treatment with 100nM Triptorelin for 0, 1 or 24h.
Protein expression was measured by RPPA in SCL60, HEK293 and SCL215 cells following treatment with 0.02% propylene glycol (vehicle control) or 100nM Triptorelin. Phospho-protein expression was wherever possible normalised to total protein expression. The expression of each protein in Triptorelin-treated cells was then normalised to the expression of that protein in vehicle control-treated cells. Bars show normalised mean protein expression of three independent experiments. Error bars show standard deviation. Figure continues on the next page.

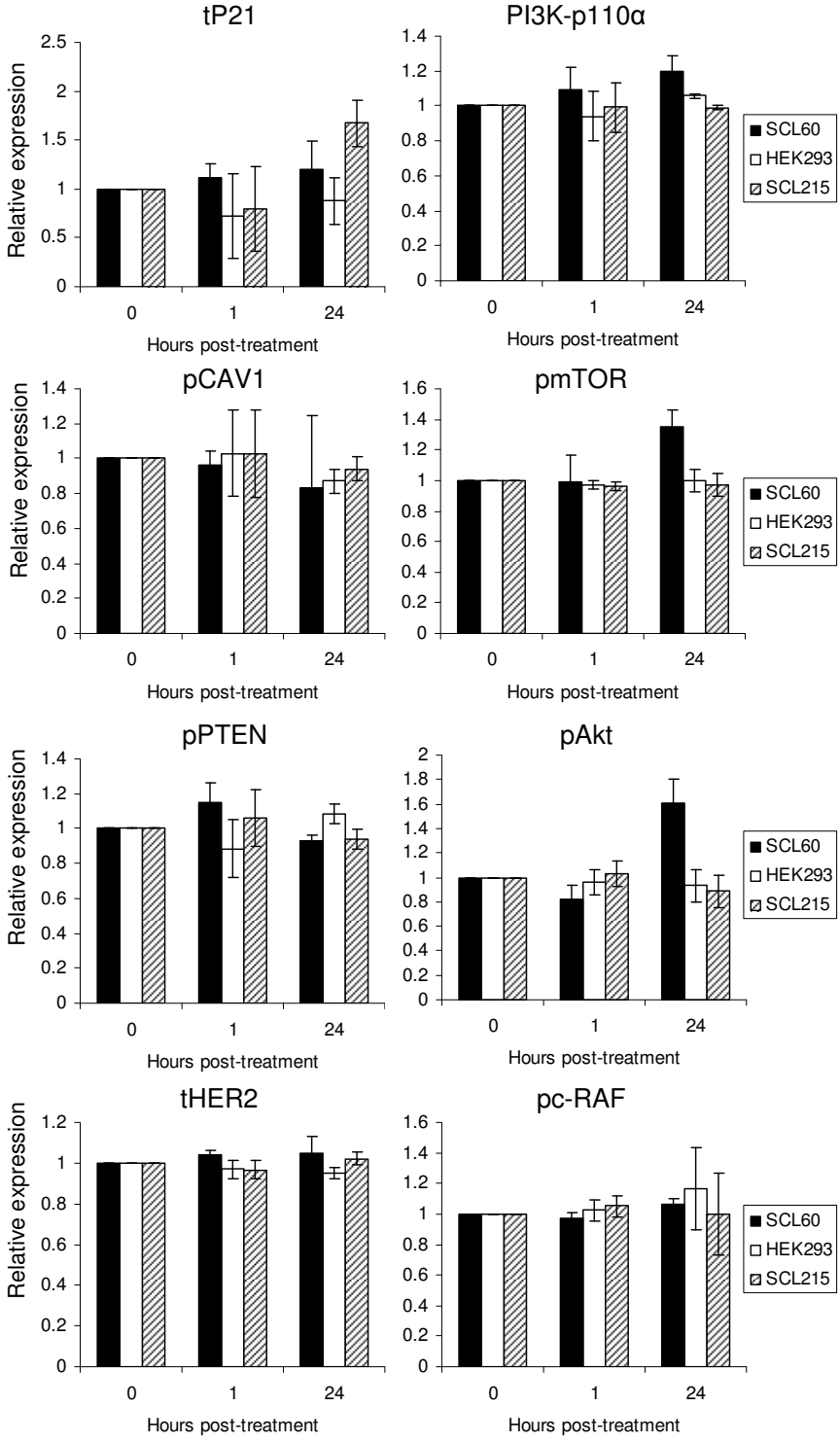

Figure 39 (continued): Protein expression (measured by RPPA) in SCL60, HEK293, and SCL215 cells following treatment with 100nM Triptorelin for 0, 1 or 24h. Protein expression was measured by RPPA in SCL60, HEK293 and SCL215 cells following treatment with 0.02% propylene glycol (vehicle control) or 100nM Triptorelin. Phospho-protein expression was wherever possible normalised to total protein expression. The expression of each protein in Triptorelin-treated cells was then normalised to the expression of that protein in vehicle control-treated cells. Bars show normalised mean protein expression of three independent experiments. Error bars show standard deviation. Figure continues on the next page.

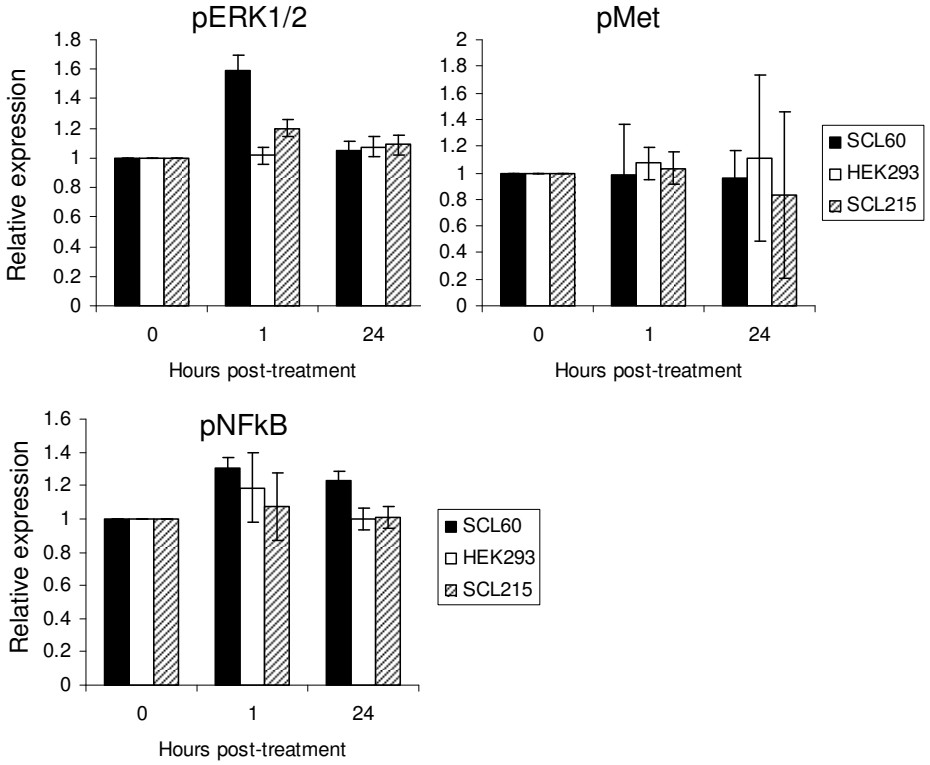

Figure 39 (continued): Protein expression (measured by RPPA) in SCL60, HEK293, and SCL215 cells following treatment with 100nM Triptorelin for 0, 1 or 24h.
Protein expression was measured by RPPA in SCL60, HEK293 and SCL215 cells following treatment with 0.02% propylene glycol (vehicle control) or 100nM Triptorelin. Phospho-protein expression was wherever possible normalised to total protein expression. The expression of each protein in Triptorelin-treated cells was then normalised to the expression of that protein in vehicle control-treated cells at the same time point. Bars show normalised mean protein expression of three independent experiments. Error bars show standard deviation.

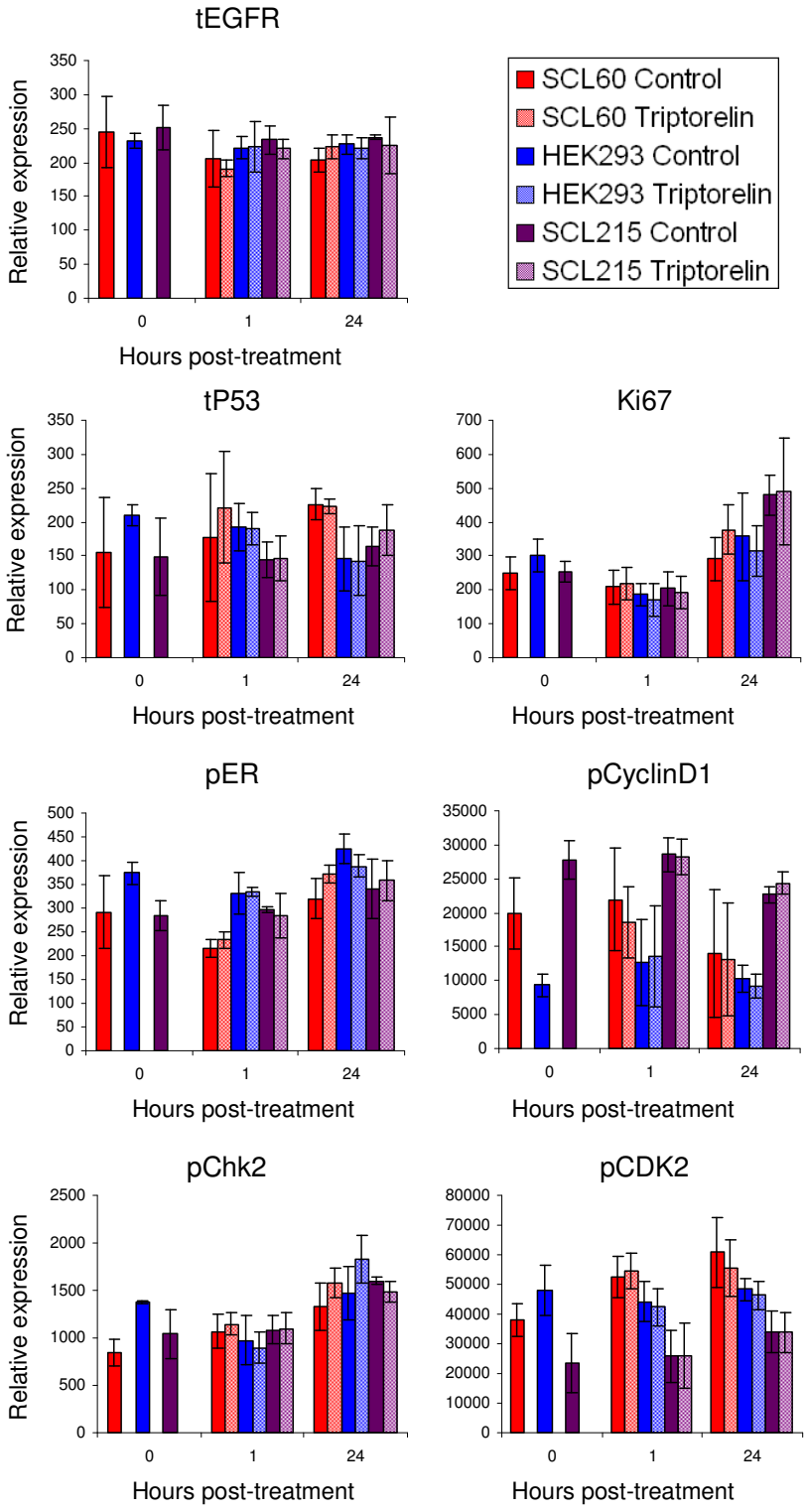

Figure 40: Protein expression (measured by RPPA) in SCL60, HEK293, and SCL215 cells following treatment with 100nM Triptorelin for 0, 1 or 24h.
Protein expression was measured by RPPA in SCL60, HEK293 and SCL215 cells following treatment with 0.02% propylene glycol (vehicle control) or 100nM Triptorelin. Phospho-protein expression was wherever possible normalised to total protein expression. Bars show mean protein expression of three independent experiments. Error bars show standard deviation.
Figure continues on the next page.

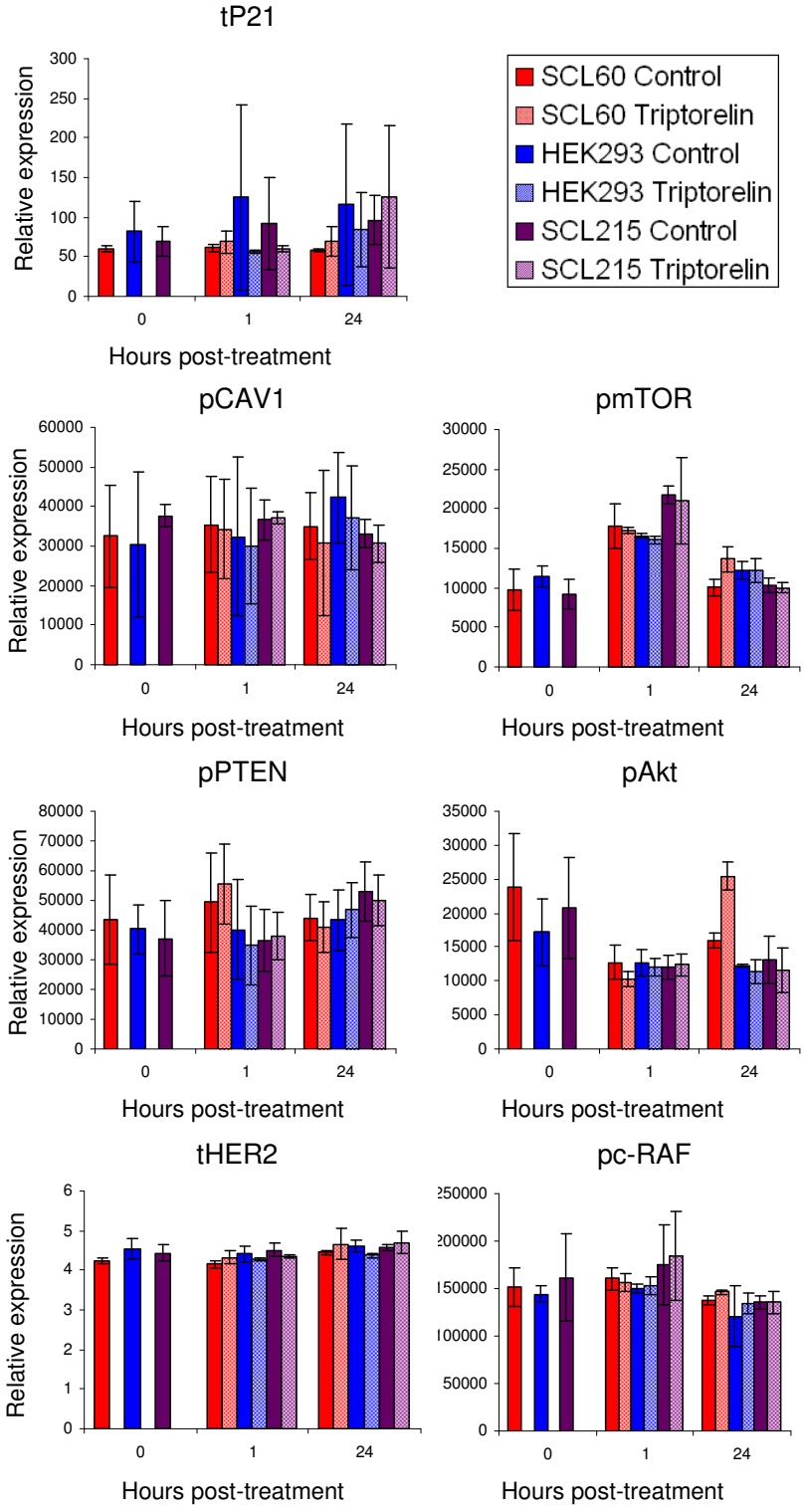

Figure 40 (continued): Protein expression (measured by RPPA) in SCL60, HEK293, and SCL215 cells following treatment with 100nM Triptorelin for 0, 1 or 24h.
Protein expression was measured by RPPA in SCL60, HEK293 and SCL215 cells following treatment with 0.02% propylene glycol (vehicle control) or 100nM Triptorelin. Phospho-protein expression was wherever possible normalised to total protein expression. Bars show mean protein expression of three independent experiments. Error bars show standard deviation.
Figure continues on the next page.

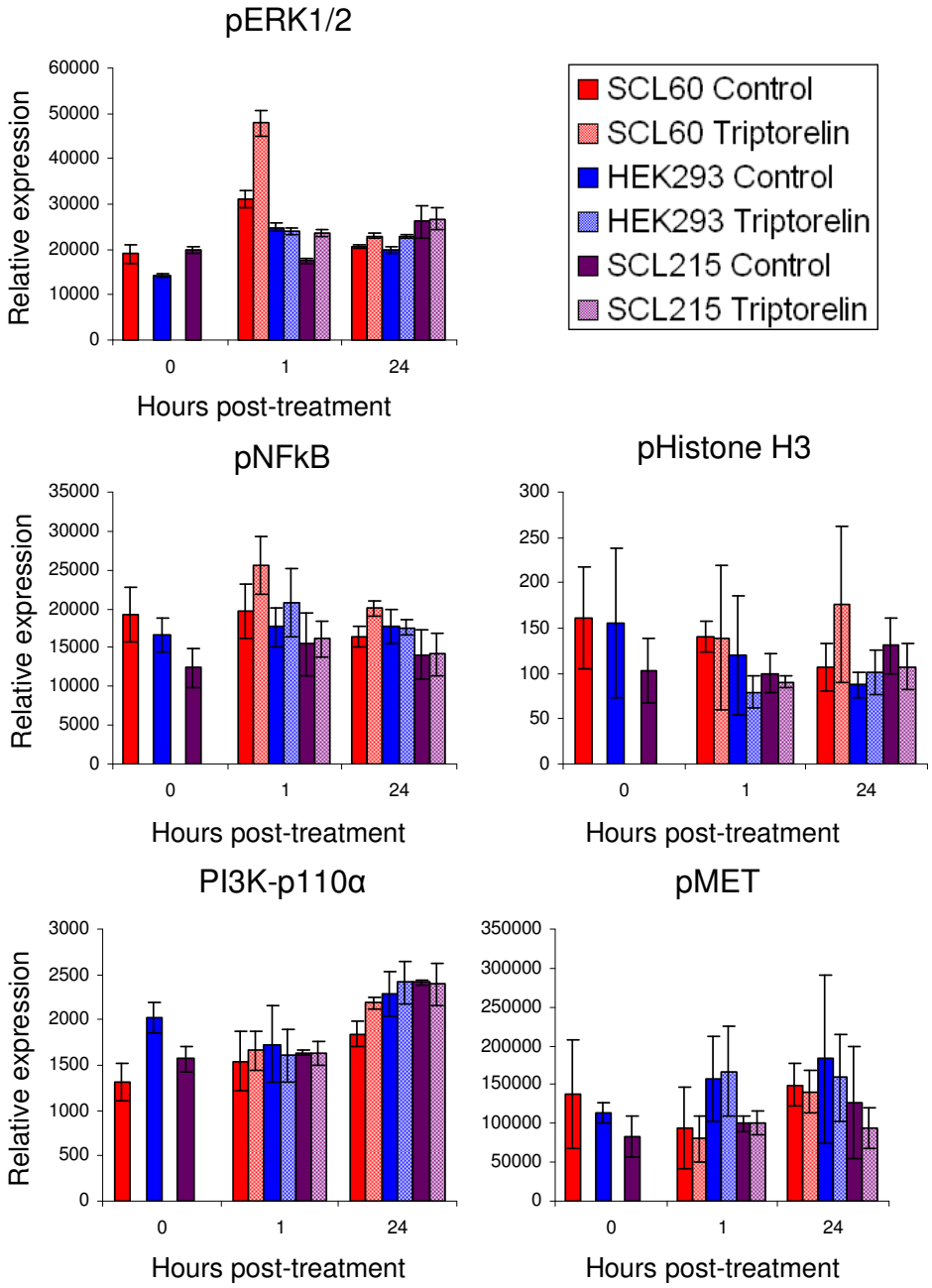

Figure 40 (continued): Protein expression (measured by RPPA) in SCL60, HEK293, and SCL215 cells following treatment with 100nM Triptorelin for 0, 1 or 24h.
Protein expression was measured by RPPA in SCL60, HEK293 and SCL215 cells following treatment with 0.02% propylene glycol (vehicle control) or 100nM Triptorelin. Phospho-protein expression was wherever possible normalised to total protein expression. Bars show mean protein expression of three independent experiments. Error bars show standard deviation.

3.3.2.3 Change in pERK1/2, pAkt and pNFkB expression in SCL60 cells from 0 to 24h

To identify proteins that may be altered in expression as a result of GnRHR stimulation, RPPA was used to measure the relative levels of several proteins in SCL60 cells following Triptorelin treatment. Figure 41 shows the expression levels of these proteins in SCL60 cells. The expression levels of each phosphoprotein was normalised to the expression level of the corresponding total protein. Figure 41 shows the expression of several proteins in Triptorelin treated cells relative to the expression of that protein in corresponding vehicle control treated cells at the same time point. Most proteins examined did not change in expression with Triptorelin treatment over 24h. However, there appeared to be some change in the level of PI3K-p110α, pmTOR, pPTEN, pAkt, pERK1/2, pMet, and pNFκB (Figure 41). The expression profiles of these proteins are shown in further detail in Figure 42.

Figure 42 shows that there is a clear difference in expression of pNFκB and pERK1/2 between Triptorelin-treated and vehicle control-treated cells at several time points. pERK1/2 was initially increased in expression in Triptorelin-treated cells compared to vehicle control-treated cells. pERK1/2 expression was more than 2 times higher in Triptorelin-treated cells than vehicle control-treated cells at 0.5h. pERK1/2 expression then decreased between 0.5 and 1h but still remained much higher than control levels. A higher level of pERK1/2 in Triptorelin-treated cells was maintained up to 8h before returning to near control level by 24h. pAkt appeared to be differentially expressed at 24h between control and Triptorelin-treated cells. pPTEN levels changed only slightly between control and treated cells at any time point and the data were quite variable. pmTOR and PI3K-p110α showed small differences in expression at at least one time point. pMet data showed changes in both control and Triptorelin treated cells, although they were very variable. To validate the changes observed here in pNFκB, pERK1/2 and pAkt, and to further investigate the unclear RPPA data surrounding pmTOR, pPTEN, pMet and PI3K-p110α expression, the expression of these proteins was measured by western blot (section 3.3.3).

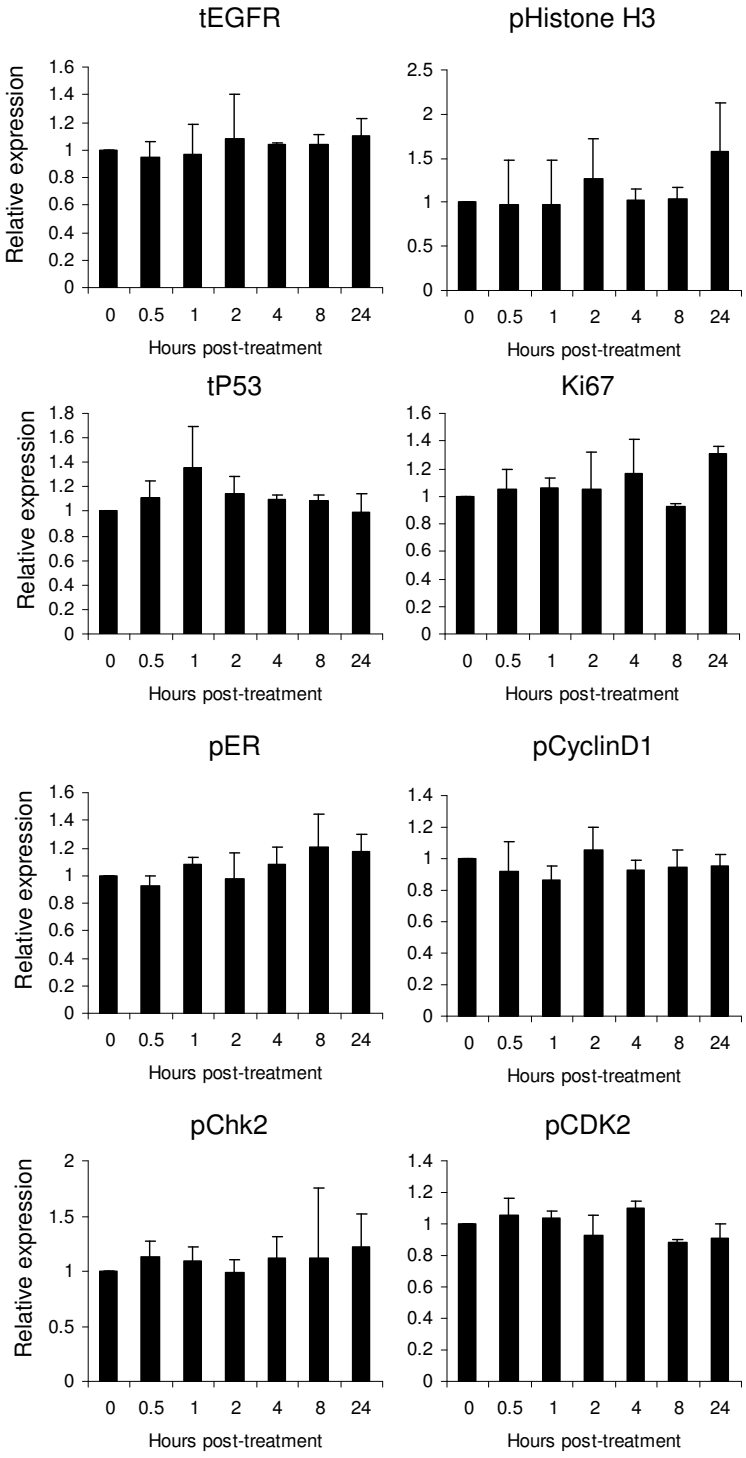

Figure 41: Protein expression (measured by RPPA) in SCL60 cells following treatment with 100nM Triptorelin for up to 24h.
Protein expression was measured by RPPA in SCL60, HEK293 and SCL215 cells following treatment with 0.02% propylene glycol (vehicle control) or 100nM Triptorelin. Phospho-protein expression was wherever possible normalised to total protein expression. The expression of each protein in Triptorelin-treated cells was then normalised to the expression level of that protein in vehicle control-treated cells at the same time point. Bars show mean protein expression of three independent experiments. Error bars show standard deviation. Figure continues on the next page.

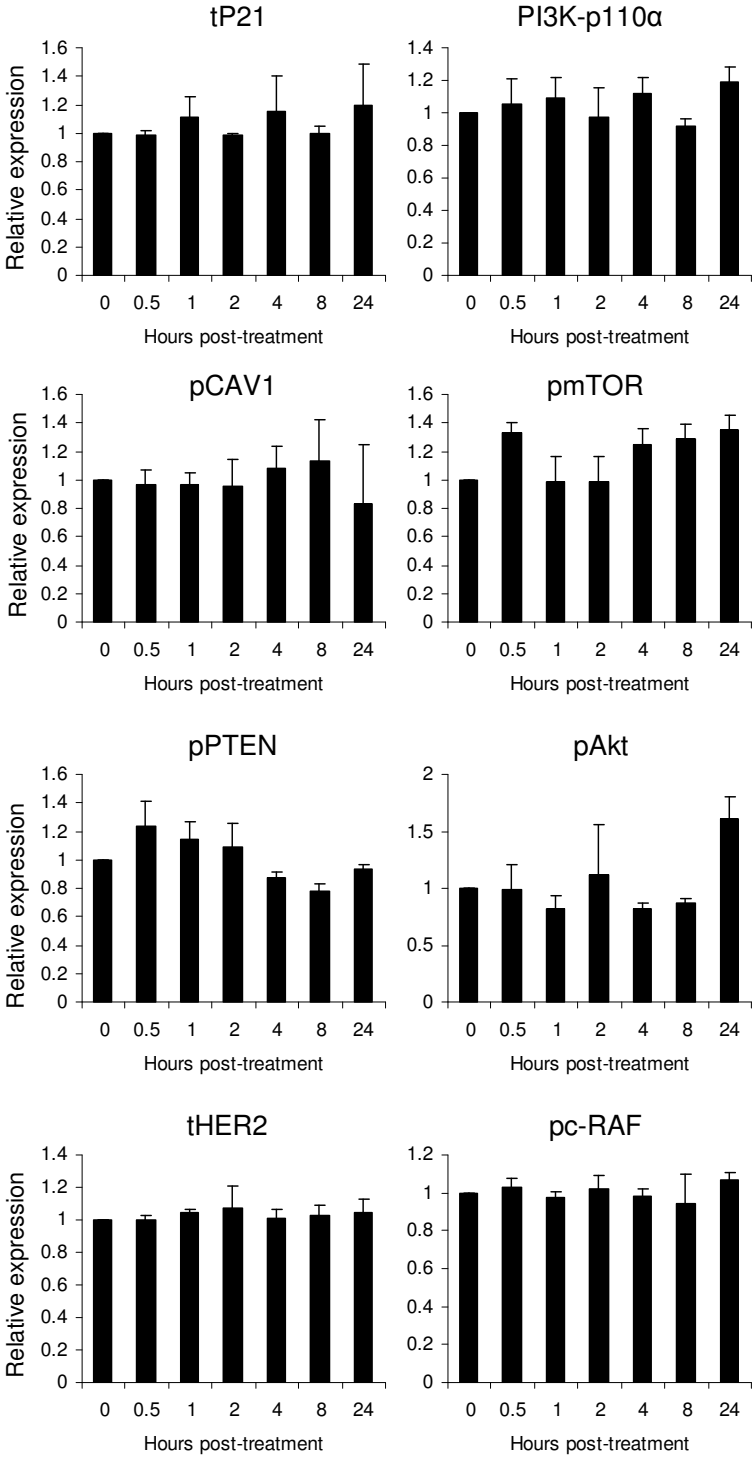

Figure 41 (continued): Protein expression (measured by RPPA) in SCL60 cells following treatment with 100nM Triptorelin for up to 24h.
Protein expression was measured by RPPA in SCL60, HEK293 and SCL215 cells following treatment with 0.02% propylene glycol (vehicle control) or 100nM Triptorelin. Phospho-protein expression was wherever possible normalised to total protein expression. The expression of each protein in Triptorelin-treated cells was then normalised to the expression level of that protein in vehicle control-treated cells at the same time point. Bars show mean protein expression of three independent experiments. Error bars show standard deviation. Figure continues on the next page.

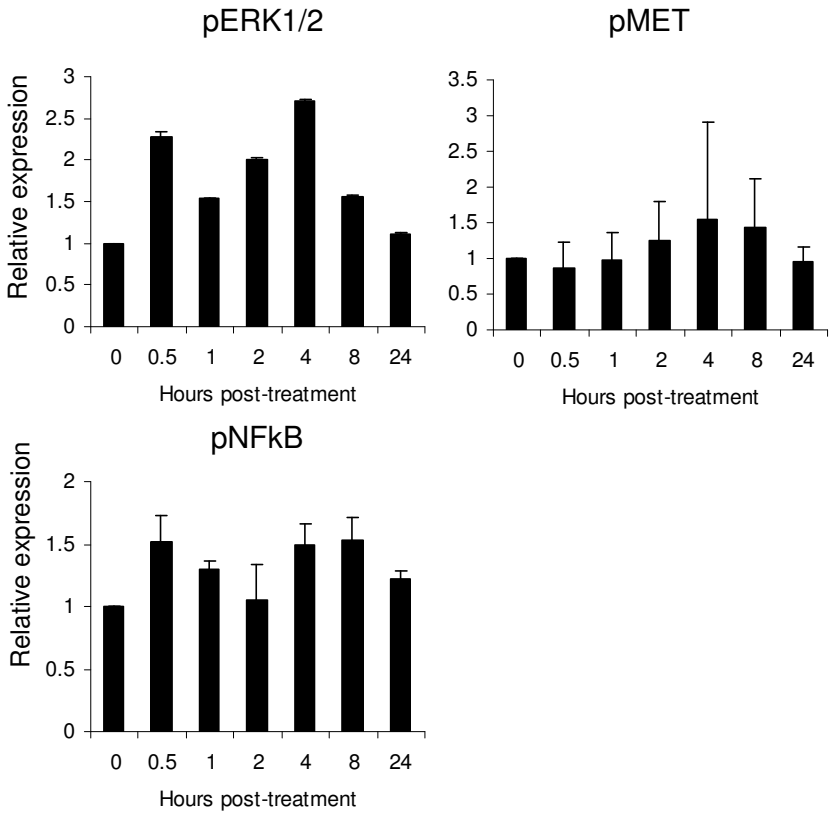

Figure 41 (continued): Protein expression (measured by RPPA) in SCL60 cells following treatment with 100nM Triptorelin for up to 24h.
Protein expression was measured by RPPA in SCL60, HEK293 and SCL215 cells following treatment with 0.02% propylene glycol (vehicle control) or 100nM Triptorelin. Phospho-protein expression was wherever possible normalised to total protein expression. The expression of each protein in Triptorelin-treated cells was then normalised to the expression level of that protein in vehicle control-treated cells at the same time point. Bars show mean protein expression of three independent experiments. Error bars show standard deviation.

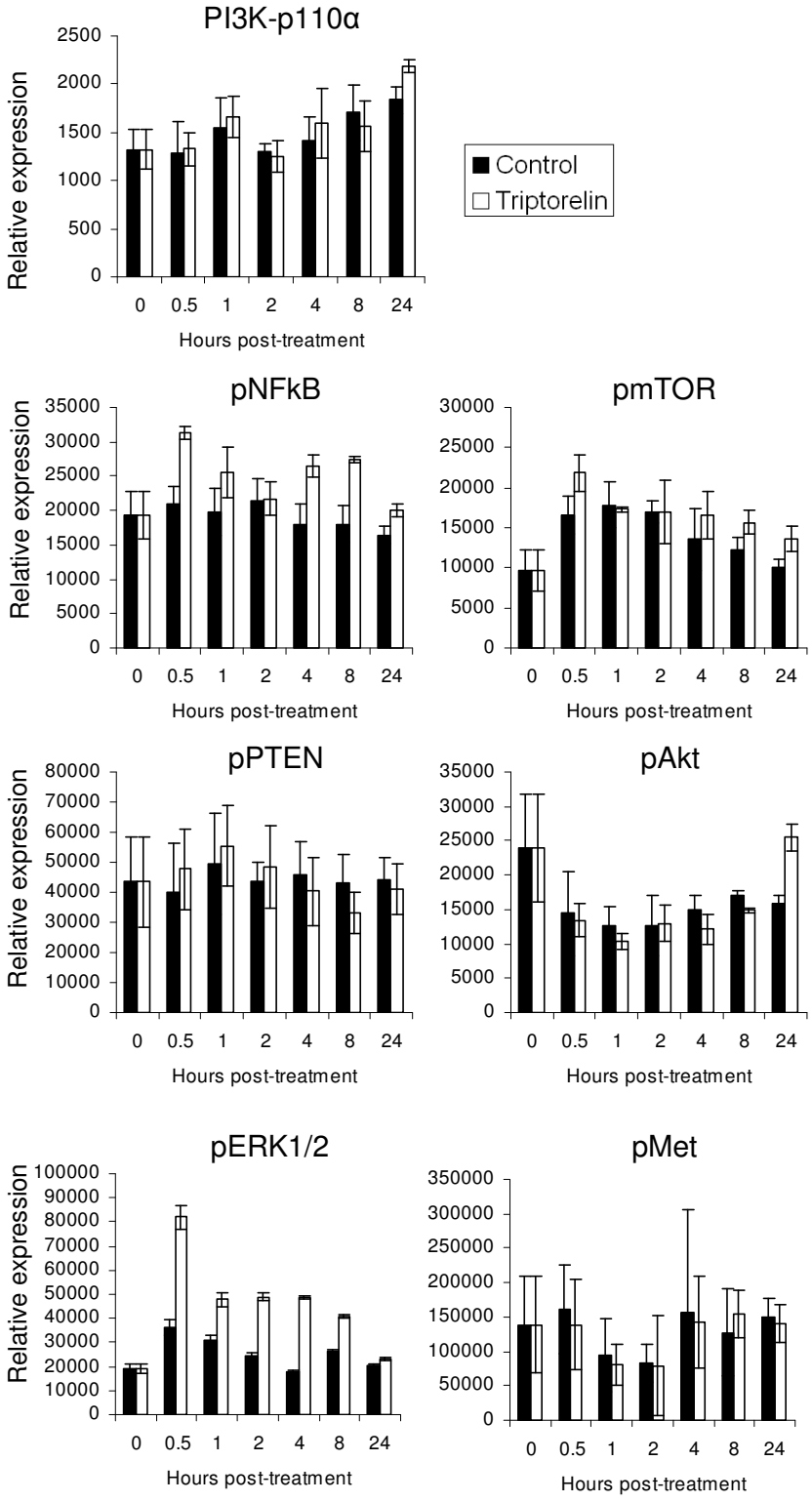

Figure 42: Protein expression (measured by RPPA) in SCL60 cells following treatment with 100nM Triptorelin or vehicle control for up to 24h.
Protein expression was measured by RPPA in SCL60, HEK293 and SCL215 cells following treatment with 0.02% propylene glycol (vehicle control) or 100nM Triptorelin. Phospho-protein expression was wherever possible normalised to total protein expression. Bars show mean protein expression of three independent experiments. Error bars show standard deviation.

3.3.2.4 RPPA Reproducibility

To assess the reproducibility of the reverse phase protein array method, a 2-pad slide was probed for pNFkB and tNFκB as usual and then the process was repeated with another 2-pad slide on a different day using freshly prepared antibody solutions. The slides were scanned under the same conditions, and for each slide the data corresponding to pNFkB expression were normalised to total NFkB expression. The expression in Triptorelin-treated samples was then divided as before by the expression in the control sample of the same time point. The results of the original and repeat measurements showed good agreement with each other (Figure 43).

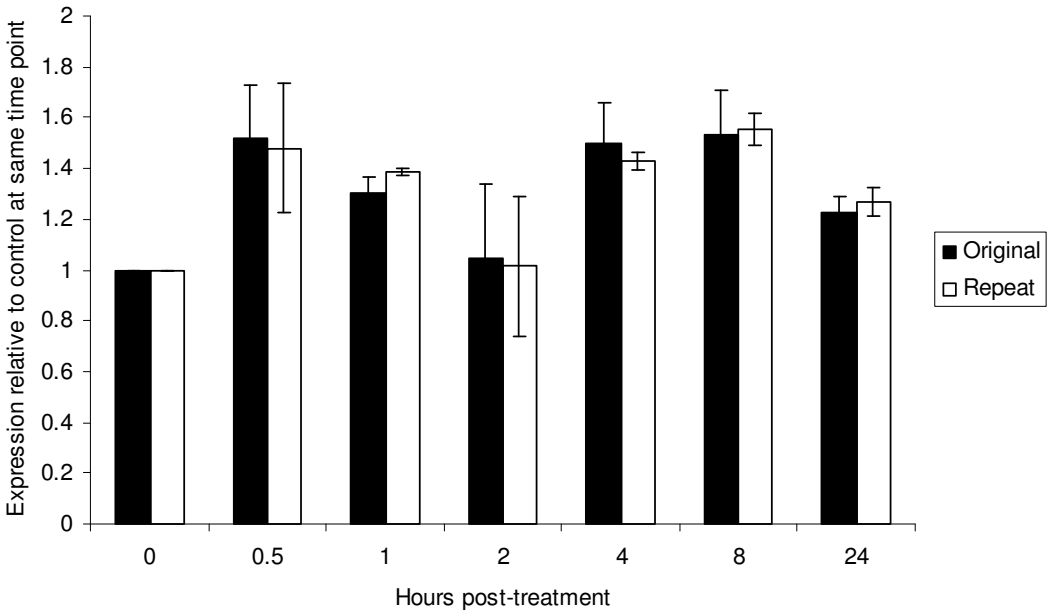

Figure 43: pNFkB protein expression (measured by RPPA) in SCL60 cells following treatment with 100nM Triptorelin for up to 24h.
Values are shown for the original measurement (black), and a repeat measurement (white). Errors bars show +/- standard deviation of three replicates.

3.3.3 Validation of RPPA phosphoprotein expression changes by western blot

Expression of the proteins identified by RPPA analysis was analysed by western blot.

3.3.3.1 pNFκB

pNFκB expression was higher in Triptorelin-treated cells at 1-24h after treatment compared to vehicle control-treated cells at the same time points (Figure 44, Figure 45). Figure 44 shows a western blot for pNFκB and tNFκB, and Figure 45 shows the quantification of this western blot. The data in Figure 45 are shown as pNFκB expression normalised to tNFκB expression, in SCL60 cells treated with Triptorelin relative to that in SCL60 cells treated with a vehicle control. RPPA data showed that pNFκB was increased slightly at all time points except 2h. The western blot data shows that pNFκB was increased in expression at all six time points investigated. The western blot data shows that there was a gradual rise in pNFκB with a peak at 2h and remaining above basal level at 24h.

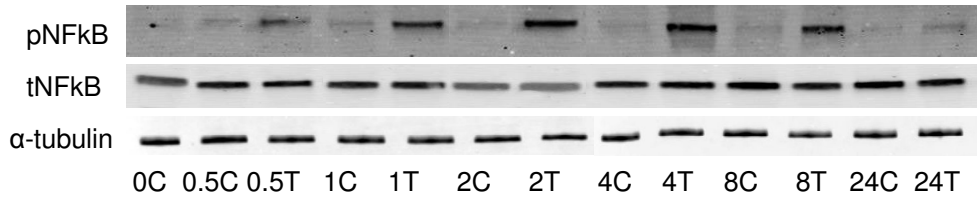

Figure 44: Western blot showing pNFκB and tNFκB expression in SCL60 cells 0-24h after treatment with Triptorelin (T) or vehicle control (C). This is representative of two independent experiments

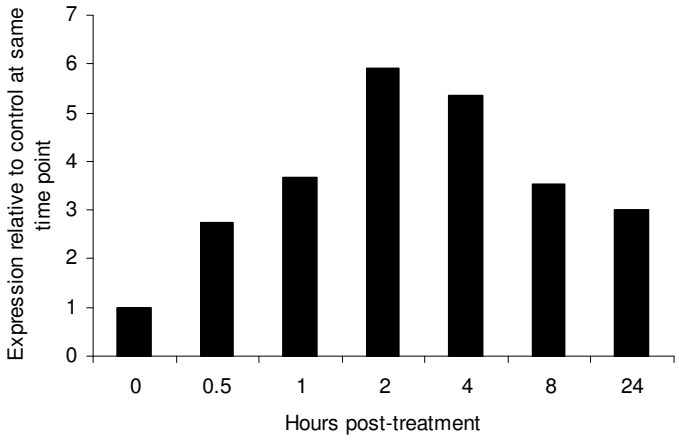

Figure 45: Quantification of western blot shown in Figure 44.
The data shown is pNFκB expression (normalised to tNFκB expression) in SCL60 cells treated with Triptorelin relative to that in cells treated with a vehicle control at the same time point. This figure shows data from a single experiment.

3.3.3.2 pERK1/2

Figure 46 shows a western blot for pERK1/2 and tERK1/2, and Figure 47 shows the quantification of this western blot. The data in Figure 47 show pERK1/2 expression normalised to tERK1/2 expression, in SCL60 cells treated with Triptorelin relative to that in SCL60 cells treated with a vehicle control. By western blot, pERK1/2 appeared to be initially increased in expression in Triptorelin-treated cells compared to vehicle control-treated cells (Figure 46, Figure 47). pERK1/2 levels peaked at 4h after treatment and a higher level of pERK1/2 in Triptorelin-treated cells was maintained up to 8h after treatment before returning to nearer control level by 24h (Figure 46, Figure 47). Western blot-detected changes in pERK1/2 and tERK1/2 expression levels following Triptorelin largely supported the changes detected by RPPA, although the magnitude of differential expression was higher in western blot data (Figure 47, Figure 42).

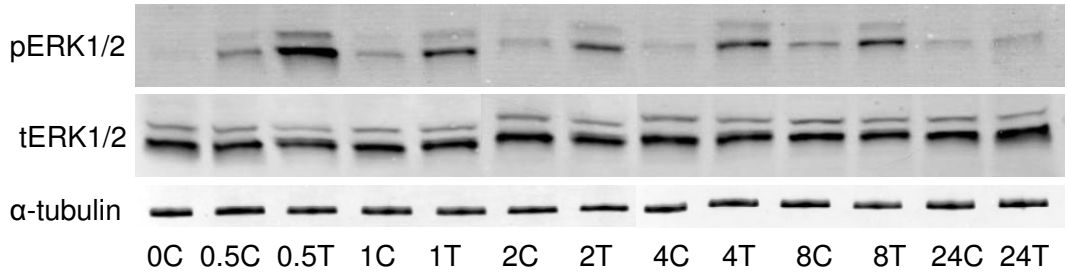

Figure 46: Western blot showing pERK1/2 and tERK1/2 expression in SCL60 cells 0-24h after treatment with Triptorelin (T) or vehicle control (C). This figure is representative of two independent experiments.

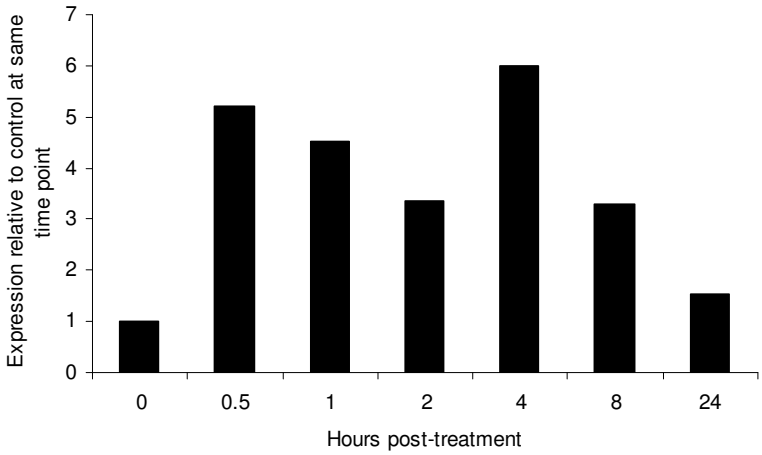

Figure 47: Quantification of western blot shown in Figure 46.
The data shown is pERK1/2 expression (normalised to tERK1/2 expression) in SCL60 cells treated with Triptorelin relative to that in cells treated with a vehicle control at the same time point. This figure shows data from a single experiment.

3.3.3.3 pAkt

Figure 48 shows a western blot for pAkt and tAkt, and Figure 49 shows the quantification of this western blot. By western blot, pAkt appeared to be lower in Triptorelin-treated cells at all time points after treatment compared to vehicle control-treated cells at the same time points (Figure 48, Figure 49). The data in Figure 49 show pAkt expression normalised to tAkt expression, in SCL60 cells treated with Triptorelin relative to that in SCL60 cells treated with a vehicle control.

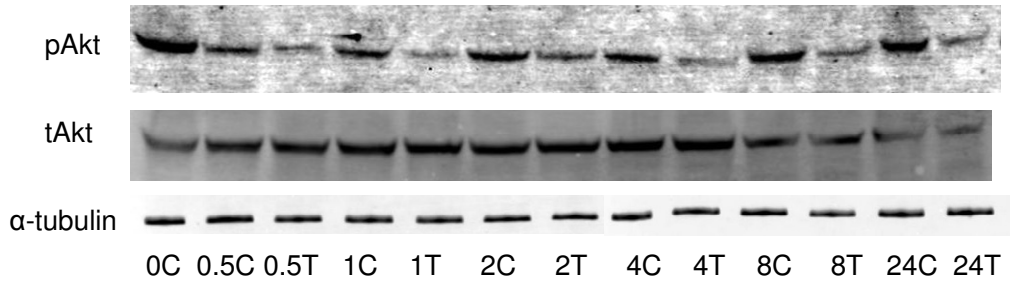

Figure 48: Western blot showing pAkt and tAkt expression in SCL60 cells 0-24h after treatment with Triptorelin (T) or vehicle control (C). These data are from a single experiment.

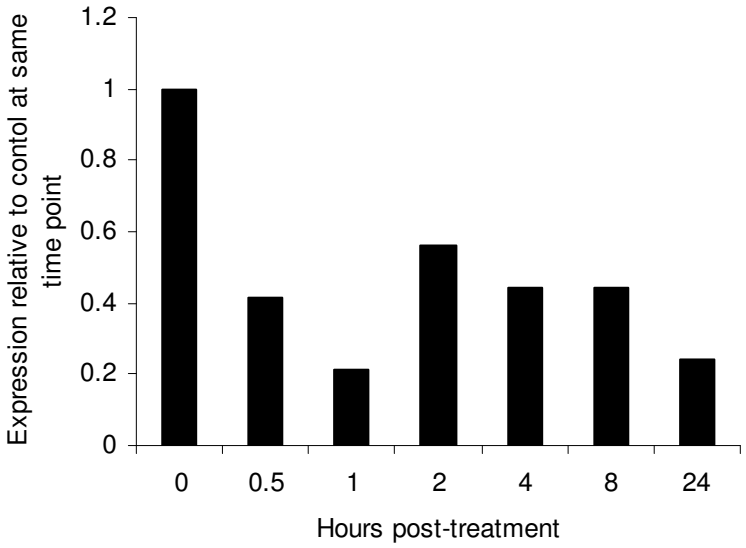

Figure 49: Quantification of western blot shown in Figure 48.
The data shown is pAkt expression (normalised to tAkt expression) in SCL60 cells treated with Triptorelin relative to that in cells treated with a vehicle control at the same time point. These data are from a single experiment.

3.3.3.4 PI3K-p110α

Figure 50 shows a western blot for PI3K-p110α, and Figure 51 shows the quantification of this western blot. The data in Figure 51 show PI3K-p110α expression in Triptorelin treated SCL60 cells relative to that in SCL60 cells treated with a vehicle control. The level of PI3K-p110α fluctuated in both vehicle control and Triptorelin-treated cells over the 24h treatment period. Western blot measurement of PI3K-p110α expression (Figure 50, Figure 51) did not support the small difference in PI3K-p110α between vehicle control and Triptorelin-treated cells at 24h observed by RPPA (Figure 42).

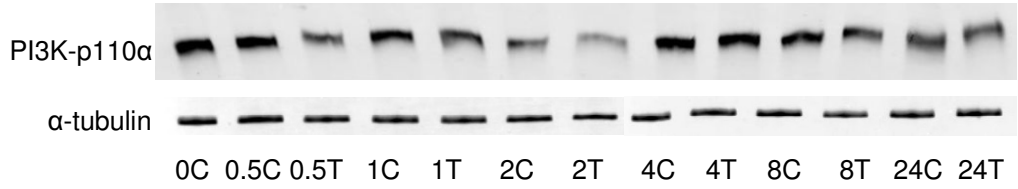

Figure 50: Western blot showing PI3K-p110α expression in SCL60 cells 0-24h after treatment with Triptorelin (T) or vehicle control (C). These data are from a single experiment.

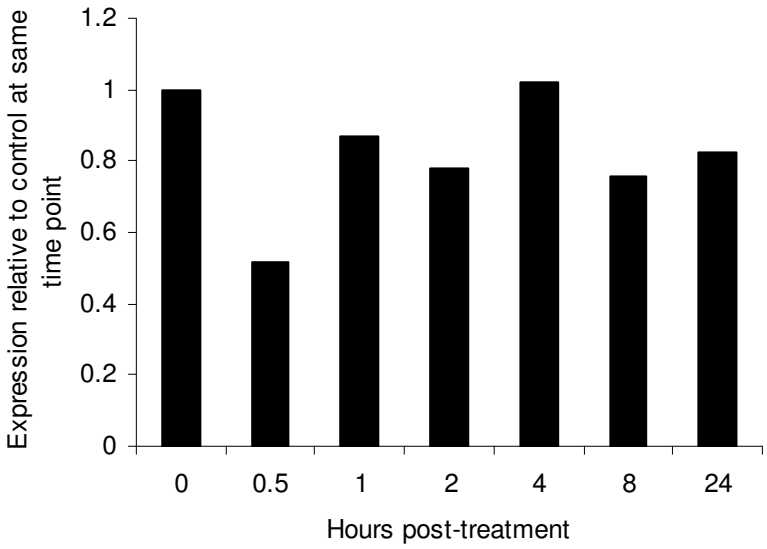

Figure 51: Quantification of western blot shown in Figure 50.
The data shown is PI3K-p110α expression in SCL60 cells treated with Triptorelin, relative to that in cells treated with a vehicle control. These data are from a single experiment.

3.3.3.5 pmTOR

Figure 52 shows a western blot for pmTOR and tmTOR, and Figure 53 shows the quantification of this western blot. The data in Figure 53 are shown as pmTOR expression normalised to tmTOR expression, in SCL60 cells treated with Triptorelin relative to that in SCL60 cells treated with a vehicle control. pmTOR appeared to be higher in Triptorelin-treated cells at 0.5, 1 and 8h after treatment compared to vehicle control-treated cells at the same time points (Figure 52, Figure 53).

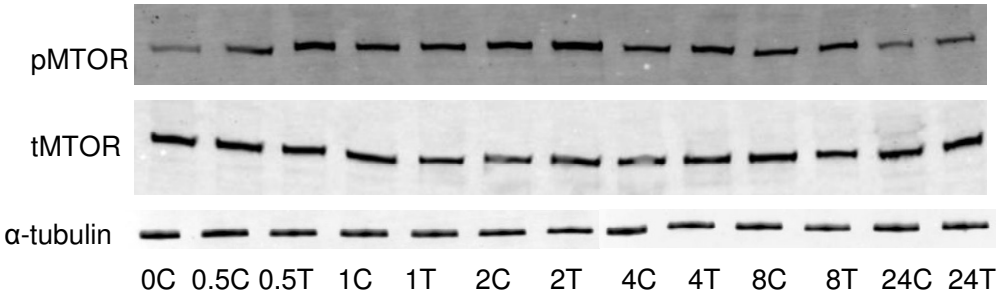

Figure 52: Western blot showing pmTOR and tmTOR expression in SCL60 cells 0-24h after treatment with Triptorelin (T) or vehicle control (C). These data are from a single experiment.

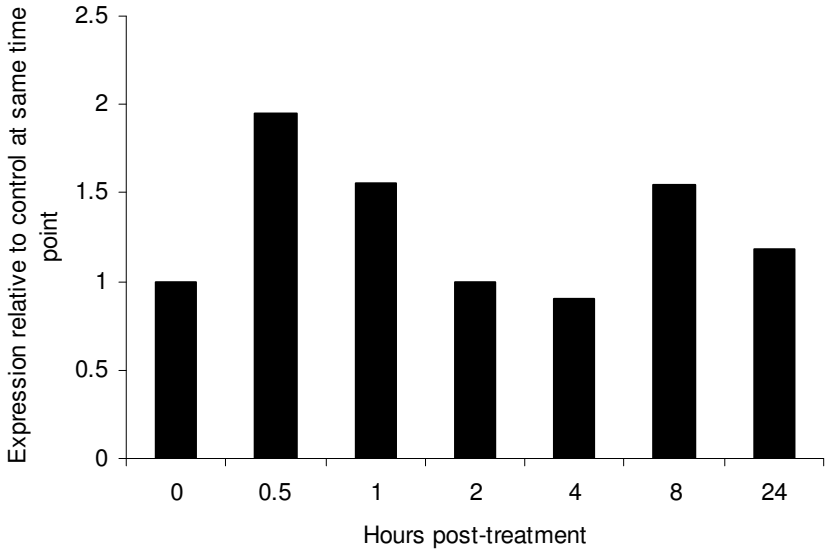

Figure 53: Quantification of western blot shown in Figure 52.
The data shown is pmTOR expression (normalised to tmTOR expression) in SCL60 cells treated with Triptorelin relative to that in cells treated wtih a vehicle control. These data are from a single experiment.

3.3.3.6 pPTEN

Figure 54 shows a western blot for pPTEN, and Figure 55 shows the quantification of this western blot. The data in Figure 55 show pPTEN expression in SCL60 cells treated with Triptorelin relative to that in SCL60 cells treated with a vehicle control. The level of pPTEN expression changed in both vehicle control and Triptorelin-treated cells over the 24h treatment period. Little difference could be detected in the level of pPTEN between control and Triptorelin-treated cells at the same time point, although pPTEN did appear slightly lower with Triptorelin treatment at 24h when measured by western blot (Figure 54, Figure 55).

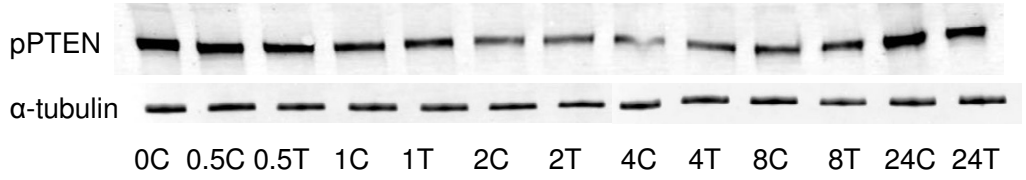

Figure 54: Western blot showing pPTEN expression in SCL60 cells 0-24h after treatment with Triptorelin (T) or vehicle control (C). These data are from a single experiment.

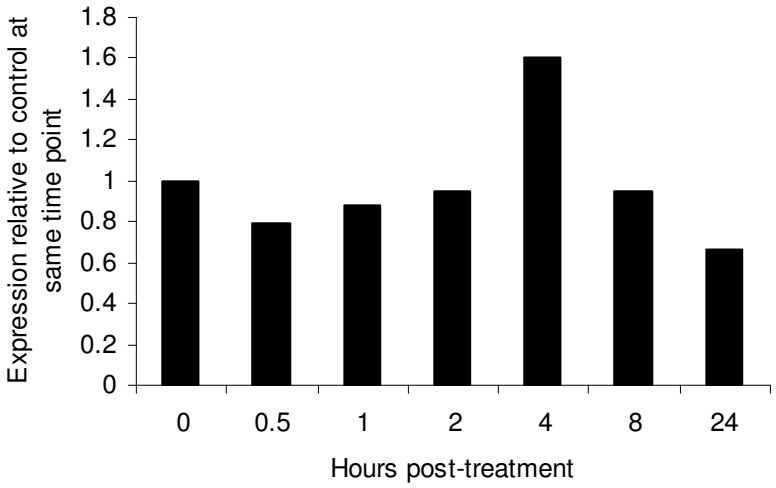

Figure 55: Quantification of western blot shown in Figure 54.
The data shown is pPTEN expression in SCL60 cells treated with Triptorelin relative to that in cells treated wtih a vehicle control. These data are from a single experiment.

3.3.3.7 pMet

Figure 56 shows a western blot for pMet and tMet, and Figure 57 shows the quantification of this western blot. The data in Figure 57 show pMet expression normalised to tMet expression, in SCL60 cells treated with Triptorelin relative to that in SCL60 cells treated with a vehicle control. By western blot, pMet appeared to be higher in Triptorelin-treated cells at 2 and 4h after treatment compared to vehicle control-treated cells at the same time points. However, pMet was poorly detected by western blot and this does not support the RPPA data.

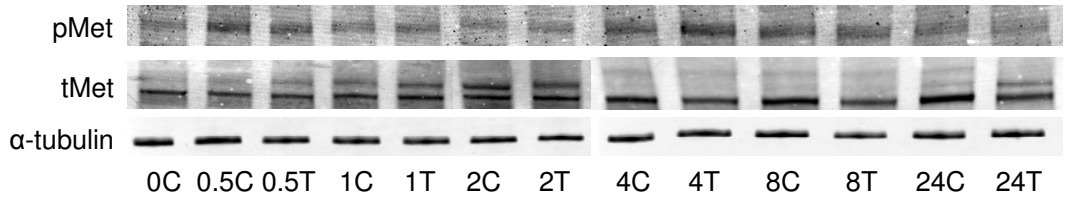

Figure 56: Western blot showing pMet and tMet expression in SCL60 cells 0-24h after treatment with Triptorelin (T) or vehicle control (C). These data are from a single experiment.

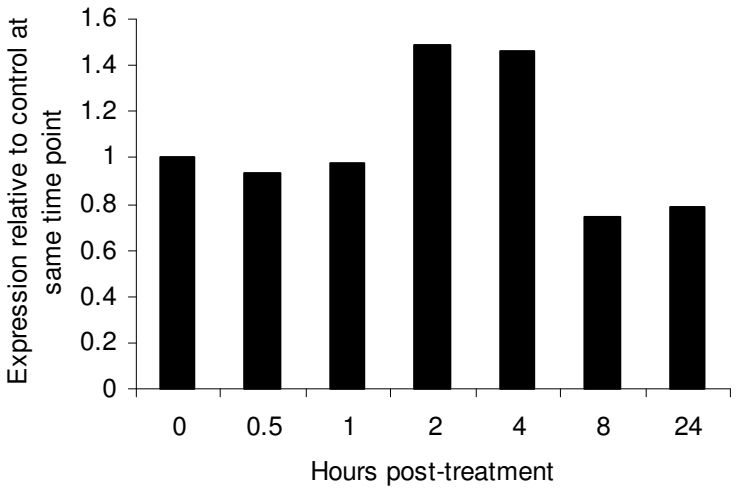

Figure 57: Quantification of western blot shown in Figure 56.
The data shown is pMet expression (normalised to tMet expression) in SCL60 cells treated with Triptorelin relative to that in cells treated wtih a vehicle control. These data are from a single experiment.

3.3.4 Discussion

3.3.4.1 In vivo phosphoproteomic array

The antibody array identified a number of phosphoproteins that were changed in response to Triptorelin in SCL60 xenografts. After 4 days of treatment, a decrease was noted in the ratio of phosphorylated to non-phosphorylated Met (growth factor receptor) and Caveolin-1 (membrane-associated protein) compared to untreated controls (Figure 32). In contrast, phosphorylation of Myc (multifunctional DNA binding proto-oncogene) was increased (Figure 32). It was interesting to note increases in phosphorylation of both NFκB-p65 and IκBε (Figure 32), since there is limited evidence in the literature that NFκB pathway members may be involved in GnRHR-mediated signalling [42, 65, 100, 101]. Triptorelin has been shown to induce NFκB activation in ovarian cancer cells (EFO-21 and EFO-27), which inhibited Doxorubicin-induced apoptosis in these cells [65]. GnRH has also been shown to stimulate the rapid phosphorylation of NFκB-p65 in LβT2 cells [100]. NFκB signalling may warrant further investigation as a downstream signalling pathway of GnRHR.

The phosphoproteins that were differentially modulated following treatment in the SCL60 xenografts were quite different between days 4 and 7, indicative of dynamic changes which may be consistent with differences seen *in vitro*. An example of this was phosphorylated AMPK1, which was increased after 4 days but decreased after 7 days (Figure 32). However, phosphorylated Myc levels remained elevated after 7 days of Triptorelin treatment compared to untreated controls, although to a lesser extent (1.4 fold; Figure 32). Phosphorylated 4E-BP1 was also increased with Triptorelin treatment at both 4 and 7 days after treatment (Figure 32).

Phosphoproteins that were decreased *in vivo* at day 7 included Akt (1.5 fold) and Chk2 (1.5 fold). Changes observed in the cell cycle proteins p27 (increased at day 4), CDC25C (increased at day 7), and Chk2 (decreased at day 7), may be relevant in understanding the disruption to cell cycle progression observed *in vitro*. CDC25C is a dual-specificity protein phosphatase that dephosphorylates and activates CDC2 to

allow entry into mitosis [185]. CDC25C is constitutively phosphorylated at Ser216 (inactivated) throughout interphase and sequestered in the cytoplasm through binding to 14-3-3 family proteins to prevent premature entry into mitosis [186, 187]. CDC25C is also phosphorylated by Chk1 and Chk2 after DNA damage at the G2/M checkpoint [188, 189]. Phosphorylation of Chk2 at Thr68 is required for further phosphorylation and activation of Chk2 in response to DNA damage [190]. Changes in the phosphorylation levels of the apoptosis regulators BCL-2 (anti-apoptotic when phosphorylated at Thr56 [191, 192], decreased at day 7) and BAD (anti-apoptotic when phosphorylated at Ser155 [193], increased at day 4) may be relevant to understanding the apoptosis observed both *in vitro* and *in vivo*.

It should be acknowledged that the array comprised phosphoproteins specifically selected because they are known to regulate cell proliferation or death and therefore some of these observations may not be a complete surprise, this was not a truly data-driven approach. Nonetheless, levels of particular phosphoproteins that consistently or very strongly changed in this dataset may be relevant to GnRHR-mediated signalling. The proteins identified in this analysis were investigated further by RPPA *in vitro* or IHC *in vivo*.

The results of the antibody array were somewhat variable due to a small sample size and the inherent variability in xenograft samples. Ideally more samples would have been included in this array. However, the antibody array was useful in that it led to the identification of a potential role for NFκB pathway signalling in the GnRHR-mediated antiproliferative response, and NFκB was further shown to be important in the antiproliferative effects of Triptorelin (see later).

The phosphoproteomic array was designed to detect changes in phosphorylation status of selected proteins. The method has an inherent systematic bias because each sample must be hybridised to a different array chip. The phosphoprotein data were normalised to corresponding total protein data, allowing relative changes in the ratio of phosphoprotein to total protein expression between samples to be analysed. However, it is not possible to normalise the measures of total protein. It would be

inappropriate to attempt to interpret a dataset that is clearly distorted by systematic bias, therefore these data are not shown. Comparisons between the level of total protein expression and the level of gene expression cannot be made for the above reason.

Immunohistochemical staining of the xenografts revealed that the level of pNFκB (normalised to tNFκB) was significantly increased with Triptorelin treatment at both 4 and 7 days after treatment (Figure 35, Figure 36).

Most of the phosphoproteins examined by immunohistochemical staining of the SCL60 xenograft tissue did not show differential staining between SCL60 Triptorelin-treated xenografts and vehicle control-treated xenografts. Despite being the most strongly and consistently differentially phosphorylated proteins according to the antibody array; no significant difference could be detected in the levels of pCav1, tCav1, pMet, or tMet between Control and Triptorelin-treated xenografts (Figure 37). It was also interesting to note that no difference in the expression of pERK1/2 or tERK1/2 could be detected between Control and Triptorelin-treated xenografts despite the proposed role of pERK1/2 *in vitro* (Figure 37) [79]. Although the sample size is limited, which could be a factor in not observing significant differences, the differences in immunostaining for the majority of targets explored were very small between control and treated groups. This suggests that even if the sample size were larger, any differences observed are unlikely to be useful in understanding the biology of GnRHR signalling.

3.3.4.2 In vitro phosphoprotein profiling

3.3.4.2.1 pNFκB

The RPPA data showed that pNFκB expression was significantly (1.8 fold) higher in SCL60 cells compared to SCL215 cells (P=0.035, 2-sample t-test), and was increased slightly with Triptorelin treatment in SCL60 cells compared to vehicle control-treated cells at all time points from 1-24h except 2h. The western blot data showed that pNFκB was increased in expression at all six time points after treatment

compared to vehicle control-treated cells at the same time points (Figure 44, Figure 45). The western blot data showed that there was a gradual rise in pNFκB expression with a peak at 2h and remaining above basal level at 24h. This increase in pNFκB expression *in vitro* was interesting because it had also been identified as differentially expressed *in vivo*. In the SCL60 xenografts, the phosphorylation of NFκB-p65 was increased after 4 days of treatment with Triptorelin. These data together gave further evidence for a role for NFκB signalling in the response to Triptorelin, and provided a basis for further investigation of the role of NFκB in response to GnRHR activation.

3.3.4.2.2 pERK1/2

A transient increase (approx 1.5 fold) was observed in the level of pERK1/2 expression at 1h following treatment with Triptorelin in both SCL60 and SCL215 cells which returned to basal levels by 24h (Figure 39). pERK1/2 was initially increased in expression in Triptorelin-treated cells compared to vehicle control-treated cells, and an elevated level of pERK1/2 in Triptorelin-treated cells was maintained up to 8h before returning to near control level by 24h.

ERK1/2 activation has previously been demonstrated in SCL60 cells to be transient, whereby increased pERK1/2 is observed within 5min of incubation with the GnRH agonist Triptorelin, which then decreases (although is still above basal levels) by 30min [79]. However, the data presented above indicates that after 30min the level of pERK1/2 expression does not decrease entirely to basal levels, but continues to be at least slightly elevated for at least 8h.

As mentioned in the Introduction to this thesis, there appears to be a role for ERK1/2 activation in response to GnRHR stimulation. In SCL60 cells, there is an immediate intense activation of ERK1/2 following Triptorelin treatment [79]. Inappropriate increase in pERK1/2 has been shown to cause G_2/M arrest [93, 194]. ERK1/2-mediated G_2 arrest appears to be dependent on PKC [93, 195] and MEK1 [92, 93]. The antiproliferative effect of Triptorelin in SCL60 cells has been shown to be dependent on PKC but not MEK [79].

3.3.4.2.3 pAkt, PI3K-p110α and pmTOR

pAkt appeared to be lower in Triptorelin-treated cells at all time points after treatment compared to vehicle control-treated cells at the same time points (Figure 48, Figure 49). By western blot, there appeared to be a clear pattern of pAkt being decreased in Triptorelin-treated cells compared to vehicle control-treated cells. This was apparent at all time points. There was a similar level of tAkt in vehicle control and Triptorelin-treated cells of each time point, indicating that the variation in pAkt is not due to variation in the level of tAkt. A decrease in pAkt is consistent with a

decrease in pAkt observed in the SCL60 xenograft *in vivo* antibody array 7 days after treatment with Triptorelin.

Cross-talk between the PI3K/Akt and NFκB signalling pathways has been suggested, and it has recently been shown that Akt inhibits FasL-dependent NFκB activity in human renal 293T and Jurkat T-lymphocytes [196, 197]. It could be speculated that the decreased Akt activity in response to Triptorelin may play a role in the increased NFκB activity, although further experimentation is required to understand the nature of any cross-talk between these pathways and the applicability of such cross-talk in this context.

When activated, Akt promotes cell survival by inhibiting several downstream targets by phosphorylation, including the pro-apoptotic factors caspase 9 and BAD [196, 198, 199]. Akt also inhibits Raf, thereby inhibiting the Raf-MEK-ERK1/2 signalling pathway [200]. Akt promotes progression through the cell cycle by inhibiting the cyclin dependent kinase inhibitors p27(Kip1) and p21 (Cip1/Waf1) [196, 201, 202] and maintaining cyclin D1 by inhibiting its phosphorylation and degradation by GSK-3β [203]. Akt also initiates a multistep signalling pathway leading to the activation of mTOR and ribosomal s6k to activate translation [204, 205]. It is plausible that the observed decrease in the level of pAkt following GnRHR stimulation may be partly responsible for the antiproliferative effect of Triptorelin in SCL60 cells.

The level of PI3K-p110α appeared to decrease in Triptorelin-treated cells compared to vehicle control-treated cells, although it fluctuated in both sample types over the 24h treatment period. Western blot measurement of PI3K-p110α expression (Figure 50, Figure 51) did not support the small difference in PI3K-p110α between vehicle control and Triptorelin-treated cells at 24h observed by RPPA, but did indicate a decrease in PI3K-p110α 0.5h after Triptorelin treatment in SCL60 cells (Figure 42).

PI3K-p110α also appeared to be decreased following GnRHR stimulation by Triptorelin in SCL60 cells. PI3K-p110α promotes the activation of Akt: PI3K

phosphorylates PIP2 to PIP3, which allows Akt to bind and be phosphorylated and activated by phosphoinositide dependent kinase 1 (PDPK1) at Thr308 and mammalian target of rapamycin complex 2 (mTORC2) at Ser473 [206, 207]. It is possible, therefore, that the decrease in PI3K-p110α mediates the decrease in pAkt.

Upon stimulation, GnRHR activates the intracellular G-protein Gαq, which is known to inhibit PI3K-p110α and therefore Akt [208, 209]. This may be the mechanism by which Triptorelin causes a decrease in pAkt. More experiments are needed to explore the downstream effects of decreased pAkt in this context.

There appeared to be a slight increase in pmTOR expression at 0.5, 1 and 8h with treatment, although this was not as clear as the change in pAkt. Akt is a key regulator of mTOR [210], but mTOR can also be activated in an Akt-independent manner [211]. RPPA data showed an increase in pmTOR expression with Triptorelin treatment at 0.5, 4, 8 and 24h. Western blot analysis supports the increased pmTOR expression at 0.5h but does not support the increased levels of pmTOR seen at later time points. Both pmTOR and tmTOR levels are variable across the 24h treatment period in both vehicle control-treated and Triptorelin-treated cells. It is not clear why pmTOR is activated in vehicle control treated cells, but this may reflect a stress-induced response. Because of the large variability in pmTOR and tmTOR detected, particularly in vehicle control-treated cells, the validity of the observed differences between control and Triptorelin-treated cells at 0.5 and 1h is questionable. Any true difference is likely to be small.

3.3.4.2.4 Other targets: pPTEN and pMet

The level of pPTEN expression changed in both vehicle control and Triptorelin-treated cells over the 24h treatment period. However, little difference could be detected in the level of pPTEN between control and Triptorelin-treated cells at any time point (Figure 54, Figure 55). It was not possible to detect tPTEN by western blot, and a stronger band of the incorrect molecular weight was detected, indicating

that this antibody unreliably detects tPTEN, therefore the level of pPTEN could not be normalised to the level of tPTEN.

By western blot, the level of pMet expression appeared to be higher in Triptorelin-treated cells at 2 and 4h after treatment compared to vehicle control-treated cells at the same time points. However, pMet was poorly detected by western blot and this does not support the RPPA data.

3.3.4.3 Comparison of RPPA and Western blot techniques

RPPA provided a high-throughput, quantitative method to study a large number of protein targets for a large number of samples. Protein expression was measured in SCL60 cells following GnRHR stimulation at multiple time points for three biological replicates (experiments performed on different days), with multiple protein dilutions. This high degree of replication allows for a more accurate quantification and indicates more reliability in the data. The disadvantage of RPPA is that the antibody used may detect a protein other than the protein of interest. RPPA may have poorer discrimination of signal from background noise compared to a western blot that gives an easily detectable band. RPPA therefore provided a useful tool for screening multiple antibodies, but western blot data is considered the more reliable for further interpretation. The results of the original and repeat measurements by RPPA showed good agreement with each other (Figure 43). Western blot data was highly supportive of RPPA data: where differential protein expression was identified by RPPA, it was generally reflected by a similar result by western blot analysis, although differences in expression between control and Triptorelin-treated cells tended to be greater in western blots.

3.4 NFκB signalling was altered at both the proteomic and transcriptomic level in SCL60 cells following GnRHR stimulation

NFκB was identified as a candidate for further investigation after an antibody array and immunohistochemistry indicated that pNFκB-p65 was differentially expressed between SCL60 xenografts treated with a vehicle control or with Triptorelin. pNFκB was also differentially expressed between vehicle control and Triptorelin-treated SCL60 cells *in vitro* by RPPA analysis. Western blotting confirmed that pNFκB was increased in response to Triptorelin at all six time points (0.5, 1, 2, 4, 8, 24h) over the 24h treatment period. A gradual rise in pNFκB was observed with a peak at 4h and remaining above basal level at 24h (Figure 44, Figure 45).

Because NFκB had been identified as being differentially modulated by Triptorelin at the proteomic level both *in vitro* and *in vivo*, it was interesting to explore its expression at the transcriptomic level.

To explore whether the expression of NFκB signalling pathway members was also altered at the transcriptomic level, their expression following Triptorelin treatment in SCL60 cells was examined. Figure 58 highlights the gene expression patterns of several NFκB pathway members that are perturbed in SCL60 cells following treatment with Triptorelin. Figure 58 shows some examples of NFκB pathway members, and demonstrates that there is a range of expression profiles within members of this pathway. Some are transiently increased (NFKBIA, IKBKB), some transiently decreased (IKBKG, NFKB1) and MAP3K8 has a prolonged increase in expression after Triptorelin treatment in SCL60 cells. NFKBIA encodes the inhibitor of NFκB, IκBα; IKBKB and IKBKG encode inhibitors of IκBα, IKKβ and IKKγ; NFKB1 encodes NFκB-p105/p50, and MAP3K8 encodes an activator of NFκB-p105, MEKK8.

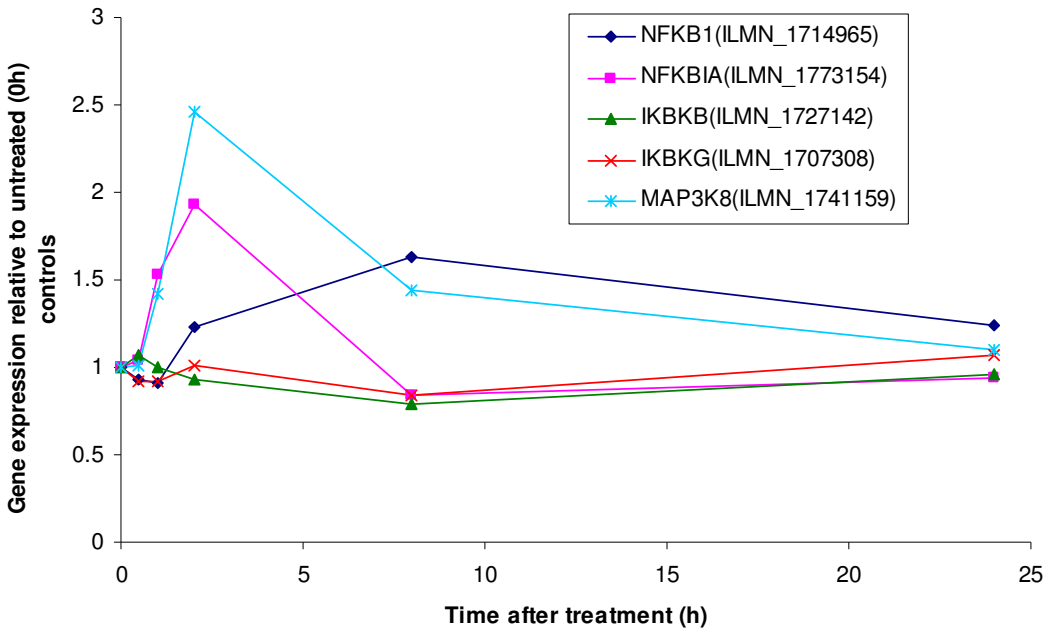

Figure 58: Gene expression profiles of several NFκB pathway members in SCL60 cells following treatment with Triptorelin for up to 24h.
Expression at 0.5, 1, 2, 8 and 24h after Triptorelin treatment is shown relative to untreated (0h) cells.

3.4.1 NFκB inhibition did not prevent the antiproliferative effect of Triptorelin in SCL60 cells

To examine the effect of NFκB on SRB activity of SCL60 cells, the cells were treated with the NFκB inhibitor 15-deoxy$\Delta^{12,14}$ prostaglandin J_2 [212] (15d-PGJ_2; 3μM) alone and in combination with Triptorelin (100nM). Cell number was measured by SRB assay. After 4 days of treatment a reduction in cell number was observed in all three treatment groups (Figure 59) compared to vehicle control-treated cells. The combination of GnRHR stimulation and NFκB inhibition had a greater impact on SRB activity than either treatment alone (Figure 59). 15d-PGJ_2 did not inhibit HEK293 SRB activity either alone or in combination with Triptorelin (Figure 60).

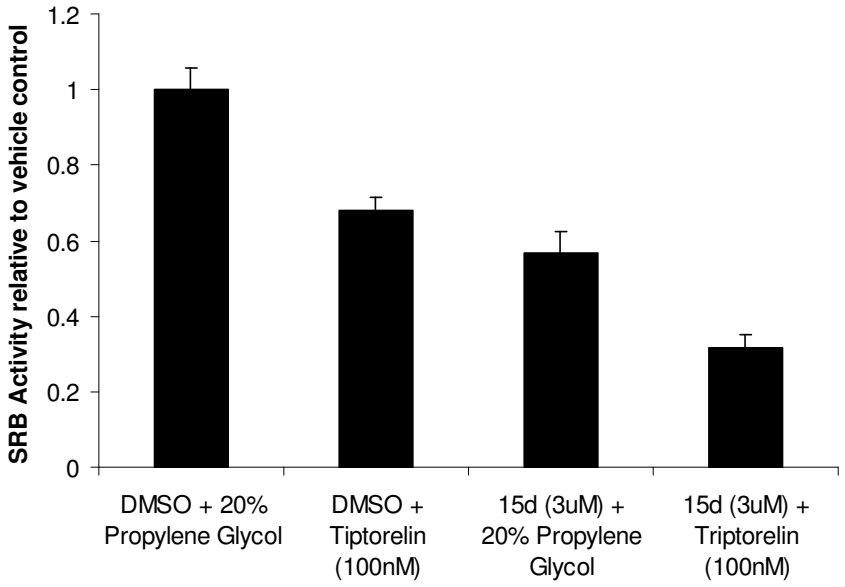

Figure 59: NFκB inhibition in SCL60 cells with 3μM 15d-PGJ_2.
NFκB inhibition with 3μM 15d-PGJ_2 (15-Deoxy-(Delta)12,14-Prostaglandin J2) caused inhibition of SCL60 SRB activity both alone and in combination with 100nM Triptorelin. Cell number was measured by SRB assay 4 days after treatment and is shown relative to that of the vehicle control-treated cells. Error bars show standard deviation of three independent experiments.

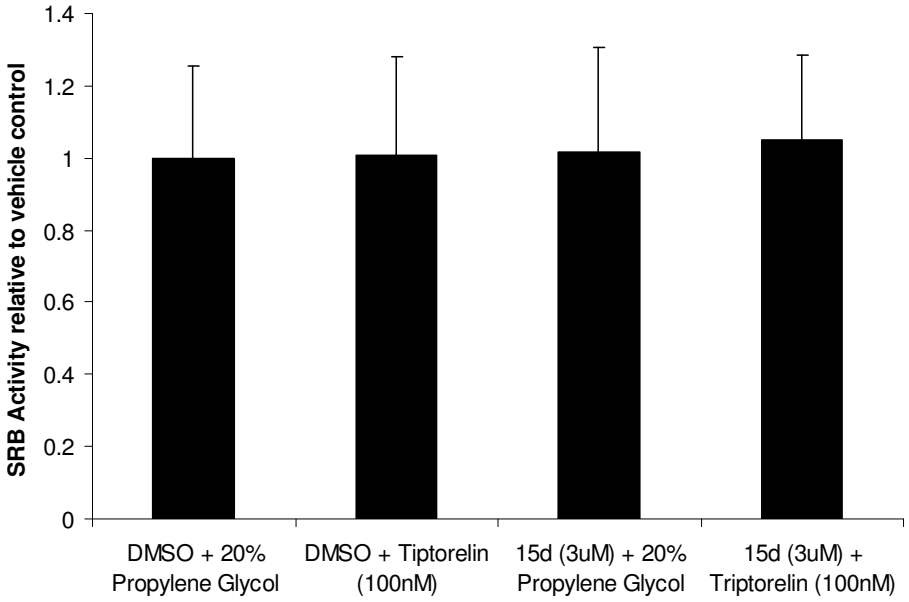

Figure 60: NFκB inhibition in HEK293 cells with 3μM 15d-PGJ_2.
NFκB inhibition with 3μM 15d-PGJ_2 did not cause inhibition of HEK293 SRB activity either alone or in combination with 100nM Triptorelin. Cell number was measured by SRB assay 4 days after treatment and is shown relative to that of the vehicle control-treated cells. Error bars show standard deviation of three intraexperimental replicates.

3.4.2 Discussion

The perturbation of NFκB pathway signalling at both the transcriptomic and proteomic level provided a basis for the hypothesis that NFκB pathway signalling may be involved in the antiproliferative response to GnRH agonist treatment. NFκB has been shown to play a role in cell survival in many model systems (reviewed in [103, 213]). NFκB inhibition enhanced the antiproliferative effect of Triptorelin in SCL60 cells (but not HEK293 cells) *in vitro*. NFκB activation may act in SCL60 cells as part of a survival mechanism in response to GnRHR stimulation.

Peroxisome proliferator-activated receptor gamma (PPARγ) is a ligand-activated transcription factor belonging to the nuclear hormone receptor superfamily [214]. 15d-PGJ_2 is a potent ligand for PPARγ, through which its anti-inflammatory functions are thought to be mediated [212, 215, 216]. However, in HEK293 cells PPARγ-mediated gene expression is not stimulated by 15d-PGJ_2 [215]. This is thought to be due to the very low level of PPARγ expression in HEK293 cells compared to other cells such as 3T3-L1 (mouse embryonic fibroblast - adipose like) cells [215]. One study reports that growth of HEK293 cells is inhibited by 15d-PGJ_2 in a mechanism that is independent of PPARγ [215]. This is in contrast to the finding above that HEK293 cells do not respond to 15d-PGJ_2 (Figure 60).

These data provide a useful insight into pathways that may interact with GnRH receptor-mediated antiproliferative signalling and suggest that NFκB pathway members may represent targets for enhancing the antiproliferative effect of GnRH agonists in some reproductive tissue cancers.

3.5 GnRHR Expression in Breast Cancer

3.5.1 Introduction

GnRH agonists and antagonists have previously been shown to have antiproliferative effects in some breast cancers [25, 26, 28, 29, 31, 32, 57, 68, 69, 71, 77, 95, 217], but further research is required to improve efficacy and prediction of response. To make these improvements, it is necessary to further understand the important signalling factors in the antiproliferative response to GnRH analogues, and to identify which breast cancers express GnRHR and therefore may be responsive to GnRH analogue treatment.

It is unclear why some cell lines respond to GnRH analogues and others do not. There is some evidence to suggest that the level of GnRHR expression at the cell surface is proportional to the antiproliferative response of that cell line [79], in that high-GnRHR expressing cell lines have tended to be inhibited by GnRH agonists [79]. It could therefore be hypothesised that breast cancers expressing the highest level of GnRHR are those most likely to respond to GnRHR treatment.

A high level of GnRHR has so far been shown to correlate with the antiproliferative response to GnRH agonist treatment [79], and increasing the expression of GnRHR can enhance the antiproliferative effect of GnRH agonists [32]. Although GnRHR binding sites have been found in breast cancer [28, 70, 74], other studies were unable to detect GnRHR in breast cancer cell lines [79, 119]. The level of GnRHR expression in breast cancer remains unclear. To explore this, the expression of GNRHR was investigated at both the transcriptional and proteomic level.

3.5.2 GnRHR mRNA expression in breast cancer cell lines

To identify breast cancer cell lines expressing high levels of GnRHR, the level of GnRHR was examined in existing published data. Neve *et al* (A Collection of Breast Cancer Cell Lines for the Study of Functionally Distinct Cancer Subtypes, Cancer Cell, 2006) [218] surveyed the expression profiles of 51 breast cancer cell lines using

Affymetrix U133A microarray chips. The expression profile of GnRHR was obtained from this dataset and the results of this are shown in Figure 61. High GnRHR expressing breast cancer cell lines tended to be of the Luminal subtype, although there was a range of GnRHR expression in each subtype.

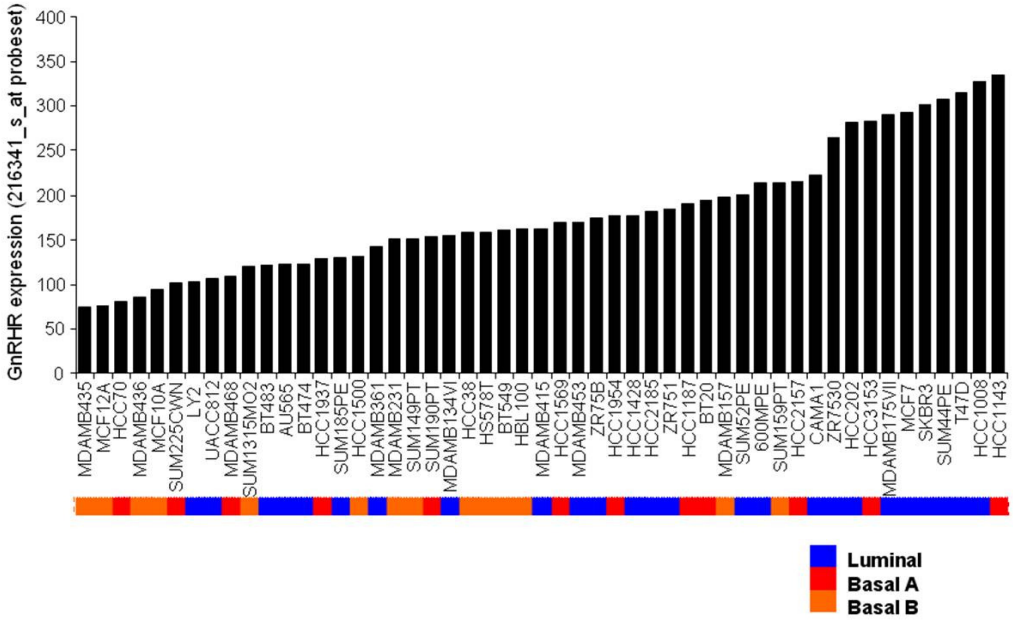

Figure 61: GNRHR gene expression in the Neve *et al* dataset, as identified using the selected probset 216341_s_at.
The subtype of each breast cancer cell line is shown beneath the x axis as either Luminal (blue), Basal A (red) or Basal B (orange). This figure was provided by Andy Sims and is in agreement with other analyses performed by myself.

3.5.3 GnRHR protein expression in breast cancer tumours

The level of GnRHR protein expression in a series of clinical breast cancer samples was measured using quantitative immunofluorescence (AQUA®). Three tissue microarrays (TMAs) were constructed with triplicate samples from each of 347 primary breast carcinomas [141]. The primary tissue was collected after surgical breast resection between 1999 and 2002 at the Breast Unit, Western General Hospital, Edinburgh [141]. Formalin-fixed paraffin-embedded pituitary was used as a positive control for GnRHR expression (Figure 62).

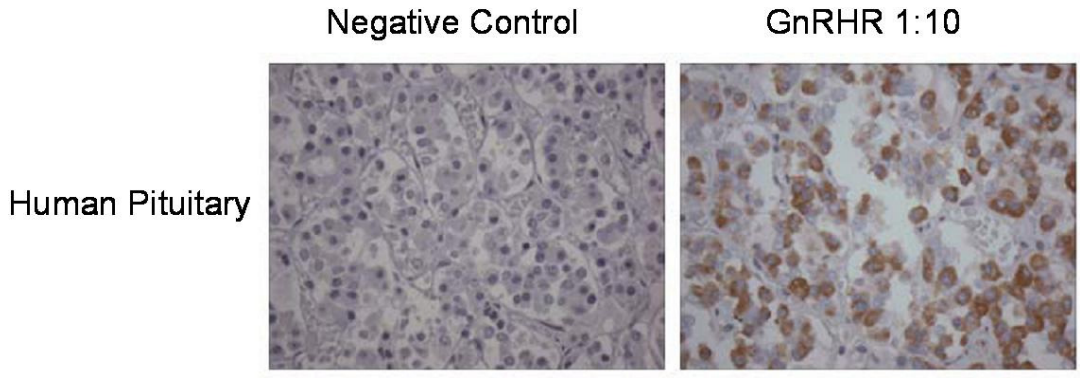

Figure 62: Human anterior pituitary GnRHR was used as a positive control for GnRHR antibody staining.
The left panel shows human pituitary incubated with antibody diluent in the absence of GnRHR antibody, and the right panel shows human pituitary incubated with Leica Microsystems A9E4GnRHR antibody (1:10 dilution). Positive staining was observed at the cell membrane and cytoplasm.

DAPI, Cy3 and Cy5 filters were applied to obtain an image for each of the nucleus, cytokeratin mask, and the target protein (GnRHR) respectively (Figure 63).

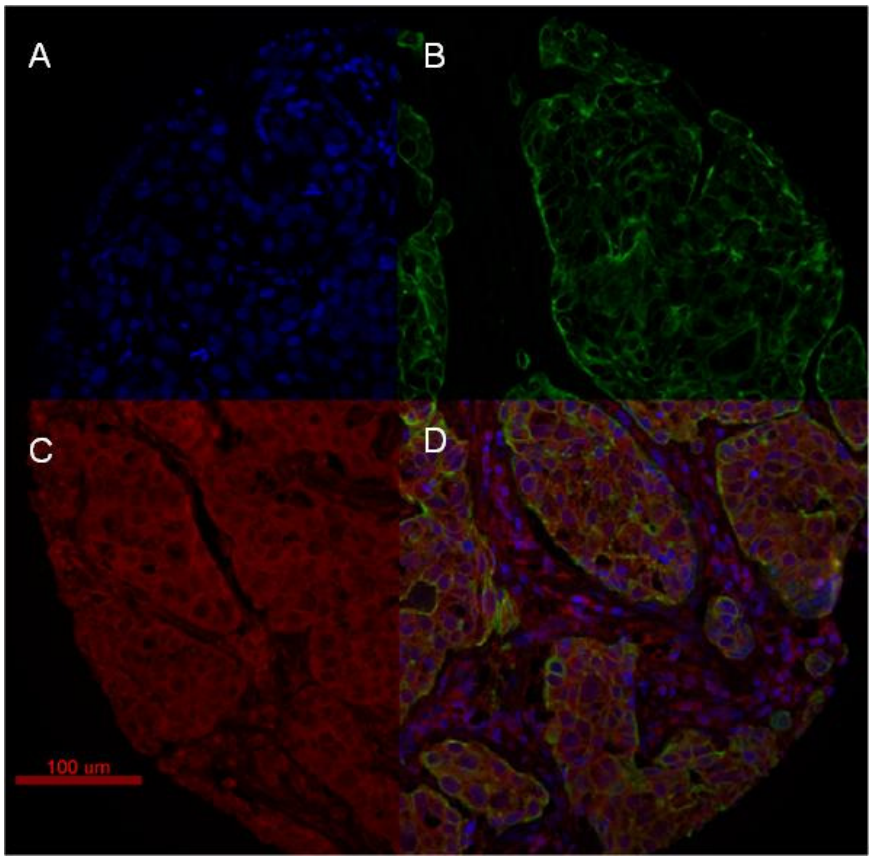

Figure 63: AQUA image analysis.
An example TMA core showing compartmentalised staining with (A) DAPI for nuclear staining, (B) Cy3 anti-cytokeratin for epithelial tissue, (C) Cy5-tyramide for target protein (GnRHR), (D) all 3 markers overlaid.

High resolution images of the TMA cores were analysed using AQUAnalysis® software. The cytokeratin mask was used to identify epithelial areas of tissue and DAPI staining was used to define cytoplasmic and nuclear compartments. Image areas that either had imaging errors, or constituted less than 5% epithelium were removed. Within the epithelial mask of the cytoplasmic compartment, the Cy5 fluorescent signal was calculated within each image pixel, totalled and then divided by the area of the cytoplasmic compartment to give a score in AQUA® units (Au) corresponding to the level of GnRHR expression in that core.

Initial observation of the data showed that there was a batch effect based on the year of tissue collection (Figure 64A). Therefore, prior to further analysis the data were mean-centred to account for this variation in staining intensity resulting from the year of tissue collection (Figure 64B). All analyses were then performed using the mean-centred GnRHR AQUA® scores.

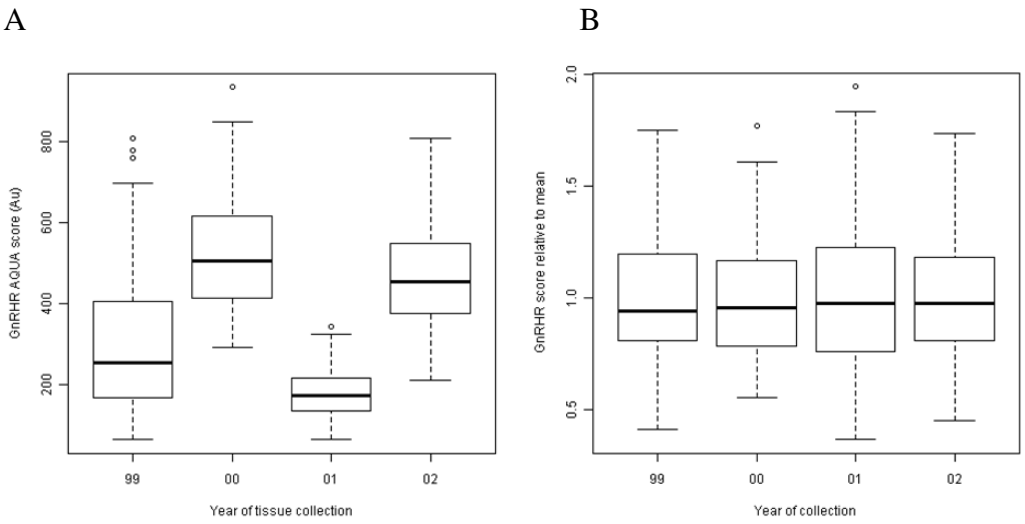

Figure 64: Batch effect in AQUA scores of GnRHR expression.
(A) A batch effect existed in the GnRHR AQUA scores based on the year of tissue collection.
(B) Mean-centring the GnRHR AQUA data reduced the batch effect.

The resulting data was analysed and associations between GnRHR expression and breast cancer subtype, grade, and expression of ER, PR, HER2, CK5/6 and EGFR were explored. These data were already available for the sample set.

The relationship between discrete variables (Grade or Phenotype) and GnRHR expression was determined by comparing the mean GnRHR expression level for each category (Grade 0/1/2/3 or phenotype HER2/Luminal/TNP) by one-way ANOVA. 298 of the 347 samples were assigned to a molecular phenotype by hormone receptor status using the annotations given by Aitken *et al* [1]. Grade information was available for 344 of the 347 samples.

There was a range of GnRHR expression in all three breast cancer subtypes, with some samples showing high immunostaining (Figure 65A and Figure 65B) and others low immunostaining (Figure 65C and Figure 65D).

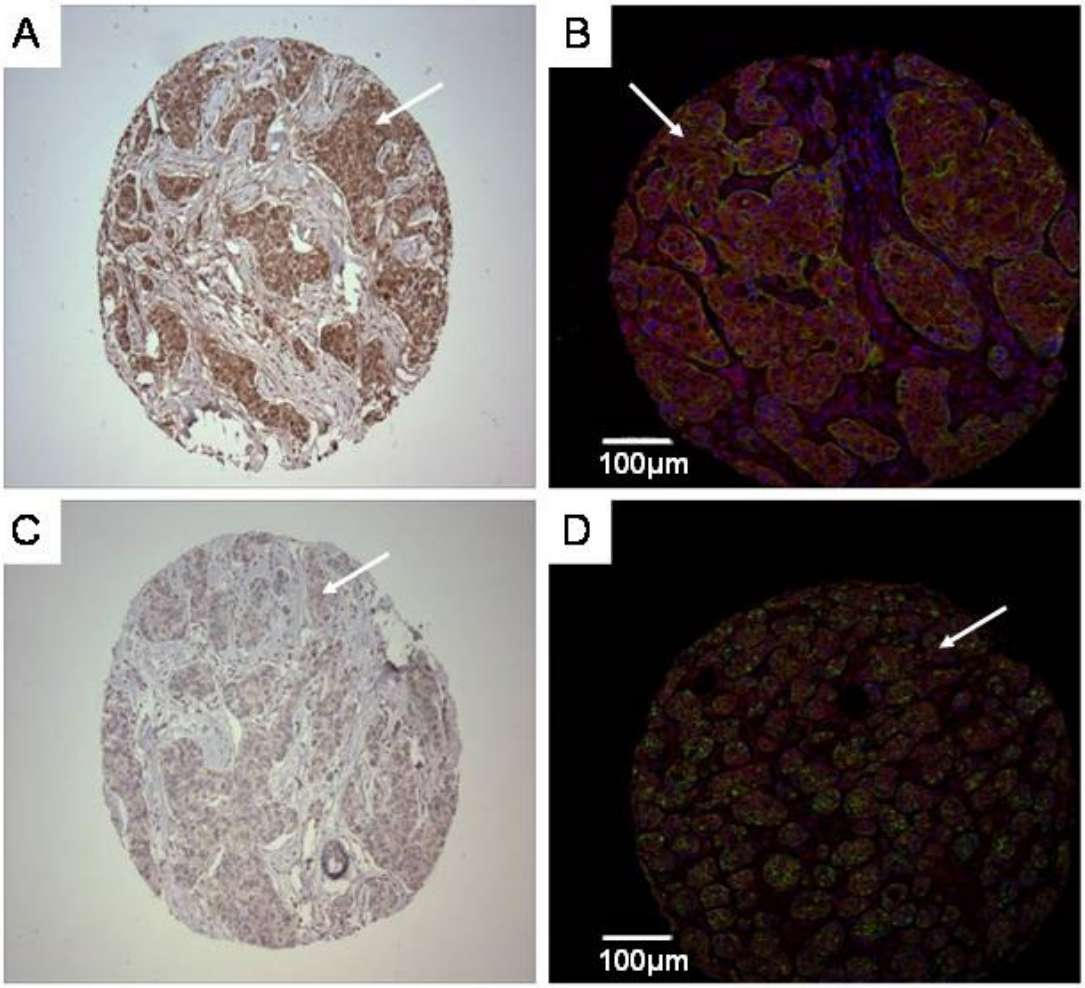

Figure 65: GnRHR immunostaining in primary breast tumours.
Representative examples of high (A and B) and low (C and D) GnRHR expression in TMA cores of breast cancers. A and C are immunohistochemical images with brown staining corresponding to GnRHR expression and blue staining to haematoxylin. B and D are immunofluorescent images with red staining corresponding to GnRHR expression, blue (DAPI) staining representing cell nuclei, and green staining for cytokeratin (carcinoma cell) staining. Arrows indicate areas of positive GnRHR expression.

Average GnRHR expression was highest in the Triple Negative Phenotype (TNP) subgroup (Figure 66; P=0.005; one-way ANOVA).

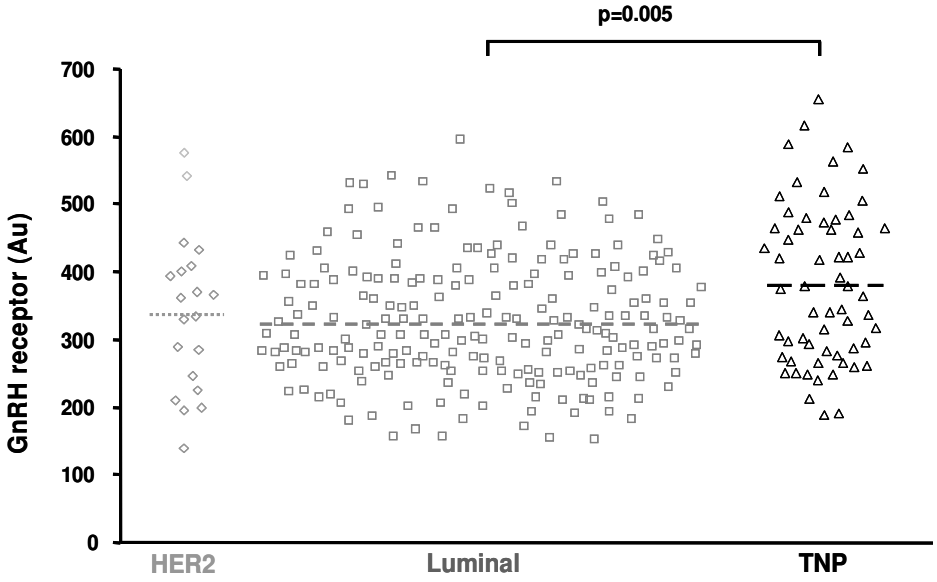

Figure 66: GnRH receptor protein expression in clinical breast cancers by breast cancer subtype.
Each point represents one breast tumour sample, dashed lines show the mean of 20 HER2, 217 Luminal and 61 TNP tumours. Protein expression was measured by quantitative immunofluoresence (AQUA).

GnRHR expression was significantly higher in grade three tumours compared to grade two tumours (Figure 67; P=0.012, one-way ANOVA).

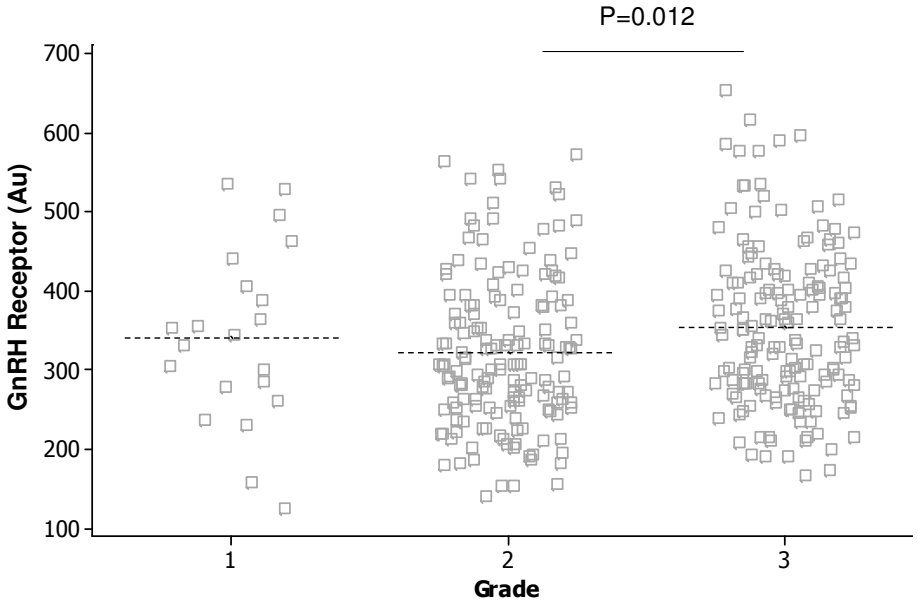

Figure 67: GnRHR protein expression (measured by AQUA) by tumour grade.
Each point represents one breast tumour sample, dashed lines show the mean GnRHR expression in 21 grade 1, 158 grade 2 and 165 grade 3 tumours.

The relationship between continuous variables (ER, PR, HER2, CK5/6, EGFR expression) and GnRHR expression was determined by non-linear regression. Expression values of ER, PR, HER2, CK5/6 and EGFR were available for 335, 336, 339, 339 and 337 of the 347 samples respectively.

High GnRHR expression was significantly associated with oestrogen receptor (ER) expression (P=0.002, regression) and progesterone receptor (PR) expression (P=0.028, regression). No significant association could be identified between GnRHR expression and HER2, CK5/6 or EGFR expression.

By defining high- and low- ER and PR expression, using cut-points previously defined by Aitken *et al* [1] (high ER > 58Au; high PR > 43Au), it was demonstrated that GnRHR expression was significantly higher in tumours expressing low ER (P=0.024, 2-sample t-test) and low PR (P=0.002, 2-sample t-test) (Figure 68 and Figure 69). This is in agreement with the finding shown above that GnRHR was higher in the TNP subgroup of breast cancer samples.

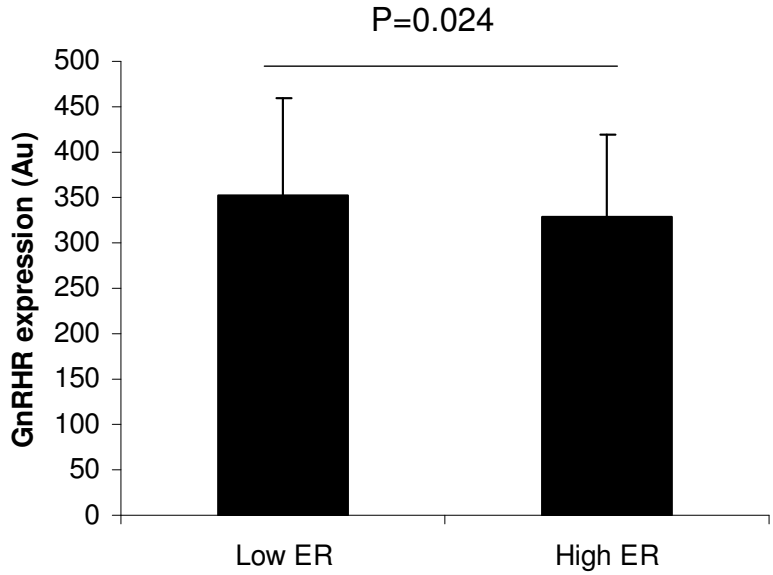

Figure 68: GnRHR expression was higher in low-ER expressing tumours (n=132) compared to high-ER expressing tumours (n=203).
Protein expression in 335 breast tumours was measured by quantitative immunofluorescence. Error bars show standard deviation. GnRHR expression was higher in low-ER expressing tumours compared to high-ER expressing tumours (P=0.024, 2-sample t-test).

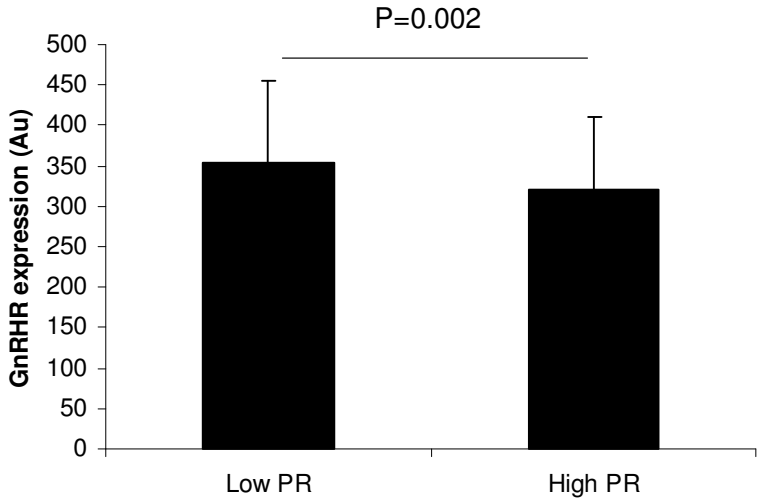

Figure 69: GnRHR expression was higher in Low-PR expressing tumours (n=182) compared to high-PR expressing tumours (n=154).
Protein expression in 335 breast tumours was measured by quantitative immunofluorescence. Error bars show standard deviation. GnRHR expression was higher in Low-PR expressing tumours compared to high-PR expressing tumours (P=0.002, 2-sample t-test).

3.5.4 Effect of GnRHR stimulation in Breast Cancer Cell Lines

Triptorelin has been reported by some groups to inhibit some breast cancer cell lines [57, 77]. In an attempt to identify a responsive cell line, a panel of 8 breast cancer cell lines were treated with Triptorelin (100nM) for up to 4 days. None of the breast cancer cell lines tested was inhibited by Triptorelin. Comparable results were observed when cells were treated once or daily, in serum-free media, and with bovine serum albumin-supplemented media. The SCL60 cell line is included as a positive control to demonstrate a response to Triptorelin.

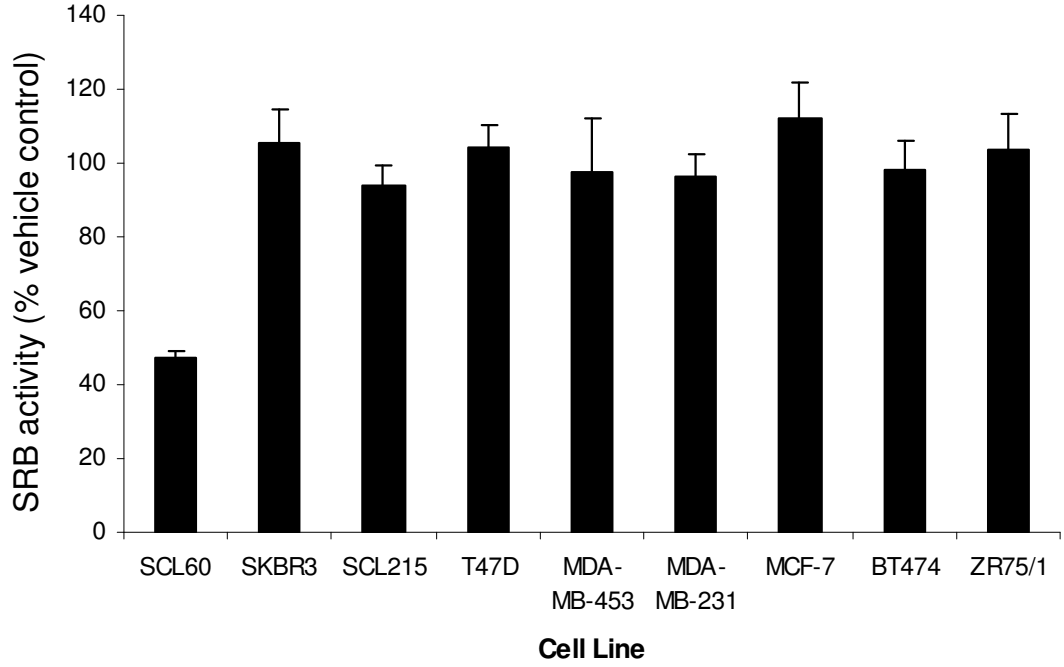

Figure 70: Effect of Triptorelin on the SRB activity of a panel of eight breast cancer cell lines. Cells were treated for up to 4 days with Triptorelin (100nM) or vehicle control. The GnRHR-transfected HEK293 cell line SCL60 is included as a positive control. Data are expressed relative to vehicle control-treated cells. Error bars show +/- standard deviation of three intraexperimental replicates. These data are representative of at least 2 experiments.

3.5.5 Discussion

At the transcript level, there was a range of GnRHR expression across the breast cancer samples. On average, GnRHR expression appeared to be higher in luminal breast cancer cell lines. Protein immunostaining for the identification of GnRHR protein expression in breast cancers showed that there was a range of GnRHR protein expression in primary breast tumours, and each subgroup of breast cancer had

samples with high and low GnRHR expression. On average, GnRHR protein expression was significantly higher in the TNP subgroup and in grade 3 tumours, and was also associated with ER and PR expression, but not with HER2, CK5/6 or EGFR expression. These associations may help to define a subgroup of breast cancers that are most likely to express high GnRHR and therefore are most likely to respond to GnRH agonist therapy.

A similar study by Baumann *et al* in 1993 measured GnRH agonist binding sites in 235 breast cancer biopsies [74]. In contrast to the data presented above, the authors found no association between GnRHR and ER or PR [74]. The association with ER and PR did not appear to be a linear relationship, and values above and below a threshold of ER and PR expression may be more important than the continuous distribution of expression values in determining a relationship with GnRHR. Baumann *et al* used a smaller sample size, and looked for a correlation between the values rather than a more complex relationship. The authors were unable to show a significant association with breast cancer subtype, although they compared only two histological subtypes ductal and lobular, rather than the molecular subtypes (TNP, HER2 and Luminal) used above [74].

Buchholz *et al* examined immunohistochemical expression of GnRHR in 17 TNP breast cancer samples and found immunoreactivity in all 17 samples [26]. They state that there was a large range of GnRHR expression in these samples with some expressing very low and some expressing high levels of GnRHR [26]. This is in line with the data presented above, which shows a large range of GnRHR expression across the primary breast tumours. The data presented by Buchholz, however, does not indicate an association with the TNP subtype of breast cancer because they did not explore GnRHR expression in other subtypes.

In support of the association of GnRHR expression with triple-negative breast cancers, it has recently been claimed by Schubert *et al* that 74% of triple-negative breast cancers express GnRH receptors [25]. In further support of the association with triple-negative breast cancers, the authors of that study showed that the growth

of triple negative (MDA-MB-453) cell line-derived xenografts was slowed by treatment with the GnRH antagonist Cetrorelix [25]. Although the cells from which these xenograft tumours were derived are defined as triple-negative, and therefore should exhibit hormone-independent growth, these cells have also been reported to express androgen receptors [219, 220]. Androgen has been shown to induce transcriptional change in MDA-MB-453 cells [221, 222] and to enhance their proliferation [219]. Therefore there remains a possibility that the anti-proliferative effect of GnRH antagonist treatment is not a result of *direct* interaction with GnRHR in the xenograft cells. The GnRH antagonist is likely to be interacting with GnRHR in the pituitary and it is possible that some inhibition of xenograft growth may be due to a resultant down-regulation of androgen secretion. It would be interesting if this result could be supported by other studies, which might benefit from a GnRHR knock-out MDA-MB-453 cell line as a control, and other triple-negative cell types. Xenografts derived from another triple-negative breast cancer cell line (MDA-MB-231) were also used in this study, and although the authors did not report whether there was an antiproliferative effect of a GnRH antagonist on these tumours, they did show that it had an anti-metastatic effect [25]. MDA-MB-231 cells have also been reported to express androgen receptors [220].

This group have previously shown an apoptosis-inducing effect of a GnRH-II antagonist on the triple-negative MDA-MB-231 and ER-positive MCF7 cells [78]. However, the authors reported that the apoptotic effect of the GnRH-II antagonist remained present when GnRHR was knocked down [78]. It is therefore unclear how this antagonist mediated the antiproliferative effect without direct interaction with the GnRHR. Since the level of GnRHR expression has been shown to be important for the antiproliferative effect of GnRH agonists in other studies [79], the results reported by Grundker *et al* are interesting.

This group reported inhibitory effects of an GnRH antagonist on proliferation of MCF7 cells [78], which contradict our and other groups' findings that MCF7 cells do not express functionally relevant levels of GnRHR at the cell surface and that their growth is not inhibited by GnRH agonists or antagonists [27, 119, 121, 223, 224]

(Figure 70). In fact, it is shown above that a panel of eight breast cancer cell lines of different subtypes, including MCF7, MDA-MB-453 and MDA-MB-231 cells did not respond to the GnRH superagonist Triptorelin, despite this having a profound effect on the SRB activity of SCL60 (GnRHR-transfected HEK293) cells (Figure 70). Screening of these breast cancer cell lines by radioligand binding assay was unable to identify any that expressed detectable levels of GnRHR, thereby accounting for the lack of response to Triptorelin. Interestingly, Saleh-Abady *et al* recently demonstrated that proliferation of SKBR3 and T47D cells was inhibited by Triptorelin [77]. The authors of that study used a daily treatment regimen and supplemented the culture medium with bovine serum albumin. In the present study, no effect of Triptorelin on SKBR3 or T47D cell number could be detected with these alterations or with serum-free media.

Fost *et al* recently showed that 31 out of 42 triple negative breast cancer specimens were GnRHR-positive [225]. Most of these GnRHR-positive specimens showed antigenicity in at least 70% of the tumour cells [225]. Fost et al used the target of GnRHR to direct a chemotherapeutic agent Doxorubicin. The GnRH agonist AEZS-108 (AN-152) consists of doxorubicin linked to [D-Lys^6]GnRH [225]. The authors showed that this induced apoptosis in triple negative breast cancer cell lines *in vitro* (MDA-MB-231, HCC1806 and HCC1937) and inhibited tumour growth of *in vivo* mouse models [225]. This study by Fost *et al* supported a previous similar report by Kahan *et al* [226]. This does not indicate that direct GnRHR signalling is involved, but does represent an interesting way of exploiting tissue-specific GnRHR expression if the doxorubicin-GnRH agonist conjugate induces apoptosis through binding to the GnRHR. The results presented above support the discovery of Fost *et al* that GnRHR expression appears to be higher in triple negative breast cancers and this group of patients may benefit from a GnRHR-directed treatment.

It is also shown above that GnRHR expression appears to be higher in grade 3 tumours compared to grade 2 tumours. An association between GnRHR expression and breast cancer grade has not previously been reported. Moriya *et al* examined the expression of GnRHR in 58 human breast carcinomas by immunohistochemistry

[73]. They defined tumours as being simply positive or negative for GnRHR immunoreactivity. By doing this, the authors identified an association between GnRHR and ER, PR and Ki-67, but were unable to demonstrate an association of GnRHR expression with grade [73]. The data presented above uses a much larger sample of breast tumours, showing that GnRHR expression is significantly higher in tumours with grade 3 status compared to grade 2, and that GnRHR expression is higher in TNP subtype of breast cancers. This information may help to further stratify a patient group most likely to benefit from GnRHR-targeted therapy.

It is important to note that positive immunohistochemical staining for GnRHR protein does not necessarily correspond to functional GnRHR protein expression or sensitivity to GnRH agonist treatment. A high level of functional GnRHR protein expression at the cell surface is believed to be required for the antiproliferative effects of GnRH agonist [79]. The staining method used does not discriminate for the subcellular localisation of GnRHR. These results therefore must be interpreted in the context of further functional investigations of receptor activity, for example with radioligand binding assays and the measurement of inositol phosphate production after receptor stimulation. It is important to note that a large proportion of the human GnRHR in particular has been shown to be retained intracellularly in the endoplasmic reticulum, more so than other mammalian forms of GnRHR such as rat and mouse [37, 121, 223]. Human and mouse GnRHR has also been shown to be expressed at the nuclear membrane [223]. However, the overall level of GnRHR expression may indicate the potential for high GnRHR cell surface expression.

An interesting finding by Finch *et al*, was that the proportion of GnRHR that is expressed at the plasma membrane can be increased using the GnRHR antagonists antide and cetrorelix [224, 227], and has also been shown to be increased with the non-peptide antagonist (2S)-2-[5-[2-(2-axabicyclo[2.2.2]oct-2-yl)-1,1-dimethy-2-oxoethyl]-2-(3,5-dimethylphenyl)-1H-indol-3-yl]-N-(2-pyridin-4-ylethyl)propan-1-amine (IN3) [121, 224, 227]. The effect of cetrorelix on the cellular localisation of GnRHR was maximal by 24h [224]. This indicates that even in cells where GnRHR expression is very low at the cell surface, if there is sufficient GnRHR protein

expression in the whole cell, its localisation can be rapidly changed. This may also indicate that part of the antiproliferative effect of a GnRH analogue may be mediated through GnRH antagonist-induced increase of GnRHR trafficking to the plasma membrane, thus increasing its signalling capacity.

3.6 Developing a breast cancer model for studying GnRHR signalling

The SCL60 model (HEK293 cells transfected with GnRHR) has been useful for studying signalling through the GnRHR, since it is well-characterised and responds well to GnRH agonists [79, 88, 104, 112, 116]. However, for it to be relevant to breast cancer patients it is necessary to use a cell line model that more accurately reflects the disease. A GnRH analogue-responsive breast cancer cell line expressing functional GnRHR may be more informative of GnRH signalling in breast cancer.

3.6.1 Transfection of several breast cancer cell lines produced an MCF-7 clone expressing high GnRHR

A panel of breast cancer cell lines was found to be unresponsive to GnRH agonist (Triptorelin) treatment (section 3.5.4), and endogenous GnRHR expression could not be identified by radiolabelled ligand binding assay in several breast cancer cell lines. To develop a model more relevant to breast cancer, several breast cancer cell lines were transfected with GnRHR. Kevin Morgan transfected these cell lines to produce clones with varying levels of GnRHR expression (Figure 71). It should be noted that in this chapter, it is assumed that the level of GnRHR is proportional to the specific binding that is measured by radioligand binding assay. The possibility that this is not true is discussed at the end of the chapter.

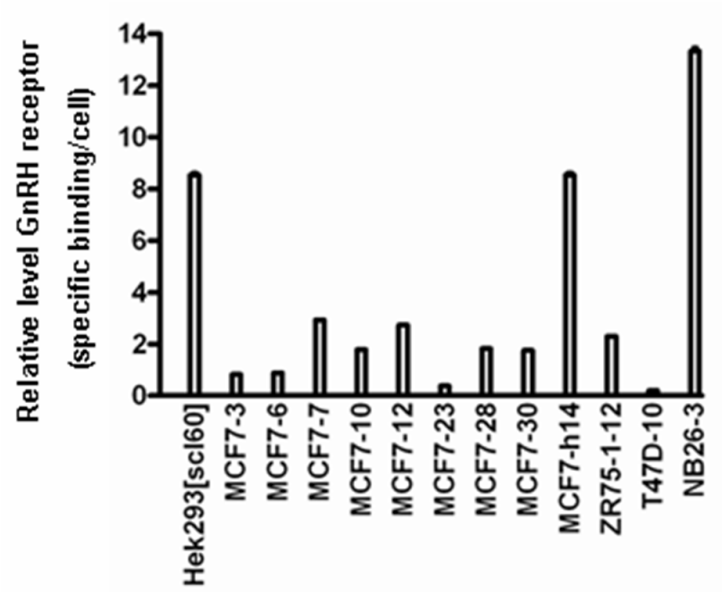

Figure 71: GnRHR cell surface expression in transfected breast cancer cell line-derived clones. The level of GnRHR cell surface expression, as detected by radioligand binding assay, in a representative selection of transfected breast cancer cell line-derived clones, including the MCF7 subclone MCF7-h14. Also shown are the GnRHR-transfected cell lines SCL60 (derived from HEK293 cells), and WPE1-NB26-3 (derived from prostate epithelial cells). MCF7-h14 cells express a similar level of GnRHR as SCL60 cells. This figure is representative of multiple experiments performed by myself and Kevin Morgan.

The extent of cell number reduction following GnRHR activation has been shown to correlate with the level of GnRHR cell surface expression [79]. To show any inhibition of proliferation, it appears that a cell line must have a minimum level of specific GnRH agonist binding (determined by radioligand binding assay) for GnRHR and must show receptor functionality, which can be measured by inositol phosphate assay [80].

Endogenous GnRHR expression at the cell surface of the breast cancer cells MCF7, T47D and ZR75/1 could not be detected by binding assay (data not shown). Transfection of these cell lines with GnRHR produced 25 T47D clones with undetectable GnRHR levels, approximately 15 MCF7 clones with low to moderate levels of receptor, and approximately 30 ZR75-1 clones with low to very high levels of GnRHR (as measured by radioligand binding assay). The isolated ZR75-1 clones grew too slowly to be practically used for further experiments. Instead, one MCF7 clone (MCF7-30) was re-transfected with GnRHR with hygromycin B

phosphotransferase to produce subclones with higher levels of GnRHR at the cell surface. The subclone MCF7-h14 showed high GnRHR cell surface expression (Figure 71, Figure 72), at a similar level to SCL60 cells, and this clone was used for further experiments.

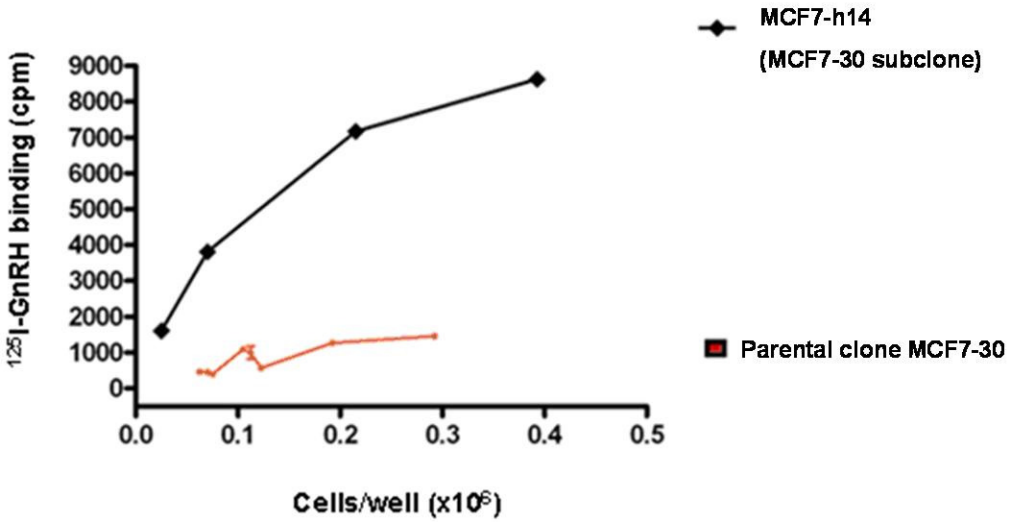

Figure 72: The level of GnRHR cell surface expression in the MCF7-30-7-H14 subclone compared to its parental clone, as detected by radioligand binding assay
This figure is representative of experiments performed by myself and Kevin Morgan.

MCF7 is a cell line derived from a pleural effusion of an invasive ductal carcinoma of a 69 year old Caucasian woman [119]. It is the most commonly used breast cancer cell line worldwide. MCF7 is classed as luminal [119]. It expresses ER and PR, has low HER2, and TP53 protein is wild type [119]. Another feature to note about the MCF7 cell line is that it has an activating mutation in PI3K [228]. Proliferation of MCF7 cells is enhanced by oestrogen and IGF-I [229, 230]. MCF7 cells proliferate relatively quickly in normal cell culture conditions, making them an ideal experimental model.

Little is clearly understood about GnRHR signalling in MCF7 cells, and it has previously been difficult to identify GnRHR cell surface expression in these cells [119]. SCL60 has been the model used to investigate GnRHR antiproliferative signalling to date since it responds well to GnRH agonists [79].

3.6.2 Aims

The first aim of the experiments in this chapter, after establishing a GnRHR-transfected breast cancer model, was to compare and contrast the response to GnRHR activation in MCF7-h14 and SCL60 cells. Specifically, to compare any change in the level of inositol phosphate production following GnRHR activation, any effect on cell number (SRB activity), and any change in the level of signalling molecules pERK1/2 and p-p38.

The second aim was to compare and contrast how the response to GnRHR activation in these cells is affected by the inhibition of other potential components of the local signalling network, such as the growth factor receptors IGF-I-R, and PI3K. Specifically, to determine for both cell lines, whether each of these inhibitors affect cell number and the level of signalling molecules pERK1/2 and p-p38 following GnRHR activation.

Two hypotheses were tested. Firstly, the mechanism of cell number reduction, including the effects on signalling molecules such as p-ERK1/2 and p-p38, may be different between these two cell types as GnRH agonists have previously been shown to act in a cell-type specific manner. Secondly, constitutive activity of one or more growth factor receptor signalling complexes (for example, IGF-I-R and PI3K) may compete with signalling induced by GnRHR activation. Inhibition of one or more of these in combination with GnRHR activation may have an addititve effect on cell number reduction in either cell type.

3.6.3 GnRH inhibits SRB activity of SCL60 cells but not MCF7h14 or untransfected MCF7 cells

The level of functional GnRHR activity in these cells was tested. Cells were stimulated with Triptorelin (100nM) and the level of inositol phosphate production was measured. MCF7-h14 cells showed a similar inositol phosphate response following GnRHR activation to that observed in SCL60 cells (Figure 73).

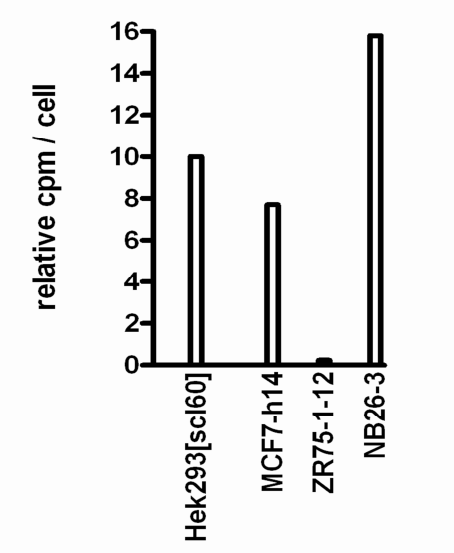

Figure 73: The relative levels of inositol phosphate following GnRHR activation in each of 4 cell lines compared to unstimulated cells.
ZR75-1-12 is a breast cancer cell line-derived clone expressing low levels of GnRHR, NB26-3 and HEK293[SCL60] are shown as controls for high GnRHR-induced inositol phosphate production. MCF7-h14 cells show a similar level of inositol phosphate production to SCL60 cells. This figure is representative of several experiments performed by myself and Kevin Morgan.

GnRHR level at the cell surface has previously appeared to correlate with the extent of SRB activity inhibition [79], so it was predicted that MCF7-h14 cells would be inhibited by Triptorelin.

MCF7-h14 cells did not demonstrate a response, in terms of SRB activity, to GnRHR stimulation with the GnRH agonist Triptorelin (Figure 74). The parental (untransfected) MCF7 cells were also unresponsive to GnRHR activation (Figure 75). Exposure to GnRH for 5min was sufficient to inhibit SCL60 cell proliferation, and maximal inhibition was achieved by 8h (Figure 74).

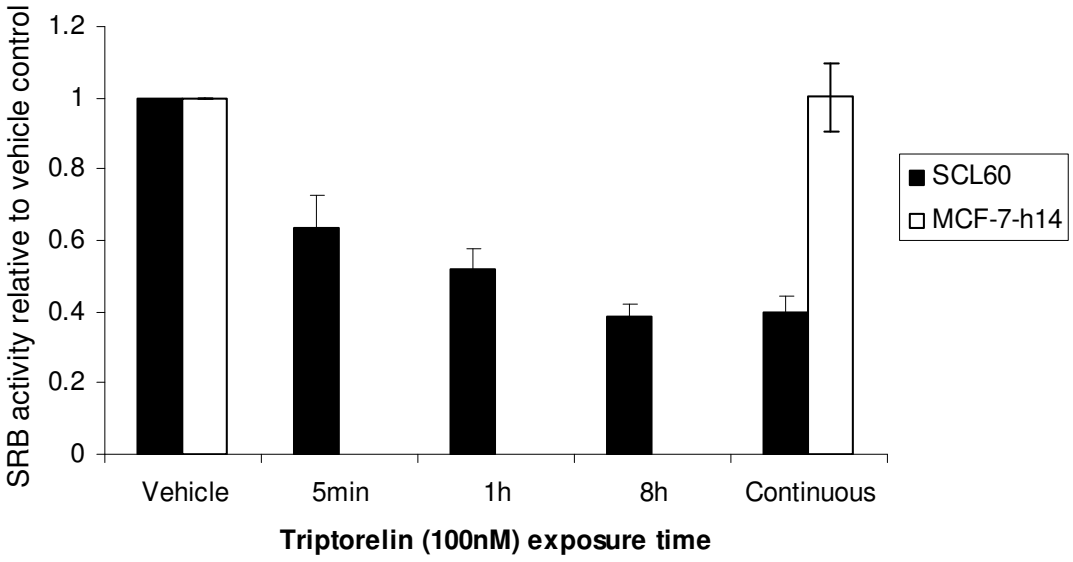

Figure 74: SRB activity of SCL60 and MCF7-h14 cells treated with 100nM Triptorelin for varying durations.
SRB activity was measured at 4 days post-treatment. SRB activity is shown relative to vehicle control. Bars represent the mean of 3 intraexperimental replicates. Error bars indicate +/- standard deviation. The differential effect of Triptorelin on SCL60 and MCF-7-h14 shown here was observed in at least 5 independent experiments.

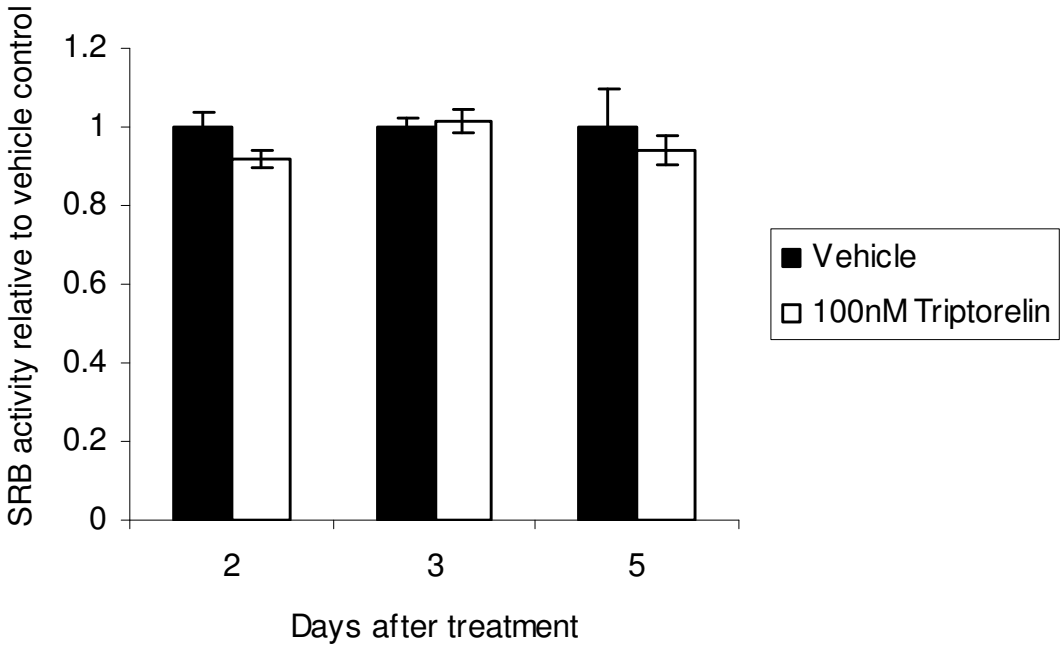

Figure 75: SRB activity of untransfected MCF7 cells treated with 100nM Triptorelin.
SRB activity was measured at 2, 3, or 5 days post-treatment. SRB activity is shown relative to vehicle control. Bars represent the mean of 3 intraexperimental replicates. Error bars indicate +/- standard deviation. These data are representative of at least 2 independent experiments.

In order to help understand why MCF7-h14 cells are not responsive to a GnRH agonist, the non-responsive MCF7-h14 cell line was compared with the responsive SCL60 cell line. In particular, the dependence of each cell line on the growth factor receptor IGF-I-R and the growth/survival signalling enzyme PI3K was examined.

3.6.3.1 The effect of GnRHR activation on signalling in MCF7-h14 and SCL60 cells

GnRHR activation causes a transient increase in pERK1/2 in SCL60 cells (Figure 76A) [79] and pERK1/2 levels were also transiently increased, but to a much lesser degree, in MCF7-h14 cells (Figure 76B). Unlike in SCL60 cells, pERK1/2 is already high in resting MCF7-h14 cells (0min, Figure 76B). This may mask an increase in pERK1/2 caused by the addition of Triptorelin. A growth factor present in the serum in the MCF7 culture medium may cause this high basal pERK1/2 activity. Serum-starved MCF7-h14 cells showed much lower basal ERK1/2 activity than those grown in normal culture conditions, and they showed a transient increase in pERK1/2 similar to that seen in SCL60 cells (Figure 76C).

Because the ERK1/2 response to GnRHR simulation is thought to be important in mediating the antiproliferative effect of Triptorelin, it was interesting to explore which growth factors may be competing with GnRHR signalling to ERK1/2.

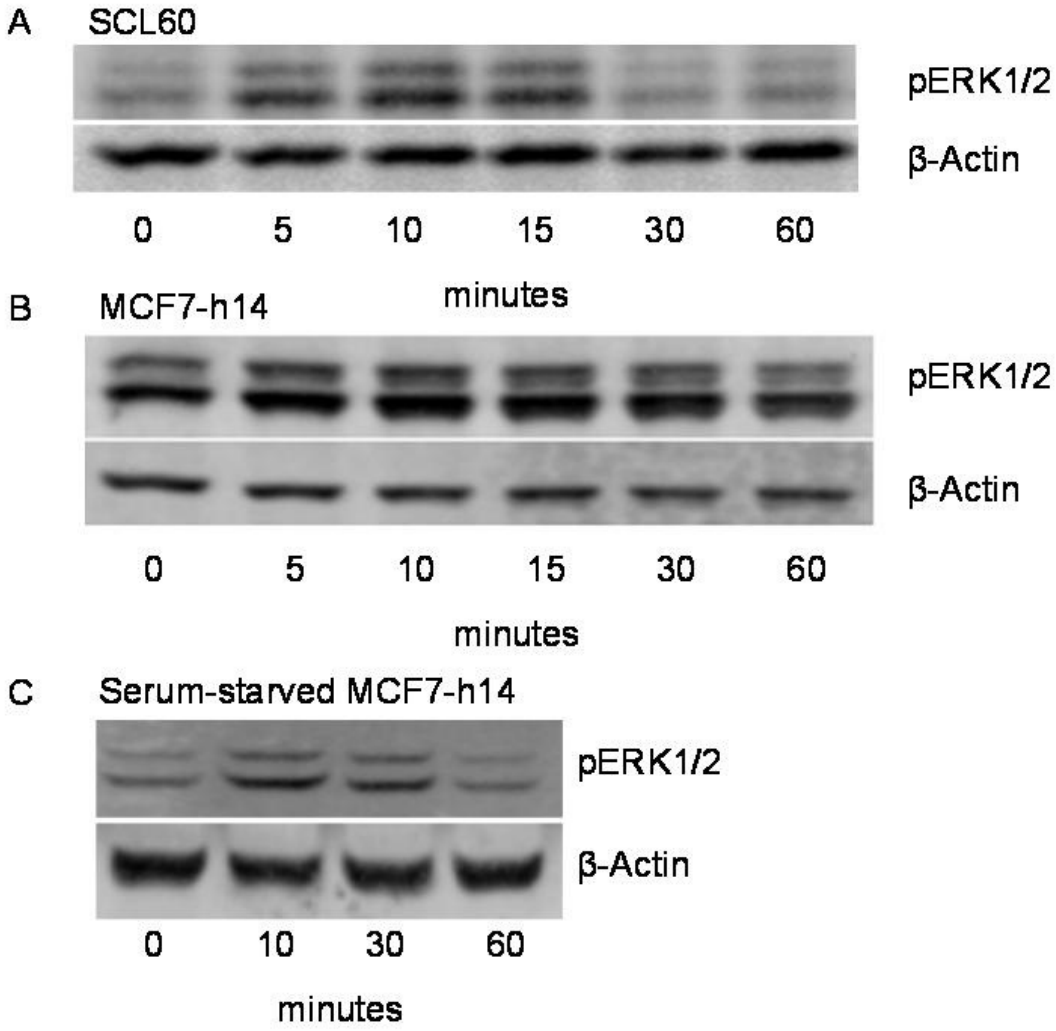

Figure 76: pERK1/2 response to GnRHR activation.
(A) Expression of pERK1/2 in SCL60 cells treated with Triptorelin or vehicle control for up to 60min, as detected by western blot.
(B) Expression of pERK1/2 in MCF7-h14 cells treated with Triptorelin or vehicle control for up to 60min, as detected by western blot.
(C) Expression of pERK1/2 in serum-starved (overnight) MCF7-h14 cells treated with Triptorelin or vehicle control for up to 60min, as detected by western blot. These data are representative of at least 3 independent experiments.

Phospho-p38 (p-p38) was transiently increased in SCL60 cells after treatment with Triptorelin (Figure 77A). To a lesser extent, p-p38 expression also appeared to transiently increase in MCF7-h14 cells after Triptorelin treatment (Figure 77B).

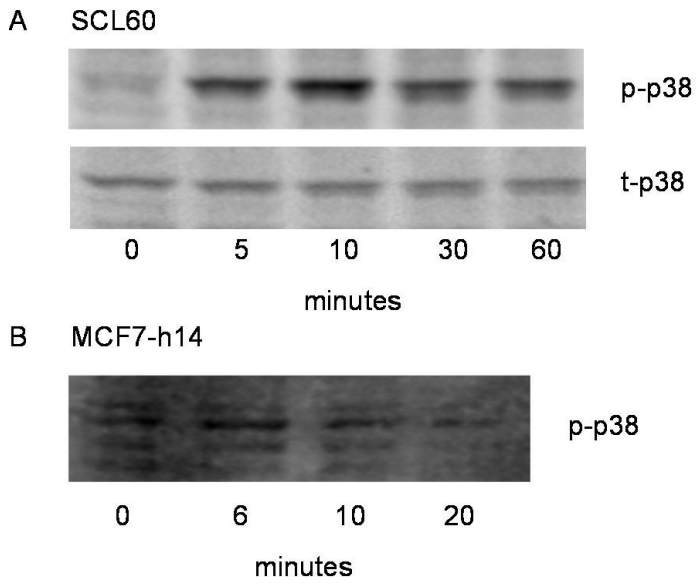

Figure 77: p-p38 response to GnRHR activation.
Expression of p-p38 in (A) SCL60 and (B) MCF7-h14 cells treated with Triptorelin (100nM) or vehicle control for up to 60min, as detected by western blot. These data are representative of at least 2 independent experiments.

3.6.4 IGF-I-R inhibition reduced SRB activity of SCL60, MCF7-h14 and MCF7 cells both alone and in combination with a GnRH agonist

IGF-I-R inhibition prevents growth of wild-type MCF7 cells [231] and this was confirmed by Kevin Morgan (Figure 78).

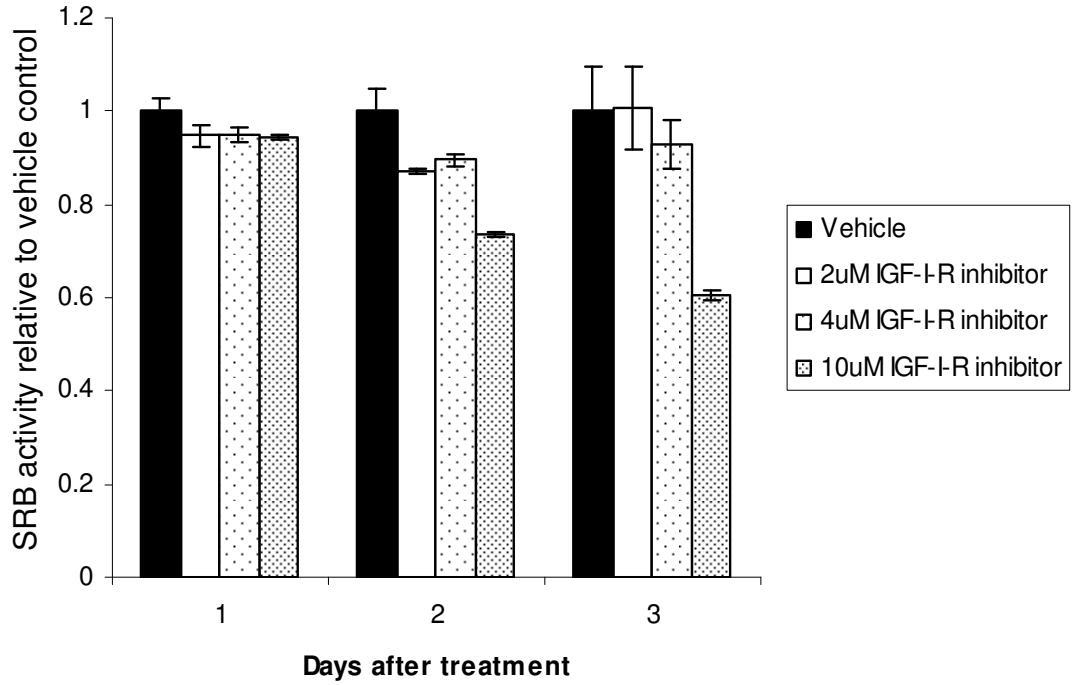

Figure 78: SRB activity of wild type MCF7 cells treated with 2, 4, or 10µM IGF-I-R inhibitor. SRB activity was measured at 1, 2, and 3 days post-treatment with 2, 4, or 10µM IGF-I-R inhibitor II (#407248 Calbiochem, EMD Biosciences, USA). Bars represent the mean of 3 intraexperimental replicates. Error bars indicate +/- standard deviation. The data for this figure was provided by Kevin Morgan.

IGF-I-R inhibition reduced SCL60 and MCF7-h14 cell number in a time-dependent manner (Figure 79). The two cell lines were inhibited to a similar extent.

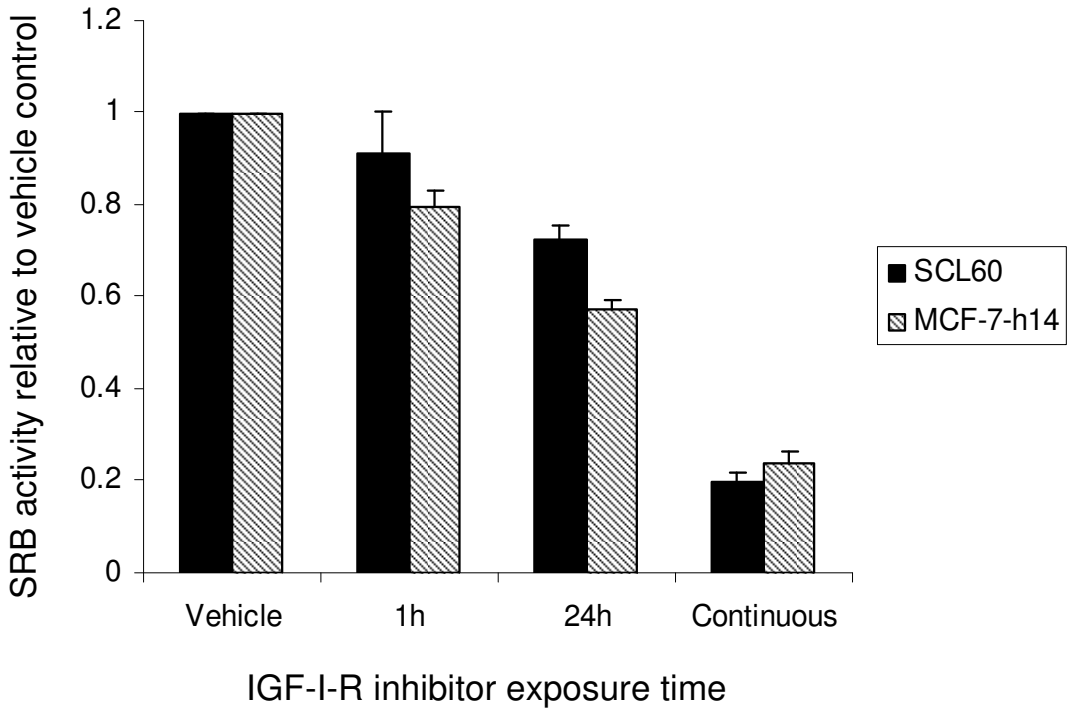

Figure 79: SRB activity of MCF7-h14 and SCL60 cells treated with 20µM IGF-I-R inhibitor for up to 24h.
SRB activity was measured at 4 days post-treatment with 20µM IGF-I-R inhibitor II (#407248 Calbiochem, EMD Biosciences, USA). Bars represent the mean of 3 intraexperimental replicates. Error bars indicate +/- standard deviation. These data are representative of at least 2 independent experiments.

IGF-I-R inhibition reduced MCF7-h14 and SCL60 cell number in a dose-dependent manner (Figure 80, Figure 81).

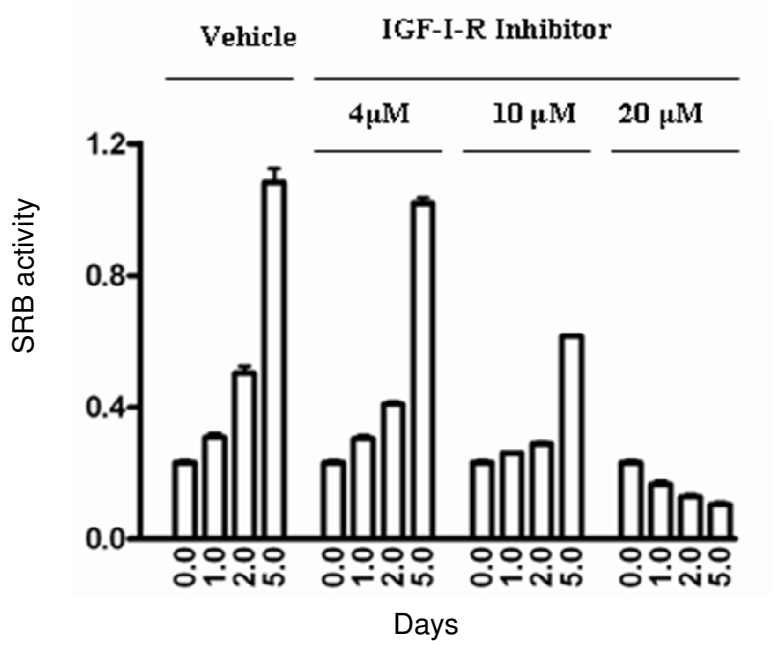

Figure 80: SRB activity of MCF7-h14 cells in response to IGF-I-R inhibitor.
SRB activity of MCF7-h14 cells treated with 4, 10 or 20µM IGF-I-R inhibitor for up to 5 days. SRB activity was measured at 1, 2, and 5 days post-treatment. Bars represent the mean of 3 independent experiments. Error bars indicate +/- standard deviation.

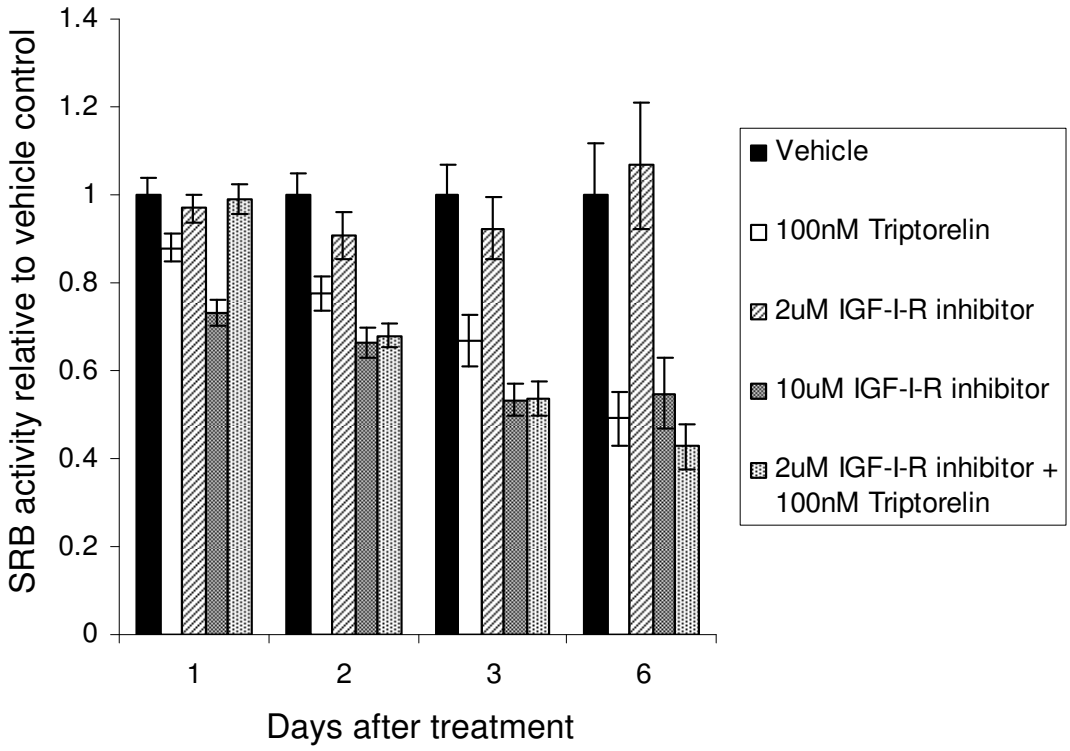

Figure 81: SRB activity of SCL60 cells treated with 2 or 10μM IGF-I-R inhibitor with or without 100nM Triptorelin, or 100nM Triptorelin alone for up to 6 days.
SRB activity was measured at 1, 2, 3 and 6 days post-treatment. Bars represent the mean of 3 intraexperimental replicates. Error bars indicate +/- standard deviation. These data are representative of at least 2 independent experiments.

When the IGF-I-R inhibitor was washed out after 1h SRB activity was unaffected (Figure 82). Triptorelin did not appear to inhibit or increase the rate of cell recovery (Figure 82).

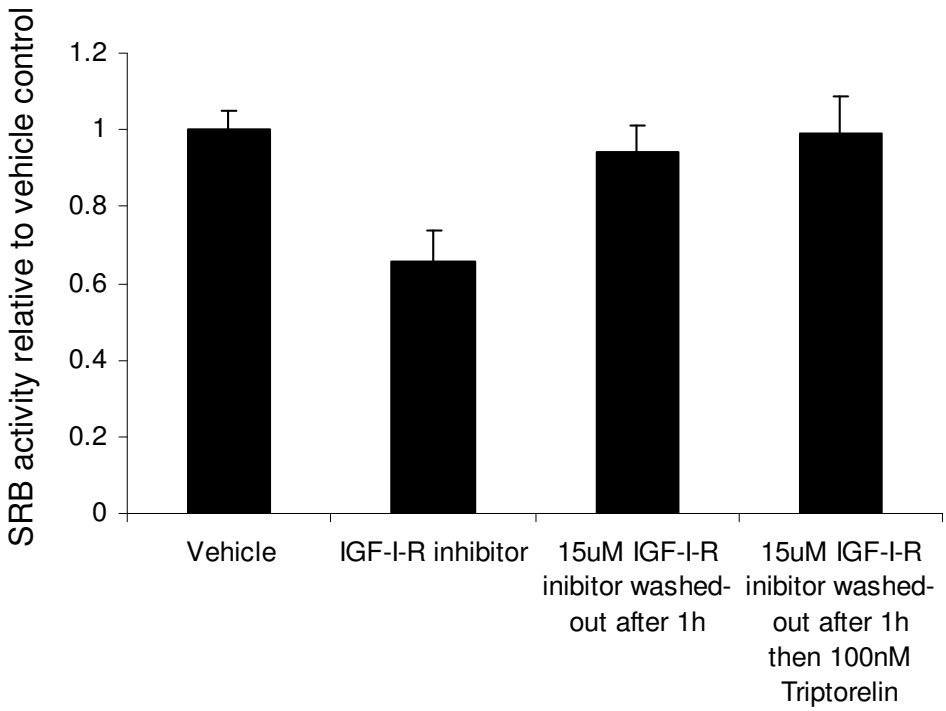

Figure 82: Effect of IGF-I-R inhibition on SRB activity of MCF7-h14 cells.
SRB activity of MCF7-h14 cells treated with 15μM IGF-I-R inhibitor continuously or for 1h then washed out and then untreated or treated with 100nM Triptorelin continuously. SRB activity was measured at 4 days post-treatment. Bars represent the mean of 3 intraexperimental replicates. Error bars indicate +/- standard deviation.

3.6.4.1 There was a sustained decrease in pERK1/2 in MCF7-h14 cells, but not SCL60 cells, following treatment with a IGF-I-R inhibitor

IGF-I-R inhibition had no detectable effect on pERK1/2 levels in SCL60 cells (Figure 83A), but appeared to cause a sustained decrease in pERK1/2 in MCF7-h14 cells (Figure 83B).

Pre-incubation with an IGF-I-R inhibitor did not prevent GnRHR-mediated transient elevation in of pERK1/2 in SCL60 cells (Figure 83A). MCF7-h14 cells showed hyper-reactivation of ERK1/2 (far above basal) after removal of IGF-I-R inhibitor, and this was not altered by GnRHR stimulation (Figure 83B).

IGF-I-R inhibition did not prevent GnRHR-mediated transient elevation in of p-p38 in SCL60 cells (Figure 84A). p-p38 appeared to be transiently decreased with IGF-I-R inhibition in MCF7-h14 cells (Figure 84B).

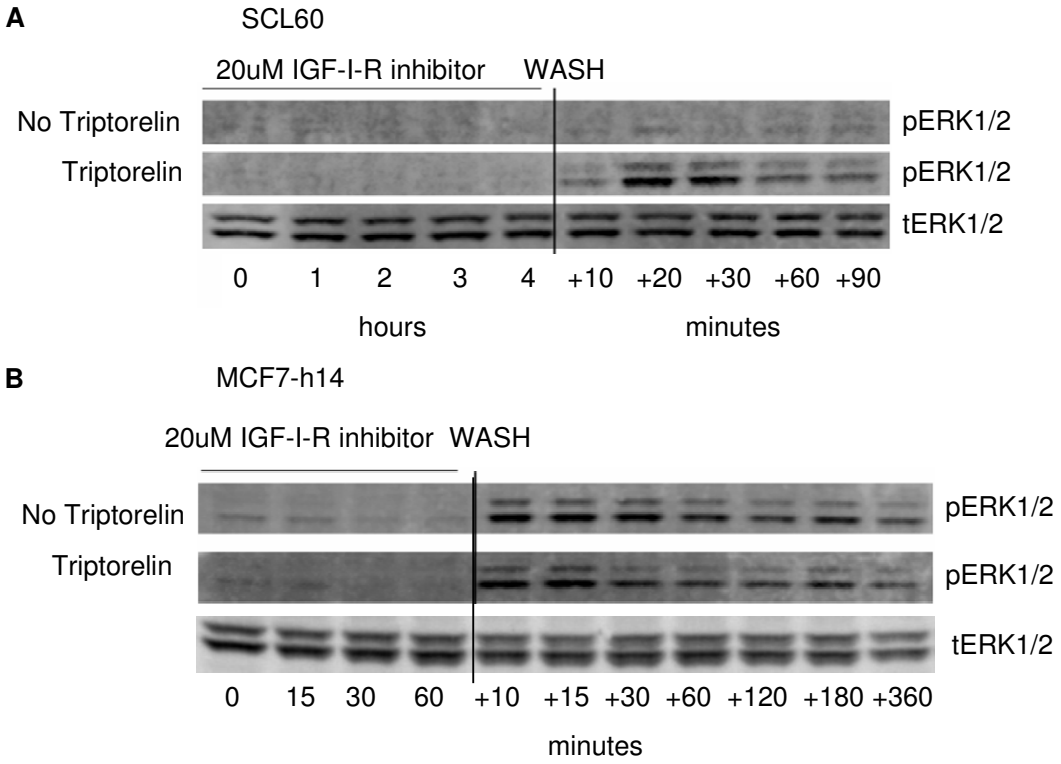

Figure 83: SCL60 and MCF7-h14 pERK1/2 response to Triptorelin and IGF-I-R inhibitor
(A) Expression of pERK1/2 in SCL60 cells treated with IGF-I-R inhibitor for up to 4h then Triptorelin or vehicle control for up to 90min, as detected by western blot.
(B) Expression of pERK1/2 in MCF7-h14 cells treated with IGF-I-R inhibitor for 60min then Triptorelin or vehicle control for up to 6h, as detected by western blot.
This figure is representative of at least 2 independent experiments.

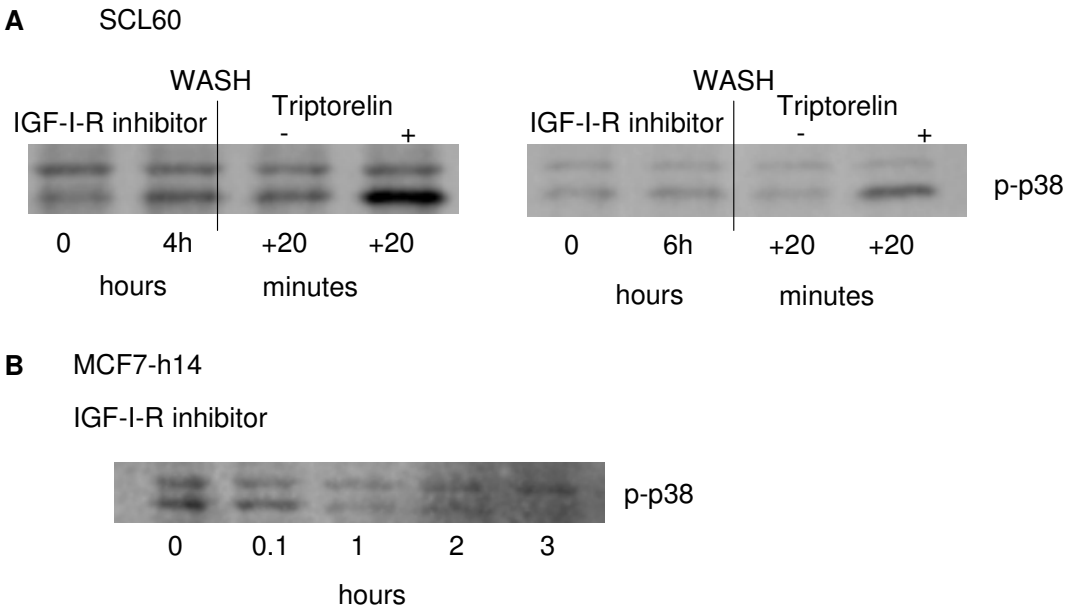

Figure 84: SCL60 and MCF7-h14 p-p38 response to Triptorelin and IGF-I-R inhibitor
(A) Expression of p-p38 in SCL60 cells treated with IGF-I-R inhibitor for up to 6h then Triptorelin or vehicle control for up to 20min, as detected by western blot.
(B) Expression of p-p38 in MCF7-h14 cells treated with IGF-I-R inhibitor up to 3h, as detected by western blot.
This figure was provided by Kevin Morgan.

3.6.5 PI3K inhibition caused mild inhibition of SCL60 SRB activity but had no effect on MCF7-h14 or WT MCF-7 cells either alone or in combination with GnRHR stimulation

PI3K inhibition caused a small reduction in SRB activity of SCL60 cells in a dose-dependent manner (Figure 85). The inhibitor used inhibits PI3K-p110γ, α, β and δ [232]. No additive effect was observed when cells were also treated with Triptorelin in combination (Figure 85). PI3K inhibition did not cause a reduction in SRB activity of MCF7-h14 cells (Figure 85) or untransfected MCF7 cells (Figure 86) either alone or in combination with GnRHR stimulation.

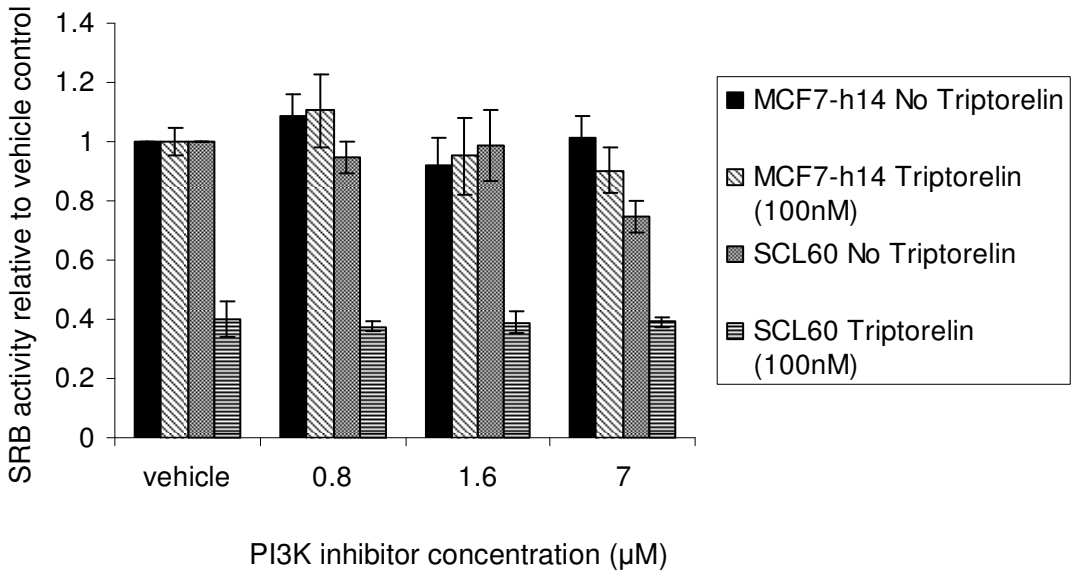

Figure 85: SRB activity of MCF7-h14 and SCL60 cells treated with 0.8, 1.6, and 7μM PI3K inhibitor with or without 100nM Triptorelin relative to vehicle control
SRB activity was measured at 4 days post-treatment. Bars represent the mean of 3 intraexperimental replicates. Error bars indicate +/- standard deviation. These data are representative of at least 2 independent experiments.

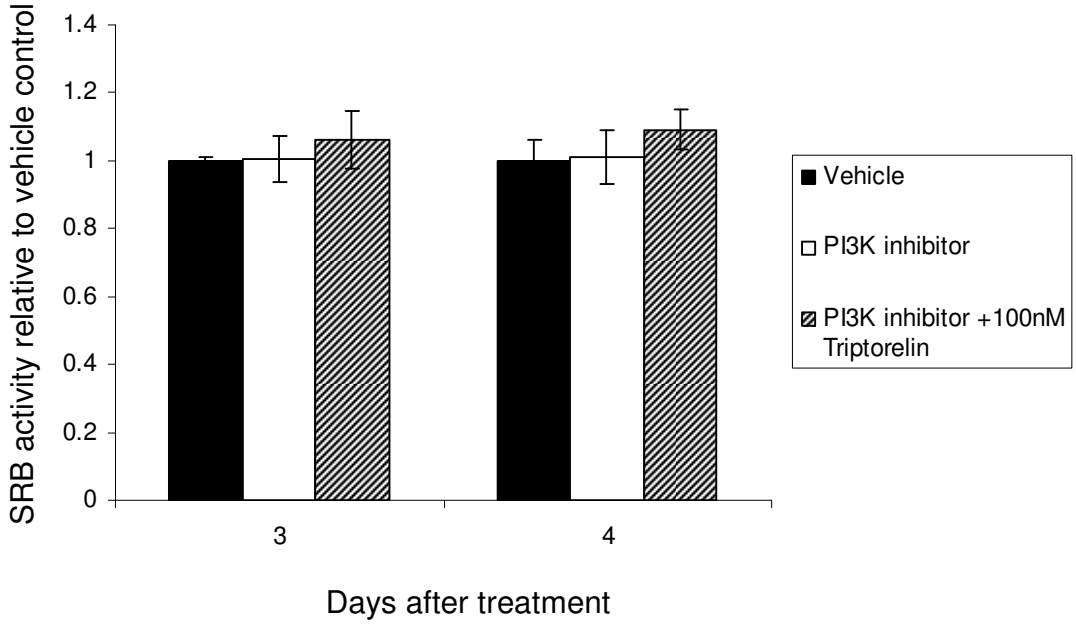

Figure 86: SRB activity of wild type MCF7 cells 7μM PI3K inhibitor with or without 100nM Triptorelin relative to vehicle control
SRB activity was measured at 3 and 4 days post-treatment. Bars represent the mean of 3 intraexperimental replicates. Error bars indicate +/- standard deviation.
These data are representative of at least 2 independent experiments.

3.6.5.1 The effects of PI3K inhibition on signalling in SCL60 and MCF7-h14 cells

No effect could be detected on the level of pERK1/2 expression in SCL60 (Figure 87A) or MCF7-h14 (Figure 87B) cells following PI3K inhibition. PI3K inhibition did not inhibit the GnRH-induced activation of pERK1/2 in SCL60 cells (Figure 87A).

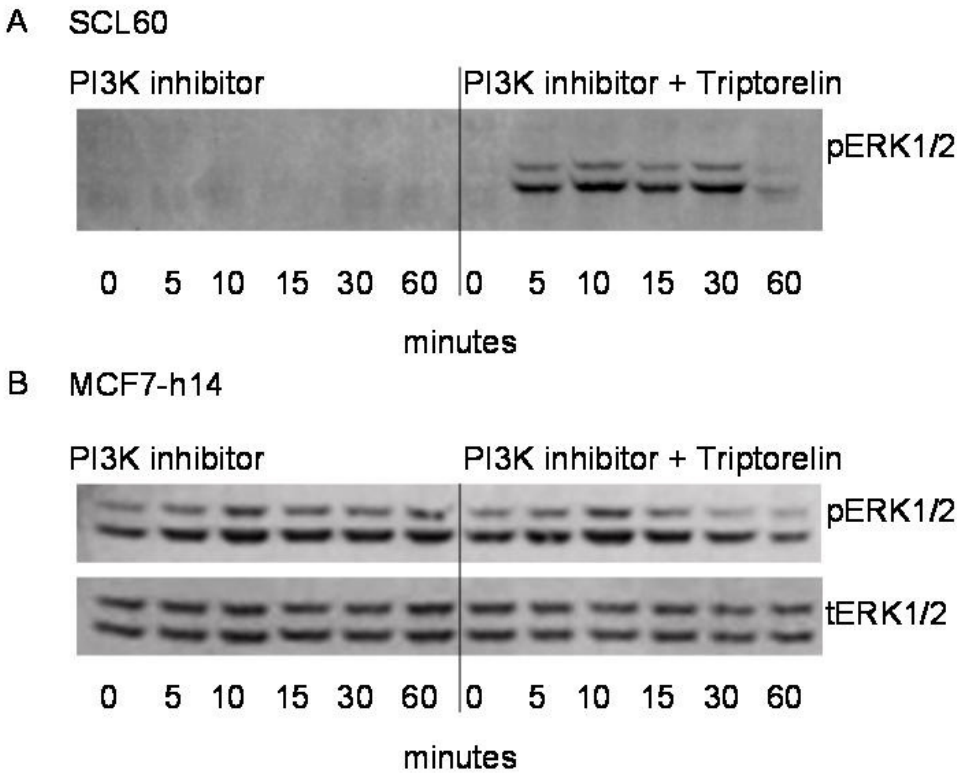

Figure 87: pERK1/2 response to PI3K inhibition
(A) Expression of pERK1/2 in SCL60 cells treated with a PI3K inhibitor, as detected by western blot.
(B) Expression of pERK1/2 in MCF7-h14 cells treated with a PI3K inhibitor, as detected by western blot.
These data are representative of 2 experiments.

A small transient increase in p-p38 in SCL60 cells was observed following treatment with a PI3K-γ inhibitor (Figure 88A). This did not appear to alter the p-p38 response to Triptorelin observed in Figure 77 (Figure 88A). A delayed decrease in p-p38 was detected in MCF7-h14 cells following PI3K-γ inhibition (Figure 88B) after 60min of treatment with PI3K-γ inhibitor. This was sustained for a further 5 hours, at which point the level of p-p38 was still below basal.

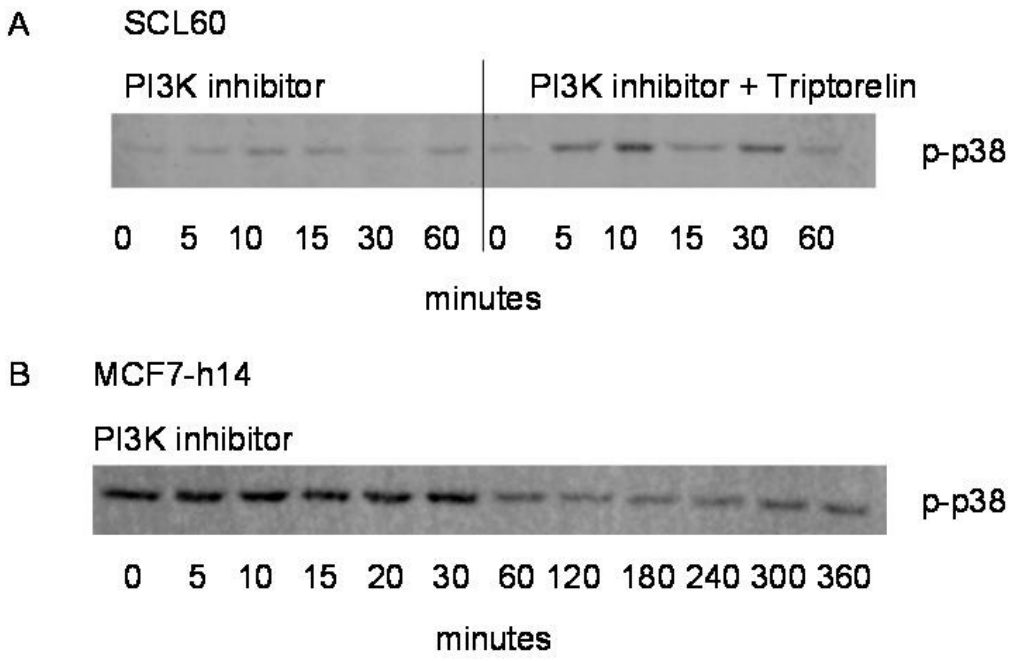

Figure 88: p-p38 response to PI3K inhibition
(A) Expression of p-p38 in SCL60 cells treated with 7μM PI3K inhibitor, as detected by western blot.
(B) Expression of p-p38 in MCF7h14 cells treated with 800nM PI3K inhibitor, as detected by western blot.
These data are from a single experiment.

3.6.6 NFκB inhibition did not inhibit the SRB activity of MCF7h14 cells either alone or in combination with Triptorelin.

Because SCL60 cells had been shown to be inhibited by 15d-PGJ_2, it was interesting to investigate whether MCF7-h14 cells might also be responsive to this NFκB inhibitor. MCF7-h14 cells were treated with 15d-PGJ_2 (3μM) alone and in combination with Triptorelin (100nM). Cell number was measured by SRB assay at 1, 4 and 6 days after treatment. No significant reduction in SRB activity could be observed in response to 15d-PGJ_2 either alone or in combination with the GnRH agonist compared to vehicle control-treated cells.

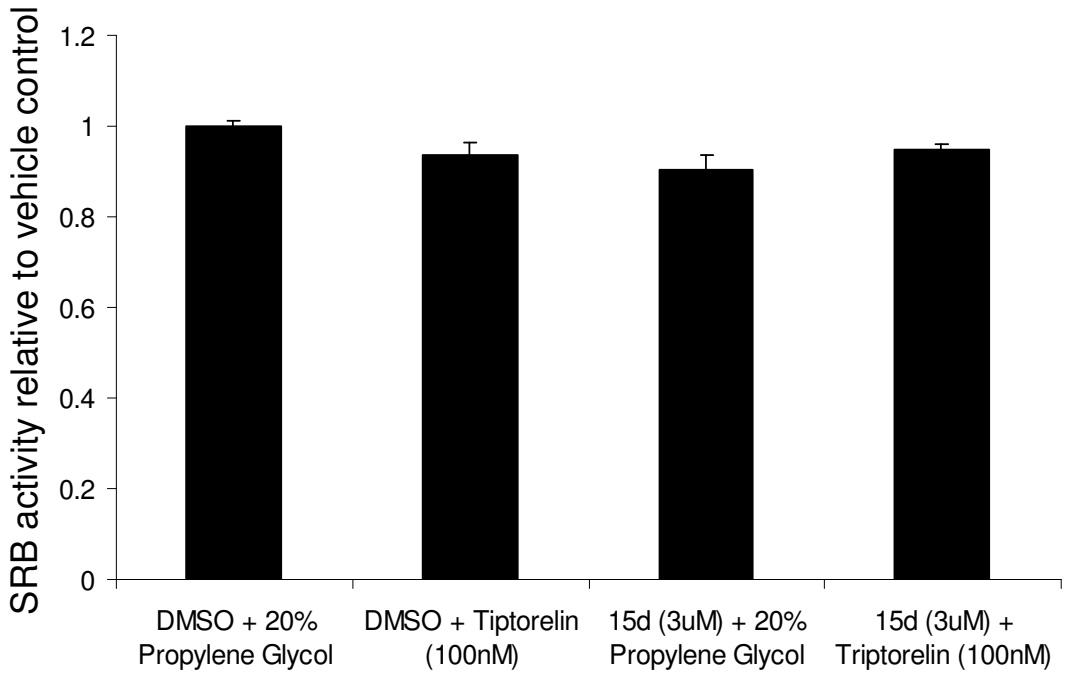

Figure 89: NFκB inhibition in MCF7-h14 cells with 3μM 15d-PGJ_2.
NFκB inhibition with 3μM 15d-PGJ_2 did not cause reduction in SRB activity of MCF7-h14 cells either alone and in combination with 100nM Triptorelin. SRB activity was measured 4 days after treatment by SRB assay and is shown relative to that of the vehicle control-treated cells. Error bars show standard deviation of three intraexperimental replicates. These data are from a single experiment.

3.6.7 Discussion

Since no breast cancer cell line expressing detectable levels of endogenous GnRH receptor could be identified, several cell lines (ZR75/1, T47D and MCF7) were transfected with GnRHR. Among the clones produced was the MCF7-h14 clone, which showed high GnRHR cell surface expression (Figure 71, Figure 72). GnRHR level has previously appeared to correlate with the extent of cell number inhibition [79], so it was predicted that MCF7-h14 cells would be inhibited by Triptorelin.

MCF7-h14 cells showed similar GnRHR expression and a similar inositol phosphate response following GnRHR activation to SCL60 cells (Figure 73). This indicated that the cells have similar levels of functional receptor activity. Despite this, MCF7-h14 cells were not responsive to GnRHR stimulation with the GnRH agonist

Triptorelin. The parental (untransfected) MCF7 cells were also unresponsive to GnRHR activation (Figure 75).

Exposure to Triptorelin for 5min was sufficient to inhibit SCL60 cell proliferation by approximately 40% after 4 days. This indicates that after 5min receptor stimulation, signalling pathway(s) downstream of the GnRHR remain active without the requirement for further ligand-receptor stimulation. Maximal inhibition after 4 days (~60%) was achieved with continuous exposure to Triptorelin for just 8h (Figure 74). This indicates that continuous exposure for 8h maintains the antiproliferative signalling.

Until now, cell lines transfected with a high level of GnRHR have been shown to be sensitive to GnRH agonist treatment [50, 79]. It is not clear why this MCF-7-h14 clone, that expresses a high level of GnRHR at the cell surface, is not responsive to a GnRH agonist.

It has previously been shown that the proliferation of MCF7-h14 cells may be inhibited by targeting the GnRHR [32]. Everest *et al* were unable to detect endogenous GnRHR in MCF7 cells, so the authors infected the cells with adenovirus expressing sheep GnRHR (which has high affinity for GnRH-I). They report that 80% of the cells then transiently expressed GnRHR and that GnRH and GnRH-I agonists (but not antagonists) inhibited thymidine incorporation in the MCF7 cells [32]. This indicated that MCF7 cells can have the required cellular machinery to elicit an antiproliferative response to GnRHR stimulation. This is in contrast to the data presented above, with the stably transfected MCF7-h14 model. The differences in response may be explained by a number of factors. Firstly, MCF7-h14 cells express rat GnRHR and were treated with the GnRH agonist Triptorelin, whereas the MCF7 cells in Everest *et al*'s study expressed sheep GnRHR and were treated with the GnRH agonist Buserelin. The two different receptors, or the different GnRH agonists, may induce differential downstream signalling. Secondly, the transfection process to stably express GnRHR in MCF7-h14 cells involves incorporation of GnRHR DNA into the host DNA. This can damage the host DNA and impact upon

cellular function such that the corresponding antiproliferative signalling pathway is not functional. Additionally, it is widely appreciated that a cell line may differ between laboratories due to genetic drift arising from independent culture, or subtle differences in the culturing environment. These differences may in part explain the absence of a response to Triptorelin in MCF7-h14 cells.

It is assumed here that specific binding is directly proportional to the level of GNRHR cell surface expression. However, it is important to be aware that this may not necessarily be true. There may be variation in the affinity for GnRH agonist within the population of cell surface GnRHRs on a given cell, on different cells, and between cells of different cell lines. A small number of receptors with a high affinity may give the same level of specific binding as a high number of receptors with a low affinity. It is also important to consider that a the affinity of a GnRHR, or population of GnRHRs, for the agonist used in the ligand binding assay may differ from its affinity for other agonists. The level of GnRHR expression at the cell surface may not necessarily be the most important factor in determining receptor functionality. It has previously been shown that a large proportion of human GnRHR is retained intracellularly [223]. The rate at which GnRHR is trafficked to and from the plasma membrane is likely to be more important in determining the extent of GnRHR signalling activation. The ligand binding assays used in this study focus on one concentration of radioligand. A single concentration of ligand can give misleading results on the estimated binding affinity of the receptor population because the competitive equilibrium will be shifted depending on the ligand concentration. Multiple concentrations of radioligand have been used previously to determine the range of ligand concentration which gives a linear relationship to specific binding. ^{3}[H]IP accumulation is used as a measure of receptor function. It should be noted that a limitation of this assumption is that the pool of inositol within different cells may be variable and if limited this may give misleading results indicating poor receptor functionality.

MCF7-h14 cells and SCL60 cells appeared to have a comparable level of GnRHR (assuming that the binding affinities of GnRHR are equal between the cell lines) and

GnRHR-induced inositol phosphate production. Both SCL60 and MCF7-h14 cells express the rat GnRHR. This is used because it is more efficiently trafficked the plasma membrane, whereas human GnRHR is retained intracellularly. In real human proliferative diseases (cancer), only the human receptor may be present, and is likely to be intracellular. GnRHR signalling in SCL60 cells is signalling that appears to occur as a result of high GnRHR expression at the cell surface. In human cancers, in which GnRHR is largely intracellular, the nature of the signalling may differ. As discussed above, in human cancers it may be more important that the cells have a high rate of GnRHR trafficking to and from the cell membrane, as this would allow higher signalling even with a low proportion of the receptors at the membrane at any one time. Transfection may alter cells in ways additional to the presence of receptor, and these changes may be a requirement for (or a hindrance to) the antiproliferative effects of a GnRH agonist. It is possible that in MCF7-h14 cells, the transfection process has caused damage which may prevent the equivalent GnRHR-induced antiproliferative signalling pathway from being activated or propagated to the same outcome as in SCL60 cells.

Unlike in SCL60 cells, a change in the level of pERK1/2 could not be detected in MCF7-h14 cells in the presence of serum, perhaps due to a higher basal level of pERK1/2 in MCF7-h14 relative to SCL60 (Figure 76B). A small increase in pERK1/2 was observed in serum-starved MCF7-h14 cells (Figure 76C), although transient alterations in the level of pERK1/2 have been observed in other cells that are inhibited by GnRHR activation even in the presence of serum, such as SCL60 (Figure 76A) and prostate-derived WPE-NB-26-3 cells [50, 79]. The lack of change in pERK1/2 might account for the lack of inhibitory effect of GnRHR stimulation on MCF7-h14 cell number.

p-p38 was also transiently increased in SCL60 cells after treatment with Triptorelin (Figure 77A), following a similar activation pattern to pERK1/2, although p-p38 remained above basal level at 60min post-treatment whereas pERK1/2 returned to, or was even below, basal level by 30min (Figure 77A). This is in agreement with previously published data showing rapid activation of p38 in SCL60 cells [79]. This

supports the role of multiple MAPK pathways in the antiproliferative response to Triptorelin, although in that study by Morgan *et al*, a p38 inhibitor had no effect on cell survival following Triptorelin treatment in SCL60 cells [79].

IGF-I-R inhibition reduced SCL60 and MCF7-h14 cell number in a time- (Figure 79) and dose-dependent manner (Figure 80, Figure 81). The two cell lines were inhibited to a similar extent. IGF-I-R inhibition also reduces SRB activity of wild-type MCF7 cells [231] and this was confirmed by Kevin Morgan (Figure 78). This is consistent with previous literature describing the growth-stimulatory role of IGF-I in MCF7 cells [233-237]. When the IGF-I-R inhibitor was washed out after 1h, MCF7-h14 cell cell number was unaffected (Figure 82), indicating that the antiproliferative effect of IGF-I-R inhibition is reversible up to at least 1h. Triptorelin did not appear to inhibit or increase the rate of cell recovery (Figure 82), although, given that the cells fully recovered, any positive effect may be masked.

IGF-I-R inhibition had no detectable effect on pERK1/2 levels in SCL60 cells (Figure 83A), but caused a rapid (within 30min) decrease in pERK1/2 in MCF7-h14 cells (Figure 83B). This discrepancy may be due to the lower level of basal pERK1/2 activity in SCL60 cells relative to MCF7-h14 cells. Pre-incubation with an IGF-I-R inhibitor for 4h (and then removing the inhibitor by washing with PBS) did not prevent the GnRHR-mediated transient elevation in of pERK1/2 in SCL60 cells (Figure 83A), which has previously been shown to correlate with cell number inhibition [50, 79]. MCF7-h14 cells showed hyper-reactivation of ERK1/2 (far above basal) after removal of IGF-I-R inhibitor, and this was not altered by GnRHR stimulation (Figure 83B).

MCF7 cells have an activating PI3K mutation, whereas SCL60 cells do not [228]. It is possible that this may underlie the differential signalling response to IGF-I-R removal in these cells. The decrease in pERK1/2 in MCF7-h14 cells may be due to decreased signalling from IGF-I-R to pERK1/2 via PI3K. Since PI3K is not mutated in SCL60 cells there is no significant decrease in pERK1/2 levels with IGF-I-R inhibition. In MCF7-h14 cells, when IGF-I-R inhibition is removed, the already

activated PI3K may interact with the IGF-I-R complex to re-phosphorylate ERK1/2, whereas since PI3K is not mutated in SCL60 cells and there is no significant re-phosphorylation of ERK1/2 in these cells.

Proliferation of MCF7 cells is enhanced by oestrogen [229, 230], whereas SCL60 does not endogenously express ERα. ERα-mediated growth promoting signalling may act in opposition to the GnRHR-mediated antiproliferative pathway, since it has been shown that ERα interacts with MAPK and Akt pathways and participates in cross-talk with IGF-I-R [238, 239]. This may contribute to the differential effect of GnRHR activation in these cells. ERα is known to interact with RTK signalling such as IGF-I-R, EGFR and the MAPK and Akt signalling pathways [235, 236, 240].

GnRHR mediated changes in ERK1/2 may be masked by constitutive growth factor receptor activity which may maintain (high) levels of pERK1/2. This may explain why no change in pERK1/2 is seen upon GnRHR activation in MCF7-h14 cells in the presence of growth factors. Both SCL60 and MCF7-h14 cells were sensitive to IGF-I-R inhibition. This was much less pronounced in SCL60 than MCF7-h14 which suggests that IGF-I-R signalling plays a more dominant role in MCF7-h14 than SCL60 cells. This may explain why GnRHR activation is unable to overcome IGF-I-R-driven signalling in MCF7-h14 cells.

Gαq binds PLC, which signals to activate ERK1/2 via PKC and Raf [241]. This is thought to be the mechanism by which GnRHR induces a transient increase in pERK1/2 in SCL60 cells [79]. Transient ERK1/2 activation may be relevant to the mechanism of GnRH agonist-induced reduction in SRB activity of SCL60 cells. Gαq is also able to inhibit PI3K and Akt [208, 209, 241], and the level of pERK1/2 may be dependent on a balance of ERK1/2 activation through Gαq-PLC and ERK1/2 inhibition through Gαq-PI3K (Figure 91). GnRHR activation did not cause a reduction in SRB activity of MCF7-h14 cells. PI3K is constitutively active in MCF7 cells and may maintain high levels of pERK1/2 [228]. Gαq can still inhibit constitutively active PI3K, but this may not be sufficient to induce apoptosis [209].

Alternatively, a transient decrease in pERK1/2 is associated with the antiproliferative effect of GnRHR activation in neuroblastoma (B35) cells and in prostate cells WPE-1-NB26-3 [50]. Gαq is also able to inhibit PI3K and Akt [208, 209, 241], and this may compete with the Gαq-PLC pathway to ERK1/2. This physical interaction between activated Gαq and PI3K may be responsible for the transient decrease in pERK1/2 in B35 and WPE-NB26-3 cells. Since MCF7 cells have an activating PI3K mutation, this pathway may be blocked, thus preventing a GnRHR-mediated transient decrease in pERK1/2.

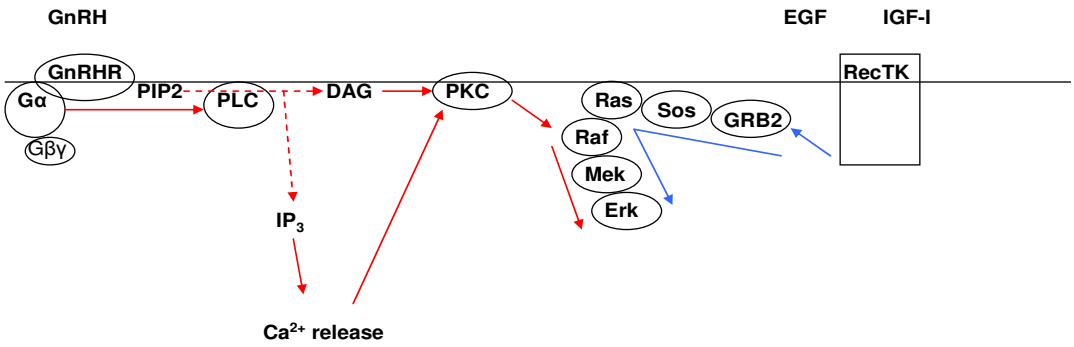

Figure 90: Possible model of GnRHR signalling based on constitutive growth factor receptor activity
GnRHR mediated changes in ERK1/2 may be masked by constitutive growth factor receptor activity which may maintain (high) levels of pERK1/2. This may explain why no change in pERK1/2 is seen upon GnRHR activation in MCF7-h14 cells. Both SCL60 and MCF7-h14 cells were sensitive to IGF-I-R inhibition. This was much less pronounced in SCL60 than MCF7-h14 which suggests that IGF-I-R signalling plays a more dominant role in MCF7-h14 than SCL60 cells. This may explain why GnRHR activation is unable to overcome IGF-I-R-driven signalling in MCF7-h14 cells.

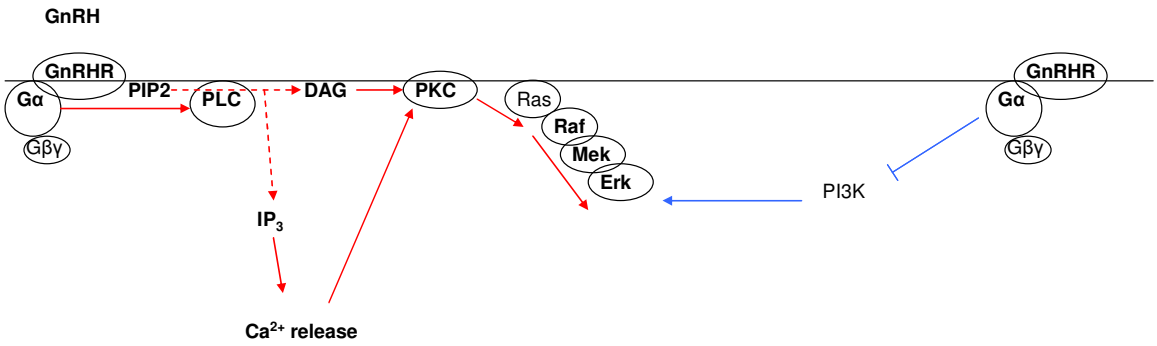

Figure 91: Possible model of GnRHR signalling based on PI3K activity
Transient ERK1/2 activation is thought to be the mechanism of GNRH-induced reduction in SCL60 cell number. The level of pErk1/2 may be dependent on a balance of Erk activation through Gαq-PLC and Erk inhibition through Gαq-PI3K. GnRHR activation did not cause a reduction in the SRB activity of MCF7-h14 cells. PI3K is constitutively active in MCF7 cells and may maintain high levels of pERK1/2. Gαq can still inhibit constitutively active PI3K, but this may not be sufficient to induce apoptosis.

In summary, Kevin Morgan developed a GnRHR-transfected breast cancer cell line, MCF7-h14. The response of MCF7-h14 cells to GnRHR stimulation was compared to that of SCL60 cells. Unlike SCL60 cells, MCF7-h14 cells were not inhibited by GnRHR activation despite the cell lines having similar levels of receptor expression. This may be explained by an inability of GnRHR-signalling to overcome constitutive PI3K activity in MCF7-h14 cells. Both cell lines appeared to be dependent on IGF-I-R for normal proliferation. In MCF7-h14 cells a small reduction in pERK1/2 expression was observed following IGF-I-R inhibition, but a similar effect on pERK1/2 expression was could not be detected in SCL60 cells. IGF-I-R inhibition did not affect GnRHR-mediated changes in pERK1/2 or p-p38 in SCL60 cells. PI3K inhibition did not affect GnRHR-mediated changes in pERK1/2 and p-p38 in either cell line; PI3K reduced SRB activity in SCL60 cells at 7μM.

Both cell lines were sensitive to IGF-I-R inhibition, and blocking PI3K activity caused a mild reduction in SRB activity of SCL60 cells only. This information, coupled with knowledge of MAPK signalling involvement, aids the formation of further models which may explain the differential outcomes of GnRHR stimultation in these cell types (Figure 90, Figure 91), and therefore which factors may be required for the direct antiproliferative action of GnRH agonists.

Chapter 4: Final Discussion

4 Final Discussion

The GnRH agonist Triptorelin inhibited SCL60 cell number by a combination of apoptosis and inhibition of proliferation both *in vitro* and *in vivo*, and cell cycle arrest appears to be involved *in vitro*. A global gene expression time series in SCL60 cells following Triptorelin treatment implicated transcriptional changes in cell cycle, MAPK and adhesion-related genes, with good support from other gene expression studies [108, 109]. Gene expression data would benefit from computational modelling to understand the complex interactions at the transcriptomic level to identify how pathways may be interacting to mediate the antiproliferative effects of a GnRH agonist. The models indicated above may represent useful starting points.

The level of pAkt was decreased at multiple time-points following GnRHR stimulation, and NFκB was activated following GnRHR stimulation. SCL60 cells (but not HEK293 cells) were sensitive to NFκB inhibition and the combination of GnRHR stimulation and NFκB inhibition enhanced the antiproliferative effect observed with either drug alone. This suggested that NFκB may be activated as part of a survival response to GnRH agonist treatment. A role for Akt and NFκB has not previously been indicated in the response of SCL60 cells to GnRH agonists.

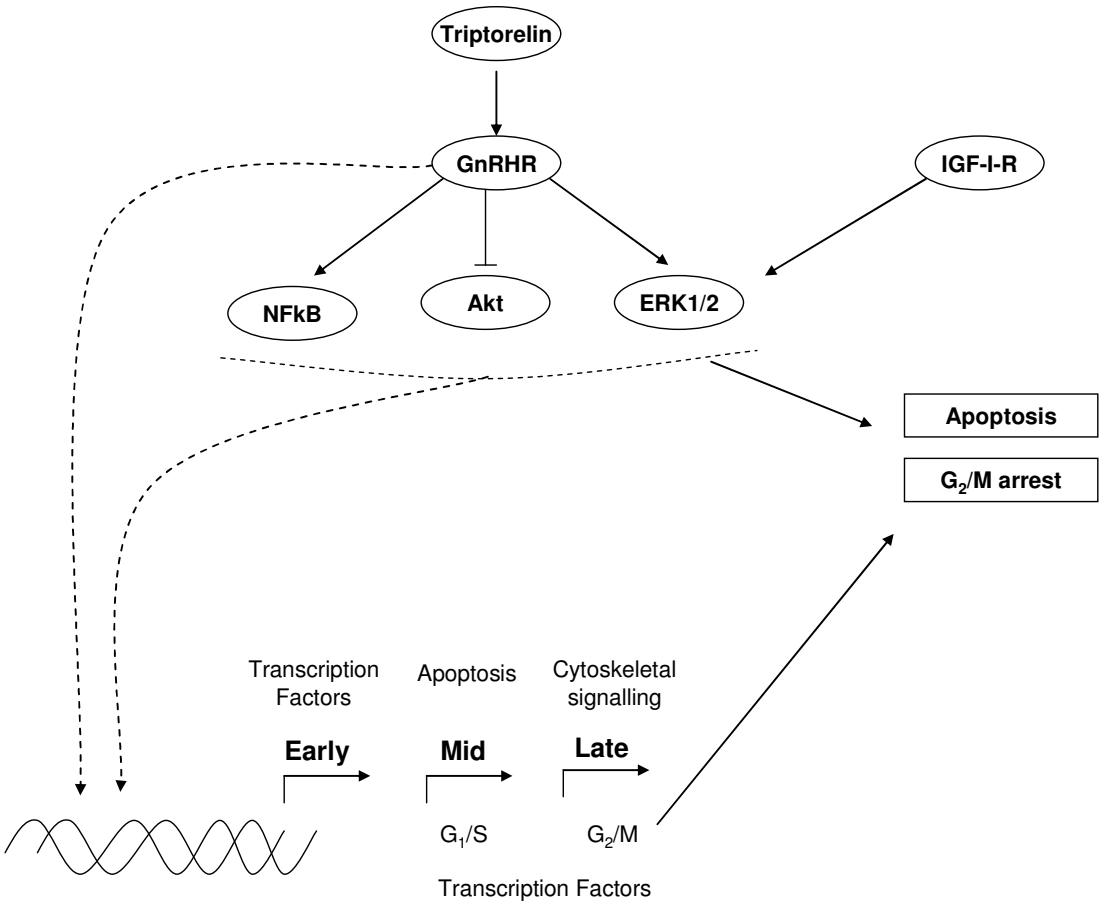

Figure 92: Schematic diagram summarising the proteomic and transcriptomic responses to Triptorelin in SCL60 cells, which may contribute to the induction of G_2/M arrest and apoptosis. At the protein level, Triptorelin appears to activate NFκB and ERK1/2, but inhibit Akt. These proteins may potentially drive the transcriptional responses to GnRHR stimulation. Early changes were observed in the expression levels of many transcription factors, some of which were transient and others maintained for up to 24h. Triptorelin influenced the expression of genes involved in apoptosis and G_1/S phase progression after 1-8h of treatment, whereas the expression of cytoskeletal/adhesion signalling components and genes involved in G_2/M phase progression was altered slightly later at around 8h after treatment.

At the protein level, Triptorelin appears to activate NFκB and ERK1/2, but inhibit Akt. These proteins may drive the transcriptional responses to GnRHR stimulation, which consisted of early changes in the expression levels of transcription factors, some of which were transient and others maintained for up to 24h. Triptorelin influenced the expression of genes involved in apoptosis and G_1/S phase progression after 1-8h of treatment, whereas the expression of cytoskeletal/adhesion signalling components and genes involved in G_2/M phase progression was altered slightly later at 8-24h after treatment.

GnRHR protein expression was significantly higher in the Triple Negative Phenotype (TNP) subgroup of breast cancer and in grade 3 tumours. However, SRB activity of a breast cancer clone expressing high GnRHR (MCF7-h14) was not inhibited by Triptorelin despite these cells expressing a similar level of GnRHR to SCL60 cells, suggesting that a high level of functional GnRHR is not sufficient for the direct antiproliferative effects of Triptorelin. This may have implications for the identification of a subgroup of breast cancers that are most likely to respond to GnRH agonist therapy, since identifying breast tumours with high GnRHR may not be sufficient to predict a response.

The comparison between the responsive high GnRHR-expressing SCL60 and the unresponsive high GnRHR-expressing MCF7-h14 cells could be expanded further. A high-throughput gene and protein expression profiling approach to compare these cells, and their responses to Triptorelin would help to identify critical signalling factors that are absent, or may be competing with GnRHR-mediated antiproliferative signalling, in MCF7h14 cells. It may also be interesting to investigate any role of pAkt and NFκB in MCF7h14 cells, since these appear to be important in the SCL60 response to GnRHR stimulation.

It is important to note that many of the results presented here, particularly western blots, are derived from single or duplicate experiments (n=1 or n=2). Any conclusions drawn from these therefore must be tentative and further validation, ideally with different methodologies, is required to affirm them. These data do however indicate signalling molecules of interest and provide hypotheses on which to base further experiments.

The observation that proliferation of MCF7-h14 cells was not inhibited by Triptorelin, despite the cells expressing a high level of GnRHR, is a particularly important step in understanding the antiproliferative effects of GnRHR signalling. It demonstrates that a high level of GnRHR is insufficient for the antiproliferative response, and underlines the role of multiple pathways interacting with GnRHR. The

experiments above have indicated that growth factor signalling (such as IGF-I) appears to out-compete GnRHR signalling in breast cancer cells, and understanding how these pathways interact may help to identify a combination therapy to enhance the antiproliferative effects of GnRHR signalling in breast cancer.

Further work may expand the current gene expression study of the SCL60 response to Triptorelin to explore the response to Triptorelin *in vivo* SCL60 xenografts. In addition, a comparison between the transcriptional response to Triptorelin in MCF7-h14 cells and SCL60 cells may highlight further reasons for the differential outcome of GnRHR stimulation. It would be important in future work to evaluate the limitations and caveats discussed above, particularly with regard to GnRHR number and function in SCL60 and MCF7-h14 cells. It would be interesting to further explore the role of pNFκB and pAkt pathways at the proteomic level in response to GnRHR stimulation, and how this may relate to the antiproliferative effects of Triptorelin. This study focussed on only one GnRH agonist, but the possibility of differential effects of other GnRH agonists and antagonists would be interesting to investigate.

In conclusion, GnRHR activation in SCL60 cells resulted in changes in the expression of cell cycle, MAPK and adhesion-related genes. At the protein level, pAkt expression was decreased, and NFκB was activated following Triptorelin treatment. NFκB inhibition enhanced the antiproliferative effect of Triptorelin in SCL60 cells, and may play a survival role in response to GnRHR activation. A range of GnRHR expression was observed in breast cancer tumours, and on average GnRHR expression was higher in the TNP subgroup. Despite MCF7-h14 cells expressing a similar high level of functional GnRHR to SCL60 cells, their SRB activity was unaffected by Triptorelin, indicating for the first time that a high level of GnRHR is insufficient for the direct antiproliferative effects of the GnRH agonist Triptorelin.

Bibliography

5 Bibliography

1. Aitken SJ, Thomas JS, Langdon SP, Harrison DJ, Faratian D: **Quantitative analysis of changes in ER, PR and HER2 expression in primary breast cancer and paired nodal metastases**. *Ann Oncol* 2009, **21**(6):1254-1261.
2. Sherr CJ: **Principles of tumor suppression**. *Cell* 2004, **116**(2):235-246.
3. Croce CM: **Oncogenes and cancer**. *N Engl J Med* 2008, **358**(5):502-511.
4. Hanahan D, Weinberg RA: **The hallmarks of cancer**. *Cell* 2000, **100**(1):57-70.
5. Hanahan D, Weinberg RA: **Hallmarks of cancer: the next generation**. *Cell* 2011, **144**(5):646-674.
6. **Breast Anatomy, Patrick J. Lynch (Accessed 10 May 2011)** [http://en.wikipedia.org/wiki/File:Breast_anatomy_normal_scheme.png]
7. Vinay Kumar AKA, Nelson Fausto **Robbins and Cotran Pathologic Basis of Disease**; 2004.
8. David Levison RR, Stewart Fleming, David Harrison, Alastair Burt: **Muir's Textbook of Pathology**, 14 edn: Hodder Arnold; 2008.
9. Ramsay DT, Kent JC, Hartmann RA, Hartmann PE: **Anatomy of the lactating human breast redefined with ultrasound imaging**. *J Anat* 2005, **206**(6):525-534.
10. **Breast Cancer Statistics - Key Facts, Cancer Research UK (Accessed 11 Aug 2010)** [http://info.cancerresearchuk.org/cancerstats/types/breast/#mortality]
11. **Breast Cancer Risk Factors, Cancer Research UK (30 June 2010)** [http://info.cancerresearchuk.org/cancerstats/types/breast/riskfactors/#source3]
12. Barnes BB, Steindorf K, Hein R, Flesch-Janys D, Chang-Claude J: **Population attributable risk of invasive postmenopausal breast cancer and breast cancer subtypes for modifiable and non-modifiable risk factors**. *Cancer Epidemiol* 2010, **13**:13.
13. Polyak K: **Breast cancer: origins and evolution**. *J Clin Invest* 2007, **117**(11):3155-3163.
14. Hu Z, Fan C, Oh DS, Marron JS, He X, Qaqish BF, Livasy C, Carey LA, Reynolds E, Dressler L, Nobel A, Parker J, Ewend MG, Sawyer LR, Wu J, Liu Y, Nanda R, Tretiakova M, Ruiz Orrico A, Dreher D, Palazzo JP, Perreard L, Nelson E, Mone M, Hansen H, Mullins M, Quackenbush JF, Ellis MJ, Olopade OI, Bernard PS, Perou CM: **The molecular portraits of breast tumors are conserved across microarray platforms**. *BMC Genomics* 2006, **7**(96):96.
15. Mullan PB, Millikan RC: **Molecular subtyping of breast cancer: opportunities for new therapeutic approaches**. *Cell Mol Life Sci* 2007, **64**(24):3219-3232.
16. **Breast cancer: prevention and control** [http://www.who.int/cancer/detection/breastcancer/en/]
17. **Breast Cancer (female), NHS (Accessed 05 July 2010)** [http://www.nhs.uk/conditions/cancer-of-the-breast-female/Pages/Introduction.aspx]

18. Morrison BJ, Schmidt CW, Lakhani SR, Reynolds BA, Lopez JA: **Breast cancer stem cells: implications for therapy of breast cancer**. *Breast Cancer Res* 2008, **10**(4):210.
19. Lawson JC, Blatch GL, Edkins AL: **Cancer stem cells in breast cancer and metastasis**. *Breast Cancer Res Treat* 2009, **118**(2):241-254.
20. Tobias J: **Cancer and its Management**, 6th edn: Wiley-Blackwell; 2010.
21. Weinstein IB, Joe A: **Oncogene addiction**. *Cancer Res* 2008, **68**(9):3077-3080; discussion 3080.
22. Kaelin WG, Jr.: **The concept of synthetic lethality in the context of anticancer therapy**. *Nat Rev Cancer* 2005, **5**(9):689-698.
23. Farmer H, McCabe N, Lord CJ, Tutt AN, Johnson DA, Richardson TB, Santarosa M, Dillon KJ, Hickson I, Knights C, Martin NM, Jackson SP, Smith GC, Ashworth A: **Targeting the DNA repair defect in BRCA mutant cells as a therapeutic strategy**. *Nature* 2005, **434**(7035):917-921.
24. Dunn BK, Jegalian K, Greenwald P: **Biomarkers for early detection and as surrogate endpoints in cancer prevention trials: issues and opportunities**. *Recent Results Cancer Res* 2011, **188**:21-47.
25. Schubert A, Hawighorst T, Emons G, Grundker C: **Agonists and antagonists of GnRH-I and -II reduce metastasis formation by triple-negative human breast cancer cells in vivo**. *Breast Cancer Res Treat* 2011, **2011**:30.
26. Buchholz S, Seitz S, Schally AV, Engel JB, Rick FG, Szalontay L, Hohla F, Krishan A, Papadia A, Gaiser T, Brockhoff G, Ortmann O, Diedrich K, Koster F: **Triple-negative breast cancers express receptors for luteinizing hormone-releasing hormone (LHRH) and respond to LHRH antagonist cetrorelix with growth inhibition**. *Int J Oncol* 2009, **35**(4):789-796.
27. Finch AR, Green L, Hislop JN, Kelly E, McArdle CA: **Signaling and antiproliferative effects of type I and II gonadotropin-releasing hormone receptors in breast cancer cells**. *J Clin Endocrinol Metab* 2004, **89**(4):1823-1832.
28. Eidne KA, Flanagan CA, Harris NS, Millar RP: **Gonadotropin-releasing hormone (GnRH)-binding sites in human breast cancer cell lines and inhibitory effects of GnRH antagonists**. *J Clin Endocrinol Metab* 1987, **64**(3):425-432.
29. Miller WR, Scott WN, Morris R, Fraser HM, Sharpe RM: **Growth of human breast cancer cells inhibited by a luteinizing hormone-releasing hormone agonist**. *Nature* 1985, **313**(5999):231-233.
30. Cassano A, Astone A, Garufi C, Noviello MR, Pietrantonio F, Barone C: **A response in advanced post-menopausal breast cancer during treatment with the luteinising hormone releasing hormone agonist--Zoladex**. *Cancer Lett* 1989, **48**(2):123-124.
31. Segal-Abramson T, Kitroser H, Levy J, Schally AV, Sharoni Y: **Direct effects of luteinizing hormone-releasing hormone agonists and antagonists on MCF-7 mammary cancer cells**. *Proc Natl Acad Sci U S A* 1992, **89**(6):2336-2339.
32. Everest HM, Hislop JN, Harding T, Uney JB, Flynn A, Millar RP, McArdle CA: **Signaling and antiproliferative effects mediated by GnRH receptors after expression in breast cancer cells using recombinant adenovirus**. *Endocrinology* 2001, **142**(11):4663-4672.

33. Millar RP: **GnRHs and GnRH receptors**. *Anim Reprod Sci* 2005, **88**(1-2):5-28.
34. Naor Z: **Signaling by G-protein-coupled receptor (GPCR): Studies on the GnRH receptor**. *Front Neuroendocrinol* 2008, **5**:5.
35. Chi L, Zhou W, Prikhozhan A, Flanagan C, Davidson JS, Golembo M, Illing N, Millar RP, Sealfon SC: **Cloning and characterization of the human GnRH receptor**. *Mol Cell Endocrinol* 1993, **91**(1-2):R1-6.
36. Millar RP, Lu ZL, Pawson AJ, Flanagan CA, Morgan K, Maudsley SR: **Gonadotropin-releasing hormone receptors**. *Endocr Rev* 2004, **25**(2):235-275.
37. Janovick JA, Knollman PE, Brothers SP, Ayala-Yanez R, Aziz AS, Conn PM: **Regulation of G protein-coupled receptor trafficking by inefficient plasma membrane expression: molecular basis of an evolved strategy**. *J Biol Chem* 2006, **281**(13):8417-8425.
38. Stewart AJ, Katz AA, Millar RP, Morgan K: **Retention and silencing of prepro-GnRH-II and type II GnRH receptor genes in mammals**. *Neuroendocrinology* 2009, **90**(4):416-432.
39. Millar RP, Pawson AJ, Morgan K, Rissman EF, Lu ZL: **Diversity of actions of GnRHs mediated by ligand-induced selective signaling**. *Front Neuroendocrinol* 2008, **29**(1):17-35.
40. Pawson AJ, Maudsley S, Morgan K, Davidson L, Naor Z, Millar RP: **Inhibition of human type i gonadotropin-releasing hormone receptor (GnRHR) function by expression of a human type II GnRHR gene fragment**. *Endocrinology* 2005, **146**(6):2639-2649.
41. Pfleger KD, Bogerd J, Millar RP: **Conformational constraint of mammalian, chicken, and salmon GnRHs, but not GnRH II, enhances binding at mammalian and nonmammalian receptors: evidence for preconfiguration of GnRH II**. *Mol Endocrinol* 2002, **16**(9):2155-2162.
42. Cheng CK, Leung PC: **Molecular biology of gonadotropin-releasing hormone (GnRH)-I, GnRH-II, and their receptors in humans**. *Endocr Rev* 2005, **26**(2):283-306.
43. Heding A, Vrecl M, Bogerd J, McGregor A, Sellar R, Taylor PL, Eidne KA: **Gonadotropin-releasing hormone receptors with intracellular carboxyl-terminal tails undergo acute desensitization of total inositol phosphate production and exhibit accelerated internalization kinetics**. *J Biol Chem* 1998, **273**(19):11472-11477.
44. McArdle CA, Franklin J, Green L, Hislop JN: **Signalling, cycling and desensitisation of gonadotrophin-releasing hormone receptors**. *J Endocrinol* 2002, **173**(1):1-11.
45. Davidson JS, Wakefield IK, Millar RP: **Absence of rapid desensitization of the mouse gonadotropin-releasing hormone receptor**. *Biochem J* 1994, **300 (Pt 2)**(Pt 2):299-302.
46. Willars GB, Heding A, Vrecl M, Sellar R, Blomenrohr M, Nahorski SR, Eidne KA: **Lack of a C-terminal tail in the mammalian gonadotropin-releasing hormone receptor confers resistance to agonist-dependent phosphorylation and rapid desensitization**. *J Biol Chem* 1999, **274**(42):30146-30153.

47. **Breast Cancer Treatment for Premenopausal Women** [http://www.cancer.gov/clinicaltrials/featured/trials/ibcsg-25-03]
48. Cuzick J, Ambroisine L, Davidson N, Jakesz R, Kaufmann M, Regan M, Sainsbury R: **Use of luteinising-hormone-releasing hormone agonists as adjuvant treatment in premenopausal patients with hormone-receptor-positive breast cancer: a meta-analysis of individual patient data from randomised adjuvant trials**. *Lancet* 2007, **369**(9574):1711-1723.
49. Coy DH, Vilchez-Martinez JA, Coy EJ, Schally AV: **Analogs of luteinizing hormone-releasing hormone with increased biological activity produced by D-amino acid substitutions in position 6**. *J Med Chem* 1976, **19**(3):423-425.
50. Morgan K, Stavrou E, Leighton SP, Miller N, Sellar R, Millar RP: **Elevated GnRH receptor expression plus GnRH agonist treatment inhibits the growth of a subset of papillomavirus 18-immortalized human prostate cells**. *Prostate* 2010, **6**:6.
51. Gnanapragasam VJ, Darby S, Khan MM, Lock WG, Robson CN, Leung HY: **Evidence that prostate gonadotropin-releasing hormone receptors mediate an anti-tumourigenic response to analogue therapy in hormone refractory prostate cancer**. *J Pathol* 2005, **206**(2):205-213.
52. Tolis G, Ackman D, Stellos A, Mehta A, Labrie F, Fazekas AT, Comaru-Schally AM, Schally AV: **Tumor growth inhibition in patients with prostatic carcinoma treated with luteinizing hormone-releasing hormone agonists**. *Proc Natl Acad Sci U S A* 1982, **79**(5):1658-1662.
53. Celio L, Martinetti A, Ferrari L, Buzzoni R, Mariani L, Miceli R, Seregni E, Procopio G, Cassata A, Bombardieri E, Bajetta E: **Premenopausal breast cancer patients treated with a gonadotropin-releasing hormone analog alone or in combination with an aromatase inhibitor: a comparative endocrine study**. *Anticancer Res* 1999, **19**(3B):2261-2268.
54. Martinetti A, Ferrari L, Celio L, Mariani L, Miceli R, Zilembo N, Di Bartolomeo M, Toffolatti L, Pozzi P, Seregni E, Bombardieri E, Bajetta E: **The luteinising hormone-releasing hormone analogue triptorelin with or without the aromatase inhibitor formestane in premenopausal breast cancer: effects on bone metabolism markers**. *J Steroid Biochem Mol Biol* 2000, **75**(1):65-73.
55. **The electronic Medicines Compendium (Accessed 12 Aug 2011)** [www.medicines.org.uk]
56. Vincze B, Palyi I, Daubner D, Kremmer T, Szamel I, Bodrogi I, Sugar J, Seprodi J, Mezo I, Teplan I, et al.: **Influence of luteinizing hormone-releasing hormone agonists on human mammary carcinoma cell lines and their xenografts**. *J Steroid Biochem Mol Biol* 1991, **38**(2):119-126.
57. Marini L, Iacopino F, Schinzari G, Robustelli della Cuna FS, Mantovani G, Sica G: **Direct antiproliferative effect of triptorelin on human breast cancer cells**. *Anticancer Res* 1994, **14**(5A):1881-1885.
58. Emons G, Grundker C, Gunthert AR, Westphalen S, Kavanagh J, Verschraegen C: **GnRH antagonists in the treatment of gynecological and breast cancers**. *Endocr Relat Cancer* 2003, **10**(2):291-299.
59. Maudsley S, Davidson L, Pawson AJ, Chan R, Lopez de Maturana R, Millar RP: **Gonadotropin-releasing hormone (GnRH) antagonists promote**

proapoptotic signaling in peripheral reproductive tumor cells by activating a Galphai-coupling state of the type I GnRH receptor. *Cancer Res* 2004, **64**(20):7533-7544.

60. Emons G, Ortmann O, Becker M, Irmer G, Springer B, Laun R, Holzel F, Schulz KD, Schally AV: **High affinity binding and direct antiproliferative effects of LHRH analogues in human ovarian cancer cell lines**. *Cancer Res* 1993, **53**(22):5439-5446.
61. Emons G, Pahwa GS, Brack C, Sturm R, Oberheuser F, Knuppen R: **Gonadotropin releasing hormone binding sites in human epithelial ovarian carcinomata**. *Eur J Cancer Clin Oncol* 1989, **25**(2):215-221.
62. Emons G, Schroder B, Ortmann O, Westphalen S, Schulz KD, Schally AV: **High affinity binding and direct antiproliferative effects of luteinizing hormone-releasing hormone analogs in human endometrial cancer cell lines**. *J Clin Endocrinol Metab* 1993, **77**(6):1458-1464.
63. Emons G, Ortmann O, Teichert HM, Fassl H, Lohrs U, Kullander S, Kauppila A, Ayalon D, Schally A, Oberheuser F: **Luteinizing hormone-releasing hormone agonist triptorelin in combination with cytotoxic chemotherapy in patients with advanced ovarian carcinoma. A prospective double blind randomized trial. Decapeptyl Ovarian Cancer Study Group**. *Cancer* 1996, **78**(7):1452-1460.
64. Emons G, Schulz KD: **Primary and salvage therapy with LH-RH analogues in ovarian cancer**. *Recent Results Cancer Res* 2000, **153**:83-94.
65. Grundker C, Schulz K, Gunthert AR, Emons G: **Luteinizing hormone-releasing hormone induces nuclear factor kappaB-activation and inhibits apoptosis in ovarian cancer cells**. *J Clin Endocrinol Metab* 2000, **85**(10):3815-3820.
66. Grundker C, Volker P, Emons G: **Antiproliferative signaling of luteinizing hormone-releasing hormone in human endometrial and ovarian cancer cells through G protein alpha(I)-mediated activation of phosphotyrosine phosphatase**. *Endocrinology* 2001, **142**(6):2369-2380.
67. Grundker C, Gunthert AR, Millar RP, Emons G: **Expression of gonadotropin-releasing hormone II (GnRH-II) receptor in human endometrial and ovarian cancer cells and effects of GnRH-II on tumor cell proliferation**. *J Clin Endocrinol Metab* 2002, **87**(3):1427-1430.
68. Blankenstein MA, Henkelman MS, Klijn JG: **Direct inhibitory effect of a luteinizing hormone-releasing hormone agonist on MCF-7 human breast cancer cells**. *Eur J Cancer Clin Oncol* 1985, **21**(12):1493-1499.
69. Mullen P, Scott WN, Miller WR: **Growth inhibition observed following administration of an LHRH agonist to a clonal variant of the MCF-7 breast cancer cell line is accompanied by an accumulation of cells in the G0/G1 phase of the cell cycle**. *Br J Cancer* 1991, **63**(6):930-932.
70. Eidne KA, Flanagan CA, Millar RP: **Gonadotropin-releasing hormone binding sites in human breast carcinoma**. *Science* 1985, **229**(4717):989-991.
71. Sharoni Y, Bosin E, Miinster A, Levy J, Schally AV: **Inhibition of growth of human mammary tumor cells by potent antagonists of luteinizing hormone-releasing hormone**. *Proc Natl Acad Sci U S A* 1989, **86**(5):1648-1651.

72. Mangia A, Tommasi S, Reshkin SJ, Simone G, Stea B, Schittulli F, Paradiso A: **Gonadotropin releasing hormone receptor expression in primary breast cancer: comparison of immunohistochemical, radioligand and Western blot analyses**. *Oncol Rep* 2002, **9**(5):1127-1132.
73. Moriya T, Suzuki T, Pilichowska M, Ariga N, Kimura N, Ouchi N, Nagura H, Sasano H: **Immunohistochemical expression of gonadotropin releasing hormone receptor in human breast carcinoma**. *Pathol Int* 2001, **51**(5):333-337.
74. Baumann KH, Kiesel L, Kaufmann M, Bastert G, Runnebaum B: **Characterization of binding sites for a GnRH-agonist (buserelin) in human breast cancer biopsies and their distribution in relation to tumor parameters**. *Breast Cancer Res Treat* 1993, **25**(1):37-46.
75. Fekete M, Wittliff JL, Schally AV: **Characteristics and distribution of receptors for [D-TRP6]-luteinizing hormone-releasing hormone, somatostatin, epidermal growth factor, and sex steroids in 500 biopsy samples of human breast cancer**. *J Clin Lab Anal* 1989, **3**(3):137-147.
76. Chen A, Kaganovsky E, Rahimipour S, Ben-Aroya N, Okon E, Koch Y: **Two forms of gonadotropin-releasing hormone (GnRH) are expressed in human breast tissue and overexpressed in breast cancer: a putative mechanism for the antiproliferative effect of GnRH by down-regulation of acidic ribosomal phosphoproteins P1 and P2**. *Cancer Res* 2002, **62**(4):1036-1044.
77. Saleh-Abady MM, Naderi-Manesh H, Alizadeh A, Shamsipour F, Balalaie S, Arabanian A: **Anticancer activity of a new gonadotropin releasing hormone analogue**. *Biopolymers* 2010, **94**(3):292-297.
78. Grundker C, Fost C, Fister S, Nolte N, Gunthert AR, Emons G: **Gonadotropin-releasing hormone type II antagonist induces apoptosis in MCF-7 and triple-negative MDA-MB-231 human breast cancer cells in vitro and in vivo**. *Breast Cancer Res* 2010, **12**(4):R49.
79. Morgan K, Stewart AJ, Miller N, Mullen P, Muir M, Dodds M, Medda F, Harrison D, Langdon S, Millar RP: **Gonadotropin-releasing hormone receptor levels and cell context affect tumor cell responses to agonist in vitro and in vivo**. *Cancer Res* 2008, **68**(15):6331-6340.
80. Morgan K: **Personal communication**. In.; 2009.
81. Lopez de Maturana R, Pawson AJ, Lu ZL, Davidson L, Maudsley S, Morgan K, Langdon SP, Millar RP: **Gonadotropin-releasing hormone analog structural determinants of selectivity for inhibition of cell growth: support for the concept of ligand-induced selective signaling**. *Mol Endocrinol* 2008, **22**(7):1711-1722.
82. Millar RP, Pawson AJ: **Outside-in and inside-out signaling: the new concept that selectivity of ligand binding at the gonadotropin-releasing hormone receptor is modulated by the intracellular environment**. *Endocrinology* 2004, **145**(8):3590-3593.
83. **Activation cycle of G-proteins by G-protein-coupled receptors, Sven Jähnichen (Accessed 10 Aug 2011)** [http://en.wikipedia.org/wiki/File:GPCR-Zyklus.png]
84. Neves SR, Ram PT, Iyengar R: **G protein pathways**. *Science* 2002, **296**(5573):1636-1639.

85. Hewavitharana T, Wedegaertner PB: **Non-canonical signaling and localizations of heterotrimeric G proteins**. *Cell Signal* 2011, **1**:1.
86. Grosse R, Schmid A, Schoneberg T, Herrlich A, Muhn P, Schultz G, Gudermann T: **Gonadotropin-releasing hormone receptor initiates multiple signaling pathways by exclusively coupling to G(q/11) proteins**. *J Biol Chem* 2000, **275**(13):9193-9200.
87. Limonta P, Moretti RM, Marelli MM, Motta M: **The biology of gonadotropin hormone-releasing hormone: role in the control of tumor growth and progression in humans**. *Front Neuroendocrinol* 2003, **24**(4):279-295.
88. White CD, Coetsee M, Morgan K, Flanagan CA, Millar RP, Lu ZL: **A Crucial Role for G{alpha}q/11, but not G{alpha}i/o or G{alpha}s, in Gonadotropin-Releasing Hormone Receptor-Mediated Cell Growth Inhibition**. *Mol Endocrinol* 2008, **18**:18.
89. Cagnol S, Chambard JC: **ERK and cell death: mechanisms of ERK-induced cell death--apoptosis, autophagy and senescence**. *Febs J* 2010, **277**(1):2-21.
90. Zhuang S, Schnellmann RG: **A death-promoting role for extracellular signal-regulated kinase**. *J Pharmacol Exp Ther* 2006, **319**(3):991-997.
91. Mebratu Y, Tesfaigzi Y: **How ERK1/2 activation controls cell proliferation and cell death: Is subcellular localization the answer?** *Cell Cycle* 2009, **8**(8):1168-1175.
92. Astuti P, Pike T, Widberg C, Payne E, Harding A, Hancock J, Gabrielli B: **MAPK pathway activation delays G2/M progression by destabilizing Cdc25B**. *J Biol Chem* 2009, **284**(49):33781-33788.
93. Dangi S, Chen FM, Shapiro P: **Activation of extracellular signal-regulated kinase (ERK) in G2 phase delays mitotic entry through p21CIP1**. *Cell Prolif* 2006, **39**(4):261-279.
94. Wagner EF, Nebreda AR: **Signal integration by JNK and p38 MAPK pathways in cancer development**. *Nat Rev Cancer* 2009, **9**(8):537-549.
95. Gunthert AR, Grundker C, Olota A, Lasche J, Eicke N, Emons G: **Analogs of GnRH-I and GnRH-II inhibit epidermal growth factor-induced signal transduction and resensitize resistant human breast cancer cells to 4OH-tamoxifen**. *Eur J Endocrinol* 2005, **153**(4):613-625.
96. Levin ER: **Integration of the extranuclear and nuclear actions of estrogen**. *Mol Endocrinol* 2005, **19**(8):1951-1959.
97. Robinson DR, Wu YM, Lin SF: **The protein tyrosine kinase family of the human genome**. *Oncogene* 2000, **19**(49):5548-5557.
98. Zwick E, Bange J, Ullrich A: **Receptor tyrosine kinase signalling as a target for cancer intervention strategies**. *Endocr Relat Cancer* 2001, **8**(3):161-173.
99. Scott WN, Mullen P, Miller WR: **Factors influencing the response of MCF-7 cells to an agonist of luteinising hormone-releasing hormone**. *Eur J Cancer* 1991, **27**(11):1458-1461.
100. Naidich M, Shterntal B, Furman R, Pawson AJ, Jabbour HN, Morgan K, Millar RP, Jia J, Tomic M, Stojilkovic S, Stern N, Naor Z: **Elucidation of mechanisms of the reciprocal cross talk between gonadotropin-releasing**

hormone and prostaglandin receptors. *Endocrinology* 2010, **151**(6):2700-2712.
101. Chaturvedi MM, Sung B, Yadav VR, Kannappan R, Aggarwal BB: **NF-kappaB addiction and its role in cancer: 'one size does not fit all'**. *Oncogene* 2011, **30**(14):1615-1630.
102. Schneider G, Kramer OH: **NFkappaB/p53 crosstalk-a promising new therapeutic target**. *Biochim Biophys Acta* 2011, **1815**(1):90-103.
103. Bubici C, Papa S, Pham CG, Zazzeroni F, Franzoso G: **NF-kappaB and JNK: an intricate affair**. *Cell Cycle* 2004, **3**(12):1524-1529.
104. Anderson L, McGregor A, Cook JV, Chilvers E, Eidne KA: **Rapid desensitization of GnRH-stimulated intracellular signalling events in alpha T3-1 and HEK-293 cells expressing the GnRH receptor**. *Endocrinology* 1995, **136**(11):5228-5231.
105. Anderson L, Milligan G, Eidne KA: **Characterization of the gonadotrophin-releasing hormone receptor in alpha T3-1 pituitary gonadotroph cells**. *J Endocrinol* 1993, **136**(1):51-58.
106. Shah BH, Milligan G: **The gonadotrophin-releasing hormone receptor of alpha T3-1 pituitary cells regulates cellular levels of both of the phosphoinositidase C-linked G proteins, Gq alpha and G11 alpha, equally**. *Mol Pharmacol* 1994, **46**(1):1-7.
107. Fink MY, Pincas H, Choi SG, Nudelman G, Sealfon SC: **Research resource: Gonadotropin-releasing hormone receptor-mediated signaling network in LbetaT2 cells: a pathway-based web-accessible knowledgebase**. *Mol Endocrinol* 2010, **24**(9):1863-1871.
108. Kakar SS, Winters SJ, Zacharias W, Miller DM, Flynn S: **Identification of distinct gene expression profiles associated with treatment of LbetaT2 cells with gonadotropin-releasing hormone agonist using microarray analysis**. *Gene* 2003, **308**:67-77.
109. Wurmbach E, Yuen T, Ebersole BJ, Sealfon SC: **Gonadotropin-releasing hormone receptor-coupled gene network organization**. *J Biol Chem* 2001, **276**(50):47195-47201.
110. Graham FL, Smiley J, Russell WC, Nairn R: **Characteristics of a human cell line transformed by DNA from human adenovirus type 5**. *J Gen Virol* 1977, **36**(1):59-74.
111. Millar R: **Personal Communication**. 2011.
112. Miles LE, Hanyaloglu AC, Dromey JR, Pfleger KD, Eidne KA: **Gonadotropin-releasing hormone receptor-mediated growth suppression of immortalized LbetaT2 gonadotrope and stable HEK293 cell lines**. *Endocrinology* 2004, **145**(1):194-204.
113. Lodwick Na: **Flesh and Bones of Medical Cell Biology**, 1 edn: Mosby; 2007.
114. Manson Ea: **Cell Biology and Genetics**, 3 edn: Mosby; 2008.
115. Malumbres M, Barbacid M: **Cell cycle, CDKs and cancer: a changing paradigm**. *Nat Rev Cancer* 2009, **9**(3):153-166.
116. Davidson L, Pawson AJ, Lopez de Maturana R, Freestone SH, Barran P, Millar RP, Maudsley S: **Gonadotropin-releasing hormone-induced activation of diacylglycerol kinase-zeta and its association with active c-src**. *J Biol Chem* 2004, **279**(12):11906-11916.

117. Davidson L, Pawson AJ, Millar RP, Maudsley S: **Cytoskeletal reorganization dependence of signaling by the gonadotropin-releasing hormone receptor**. *J Biol Chem* 2004, **279**(3):1980-1993.
118. Emons G, Muller V, Ortmann O, Grossmann G, Trautner U, Stuckrad B, Schulz K, Schally A: **Luteinizing hormone-releasing hormone agonist triptorelin antagonizes signal transduction and mitogenic activity of epidermal growth factor in human ovarian and endometrial cancer cell lines**. *Int J Oncol* 1996, **9**(6):1129-1137.
119. Mullen P, Bramley T, Menzies G, Miller B: **Failure to detect gonadotrophin-releasing hormone receptors in human benign and malignant breast tissue and in MCF-7 and MDA-MB-231 cancer cells**. *Eur J Cancer* 1993, **29A**(2):248-252.
120. Harris N, Dutlow C, Eidne K, Dong KW, Roberts J, Millar R: **Gonadotropin-releasing hormone gene expression in MDA-MB-231 and ZR-75-1 breast carcinoma cell lines**. *Cancer Res* 1991, **51**(10):2577-2581.
121. Sedgley KR, Finch AR, Caunt CJ, McArdle CA: **Intracellular gonadotropin-releasing hormone receptors in breast cancer and gonadotrope lineage cells**. *J Endocrinol* 2006, **191**(3):625-636.
122. Vrecl M, Anderson L, Hanyaloglu A, McGregor AM, Groarke AD, Milligan G, Taylor PL, Eidne KA: **Agonist-induced endocytosis and recycling of the gonadotropin-releasing hormone receptor: effect of beta-arrestin on internalization kinetics**. *Mol Endocrinol* 1998, **12**(12):1818-1829.
123. Kim LS, Kim JH: **Heat shock protein as molecular targets for breast cancer therapeutics**. *J Breast Cancer*, **14**(3):167-174.
124. Spurrier B, Ramalingam S, Nishizuka S: **Reverse-phase protein lysate microarrays for cell signaling analysis**. *Nat Protoc* 2008, **3**(11):1796-1808.
125. **NanoDrop 2000 User Manual** [http://www.nanodrop.com/Library/NanoDrop%202000%20User%20Manual.pdf]
126. **Illumina** [www.illumina.com]
127. Sims AH, Smethurst GJ, Hey Y, Okoniewski MJ, Pepper SD, Howell A, Miller CJ, Clarke RB: **The removal of multiplicative, systematic bias allows integration of breast cancer gene expression datasets - improving meta-analysis and prediction of prognosis**. *BMC Med Genomics* 2008, **1**(42):42.
128. Leek JT, Scharpf RB, Bravo HC, Simcha D, Langmead B, Johnson WE, Geman D, Baggerly K, Irizarry RA: **Tackling the widespread and critical impact of batch effects in high-throughput data**. *Nat Rev Genet* 2010, **11**(10):733-739.
129. **NCBI Database** [http://www.ncbi.nlm.nih.gov]
130. Dunning MJ, Smith ML, Ritchie ME, Tavare S: **beadarray: R classes and methods for Illumina bead-based data**. *Bioinformatics* 2007, **23**(16):2183-2184.
131. **The R Project for Statistical Computing (Accessed 2009)** [http://www.r-project.org/]
132. Ihaka R GR: **R: a language for data analysis and graphics.** *Journal of Computational and Graphical Statistics* 1996, **5**:299-314.
133. **Bioconductor (Accessed 2009-2010)** [http://www.bioconductor.org/]

134. Gentleman RC, Carey VJ, Bates DM, Bolstad B, Dettling M, Dudoit S, Ellis B, Gautier L, Ge Y, Gentry J, Hornik K, Hothorn T, Huber W, Iacus S, Irizarry R, Leisch F, Li C, Maechler M, Rossini AJ, Sawitzki G, Smith C, Smyth G, Tierney L, Yang JY, Zhang J: **Bioconductor: open software development for computational biology and bioinformatics**. *Genome Biol* 2004, **5**(10):R80.
135. Breitling R, Armengaud P, Amtmann A, Herzyk P: **Rank products: a simple, yet powerful, new method to detect differentially regulated genes in replicated microarray experiments**. *FEBS Lett* 2004, **573**(1-3):83-92.
136. **Cluster and Treeview Manual, Eisen (Accessed 25 August 2010)** [http://rana.lbl.gov/manuals/ClusterTreeView.pdf]
137. Huang da W, Sherman BT, Lempicki RA: **Systematic and integrative analysis of large gene lists using DAVID bioinformatics resources**. *Nat Protoc* 2009, **4**(1):44-57.
138. Huckle WR, Conn PM: **Use of lithium ion in measurement of stimulated pituitary inositol phospholipid turnover**. *Methods Enzymol* 1987, **141**:149-155.
139. Liotta LA, Espina V, Mehta AI, Calvert V, Rosenblatt K, Geho D, Munson PJ, Young L, Wulfkuhle J, Petricoin EF, 3rd: **Protein microarrays: meeting analytical challenges for clinical applications**. *Cancer Cell* 2003, **3**(4):317-325.
140. Kononen J, Bubendorf L, Kallioniemi A, Barlund M, Schraml P, Leighton S, Torhorst J, Mihatsch MJ, Sauter G, Kallioniemi OP: **Tissue microarrays for high-throughput molecular profiling of tumor specimens**. *Nat Med* 1998, **4**(7):844-847.
141. Somner JE, Dixon JM, Thomas JS: **Node retrieval in axillary lymph node dissections: recommendations for minimum numbers to be confident about node negative status**. *J Clin Pathol* 2004, **57**(8):845-848.
142. Camp RL, Chung GG, Rimm DL: **Automated subcellular localization and quantification of protein expression in tissue microarrays**. *Nat Med* 2002, **8**(11):1323-1327.
143. Langdon S: **Personal communication**. In.; 2008.
144. Qvarnstrom OF, Simonsson M, Eriksson V, Turesson I, Carlsson J: **gammaH2AX and cleaved PARP-1 as apoptotic markers in irradiated breast cancer BT474 cellular spheroids**. *Int J Oncol* 2009, **35**(1):41-47.
145. Goto H, Tomono Y, Ajiro K, Kosako H, Fujita M, Sakurai M, Okawa K, Iwamatsu A, Okigaki T, Takahashi T, Inagaki M: **Identification of a novel phosphorylation site on histone H3 coupled with mitotic chromosome condensation**. *J Biol Chem* 1999, **274**(36):25543-25549.
146. Hendzel MJ, Wei Y, Mancini MA, Van Hooser A, Ranalli T, Brinkley BR, Bazett-Jones DP, Allis CD: **Mitosis-specific phosphorylation of histone H3 initiates primarily within pericentromeric heterochromatin during G2 and spreads in an ordered fashion coincident with mitotic chromosome condensation**. *Chromosoma* 1997, **106**(6):348-360.
147. Preuss U, Landsberg G, Scheidtmann KH: **Novel mitosis-specific phosphorylation of histone H3 at Thr11 mediated by Dlk/ZIP kinase**. *Nucleic Acids Res* 2003, **31**(3):878-885.

148. Nicholson DW, Ali A, Thornberry NA, Vaillancourt JP, Ding CK, Gallant M, Gareau Y, Griffin PR, Labelle M, Lazebnik YA, et al.: **Identification and inhibition of the ICE/CED-3 protease necessary for mammalian apoptosis**. *Nature* 1995, **376**(6535):37-43.
149. Gunthert AR, Grundker C, Hollmann K, Emons G: **Luteinizing hormone-releasing hormone induces JunD-DNA binding and extends cell cycle in human ovarian cancer cells**. *Biochem Biophys Res Commun* 2002, **294**(1):11-15.
150. Bratt A, Birot O, Sinha I, Veitonmaki N, Aase K, Ernkvist M, Holmgren L: **Angiomotin regulates endothelial cell-cell junctions and cell motility**. *J Biol Chem* 2005, **280**(41):34859-34869.
151. **GeneCards Database (Accessed April 2011)** [http://www.genecards.org/]
152. Ogata S, Morokuma J, Hayata T, Kolle G, Niehrs C, Ueno N, Cho KW: **TGF-beta signaling-mediated morphogenesis: modulation of cell adhesion via cadherin endocytosis**. *Genes Dev* 2007, **21**(14):1817-1831.
153. Karaulanov EE, Bottcher RT, Niehrs C: **A role for fibronectin-leucine-rich transmembrane cell-surface proteins in homotypic cell adhesion**. *EMBO Rep* 2006, **7**(3):283-290.
154. Kikkawa Y, Sudo R, Kon J, Mizuguchi T, Nomizu M, Hirata K, Mitaka T: **Laminin alpha 5 mediates ectopic adhesion of hepatocellular carcinoma through integrins and/or Lutheran/basal cell adhesion molecule**. *Exp Cell Res* 2008, **314**(14):2579-2590.
155. Nakashima Y, Nishimura S, Maeda A, Barsoumian EL, Hakamata Y, Nakai J, Allen PD, Imoto K, Kita T: **Molecular cloning and characterization of a human brain ryanodine receptor**. *FEBS Lett* 1997, **417**(1):157-162.
156. Kireeva ML, Mo FE, Yang GP, Lau LF: **Cyr61, a product of a growth factor-inducible immediate-early gene, promotes cell proliferation, migration, and adhesion**. *Mol Cell Biol* 1996, **16**(4):1326-1334.
157. Pi L, Ding X, Jorgensen M, Pan JJ, Oh SH, Pintilie D, Brown A, Song WY, Petersen BE: **Connective tissue growth factor with a novel fibronectin binding site promotes cell adhesion and migration during rat oval cell activation**. *Hepatology* 2008, **47**(3):996-1004.
158. Salisbury TB, Binder AK, Nilson JH: **Welcoming beta-catenin to the gonadotropin-releasing hormone transcriptional network in gonadotropes**. *Mol Endocrinol* 2008, **22**(6):1295-1303.
159. Armstrong SP, Caunt CJ, Fowkes RC, Tsaneva-Atanasova K, McArdle CA: **Pulsatile and sustained gonadotropin-releasing hormone (GnRH) receptor signaling: does the ERK signaling pathway decode GnRH pulse frequency?** *J Biol Chem* 2010, **285**(32):24360-24371.
160. Armstrong SP, Caunt CJ, McArdle CA: **Gonadotropin-releasing hormone and protein kinase C signaling to ERK: spatiotemporal regulation of ERK by docking domains and dual-specificity phosphatases**. *Mol Endocrinol* 2009, **23**(4):510-519.
161. Kehrl JH, Sinnarajah S: **RGS2: a multifunctional regulator of G-protein signaling**. *Int J Biochem Cell Biol* 2002, **34**(5):432-438.
162. Ferris HA, Shupnik MA: **Mechanisms for pulsatile regulation of the gonadotropin subunit genes by GNRH1**. *Biol Reprod* 2006, **74**(6):993-998.

163. Cunningham ML, Waldo GL, Hollinger S, Hepler JR, Harden TK: **Protein kinase C phosphorylates RGS2 and modulates its capacity for negative regulation of Galpha 11 signaling**. *J Biol Chem* 2001, **276**(8):5438-5444.
164. Salisbury TB, Binder AK, Grammer JC, Nilson JH: **Maximal activity of the luteinizing hormone beta-subunit gene requires beta-catenin**. *Mol Endocrinol* 2007, **21**(4):963-971.
165. Gardner S, Maudsley S, Millar RP, Pawson AJ: **Nuclear stabilization of beta-catenin and inactivation of glycogen synthase kinase-3beta by gonadotropin-releasing hormone: targeting Wnt signaling in the pituitary gonadotrope**. *Mol Endocrinol* 2007, **21**(12):3028-3038.
166. Ramos HJ, Gale M, Jr.: **RIG-I Like Receptors and Their Signaling Crosstalk in the Regulation of Antiviral Immunity**. *Curr Opin Virol* 2011, **1**(3):167-176.
167. Saleh M: **The machinery of Nod-like receptors: refining the paths to immunity and cell death**. *Immunol Rev* 2011, **243**(1):235-246.
168. Schwanbeck R, Martini S, Bernoth K, Just U: **The Notch signaling pathway: molecular basis of cell context dependency**. *Eur J Cell Biol* 2011, **90**(6-7):572-581.
169. Lobry C, Oh P, Aifantis I: **Oncogenic and tumor suppressor functions of Notch in cancer: it's NOTCH what you think**. *J Exp Med* 2011, **208**(10):1931-1935.
170. Taylor SS, Ha E, McKeon F: **The human homologue of Bub3 is required for kinetochore localization of Bub1 and a Mad3/Bub1-related protein kinase**. *J Cell Biol* 1998, **142**(1):1-11.
171. Lo KW, Kogoy JM, Pfister KK: **The DYNLT3 light chain directly links cytoplasmic dynein to a spindle checkpoint protein, Bub3**. *J Biol Chem* 2007, **282**(15):11205-11212.
172. Zhu N, Shao Y, Xu L, Yu L, Sun L: **Gadd45-alpha and Gadd45-gamma utilize p38 and JNK signaling pathways to induce cell cycle G2/M arrest in Hep-G2 hepatoma cells**. *Mol Biol Rep* 2009, **36**(8):2075-2085.
173. Cho HJ, Park SM, Hwang EM, Baek KE, Kim IK, Nam IK, Im MJ, Park SH, Bae S, Park JY, Yoo J: **Gadd45b mediates Fas-induced apoptosis by enhancing the interaction between p38 and retinoblastoma tumor suppressor**. *J Biol Chem* 2010, **285**(33):25500-25505.
174. Gentile M, Latonen L, Laiho M: **Cell cycle arrest and apoptosis provoked by UV radiation-induced DNA damage are transcriptionally highly divergent responses**. *Nucleic Acids Res* 2003, **31**(16):4779-4790.
175. Montagnoli A, Guardavaccaro D, Starace G, Tirone F: **Overexpression of the nerve growth factor-inducible PC3 immediate early gene is associated with growth inhibition**. *Cell Growth Differ* 1996, **7**(10):1327-1336.
176. Guardavaccaro D, Corrente G, Covone F, Micheli L, D'Agnano I, Starace G, Caruso M, Tirone F: **Arrest of G(1)-S progression by the p53-inducible gene PC3 is Rb dependent and relies on the inhibition of cyclin D1 transcription**. *Mol Cell Biol* 2000, **20**(5):1797-1815.
177. Hummer S, Mayer TU: **Cdk1 negatively regulates midzone localization of the mitotic kinesin Mklp2 and the chromosomal passenger complex**. *Curr Biol* 2009, **19**(7):607-612.

178. Kimura A, Ohmichi M, Kurachi H, Ikegami H, Hayakawa J, Tasaka K, Kanda Y, Nishio Y, Jikihara H, Matsuura N, Murata Y: **Role of mitogen-activated protein kinase/extracellular signal-regulated kinase cascade in gonadotropin-releasing hormone-induced growth inhibition of a human ovarian cancer cell line**. *Cancer Res* 1999, **59**(20):5133-5142.
179. Nguyen KA, Intriago RE, Upadhyay HC, Santos SJ, Webster NJ, Lawson MA: **Modulation of gonadotropin-releasing hormone-induced extracellular signal-regulated kinase activation by dual-specificity protein phosphatase 1 in LbetaT2 gonadotropes**. *Endocrinology* 2010, **151**(10):4882-4893.
180. Dobkin-Bekman M, Naidich M, Pawson AJ, Millar RP, Seger R, Naor Z: **Activation of mitogen-activated protein kinase (MAPK) by GnRH is cell-context dependent**. *Mol Cell Endocrinol* 2006, **252**(1-2):184-190.
181. Farshori PQ, Shah BH, Arora KK, Martinez-Fuentes A, Catt KJ: **Activation and nuclear translocation of PKCdelta, Pyk2 and ERK1/2 by gonadotropin releasing hormone in HEK293 cells**. *J Steroid Biochem Mol Biol* 2003, **85**(2-5):337-347.
182. Kanehisa M, Goto S, Furumichi M, Tanabe M, Hirakawa M: **KEGG for representation and analysis of molecular networks involving diseases and drugs**. *Nucleic Acids Res* 2010, **38**(Database issue):D355-360.
183. Kanehisa M, Goto S, Hattori M, Aoki-Kinoshita KF, Itoh M, Kawashima S, Katayama T, Araki M, Hirakawa M: **From genomics to chemical genomics: new developments in KEGG**. *Nucleic Acids Res* 2006, **34**(Database issue):D354-357.
184. Kanehisa M, Goto S: **KEGG: kyoto encyclopedia of genes and genomes**. *Nucleic Acids Res* 2000, **28**(1):27-30.
185. Jessus C, Ozon R: **Function and regulation of cdc25 protein phosphate through mitosis and meiosis**. *Prog Cell Cycle Res* 1995, **1**:215-228.
186. Kumagai A, Dunphy WG: **Binding of 14-3-3 proteins and nuclear export control the intracellular localization of the mitotic inducer Cdc25**. *Genes Dev* 1999, **13**(9):1067-1072.
187. Peng CY, Graves PR, Thoma RS, Wu Z, Shaw AS, Piwnica-Worms H: **Mitotic and G2 checkpoint control: regulation of 14-3-3 protein binding by phosphorylation of Cdc25C on serine-216**. *Science* 1997, **277**(5331):1501-1505.
188. Furnari B, Blasina A, Boddy MN, McGowan CH, Russell P: **Cdc25 inhibited in vivo and in vitro by checkpoint kinases Cds1 and Chk1**. *Mol Biol Cell* 1999, **10**(4):833-845.
189. Blasina A, de Weyer IV, Laus MC, Luyten WH, Parker AE, McGowan CH: **A human homologue of the checkpoint kinase Cds1 directly inhibits Cdc25 phosphatase**. *Curr Biol* 1999, **9**(1):1-10.
190. Lee CH, Chung JH: **The hCds1 (Chk2)-FHA domain is essential for a chain of phosphorylation events on hCds1 that is induced by ionizing radiation**. *J Biol Chem* 2001, **276**(32):30537-30541.
191. Ito T, Deng X, Carr B, May WS: **Bcl-2 phosphorylation required for anti-apoptosis function**. *J Biol Chem* 1997, **272**(18):11671-11673.

192. Huang ST, Cidlowski JA: **Phosphorylation status modulates Bcl-2 function during glucocorticoid-induced apoptosis in T lymphocytes**. *Faseb J* 2002, **16**(8):825-832.
193. Tan Y, Demeter MR, Ruan H, Comb MJ: **BAD Ser-155 phosphorylation regulates BAD/Bcl-XL interaction and cell survival**. *J Biol Chem* 2000, **275**(33):25865-25869.
194. Yan Y, Spieker RS, Kim M, Stoeger SM, Cowan KH: **BRCA1-mediated G2/M cell cycle arrest requires ERK1/2 kinase activation**. *Oncogene* 2005, **24**(20):3285-3296.
195. Barboule N, Lafon C, Chadebech P, Vidal S, Valette A: **Involvement of p21 in the PKC-induced regulation of the G2/M cell cycle transition**. *FEBS Lett* 1999, **444**(1):32-37.
196. Manning BD, Cantley LC: **AKT/PKB signaling: navigating downstream**. *Cell* 2007, **129**(7):1261-1274.
197. Iyer AK, Azad N, Talbot S, Stehlik C, Lu B, Wang L, Rojanasakul Y: **Antioxidant c-FLIP Inhibits Fas Ligand-Induced NF-{kappa}B Activation in a Phosphatidylinositol 3-Kinase/Akt-Dependent Manner**. *J Immunol* 2011, **187**(6):3256-3266.
198. Cardone MH, Roy N, Stennicke HR, Salvesen GS, Franke TF, Stanbridge E, Frisch S, Reed JC: **Regulation of cell death protease caspase-9 by phosphorylation**. *Science* 1998, **282**(5392):1318-1321.
199. Brunet A, Bonni A, Zigmond MJ, Lin MZ, Juo P, Hu LS, Anderson MJ, Arden KC, Blenis J, Greenberg ME: **Akt promotes cell survival by phosphorylating and inhibiting a Forkhead transcription factor**. *Cell* 1999, **96**(6):857-868.
200. Zimmermann S, Moelling K: **Phosphorylation and regulation of Raf by Akt (protein kinase B)**. *Science* 1999, **286**(5445):1741-1744.
201. Gesbert F, Sellers WR, Signoretti S, Loda M, Griffin JD: **BCR/ABL regulates expression of the cyclin-dependent kinase inhibitor p27Kip1 through the phosphatidylinositol 3-Kinase/AKT pathway**. *J Biol Chem* 2000, **275**(50):39223-39230.
202. Zhou BP, Liao Y, Xia W, Spohn B, Lee MH, Hung MC: **Cytoplasmic localization of p21Cip1/WAF1 by Akt-induced phosphorylation in HER-2/neu-overexpressing cells**. *Nat Cell Biol* 2001, **3**(3):245-252.
203. Diehl JA, Cheng M, Roussel MF, Sherr CJ: **Glycogen synthase kinase-3beta regulates cyclin D1 proteolysis and subcellular localization**. *Genes Dev* 1998, **12**(22):3499-3511.
204. Inoki K, Li Y, Zhu T, Wu J, Guan KL: **TSC2 is phosphorylated and inhibited by Akt and suppresses mTOR signalling**. *Nat Cell Biol* 2002, **4**(9):648-657.
205. Manning BD, Tee AR, Logsdon MN, Blenis J, Cantley LC: **Identification of the tuberous sclerosis complex-2 tumor suppressor gene product tuberin as a target of the phosphoinositide 3-kinase/akt pathway**. *Mol Cell* 2002, **10**(1):151-162.
206. Sarbassov DD, Guertin DA, Ali SM, Sabatini DM: **Phosphorylation and regulation of Akt/PKB by the rictor-mTOR complex**. *Science* 2005, **307**(5712):1098-1101.

207. Jacinto E, Facchinetti V, Liu D, Soto N, Wei S, Jung SY, Huang Q, Qin J, Su B: **SIN1/MIP1 maintains rictor-mTOR complex integrity and regulates Akt phosphorylation and substrate specificity**. *Cell* 2006, **127**(1):125-137.
208. Ballou LM, Chattopadhyay M, Li Y, Scarlata S, Lin RZ: **Galphaq binds to p110alpha/p85alpha phosphoinositide 3-kinase and displaces Ras**. *Biochem J* 2006, **394**(Pt 3):557-562.
209. Ballou LM, Lin HY, Fan G, Jiang YP, Lin RZ: **Activated G alpha q inhibits p110 alpha phosphatidylinositol 3-kinase and Akt**. *J Biol Chem* 2003, **278**(26):23472-23479.
210. Hahn-Windgassen A, Nogueira V, Chen CC, Skeen JE, Sonenberg N, Hay N: **Akt activates the mammalian target of rapamycin by regulating cellular ATP level and AMPK activity**. *J Biol Chem* 2005, **280**(37):32081-32089.
211. Arvisais EW, Romanelli A, Hou X, Davis JS: **AKT-independent phosphorylation of TSC2 and activation of mTOR and ribosomal protein S6 kinase signaling by prostaglandin F2alpha**. *J Biol Chem* 2006, **281**(37):26904-26913.
212. Straus DS, Pascual G, Li M, Welch JS, Ricote M, Hsiang CH, Sengchanthalangsy LL, Ghosh G, Glass CK: **15-deoxy-delta 12,14-prostaglandin J2 inhibits multiple steps in the NF-kappa B signaling pathway**. *Proc Natl Acad Sci U S A* 2000, **97**(9):4844-4849.
213. Kucharczak J, Simmons MJ, Fan Y, Gelinas C: **To be, or not to be: NF-kappaB is the answer--role of Rel/NF-kappaB in the regulation of apoptosis**. *Oncogene* 2003, **22**(56):8961-8982.
214. Michalik L, Auwerx J, Berger JP, Chatterjee VK, Glass CK, Gonzalez FJ, Grimaldi PA, Kadowaki T, Lazar MA, O'Rahilly S, Palmer CN, Plutzky J, Reddy JK, Spiegelman BM, Staels B, Wahli W: **International Union of Pharmacology. LXI. Peroxisome proliferator-activated receptors**. *Pharmacol Rev* 2006, **58**(4):726-741.
215. Maekawa N, Hiramoto M, Sakamoto S, Azuma M, Ito T, Ikeda M, Naitou M, Acharya HP, Kobayashi Y, Suematsu M, Handa H, Imai T: **High-performance affinity purification for identification of 15-deoxy-Delta 12,14 -PGJ interacting factors using magnetic nanobeads**. *Biomed Chromatogr* 2011, **25**(4):466-471.
216. Scher JU, Pillinger MH: **15d-PGJ2: the anti-inflammatory prostaglandin?** *Clin Immunol* 2005, **114**(2):100-109.
217. Sica G, Iacopino F, Marini L, Robustelli della Cuna G: **Antiproliferative effect of leuprorelin acetate, alone or combined with tamoxifen or medroxyprogesterone acetate, on human breast cancer cell lines**. *Clin Ther* 1992, **14 Suppl A**:87-96.
218. Neve RM, Chin K, Fridlyand J, Yeh J, Baehner FL, Fevr T, Clark L, Bayani N, Coppe JP, Tong F, Speed T, Spellman PT, DeVries S, Lapuk A, Wang NJ, Kuo WL, Stilwell JL, Pinkel D, Albertson DG, Waldman FM, McCormick F, Dickson RB, Johnson MD, Lippman M, Ethier S, Gazdar A, Gray JW: **A collection of breast cancer cell lines for the study of functionally distinct cancer subtypes**. *Cancer Cell* 2006, **10**(6):515-527.
219. Hall RE, Birrell SN, Tilley WD, Sutherland RL: **MDA-MB-453, an androgen-responsive human breast carcinoma cell line with high level androgen receptor expression**. *Eur J Cancer* 1994, **30A**(4):484-490.

220. Subik K, Lee JF, Baxter L, Strzepek T, Costello D, Crowley P, Xing L, Hung MC, Bonfiglio T, Hicks DG, Tang P: **The Expression Patterns of ER, PR, HER2, CK5/6, EGFR, Ki-67 and AR by Immunohistochemical Analysis in Breast Cancer Cell Lines**. *Breast Cancer (Auckl)* 2010, **4**:35-41.
221. Doane AS, Danso M, Lal P, Donaton M, Zhang L, Hudis C, Gerald WL: **An estrogen receptor-negative breast cancer subset characterized by a hormonally regulated transcriptional program and response to androgen**. *Oncogene* 2006, **25**(28):3994-4008.
222. Robinson JL, Macarthur S, Ross-Innes CS, Tilley WD, Neal DE, Mills IG, Carroll JS: **Androgen receptor driven transcription in molecular apocrine breast cancer is mediated by FoxA1**. *Embo J* 2011, **30**(15):3019-3027.
223. Re M, Pampillo M, Savard M, Dubuc C, McArdle CA, Millar RP, Conn PM, Gobeil F, Jr., Bhattacharya M, Babwah AV: **The human gonadotropin releasing hormone type I receptor is a functional intracellular GPCR expressed on the nuclear membrane**. *PLoS One* 2010, **5**(7):e11489.
224. Finch AR, Sedgley KR, Caunt CJ, McArdle CA: **Plasma membrane expression of GnRH receptors: regulation by antagonists in breast, prostate, and gonadotrope cell lines**. *J Endocrinol* 2008, **196**(2):353-367.
225. Fost C, Duwe F, Hellriegel M, Schweyer S, Emons G, Grundker C, Fister S, Nolte N, Gunthert AR: **Targeted chemotherapy for triple-negative breast cancers via LHRH receptor**. *Oncol Rep* 2011, **25**(5):1481-1487.
226. Kahan Z, Nagy A, Schally AV, Halmos G, Arencibia JM, Groot K: **Administration of a targeted cytotoxic analog of luteinizing hormone-releasing hormone inhibits growth of estrogen-independent MDA-MB-231 human breast cancers in nude mice**. *Breast Cancer Res Treat* 2000, **59**(3):255-262.
227. Finch AR, Caunt CJ, Armstrong SP, McArdle CA: **Plasma membrane expression of gonadotropin-releasing hormone receptors: regulation by peptide and nonpeptide antagonists**. *Mol Endocrinol* 2010, **24**(2):423-435.
228. Wu G, Xing M, Mambo E, Huang X, Liu J, Guo Z, Chatterjee A, Goldenberg D, Gollin SM, Sukumar S, Trink B, Sidransky D: **Somatic mutation and gain of copy number of PIK3CA in human breast cancer**. *Breast Cancer Res* 2005, **7**(5):R609-616.
229. Dupont J, Le Roith D: **Insulin-like growth factor 1 and oestradiol promote cell proliferation of MCF-7 breast cancer cells: new insights into their synergistic effects**. *Mol Pathol* 2001, **54**(3):149-154.
230. Lai A, Sarcevic B, Prall OW, Sutherland RL: **Insulin/insulin-like growth factor-I and estrogen cooperate to stimulate cyclin E-Cdk2 activation and cell Cycle progression in MCF-7 breast cancer cells through differential regulation of cyclin E and p21(WAF1/Cip1)**. *J Biol Chem* 2001, **276**(28):25823-25833.
231. Mukohara T, Shimada H, Ogasawara N, Wanikawa R, Shimomura M, Nakatsura T, Ishii G, Park JO, Janne PA, Saijo N, Minami H: **Sensitivity of breast cancer cell lines to the novel insulin-like growth factor-1 receptor (IGF-1R) inhibitor NVP-AEW541 is dependent on the level of IRS-1 expression**. *Cancer Lett* 2009, **282**(1):14-24.
232. Calbiochem: **PI3Kγ inhibitor #528106**. In.; 2010.

233. Bartucci M, Morelli C, Mauro L, Ando S, Surmacz E: **Differential insulin-like growth factor I receptor signaling and function in estrogen receptor (ER)-positive MCF-7 and ER-negative MDA-MB-231 breast cancer cells**. *Cancer Res* 2001, **61**(18):6747-6754.
234. Kahlert S, Nuedling S, van Eickels M, Vetter H, Meyer R, Grohe C: **Estrogen receptor alpha rapidly activates the IGF-1 receptor pathway**. *J Biol Chem* 2000, **275**(24):18447-18453.
235. Song RX, Zhang Z, Chen Y, Bao Y, Santen RJ, Kahlert S, Nuedling S, van Eickels M, Vetter H, Meyer R, Grohe C: **Estrogen signaling via a linear pathway involving insulin-like growth factor I receptor, matrix metalloproteinases, and epidermal growth factor receptor to activate mitogen-activated protein kinase in MCF-7 breast cancer cells**. *Endocrinology* 2007, **148**(8):4091-4101.
236. Surmacz E, Bartucci M: **Role of estrogen receptor alpha in modulating IGF-I receptor signaling and function in breast cancer**. *J Exp Clin Cancer Res* 2004, **23**(3):385-394.
237. Ahmad T, Farnie G, Bundred NJ, Anderson NG: **The mitogenic action of insulin-like growth factor I in normal human mammary epithelial cells requires the epidermal growth factor receptor tyrosine kinase**. *J Biol Chem* 2004, **279**(3):1713-1719.
238. Manavathi B, Acconcia F, Rayala SK, Kumar R: **An inherent role of microtubule network in the action of nuclear receptor**. *Proc Natl Acad Sci U S A* 2006, **103**(43):15981-15986.
239. Zhang Y, Moerkens M, Ramaiahgari S, de Bont H, Price L, Meerman J, van de Water B: **Elevated insulin-like growth factor 1 receptor signaling induces antiestrogen resistance through the MAPK/ERK and PI3K/Akt signaling routes**. *Breast Cancer Res* 2011, **13**(3):R52.
240. Driggers PH, Segars JH: **Estrogen action and cytoplasmic signaling pathways. Part II: the role of growth factors and phosphorylation in estrogen signaling**. *Trends Endocrinol Metab* 2002, **13**(10):422-427.
241. Golebiewska U, Scarlata S: **Galphaq binds two effectors separately in cells: evidence for predetermined signaling pathways**. *Biophys J* 2008, **95**(5):2575-2582.

Appendix A

6 Appendix A

14-3-3 ζ(Ab-58)	JunB(Phospho-Ser259)
14-3-3 ζ(Phospho-Phospho-Ser58)	JunB(Phospho-Ser79)
4E-BP1(Ab-36)	JunD(Ab-255)
4E-BP1(Phospho-Thr36)	JunD(Phospho-Ser255)
Akt(Ab-308)	Keratin 18(Ab-33)
Akt(Ab-473)	Keratin 18(Phospho-Phospho-Ser33)
Akt(Phospho-Ser473)	MEK1(Ab-217)
Akt(Phospho-Thr308)	MEK1(Ab-221)
Akt2(Ab-474)	MEK1(Ab-291)
Akt2(Phospho-Ser474)	MEK1(Phospho-Ser217)
AMPK1(Ab-174)	MEK1(Phospho-Ser221)
AMPK1(Phospho-Phospho-Thr174)	MEK1(Phospho-Thr291)
ATM(Ab-1981)	MEK-2(Ab-394)
BAD(Ab-112)	MEK-2(Phospho-Thr394)
BAD(Ab-136)	Met(Ab-1349)
BAD(Ab-155)	Met(Phospho-Tyr1349)
BAD(Phospho-Ser112)	MKK3(Ab-189)
BAD(Phospho-Ser136)	MKK3(Phospho-Ser189)
BAD(Phospho-Ser155)	MSK1(Ab-376)
BCL-2(Ab-56)	MSK1(Phospho-Ser376)
BCL-2(Ab-70)	mTOR(Ab-2448)
BCL-2(Phospho-Ser70)	mTOR(Phospho-Ser2448)
BCL-2(Phospho-Thr56)	Myc(Ab-358)
BCL-XL(Ab-62)	Myc(Ab-373)
BCL-XL(Phospho-Ser62)	Myc(Ab-58)
BRCA1(Ab-1423)	Myc(Ab-62)
BRCA1(Ab-1524)	Myc(Phospho-Phospho-Ser62)
BRCA1(Phospho-Ser1423)	Myc(Phospho-Ser373)
BRCA1(Phospho-Ser1524)	Myc(Phospho-Thr358)
CaMKII (Ab-286)	Myc(Phospho-Thr58)
CaMKII (Phospho-Thr286)	NFκB-p100/p52(Ab-865)
Caveolin-1(Ab-14)	NFκB-p100/p52(Ab-869)
Caveolin-1(Phospho-Tyr14)	NFκB-p100/p52(Phospho-Ser869)
CDC2(Ab-15)	NFκB-p105/p50(Ab-337)
CDC2(Phospho-Tyr15)	NFκB-p105/p50(Ab-337)
cdc25A (Ab-75)	NFκB-p105/p50(Ab-893)
cdc25A (Phospho-Ser75)	NFκB-p105/p50(Ab-907)
cdc25C(Ab-216)	NFκB-p105/p50(Phospho-Ser893)
cdc25C(Phospho-Ser216)	NFκB-p105/p50(Phospho-Ser907)
CDK2(Ab-160)	NFκB-p105/p50(Phospho-Ser932)
CDK2(Phospho-Thr160)	NFκB-p65(Ab-254)
Chk1(Ab-280)	NFκB-p65(Ab-529)
Chk1(Ab-317)	NFκB-p65(Phospho-Ser529)
Chk1(Ab-345)	NFκB-p65(Phospho-Thr254)
Chk1(Phospho-Ser280)	p21Cip1(Ab-145)

Chk1(Phospho-Ser317)	p21Cip1(Phospho-Thr145)
Chk1(Phospho-Ser345)	p27Kip1(Ab-10)
Chk2(Ab-516)	p27Kip1(Ab-187)
Chk2(Ab-68)	p27Kip1(Phospho-Ser10)
Chk2(Phospho-Ser516)	p27Kip1(Phospho-Thr187)
Chk2(Phospho-Thr68)	P38 MAPK(Ab-182)
c-Jun (Phospho-Thr239)	P38 MAPK(Phospho-Thr180)
c-Jun(Ab-239)	P38 MAPK(Phospho-Tyr182)
c-Jun(Ab-243)	p44/42 MAP Kinase(Ab-202)
c-Jun(Ab-73)	p44/42 MAP Kinase(Ab-204)
c-Jun(Phospho-Ser243)	p44/42 MAP Kinase(Phospho-Thr202)
c-Jun(Phospho-Ser73)	p44/42 MAP Kinase(Phospho-Tyr204)
c-Kit(Ab-721)	p53(Ab-315)
c-Kit(Phospho-Tyr721)	p53(Ab-6)
CREB(Ab-133)	p53(Phospho-Ser315)
CREB(Phospho-Ser133)	p53(Phospho-Ser6)
CrkII(Ab-221)	p70 S6 Kinase (Ab-424)
CrkII(Phospho-Phospho-Tyr221)	p70 S6 Kinase (Phospho-Ser424)
eEF2K(Ab-366)	PDGF Receptor β(Ab-751)
eEF2K(Phospho-Phospho-Ser366)	PDGF Receptor β(Phospho-Tyr751)
EGFR(Ab-1110)	PDK1(Ab-241)
EGFR(Phospho-Tyr1110)	PDK1(Phospho-Ser241)
eIF2α(Ab-51)	PTEN(Ab-380/382/383)
eIF2α(Phospho-Ser51)	PTEN(Phospho-Ser380/Phospho-Thr382/Phospho-Thr383)
eIF4E(Ab-209)	Pyk2(Ab-402)
eIF4E(Phospho-Ser209)	Pyk2(Phospho-Tyr402)
Elk-1(Ab-383)	Rac1/cdc42(Ab-71)
Elk-1(Phospho-Ser383)	Rac1/cdc42(Phospho-Ser71)
Estrogen Receptor-α (Ab-167)	Raf1(Ab-259)
Estrogen Receptor-α (Phospho-Ser167)	Raf1(Phospho-Ser259)
FAK(Ab-397)	Rb(Ab-780)
FAK(Ab-861)	Rb(Phospho-Ser780)
FAK(Ab-925)	Rel(Ab-503)
FAK(Phospho-Tyr861)	Rel(Phospho-Ser503)
FAK(Phospho-Tyr925)	SAPK/JNK(Ab-183)
FGF Receptor 1(Ab-154)	SAPK/JNK(Phospho-Thr183)
FGF Receptor 1(Phospho-Tyr154)	Shc(Ab-349)
FKHR(Ab-256)	Shc(Phospho-Phospho-Tyr349)
FKHR(Phospho-Ser256)	SHP-2(Ab-580)
GSK3α(Ab-21)	SHP-2(Phospho-Phospho-Tyr580)
GSK3α(Phospho-Ser21)	Smad3(Phospho-Phospho-Ser425)
GSK3β(Ab-9)	Src(Ab-418)
GSK3β(Phospho-Ser9)	Src(Ab-529)
HDAC8(Ab-39)	Src(Phospho-Tyr418)
HDAC8(Phospho-Ser39)	Src(Phospho-Tyr529)
HER2(Ab-877)	STAT1(Ab-701)

HER2(Phospho-Tyr877)	STAT1(Ab-727)
Histone H2A.X(Ab-139)	STAT1(Phospho-Ser727)
Histone H2A.X(Phospho-Ser139)	STAT1(Phospho-Tyr701)
HSF1(Ab-303)	STAT3(Ab-705)
HSF1(Phospho-Ser303)	STAT3(Ab-727)
HSP27(Ab-15)	STAT3(Phospho-Ser727)
HSP27(Ab-78)	STAT3(Phospho-Tyr705)
HSP27(Phospho-Ser15)	STAT4(Ab-693)
HSP27(Phospho-Ser78)	STAT4(Phospho-Tyr693)
HSP90B(Ab-254)	STAT5A (Ab-694)
HSP90B(Phospho-Phospho-Ser254)	STAT5A (Ab-780)
ICAM-1(Ab-512)	STAT5A (Phospho-Ser780)
ICAM-1(Phospho-Tyr512)	STAT5A (Phospho-Tyr694)
IGF-1R (Ab-1161)	STAT6(Ab-641)
IGF-1R (Phospho-Tyr1161)	STAT6(Ab-645)
IKK α(Ab-23)	STAT6(Phospho-Thr645)
IKK α(Phospho-Thr23)	STAT6(Phospho-Tyr641)
Integrin β3(Ab-773)	Tau(Ab-404)
Integrin β3(Ab-785)	Tau(Phospho-Ser404)
Integrin β3(Phospho-Tyr773)	Trk B(Ab-515)
Integrin β3(Phospho-Tyr785)	Trk B(Phospho-Phospho-Tyr515)
IκB-α(Ab-32/36)	TYK2(Ab-1054)
IκB-α(Ab-42)	TYK2(Phospho-Tyr1054)
IκB-α(Phospho-Ser32/Phospho-Ser36)	VEGFR2(Ab-951)
IκB-α(Phospho-Tyr42)	VEGFR2(Phospho-Tyr951)
IκB-β(Phospho-Phospho-Ser23)	β-Catenin(Ab-37)
IκB-ε(Ab-22)	β-Catenin(Ab-41/45)
IκB-ε(Phospho-Phospho-Ser22)	β-Catenin(Phospho-Ser33)
JAK1(Ab-1022)	β-Catenin(Phospho-Ser37)
JAK1(Phospho-Tyr1022)	β-Catenin(Phospho-Thr41/Phospho-Ser45)
JAK2(Ab-1007)	Beta Actin
JAK2(Ab-221)	Empty
JAK2(Phospho-Tyr1007)	GAPDH
JAK2(Phospho-Tyr221)	Negative control
JunB(Ab-259)	Positive control
JunB(Ab-79)	

Appendix A Table 1: Antibodies on phosphoproteomic array

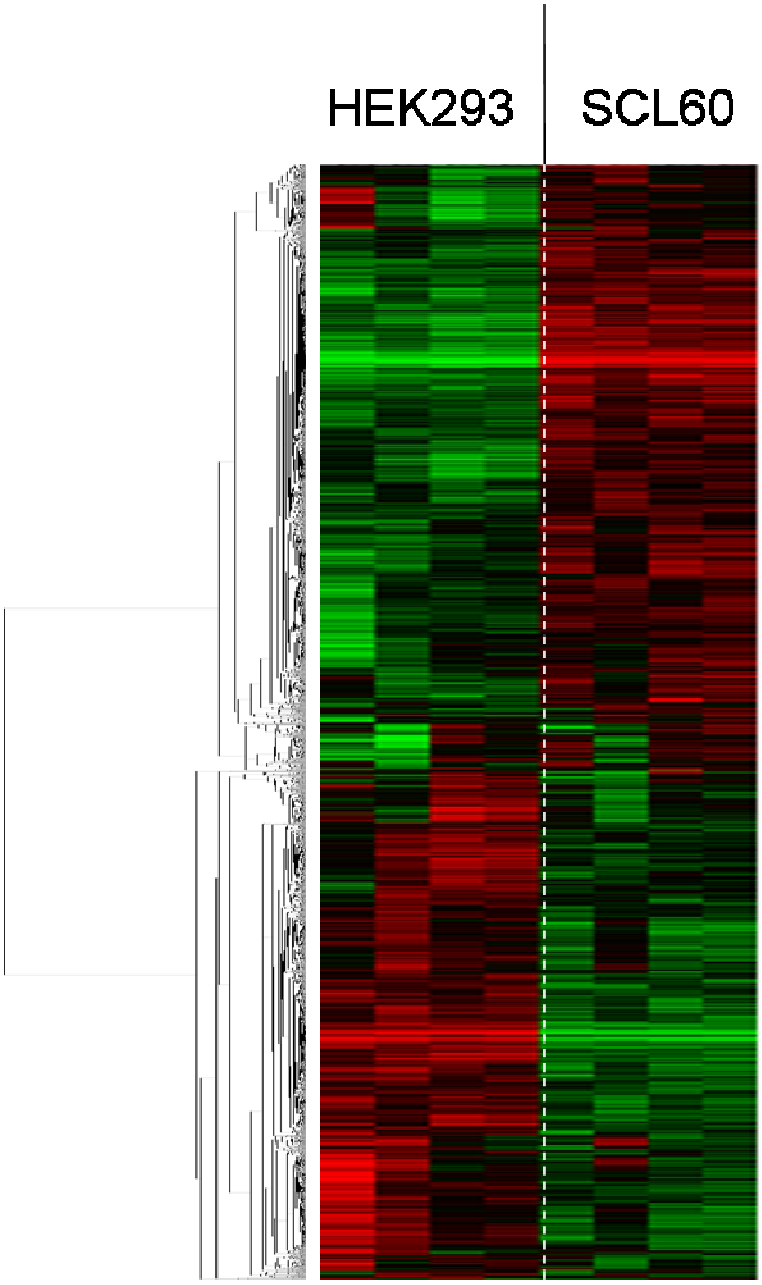

Appendix A Figure 1: Overview heatmap showing 4745 differentially expressed genes between untreated HEK293 and untreated SCL60 cells.
The heatmap shows 4 replicates for each cell line from left to right. Each horizontal line on the heatmap represents a gene. Red indicates a higher expression, green indicates a lower expression. The genes are hierarchically clustered to reveal two major, similarly sized clusters: one cluster showing genes increased in SCL60 compared to HEK293 cells, and one cluster showing genes that are decreased in SCL60 compared to HEK293 cells.

Gene	Illumina Probe ID	Fold Change	Description
SOX11	ILMN_1773459	+19	Transcriptional regulation
KRT19	ILMN_1730777	+15	Keratin
RYR3	ILMN_1796455	+14	Ryanodine receptor
MAL2	ILMN_1770653	+12	Lipid raft component
FLJ12684	ILMN_2072622	+10	Unknown
BEX1	ILMN_2234697	+6.4	Cell cycle, NGFR signalling, can inhibit NFkB
VANGL2	ILMN_1715647	+6.3	Cell polarisation
UCHL1	ILMN_1757387	+5.9	Hydrolyses ubiquitin
PRSS3	ILMN_1685699	+5.5	Serine protease
RAB17	ILMN_2052373	+5.4	Small GTPase
TCEAL3	ILMN_1734190	+5.4	Transcription regulation
HLA-DRB5	ILMN_1697499	+5.3	MHC complex
HLA-B	ILMN_1778401	+5.3	MHC complex
SFRP1	ILMN_2149164	+5.1	Wnt Signalling
EEF1A2	ILMN_2108735	+5.0	Protein biosynthesis
TCEAL3	ILMN_1749478	+4.7	Transcription regulation
HOPX	ILMN_2316236	+4.7	Interacts with serum response factor, possible tumour suppressor
CYP4X1	ILMN_2175317	+4.6	Cytochrome P450
LOC389641	ILMN_1713141	+4.6	Unknown
CD44	ILMN_1803429	+4.5	Adhesion
TACSTD1	ILMN_2160210	+4.5	Adhesion
RUNX3	ILMN_1787461	+4.5	Transcriptional regulation
MT1F	ILMN_1718766	+4.4	Metallothioneins
TNFRSF10A	ILMN_1721316	+4.2	TNF Receptor, activates NFkB
PTGER4	ILMN_1795930	+4.1	Prostaglandin E2 receptor

Appendix A Table 2: The 25 probes with the most significantly increased expression in SCL60 cells compared to HEK293 cells.
The probes changes are ordered in ascending probability of each being false positive, which for all the probes in the table is less than 0.05. Gene descriptions were taken from the GeneCards database.

Gene	Illumina Probe ID	Fold Change	Description
HSPA1A	ILMN_1789074	-210	Heat shock protein
CMBL	ILMN_1709634	-23	Cysteine hydrolase
NEFH	ILMN_1705153	-15	Neurofilament
CA2	ILMN_1662795	-14	Carbonic anhydrase II
CA2	ILMN_2199439	-14	Carbonic anhydrase II
TMEM47	ILMN_2129234	-9.9	Transmembrane protein
ZSCAN18	ILMN_1654946	-8.5	Transcriptional regulation
NEFM	ILMN_2215989	-8.4	Neurofilament
PCDH17	ILMN_1781514	-8.0	Cadherin (adhesion)
NEFL	ILMN_1659086	-7.8	Neurofilament
ZNF83	ILMN_2190414	-7.3	Transcriptional regulation
ZNF816A	ILMN_1728710	-7.3	Transcriptional regulation
ZNF135	ILMN_1726368	-6.6	Transcriptional regulation
ZNF702	ILMN_1663281	-5.7	Transcriptional regulation
FABP5	ILMN_2146761	-5.7	Fatty acid binding protein
IFITM3	ILMN_1805750	-5.1	IFN-induced antiviral protein
ZNF160	ILMN_1777049	-5.2	Transcriptional regulation
HS.572538	ILMN_1886769	-4.7	Unknown
ZNF649	ILMN_1699249	-4.4	Transcriptional regulation
HOXB5	ILMN_1674908	-4.0	Anterior-Posterior development
LOC400713	ILMN_1773367	-3.9	Transcriptional regulation
PCDH10	ILMN_1688500	-3.9	Cadherin (adhesion)
SH3PXD2A	ILMN_1743103	-3.7	ECM degradation, invasion
ZNF682	ILMN_2242998	-3.6	Transcriptional regulation
HS.200774	ILMN_1849209	-3.7	Unknown

Appendix A Table 3: The 25 probes with the most significantly decreased expression in SCL60 cells compared to HEK293 cells.
The probes changes are ordered in ascending probability of each being false positive, which for all the probes in the table is less than 0.05. Gene descriptions were taken from the GeneCards database.

	Genes	P-Value	FDR
Increased from SC0 to ST0.5			
hsa04010:MAPK signaling pathway	DUSP5, FOS, DUSP1, JUN, GADD45B	0.008	6.8
Increased from SC0 to ST1			
hsa04010:MAPK signaling pathway	DUSP5, FOS, DUSP1, JUN, MAP3K8, JUND, NR4A1, GADD45B, SRF, GADD45A, MYC, DDIT3	1E-05	0.011
hsa04620:Toll-like receptor signaling pathway	FOS, IL8, JUN, MAP3K8, IL12A, NFKBIA	0.002	1.6
hsa04115:p53 signaling pathway	RRM2, CYCS, PMAIP1, GADD45B, GADD45A	0.003	2.6
hsa04622:RIG-I-like receptor signaling pathway	DDX3X, ISG15, IL8, IL12A, NFKBIA	0.003	3.1
hsa04350:TGF-beta signaling pathway	BMP2, ID2, ID1, ID3, MYC	0.006	6.3
hsa04621:NOD-like receptor signaling pathway	CCL2, IL8, CXCL2, NFKBIA	0.02	15
Increased from SC0 to ST2			
hsa04010:MAPK signaling pathway	RELB, NR4A1, SRF, DDIT3, DUSP5, FOS, DUSP3, ATF4, DUSP1, JUND, MAP3K8, GADD45B, GADD45A	1E-04	0.12
hsa04621:NOD-like receptor signaling pathway	CCL2, IL8, CXCL2, CCL8, NFKBIA	0.008	7.9
hsa04115:p53 signaling pathway	CASP9, PMAIP1, GADD45B, THBS1, GADD45A	0.01	11
hsa04620:Toll-like receptor signaling pathway	TMED7, FOS, IL8, MAP3K8, NFKBIA	0.04	35
hsa04622:RIG-I-like receptor signaling pathway	DDX3X, ISG15, IL8, NFKBIA	0.06	49

Appendix A Table 4: Differentially expressed genes between untreated (0h) SCL60 controls and SCL60 cells treated with Triptorelin for up to 24h were enriched for several signalling pathways.
P-value was calculated within the DAVID system using a one-tail Fisher Exact test. False Discovery Rate (FDR) was also calculated within the DAVID system and is shown to 2 significant figures.

	Genes	P-Value	FDR
Increased from SC0 to ST8			
hsa04621:NOD-like receptor signaling pathway	HSP90B1, CCL2, IL8, CCL8, CHUK, CCL7	0.01	15
hsa04060:Cytokine-cytokine receptor interaction	BMP2, CCL2, IL8, TNFRSF12A, CCL8, KITLG, CCL7, IL11, TNFRSF10A, CCL20, TNFRSF10D, IL12A, IFNGR1	0.02	18
hsa04010:MAPK signaling pathway	MAP2K4, RELB, NR4A1, DUSP5, FOS, RPS6KA3, DUSP1, JUN, HSPA6, GADD45B, GADD45A, DUSP8, CHUK	0.02	20
hsa04115:p53 signaling pathway	CDKN1A, CASP9, PMAIP1, GADD45B, THBS1, GADD45A	0.02	20
hsa04620:Toll-like receptor signaling pathway	TMED7, FOS, IL8, JUN, MAP2K4, IL12A, CHUK	0.03	28
Decreased from SC0 to ST8			
hsa03410:Base excision repair	MUTYH, PARP4, XRCC1, SMUG1, NTHL1	0.01	14
hsa03030:DNA replication	PRIM1, POLA2, MCM2, MCM5	0.07	57
Increased from SC0 to ST24			
hsa04060:Cytokine-cytokine receptor interaction	CCL2, IL8, CCL20, TNFRSF12A, CCL8, CD70, CCL7, IL11, CCL26, ACVR1	0.04	35
hsa04621:NOD-like receptor signaling pathway	CCL2, IL8, CCL8, CCL7	0.09	66
Decreased from SC0 to ST24			
hsa04115:p53 signaling pathway	CDKN2A, BAX, LRDD, DDB2, CHEK2, SESN1	0.01	12
hsa00562:Inositol phosphate metabolism	ALDH6A1, ISYNA1, IMPA2, PLCG2	0.09	66

Appendix A Table 4 (continued): Differentially expressed genes between untreated (0h) SCL60 controls and SCL60 cells treated with Triptorelin for up to 24h were enriched for several signalling pathways. P-value was calculated within the DAVID system using a one-tail Fisher Exact test. False Discovery Rate (FDR) was also calculated within the DAVID system and is shown to 2 significant figures.

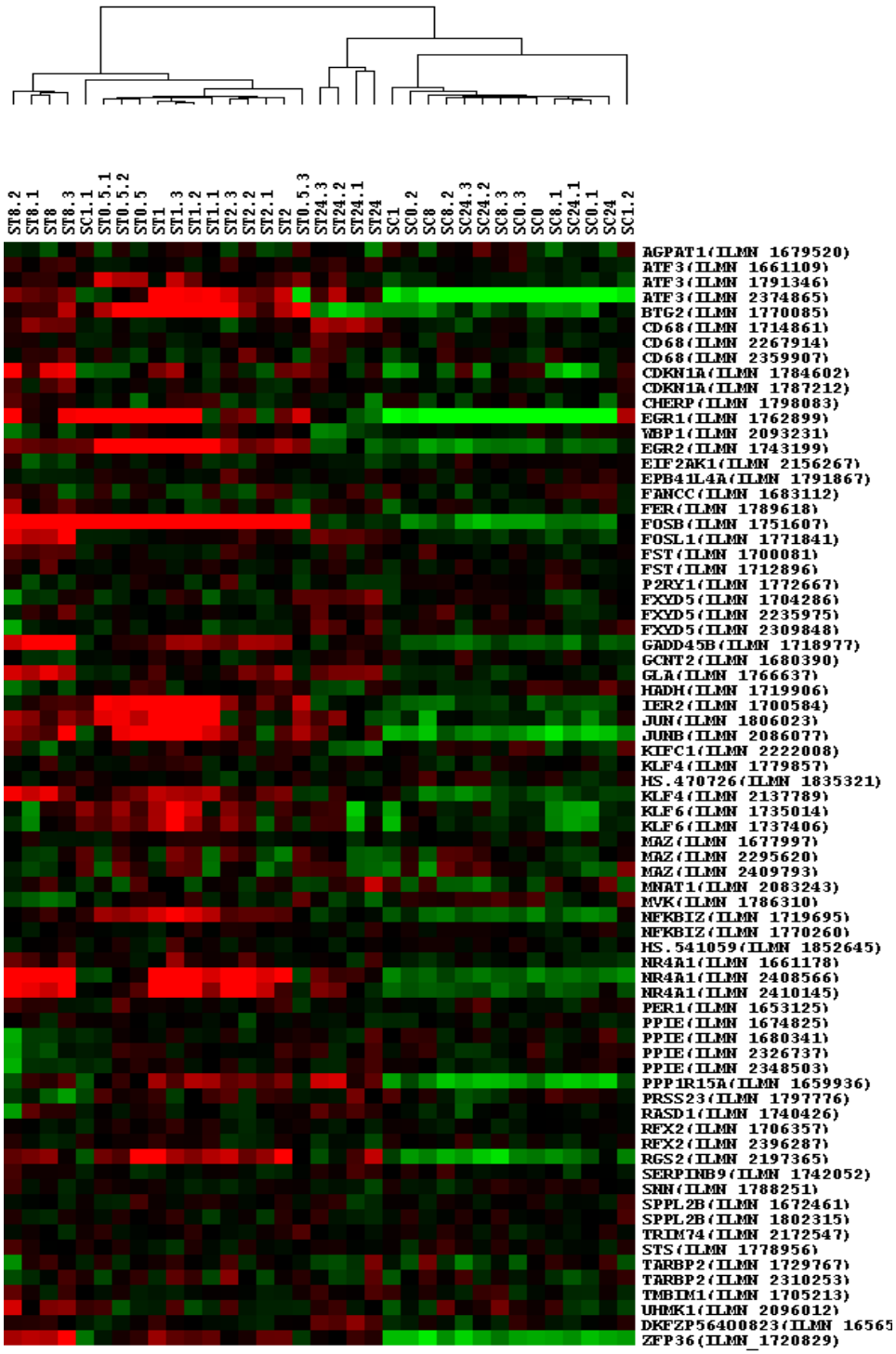

Appendix A Figure 2: The Kakar *et al* gene signature clustered the SCL60 dataset into control and Triptorelin-treated groups.
SCL60 (S) cells treated with Triptorelin (T) or vehicle control (C) for up to 24h. SCx = SCL60 treated with vehicle control for x hours, STx = SCL60 treated with Triptorelin for x hours. Four replicates are shown for each time point from left to right (except for SC1, for which there are 3 replicates). Red = higher, Green = lower expression.

Appendix B

7 Appendix B

Further supplementary material is available on the enclosed CD.

The CD contains the file *Colette Meyer PhD Thesis – Supplementary File 1.xls*, which contains further details of the differentially expressed genes between HEK293 and SCL60 cells and in SCL60 cells with Triptorelin treatment. It also details the conversion of Kakar *et al* genes to Illumina IDs and the full list of expression values observed in the phosphoproteomic antibody array (V250).

The CD also contains the published BMC cancer paper below (*BMC Cancer Morgan et al 2011.pdf)*, which is also available online at http://www.biomedcentral.com/1471-2407/11/476.

GnRH receptor activation competes at a low level with growth signaling in stably transfected human breast cell lines.
Morgan K, Meyer C, Miller N, Sims AH, Cagnan I, Faratian D, Harrison DJ, Millar RP, Langdon SP.